UNIVERSITÀ
DEGLI STUDI
FIRENZE

DOTTORATO DI RICERCA TOSCANO IN NEUROSCIENZE

CICLO XXXII

COORDINATORE Prof. Renato Corradetti

T-cell response in Relapsing-Remitting Multiple Sclerosis: a computational approach to T-cell receptor repertoire diversity before and during disease-modifying therapies

Settore Scientifico Disciplinare MED/26

Dottorando

Dott.ssa Amoriello Roberta

(firma)

Tutore

Dott.ssa Ballerini Clara

(firma)

Coordinatore

Prof. Corradetti Renato

(firma)

Anni 2016/2019

INDEX

1. Introduction

1.1 Multiple sclerosis

Multiple sclerosis (MS) is an inflammatory, chronic disease of the central nervous system (CNS), characterized by an immune-mediated degradation of myelin that leads to the formation of demyelinated lesions, impairing the nervous conduction.

With a 2,5 million of people prevalence worldwide (Atlas of Multiple Sclerosis, 2013), MS is the most common demyelinating disease of the CNS and the first cause of neurological disability among young people.

The first detailed description of MS dates back to 1868, when the French neurologist Jean-Martin Charcot identified the important relationship between clinical and anatomical findings (Marie P, 1895) and recognized MS as a distinct illness. Charcot defined the disease as "*la sclérose en plaques*", accompanying the description with an accurate illustration of the expansion of lesions from the ventricles to the cerebral hemispheres, demonstrating for the first time that the pathology of MS involves both the brain and the spinal cord (Pearce JM, 2005; Orrell RW, 2005).

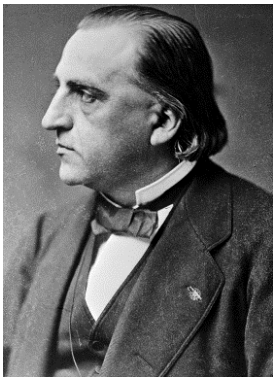

Fig.1. Jean-Martin Charcot (1825-1893).

Besides white matter lesions, Charcot also described the presence of cortical demyelinated lesions, although rare (Charcot JM, 1887). Nevertheless, due to the lack of high-sensitivity imaging techniques, MS has been considered a white-matter disease until the advent of magnetic resonance imaging (MRI), along with the histopathological evaluation of lesions, had notably improved MS understanding and diagnosis, confirming the presence of demyelinated lesions in the grey matter. These lesions were classified for the first time by Kidd D et al. in 1999, who described 7 different types of cortical lesions based on their location relative to the cortical venous supply (Kidd D et al., 1999) and Peterson JW et al. in 2001, who classified cortical lesions based on the distribution within the cortical grey matter layers in 4 different types (ref. par. 2.6). MRI confirmed the presence of cortical lesions in MS patients also at early stages and especially in progressive MS forms (Vrenken H et al., 2006).

The most common form of MS is Relapsing-Remitting MS (RRMS), characterized by

relapses interspersed with periods of partial or complete recovery; the other forms are progressive and include Primary Progressive MS (PPMS), Secondary Progressive MS (SPMS) and Progressive Relapsing multiple sclerosis (PRMS) (ref. par. 2.5) (Lublin FD and Reingold SC, 1996).

The unknown etiology, the complex pathogenesis and the wide variety of clinical manifestations make MS an extremely heterogeneous disease. Several factors have been suggested as linked to the development of the disease, from genetic background to environmental and infective factors. One of the proposed mechanisms involved in MS pathogenesis is the so-called "molecular mimicry" (ref. par. 2.2.3), in which structural homologies between the microbial and a self-protein can lead to an autosensitization (Wucherpfennig KW and Strominger JL, 1995). Despite the hypothesis, the exact event that triggers the autoreactive response remains elusive.

1.1.1 Epidemiology

Multiple sclerosis affects about 2,5 million of people worldwide, of which 1.5 million only in Europe (Rosati G, 2001). The disease is more common in world regions farther from the equator. In Europe, the major number of cases is reported in the northern populations (Compston A and Coles A, 2002; Tarlinton RE et al., 2019).

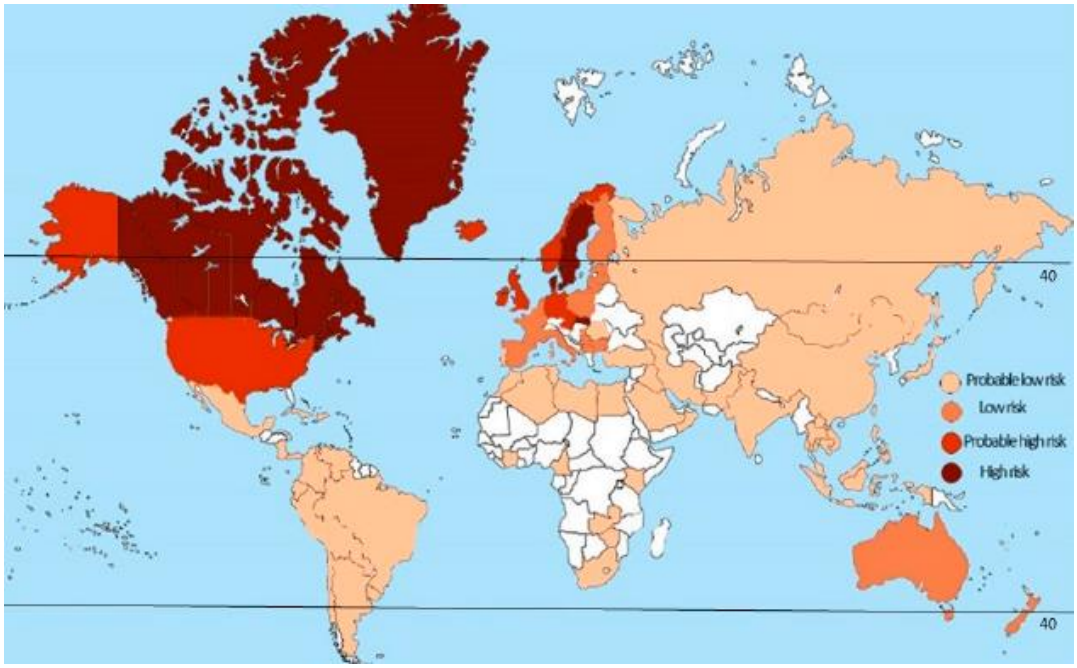

Fig. 2. Global prevalence of Multiple sclerosis (Tarlinton RE et al., 2019).

In Italy, the highest disease incidence and prevalence were found in the island of Sardinia (Rosati G, 1996).

MS usually begins between 20 and 50 years, with an average age of onset about 35 years. Women are more than twice as likely to develop multiple sclerosis as men (Alonso A and Hernán MA, 2008).

1.1.2. Etiology

MS is a heterogeneous and multifactorial disease. Although its precise etiology is currently unknown, a combination of environmental and genetic factors, as well as infectious agents, have been suggested to have a role in MS development (Compston A and Coles A, 2002).

1.1.2.1 Genetics

The study of the genetic background of MS has spanned over a period of 20 years, successfully demonstrating the involvement of several genetic loci as important risk factors for the development of the disease.

To date, MS is not considered a hereditary disease, although it has demonstrated that the probability of developing the disease is higher in relatives of patients and even greater in closely related (Compston A and Coles A, 2002). In identical twins both are affected about 30% of the time, while around 5% for non-identical twins and 2.5% of siblings are affected with a lower percentage of half-siblings (Compston A and Coles A, 2002; Hassan-Smith G and Douglas MR, 2011). Furthermore, when both parents are affected by MS, the risk in their children is 10 times that of the general population (Milo R and Kahana E, 2010).

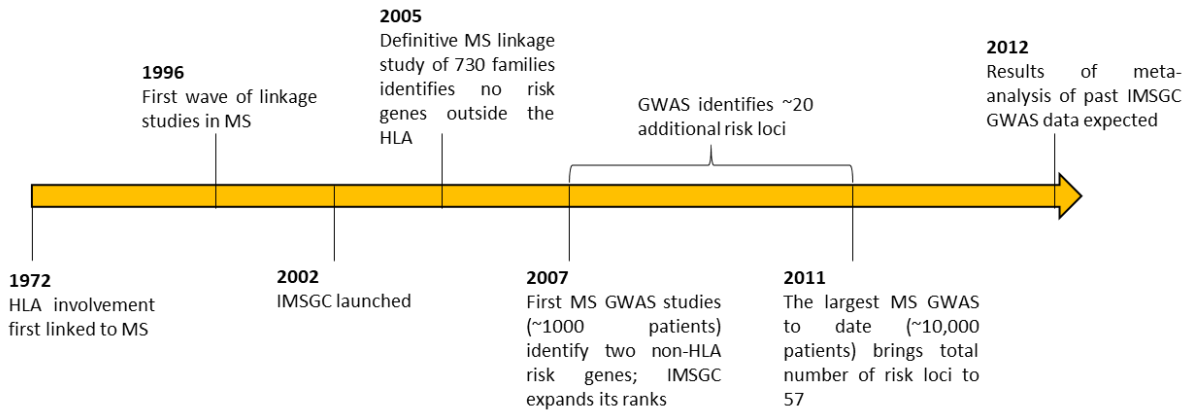

Fig. 3. Studies about the genetic background of MS over time. Timeline includes the major investigations about the genetic background of MS pathogenesis from 1972 to 2012.

The human leukocyte antigen (HLA) locus (major histocompatibility complex "MHC" in mice) was identified in 1970 as the first major genetic risk factor related to the disease. The locus is in the short arm of chromosome 6. HLA class I (A, B and C) present intracellular peptides, while HLA corresponding class II (DP, DM, DO, DQ, DR) present exogenous peptides.

Briefly, after the degradation by proteasome, the cytosol-derived peptides are transported into the endoplasmic reticulum (ER) and loaded onto MHC class I molecules; on the other hand, MHC class II are assembled in the ER where they form a complex with the invariant chain (Ii); the complex is transported through the Golgi to

the MHC class II compartment (MIIC), where the endocytosed proteins and the Ii are degraded and the remained fragment of the Ii in the peptide-binding groove is exchanged with the antigenic peptide, supported by a chaperon called HLA-DM (H2-M in mice). Finally, MHC class II are transported to the plasma membrane to present antigenic peptides to CD4 cells (Neefjes J et al., 2011).

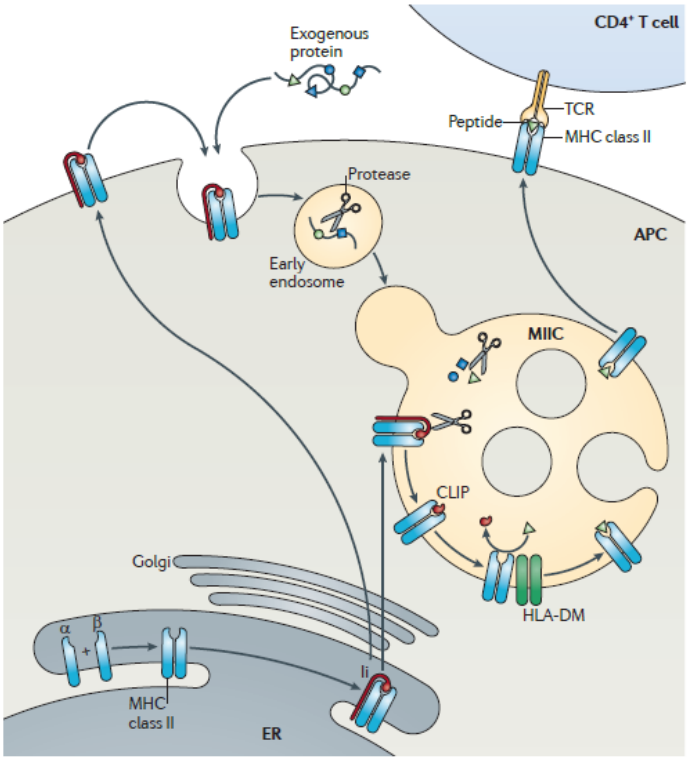

Fig. 4. MHC class II antigen presenting pathway. MHC II are assembled in RE and undergoes maturation within the Golgi, then it is exposed to the plasma cell membrane. MHC II presents antigenic peptides to CD4 cells (Neefjes J et al., 2011).

The strongest association has been identified between MS and HLA II haplotype DR15, in particular DRB1*1501 (Olerup O and Hillert J, 1991; Ballerini C et al., 2004) in European population. The island of Sardinia, in Italy, is an exception: characterized by a genetic isolated population and a high prevalence of MS and other autoimmune diseases, it shows a low frequency of DR15 haplotype and a strong association between MS and DR4 (DRB1*0405 - DQA1*0501 - DQB1*0301) and with DR3 (DRB1*0301-DQA1*0501-DQB1*0201) haplotypes (Marrosu MG et al., 1998).

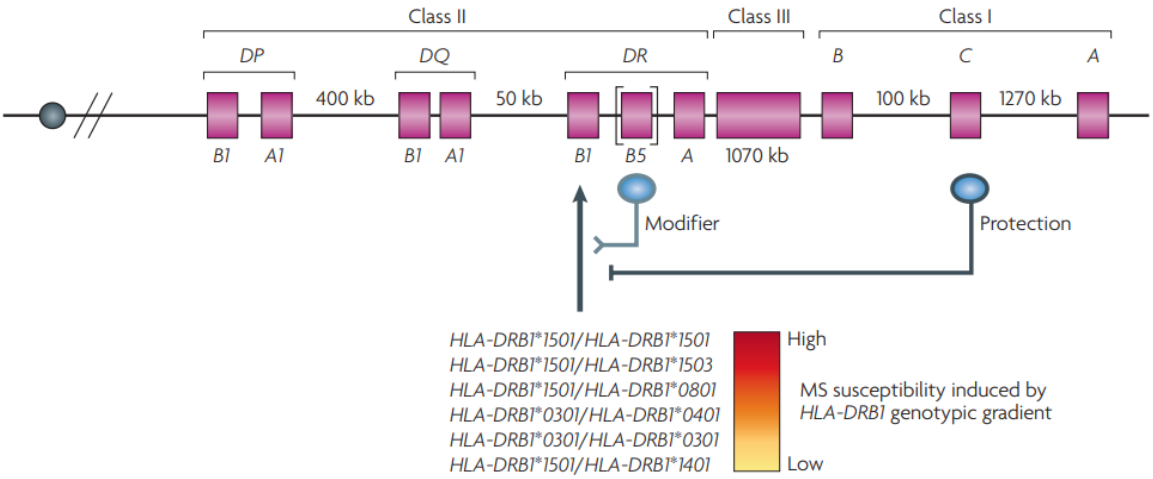

Fig. 5. HLA genes and MS susceptibility. The human leukocyte antigen (HLA) gene is located on the short arm of chromosome 6 and included HLA class I (A, B, C) and class II (DP, DQ, DR). HLA class I and II are glycoproteins expressed on cell surfaces that present peptide antigens to CD8 and CD4 T cells, respectively. HLA genes have been linked to MS susceptibility in a genotypic gradient going from high to low disease susceptibility; e.g., HLA-DRB1*1501 homozygotes and HLA- DRB1*1501/HLA-DRB1*0801 and DRB1*1501/HLA-DRB1*0801 heterozygotes were linked to high susceptibility, while HLA-DRB1*03/HLA-DRB1*04 heterozygotes and HLA-DRB1*0301 homozygotes to moderate susceptibility (Oksenberg JR et al., 2008).

In other parts of the world, MS has been associated with other haplotypes, e. g. DQB1*0602 in African-Brazilian patients (Caballero A et al., 1999) or DRB1*04:05 in Japan (Nakamura Y et al., 2016). Furthermore, a connection between HLA class I region and the increased risk of MS (Link J et al., 2010; Cree BA et al., 2010) has been recently assessed: to mention, the class I region involved in Epstein-Barr virus (EBV) recognition has been demonstrated to be associated with MS susceptibility (Jafari N et al., 2010), supporting the hypothesis of the role of EBV in the disease etiology.

Following the confirm of the association between HLA and MS risk, many non-HLA linked genes were related to the disease, beginning with the variants in the cytokine receptor genes interleukin-2 receptor alfa (IL2RA) and interleukin-7 receptor (IL7R) (Gregory SG et al., 2007; Lundmark F et al., 2007). Later, with the increase of the sample size, new genetic disease risk *loci* were found: examples are a rare variant of the non-receptor tyrosine-protein kinase TYK2 gene (Jakkula E et al., 2010), the variants of the costimulatory molecule CD40, whose lower expression level was found as associated with increased MS risk (Field J et al., 2015) and a common variant of the TNF receptor superfamily member 1 TNFRSF1A (International Multiple Sclerosis Genetics

Consortium, 2011).

1.1.2.2. Environmental factors: latitude and vitamin D

Environmental factors have a fundamental role in MS causation. The first evidence is the non-uniform worldwide disease distribution, reflecting in a geographical pattern of distribution (Lincoln JA and Cook SD, 2009): the occurrence of MS is positively correlated with the distance from the equator; indeed, higher latitude is associated with higher MS incidence. Those living beyond the 40-degree mark north or south of the equator are more likely to develop MS that those living in the warmer climates near the equator (Alonso A and Hernán MA, 2008). This occurrence has been considered a consequence of the lower sunlight exposition at higher latitudes, resulting in a vitamin D deficiency.

A lower risk of MS in women who used supplemental vitamin D (Munger KL et al., 2004) and a seasonal fluctuation of gadolinium-enhancing lesions in MS patients, with a greater number of active lesions in spring than in autumn (Embry AF et al., 2000) are two examples in supporting the hypothesis of the protective role of vitamin D. Later, vitamin D has been described as an important immunoregulator factor, stimulating the development of T lymphocytes immunomodulatory properties, increasing the levels of immunosuppressive cytokines and inhibiting the production of inflammatory ones (Correale J et al., 2009).

A gene-environment interaction has been observed between vitamin D and HLA-DRB1*1501 allele. Vitamin D, in fact, modulates the expression of several genes binding its receptor, the vitamin D receptor (VDR) and the vitamin D response elements (VDREs) in the genome. Vitamin D has been demonstrated to impact on HLA-DR genes, altering the antigen expression and presentation (Rigby WF et al., 1990). A single VDRE in the promoter region of HLA-DRB1 was found as highly conserved only in MS patients with HLA-DRB1*15 haplotype but not in non-MS-associated ones (Ramagopalan SV et al., 2009). It has been proposed that low availability in VDREs or mutations in these regions may be unable to induce the expression of HLA-DRB1*15 in early stages of life, allowing autoreactive T cells to escape thymic deletion. Interestingly, a recent study performed on MS patients in the island of Sardinia, where MS susceptibility is not linked to HLA-DRB1*1501 but to other HLA alleles as already mentioned above, the expression of

DRB1 associated alleles resulted to be VDRE-independent (Cocco E et al., 2012).

1.1.2.3. Infections involvement in MS etiology

The earliest evidence of infections involvement in MS etiology dates to 1965, when Sibley and Foley demonstrated the role for upper-respiratory infections in the promotion of MS exacerbation (Sibley WA and Foley JM, 1965). Multiple epidemiological studies indicate that periods of high-risk for obtaining any upper-respiratory viral infection correspond to increased relapse risk in MS patients (Spelman T et al., 2014; Monto AS et al., 2014).

One of the arguments proposed as involved in the link between autoimmune diseases and infections is the concept of "molecular mimicry" (Fujinami RS et al., 1983; Abromson-Leeman SR and Cantor H, 1983). It assumes that the molecular similarities between foreign (e. g. viral) and self-peptides may lead to cross-activation of autoreactive T or B cells by pathogen-derived peptides. Fujinami and Oldstone described that injection into rabbits of hepatitis B virus (HBV) polymerase peptide 589-598, which shares 6 aminoacids (a.a.) with the myelin basic protein (MBP) a. a. 66-75, induced an encephalitis due to an immune cross-reaction against the myelin peptide (Fujinami RS and Oldstone MBA, 1985). Based on the assumption that cross-recognition only occurs if two peptides share the same stretch of a.a., molecular mimicry was initially considered a rare event. With the work of Hemmer et al., who showed that a peptide that shares no a.a. with MBP (83-99) can still be a molecular mimic, it was clear that the cross-reactivity of T cells is a very frequent event (Hemmer B et al., 1998). Since *in vitro* experiments are not sufficient to clarify the impact of molecular mimicry in humans, a wide number of *in vivo* observations has followed: regarding the animal models, transgenic mice expressing MBP-specific T-cell receptor (TCR) resulted to be susceptible to Experimental Autoimmune Encephalomyelitis (EAE), the animal model of MS (Madsen LS et al., 1999).

It was hypothesized that infections acquired in childhood and reactivated in adult life may have a role in the disease, especially in the relapsing-remitting pattern of the initial stages (Steelman AJ, 2015). About 20 years ago, Human Herpesvirus 6 (HHV-6) was suggested involved in MS pathogenesis, since it was found in plaques (Challoner PB et al., 1995) and subsequently investigated for increased immunoglobulin M (IgM)

response to HHV-6 early antigen in Relapsing-Remitting Multiple Sclerosis (RRMS) patients (Soldan SS et al., 1997). Further studies showed that HHV-6 protein U24 shares an a.a. stretch, enriched in proline (PRTPPPS), with MBP and that T cells might be activated by this protein recognizing MBP peptide by cross-reaction (Tejada-Simon MV et al., 2003), supporting the hypothesis of molecular mimic; in addition, HHV-6 was found in MS plaques and expressed in oligodendrocytes and in astrocytes (Goodman AD et al., 2003). However, the role of HHV-6 in the disease etiology is still under debate. EBV, able to remain latent within the body over long periods, has been widely investigated for its probable association with MS. Anti-EBV antibodies are elevated in MS patients, who often reactivate latent EBV infections after relapses (Wandinger K et al., 2000). Analysis of serum samples obtained more than 10 years before the onset demonstrated that the risk of developing MS significantly increases together with the level of EBV-antibody titles (Levin LI et al., 2005). Furthermore, it was observed that EBV-infected B cells are present in demyelinated lesions and meninges (Serafini B et al., 2007), while in peripheral an increased frequency of lytic antigen EBV-specific CD8 T cells were found during active MS (Angelini DF et al., 2013).

Although EBV's role in MS etiology remains discussed, some interesting scenarios have been proposed by Giovannoni et al. in 2006, as illustrated in fig. 6; one of these may be the cross-reaction of Epstein-Barr virus antigen 1 (EBNA1) specific T cells with CNS autoantigens, resulting in the attack of the myelin sheath of axons.

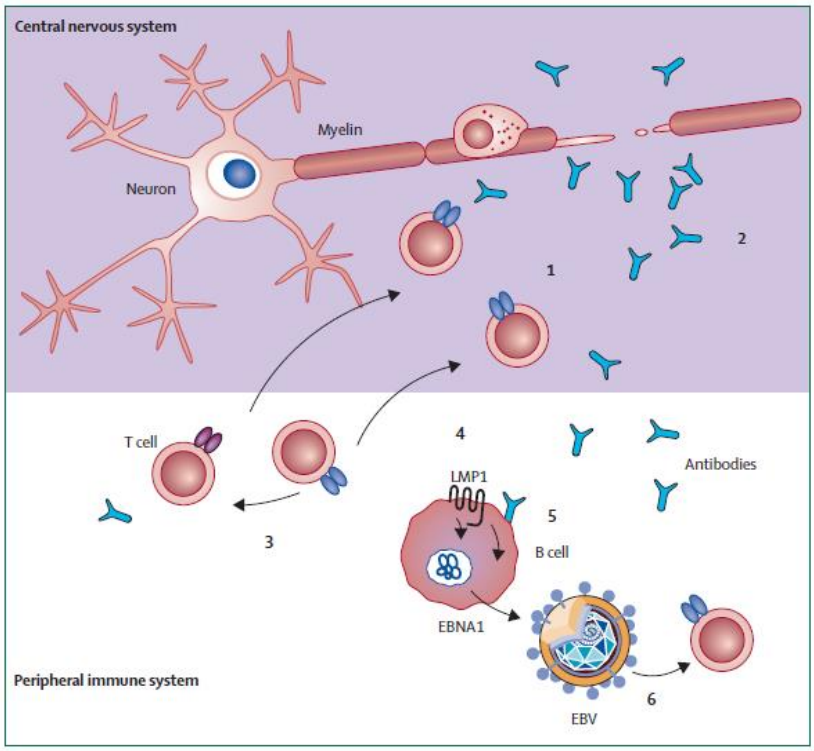

Fig. 6. Hypothesis of EBV mediation of autoimmunity in MS. EBNA1-specific T cells (1) or antibodies (2) cross-react with CNS autoantigens and attack the myelin sheath of axons. 3) EBNA1-specific T cells assist myelin specific T cells via cytokine-mediated bystander activation. 4) Latent EBV antigens sustain the survival of autoreactive B cells or the latter could be activated by autoantigens which could initiate viral replication (5) and augment EBV-specific T cell responses (6). The T-cell receptors of EBNA1-specific T cells are indicated in blue and those of myelin-specific T cells in purple. Arrows indicate interactions via cytokines (step 3), cell–cell contact (step 6), or directions of migration (from the peripheral immune system to the CNS). LMP1=latent membrane protein 1 (Giovannoni G et al., 2006).

As a neurotropic and highly infective virus, Varicella Zoster Virus (VZV) was investigated for the role in MS pathogenesis: VZV antibodies were found in the cerebrospinal fluid (CSF) of patients (Leinikki P et al., 1982); nevertheless, a strong statistical correlation with the disease pathogenesis was not found (Marrie RA and Wolfson C, 2001; Kang JH et al., 2011) and the presence of compartmentalized antibodies in patients' CSF may reflect a polyspecific activation to various neurotropic viruses, including measles and rubella (Virtanen JO and Jacobson S, 2012).

1.1.3. Pathogenesis

The description of MS as an autoimmune disease and our understandings about the role of autoreactive T cells in its pathogenesis owe much to the study of EAE, animal model of MS. In this model, encephalitogenic peptides as MBP, proteolytic protein (PLP) and

myelin oligodendrocyte glycoprotein (MOG) are the targets of autoreactive T-cell response against myelin. EAE had long been considered as a CD4-T-cells mediated disease, until several studies shed light on the pathogenic role of CD8 T cells (Ford ML et al., 2005; Sobottka B et al., 2009).

In MS, autoreactive T cells from periphery migrate across the blood-brain barrier (BBB) and infiltrate CNS parenchyma, attacking the myelin sheath and leading to neuronal damage, with the consequent formation of the typical lesions in the white matter.

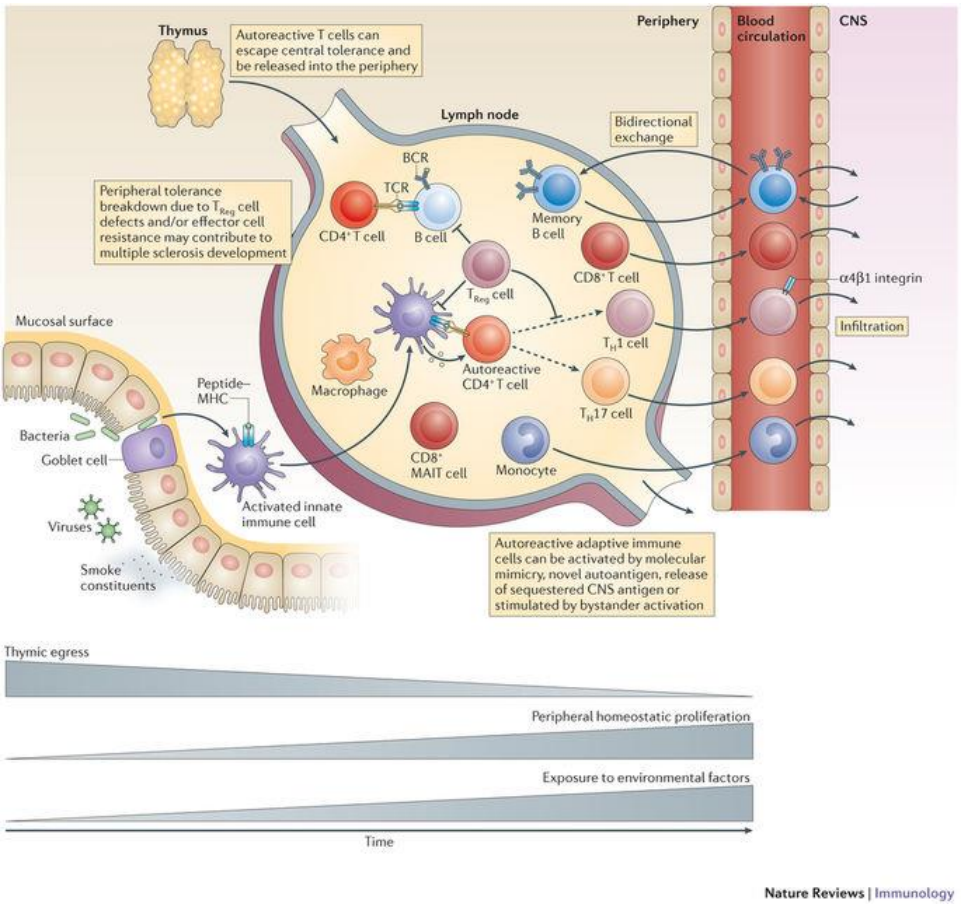

Fig. 7. Illustrated representation of immune system dysregulation mechanisms in MS pathogenesis (Dendrou CA et al., 2015).

MS lesions in the white matter have been widely described for the presence of different types of T cells involved in sustaining inflammation and CNS damage (Babbe H et al., 2000; Markovic-Plese S et al. 2001) and for some typical features that allow to distinguish between different types ("pattern") of lesions. In fact, despite all lesions are characterized by the presence of immunological infiltrates including T lymphocytes and macrophages, there are some immunopathological differences that have been described by four different patterns (Lucchinetti C et al., 2000): I and II are characterized by the

predominance of T cells and macrophages in the lesion, but the pattern II is the only one that presents deposits of Igs, mainly IgG, and complement C9neo antigens. Pattern III is characterized by infiltrates of T cells, macrophages and activated microglia, no Ig deposits, well defined borders and a loss of myelin-associated glycoprotein (MAG). Finally, pattern IV consists in infiltrates of T cells and macrophages, oligodendrocyte death around the white matter, well demarcated plaque and radial expansion of the lesion.

The histopathological observation of lesions and, later, the advent of MRI (ref. par. 2.6), provided the detection of demyelinated lesions also in the grey matter. The most recent histopathological cortical lesions classification comes from the work of Peterson JW et al. in 2001, who described 4 different types: I) leukocortical lesions, developed in the deeper layers of the grey matter or within the grey/white matter junction; II) intracortical lesions, small demyelinated lesions centered on blood vessels; III) lesions distributed from the pial surface to layers 3-4 of the cortex and IV) lesions extended within the entire cortex (Peterson JW et al., 2001).

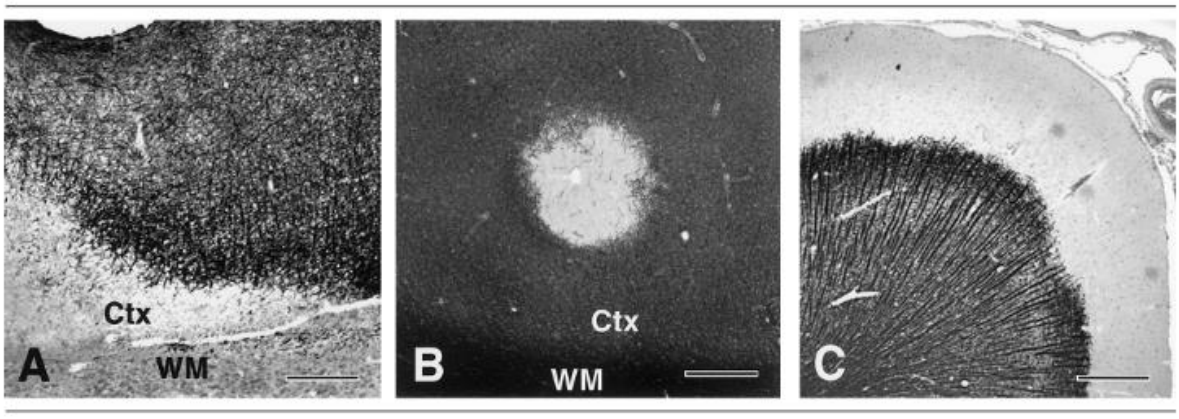

Fig. 8. Patterns I, II and III of MS cortical lesions defined by immunocytochemical distribution of myelin. (A) Cortical lesion type I, involving both white matter (WM) and cortex (Ctx). (B) Cortical lesion type II, confined within the cortex with a centrally located vessel. (C) Cortical lesion type III**,** distributed across pial surface into the cortex. Scale bars = 200 μm (Peterson JW et al., 2001).

1.1.3.1. T-cell biology and MS

T lymphocytes are the principal white blood cells involved in cell-mediated immunity. They originate from hematopoietic progenitors (or lymphoid progenitor cells), in turn derived from hematopoietic stem cells (HSCs) within the bone marrow. The hematopoietic progenitors populate the thymus where they undergo expansion, generating a population of immature thymocytes by the process called "thymopoiesis" (Schwarz BA and Bhandoola A, 2006). T cells development goes through a first phase of double-positive thymocytes, expressing both CD4 and CD8, followed by the generation of single-positive cells (CD4+CD8- or CD4-CD8+) that leave the thymus towards peripheral tissues.

Thymus is a primary lymphoid organ located in the anterior superior mediastinum and composed by an outer cortex and in an inner medulla, where T cells undergo positive and negative selection, respectively. During the positive selection, CD4 or CD8 single-positive T cells undergo TCR rearrangement (ref. par. 3.2) and then interact with the complex comprising the peptide and the MHC molecules on cortical thymic epithelial cells (cTECs); according to their affinity to MHC class II and I, T cells are positively selected (Takada K and Takahama Y, 2015). These cells next migrate from thymus cortex to medulla, where they interact with antigen presenting cells (APC) and dendritic cells (DCs), resulting in the deletion of autoreactive cells (Klein L et al., 2014). These selective processes are the major mechanisms of central immune tolerance.

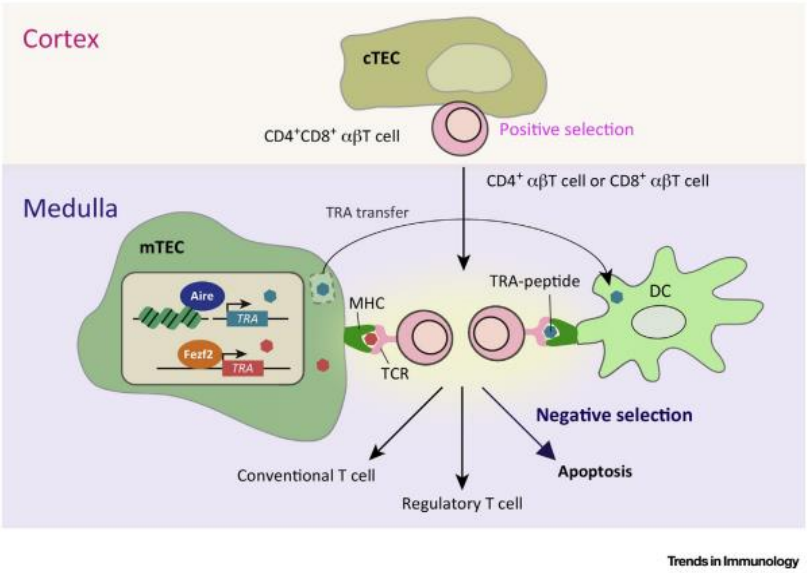

Fig. 9. Schematic illustration of T cells positive and negative selection in the thymus (Takaba H and Takayanagi H, 2017).

CD4 and CD8 are the principal glycoproteins expressed on T lymphocytes surface. CD4 characterizes T helper (Th) and CD8 is distinctive of cytotoxic T lymphocytes (CTL). CD4 and CD8 are structurally and functionally different. CD4 is a monomeric type I transmembrane glycoprotein, formed by four immunoglobulin (Ig)-like extracellular domains connected to a transmembrane domain and a cytoplasmic tail; CD4 interacts with MHC class II through its membrane-distal D1 domain which contacts the α2 and β2 domains of MHC class II; specifically, CD4 contacts a concavity formed between α2 and β2 (Li Y et al., 2013). CD8 is a heterodimeric type I transmembrane glycoprotein equipped with α and β chains, each one composed of an Ig-like domain connected to a transmembrane domain and a cytoplasmic tail. CD8 interacts with the α3 portion of MHC class I (Li Y et al., 2013).

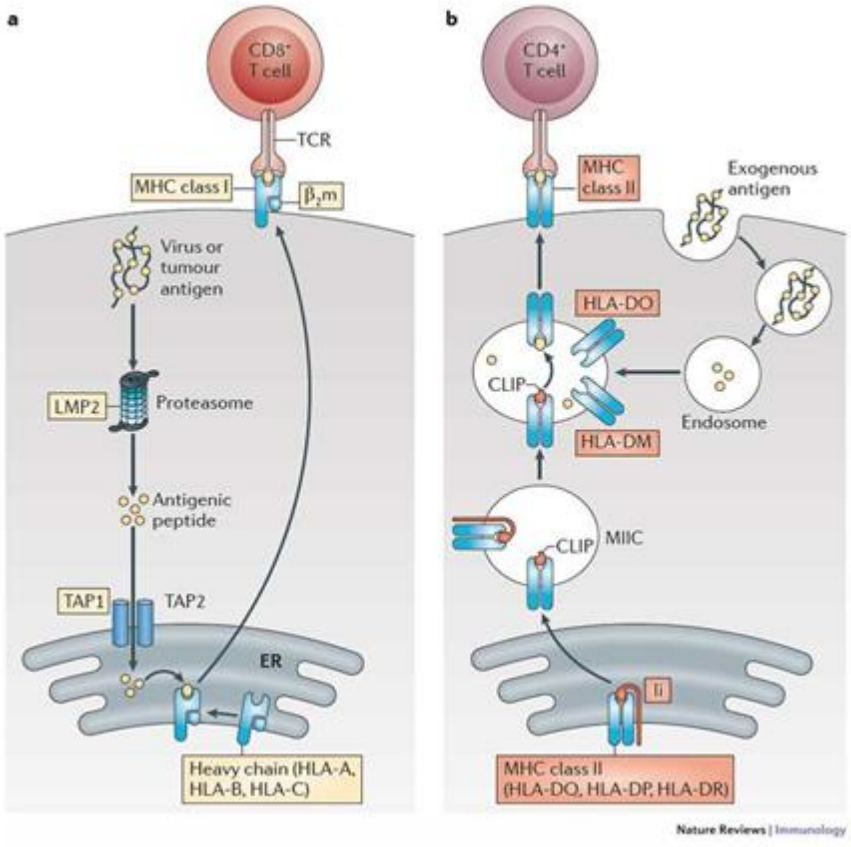

Fig. 10. Illustration of the interaction between CD8 and MHC class I (a) and between CD4 and MHC class II (b). a) Endogenous peptides presented by MHC class I to CD8 cells are transported into the endoplasmic reticulum (ER) and loaded into the groove of the MHC class I complex. b) Exogenous antigens are processed by endolysosomal enzymes into peptides that bind to the groove of the MHC class II complex by displacing the class II-associated invariant chain peptide (CLIP), which is derived from the MHC class II-associated invariant chain (Ii) (Kobayashi KS and van den Elsen PJ, 2012).

As in EAE model (Langrish CL et al., 2005; O'Connor RA et al., 2008), the main pathogenic CD4 cells in MS are T helper 1 (Th1) and T helper 17 (Th17) phenotypes, that produce the pro-inflammatory cytokines IFNγ and IL17, respectively. In human, the association between HLA class II (e. g. HLA-DR15 haplotype; Ballerini C et al., 2004) and susceptibility to MS was the first confirm supporting the role of CD4 cells in the disease pathogenesis.

In EAE, Th1 and Th17 cells have an established role in the onset and maintenance of the disease (Steinman L et al., 2007). Pathogenic cells can enter the CNS either through the BBB by the interaction between cell-surface integrins and endothelial adhesion molecules or by the choroid plexus (Engelhardt B et al., 2001). The choroid plexus is composed by an epithelium of non-ciliated cells with tight junctions and is located in the

four brain ventricles forming a blood-cerebrospinal fluid barrier, in order to regulate the circulation of immune cells and molecules into the CSF. The trafficking of T cells in steady state and during inflammation is mediated by various chemokines, and different T-cell phenotypes express different chemokines (Bromley SK et al., 2008): Th1 were found to preferentially express CXCR3 and CCR5, whereas CCR3 and CCR8 were mainly found on Th2 cells. Similarly, the CCL20-receptor CCR6 was found on Th17 cells. In this regard, it was observed that CCR6 is strictly required to induce EAE, since CCR6-deficient mice are resistant to EAE development. Specifically, CCR6- Th17 cells were not able to pass the choroid plexus and migrate into CNS at early stages of EAE, preventing the development of the disease (Reboldi A et al., 2009); such findings supported the pivotal role of Th17 in EAE pathogenesis.

In human MS, a higher frequency of Th17 in peripheral blood and CSF was found during the acute episodes (Matusevicius D et al., 1999), along with increased levels of IL17 in active brain lesions (Tzartos JS et al., 2008). The proportion of Th17 and IL17 correlated with disease activity, specifically with the number of lesions, the EDSS and the frequency of relapses (Hedegaard CJ et al., 2008).

Moreover, abnormalities in T and B cells are generally present in CSF of patients. A study performed on 221 subjects reported a significantly higher percentage of CD4 and CD8 T cells and B cells in RRMS and SPMS patients compared to PPMS, whereas PPMS were characterized by a significant higher percentage of monocytes and granulocytes in CSF compared to RRMS and SPMS (Han S et al., 2014).

In MS lesions CD4 cells localize mostly in perivascular spaces, even if fewer than CD8. Interestingly, CD4 cells producing IFNγ and IL17 seem to cross the BBB more efficiently respect other types of T cells, and this has been suggested as associated with a greater encephalitogenic capacity (Kebir H et al., 2009). Recently, the involvement in MS pathogenesis of cytotoxic CD4 T cells (CTL) has been discussed (Peeters LM et al., 2017): these cells increase in number under inflammatory conditions and seem to be costimulatory-independent. Moreover, they produce large amounts of IFNγ, granzyme b and perforin (Broux B et al., 2012).

Finally, regulatory T cells (Treg) may have a protective role in the disease, since their impairment or dysfunction were documented in MS exacerbations (Zozulya AL and

Wiendl H, 2008). In fact, Tregs control the maintenance of immune tolerance and suppress the effector activity of CD4 cells that are involved in MS as well as in other autoimmune diseases (Danikowski KM et al., 2017). Furthermore, the role of Tregs in MS is sustained by the impact of several treatments in restoring immunotolerance promoting a switch of T cells phenotype towards a regulatory one or increasing the number of Tregs (Massey JC et al., 2018; Muls N et al., 2014).

Once definitely assessed the involvement of CD4 cells in MS pathogenesis, the focus of attention shifted towards the pathogenic role of CD8 cells. The association of MHC class I with a higher risk of developing MS was initially described for HLA-A3 and B7 alleles (Jersild C et al., 1972; Naito S et al., 1972) and more recently for HLA-A*0301, associated with susceptibility to the disease. Furthermore, HLA-A*0201 was described for having a protective role (Fogdell-Hahn A et al., 2000; Harbo HF et al., 2004).

In MS lesions, CD8 cells outnumber CD4, especially at the edges of active demyelinating plaques, but they are also predominant in normal-appearing white matter (NAWM) (Hauser SL et al., 1986). Lucchinetti CF and collaborators described CD8 as being often present in cortical plaques, that are usually associated with cognitive impairment in MS (Lucchinetti CF et al., 2011). In most cases, CNS-infiltrating CD8 cells are clonally expanded (Babbe H et al., 2000) and characterized by a less diverse TCR repertoire compared to CD4 cells (Junker A et al., 2007; Skulina C et al., 2004) (ref. par. 3.4), suggesting that their clonal profile may be due to a process of antigen-driven selection. In MS, CD8 T cells may cause axonal damage by the production of perforin, granzymes and cytotoxic cytokines e. g. IL17 (Wang HH et al., 2011), that was originally considered an exclusive product of CD4 (Tzartos JS et al., 2008; Vanden ES et al., 2005). Intriguingly, some CD8 T cell populations may have a protective role, suppressing the production of pro-inflammatory cytokines and the proliferation of autoreactive CD4 T cells (Hu D et al., 2013).

Finally, resident memory CD4 and CD8 T cells (Trm), that originally belong to CNS, could contribute to MS pathogenesis. In normal condition, these cells prevent autoreactivity, i.e. by the expression of the Programmed cell death protein 1 (PD-1) on CD8 cells (Raj T et al., 2014); in MS patients, brain CD8 Trm producing IFNγ and TNFα were found as associated with neuroinflammation (Rasouli J et al., 2015).

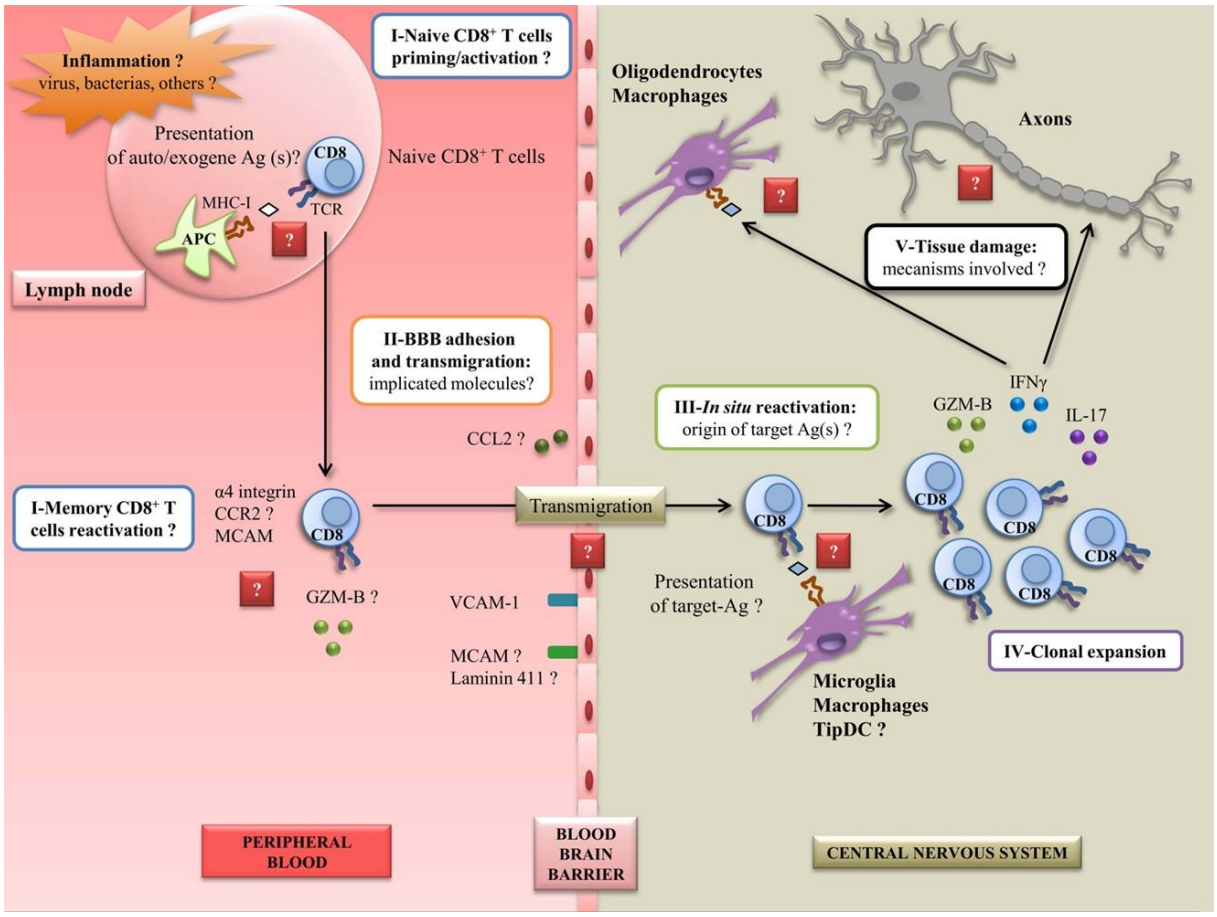

Fig. 11. Overview of possible CD8 autoreactivity mechanisms in MS pathogenesis. The activated CD8 T cells can lead to express several molecules involved in adhesion, migration and cytotoxicity. In condition of inflammation, CD8 T cells migrate across the damaged BBB, reaching the CNS, where they could be reactivated by resident antigen presenting cells (APC) and undergo to clonal expansion (Marion S et al., 2015).

1.1.3.2. T-cell subpopulations: characteristics and role in CNS inflammation

The T lymphocytes compartment consists in two main groups: naïve cells, that have not encountered their antigen (also called "antigen-inexperienced") after the maturation, and memory cells, that have previously encountered the antigen ("antigen-experienced") and are able to react by a fast and strong immune response to a second encounter with the antigen. As reviewed by van den Broek et al. (2018), human naïve T cells express CC-chemokine receptor 7 (CCR7) and CD62 ligand (CD62L or L-selectin) to recirculate between secondary lymphoid organs and peripheral blood. Naïve subpopulation (or "subset") shows a high diversity in TCR repertoire to recognize a great variety of antigens. The recognition of an antigen lead to naïve-cells differentiation

into memory cells. The turnover of naïve cells is controlled by homeostatic factors (i.e. IL7 and self-peptide MHC complexes; Takada K and Jameson SC, 2009) and probably also by epigenetic mechanisms (DNA methylation, histone modifications etc.; Moskowitz DM et al., 2017). Their differentiation and proliferation processes can be accelerated in certain conditions, e. g. in case of lymphopenia (Takada K and Jameson SC, 2009).

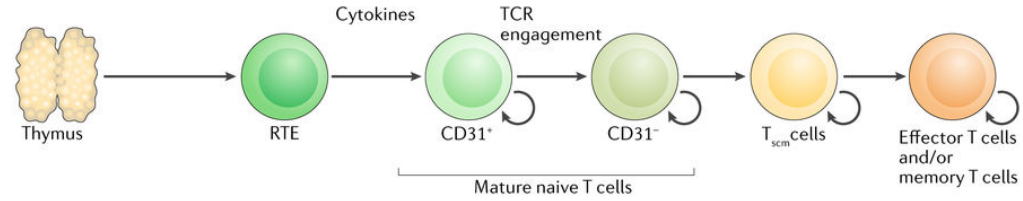

Marker	Relevant T cell subset				
TREC	CD4+, CD8+	++	+	+/–	–
PTK7	CD4+	+	–	–	–
CD31	CD4+	+	+	–	–
CD103	CD8+	+	–	–	–
IL-8	CD4+, CD8+	+	+/–	+/–	–
CR2	CD4+, CD8+	+	+/–	+/–	–
CD25dim	CD4+	–	+/–	+/–	–
CD95 (FAS)	CD4+, CD8+	–	–	–	++
CD122 (IL-2Rβ)	CD4+, CD8+	–	–	–	++
TCR diversity					
Life-span					
Proliferation		+/–	+	+	+++ ++

Fig. 12. Schematic representation of naïve T cells differentiation (van den Broek T et al., 2018).

Human naïve T lymphocytes express CD45RA and not CD45RO. CD45RA is an isoform of CD45, also known as protein tyrosine phosphatase receptor type C (PTPRC), which is an enzyme involved in TCR-signal transduction (Trowbridge IS and Thomas ML., 1994). Naïve CD4 and CD8 cells tend to decrease in number and in TCR diversity with ageing, probably because of the progressive decline of thymus output (Thome, JJ et al., 2016; Murray JM et al., 2003).

Memory T cells result from the encounter between naïve cells and antigens. Next, lymphocytes undergo clonal expansion and then maintain their antigen-specificity over the lifetime of the individual. Memory-cells compartment consists in three main subpopulations: effector memory T cells (Tem), central memory T cells (Tcm) and terminally differentiated Tem cells (Temra); these three subpopulations differ in homing capacity and effector functions (Sallusto F et al., 2004).

Human Tem migrate to inflamed peripheral tissues and exert an immediate effector function. They express CD45RO (and not CD45RA) and, in some cases, CD62L, whereas they have lost the expression of CCR7. Tem CD4 and CD8 cells produce IFN-γ, IL4 and IL5 (Sallusto F et al., 2004). In periphery, Tem are predominantly CD8. Moreover, Tem are particularly abundant in lung, liver and gut. By appropriate stimulation, Tem can rapidly differentiate in Th1 or Th2 phenotype. Upon stimulation, Tem tend to retain their Th1 or Th2 phenotype, demonstrating a certain stability (Messi M et al., 2003). Tem-proliferative capacity lies in the middle between Tcm and Temra and correlates with a different telomere length. Furthermore, Tem cells seem to be more sensitive to upregulation of antiapoptotic molecules compared to Tcm (Son NH et al., 2000).
Human Tcm, as memory cells, express CD45RO, but also CCR7 and CD62L, involved in Tcm ability to extravase through high endothelial venules (HEV) and migrate to secondary lymphoid organs, where they provide immunosurveillance against known pathogens (Gehad A et al., 2018).

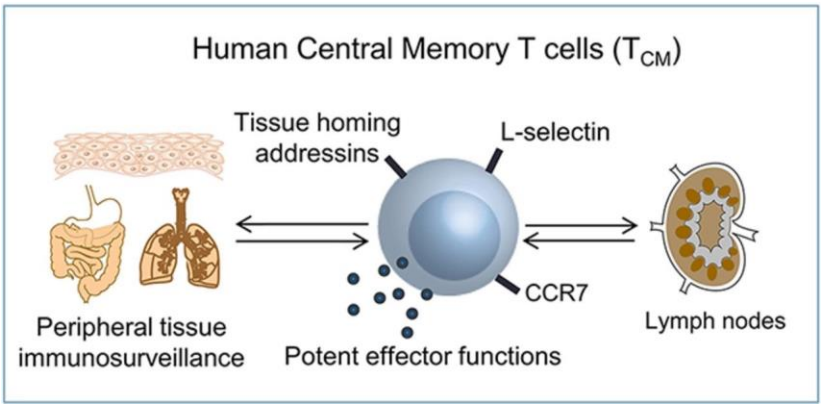

Fig. 13. Illustration of human Tcm cells, characterized by potent effector functions, ability to migrate into peripheral tissue and to guarantee immunosurveillance within lymph nodes (Gehad A et al., 2018).

Within tissue, Tcm are enriched in lymph nodes and tonsils; in periphery, these cells are predominantly CD4 and a sizable proportion of them expresses CXCR5 (CXCL13 receptor) and produces IL2 and IL10 upon activation (Gunn MD et al., 2003). Moreover, Tcm produce mainly IL2 or IFN-γ and IL4 after proliferation and differentiation into effector cells (Sallusto F et al., 2004). Tcm show a higher expansion potential and a decreased telomere length when compared to Tem. Upon stimulation, Tcm possess the ability to differentiate in two directions, going towards a non-effector state under neutral conditions or differentiating into Th1 or Th2 cells in presence of IL12 or IL-4

(Sallusto F et al., 2004), demonstrating to be tendentially more heterogeneous compared to Tem.

Temra cells lack the expression of CCR7, but are CD45RA+ as naïve cells, and are represented in the CD8 T cells compartment. These cells are more differentiated than Tcm and Tem, since they are characterized by a senescent replicative history: in fact, Temra possess shorter telomeres and a high sensitivity to apoptosis (Brenchley JM et al., 2003). Moreover, they have a very low capability to expand compared to Tcm and Tem (Sallusto F et al., 2004), but are also more differentiated than Tcm in terms of effector functions (Willinger T et al., 2005). According to literature, Temra are the 11% of CD8 global cells in peripheral blood of healthy donors, of which the 41% expresses the senescent T cells marker CD57 (Verma K et al., 2017). However, a group of CD57- Temra was identified as characterized by longer telomeres and a higher potential to proliferate compared to CD57+ (Geginat J et al., 2003). The generation and function of Temra cells are still under debate. Since they appear late during the immune response, they may be generated through homeostatic mechanism rather than antigen-dependent pathway (Sallusto F et al., 2004). Moreover, Temra produce large amount of perforin and are mostly CMV-responsive, that suggests their possible role in protection against viral infections and reactivation (Scheinberg P et al., 2009).

In normal conditions, about 150,000 T lymphocytes are present in CSF (Engelhardt B and Ransohoff RM, 2005). They contribute to cells homeostasis and have an important role in immunosurveillance, representing the first defense against opportunistic diseases that can affect CNS in condition of immunosuppression (Ellwardt E et al., 2016). In case of a primary T cell response in the CNS, some effector T cells migrate through parenchymal post-capillary venules and differentiate into tissue-resident memory T cells (Trm) supported by transforming growth factor-β (TGFβ), IL33 and IL15 signalling (Mackay LK et al., 2015). Trm are characterized by self-renewing potential and a high antigen-sensitivity and lack of molecules that mediate egress from tissues such as sphingosine-1-phosphate receptor 1 (S1PR1) and CCR7 (Skon CN et al., 2013).

Tem cells recirculate between CSF and CNS parenchyma via afferent lymphatics and blood, while Tcm recirculate via afferent lymphatics, secondary lymphoid tissue and blood. In human CSF about 90% of T cells are Tcm, while about 10% is represented by Tem (Kivisäkk P et al., 2003). Interestingly, in MS patients CSF appears quite depleted of Tem compared to healthy controls, while they are not altered in peripheral blood,

suggesting that Tem may have moved from CSF to CNS parenchyma driven by an antigen-specific response (Kivisäkk P et al., 2004).

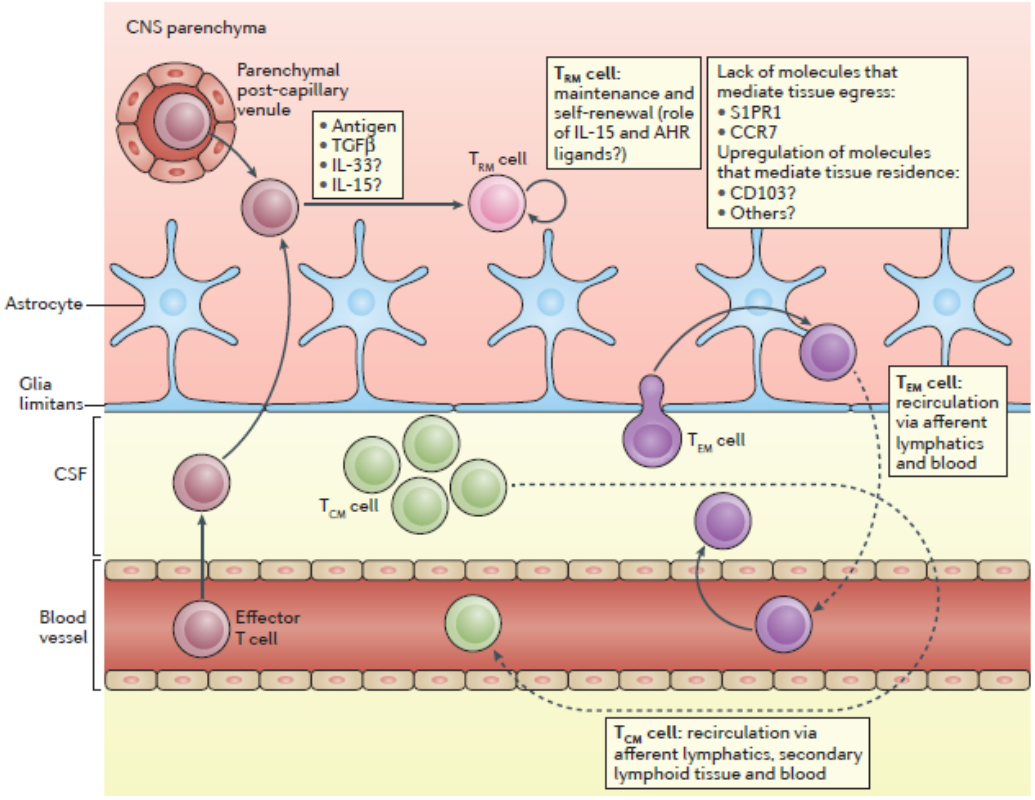

Fig. 14. Immunosurveillance in the CNS by memory T-cell subpopulations. While Trm are retained into CNS parenchyma, Tem and Tcm cells recirculate between blood, CSF and CNS via afferent lymphatics and blood or via afferent lymphatics, secondary lymphoid tissue and blood respectively (Korn T and Kallies A, 2017).

In peripheral blood, the differences among memory T-cell subpopulations in MS patients are less prominent (Nielsen BR et al., 2017). According to literature, the main significant difference in the distribution of Tcm, Tem and Temra CD4 and CD8 cells in MS compared to healthy controls is age-related, due to an accelerated immune senescence (Balint et al., 2013) associated to a reduced thymic output of naïve T cells and an augmented distribution of Temra cells in periphery, especially in patients affected with Primary-Progressive MS (PPMS) (Haegert et al., 2011).

1.1.3.3. B lymphocytes in MS

In MS pathogenesis, B cells are responsible of oligoclonal bands (OCB) production in brain parenchyma and meninges (Owens GP et al., 2003; Serafini B et al., 2004; Magliozzi R et al., 2007; Obermeier B et al., 2011), which are considered a hallmark of MS, since they are present in more than 95% of patients (Freedman MS et al., 2005) and correlate with disease course: OCB negative (OCB-) patients show a slower progression of MS than OCB positive (OCB+) ones (Joseph FG et al., 2009). Furthermore, B cells involvement in the disease pathogenesis takes evidence in the presence of lymphoid follicle-like structures in the cerebral meninges of many MS patients (Magliozzi R et al., 2007) and in the high levels in patients CSF of cytokines and chemokines involved in B cells recruitment, e. g. the chemokine C-X-C motif ligand 13 (CXCL13), correlated with CSF total leukocytes, B cell counts and intrathecal IgG synthesis (Khademi M et al., 2011).

A finding supporting the involvement of B cells in MS is the decrease of Tregs and follicular regulatory T cells (TFR) in MS patients, that may impact on the B cell tolerance development (Dhaeze T et al., 2015). Furthermore, it is known that human naive CD27- B cells can produce immunosuppressive cytokines such as IL-10 upon CD40-ligand stimulation (Correale J and Farez M, 2007) and such response was observed to be abnormal in B cells of MS patients (Duddy ME et al., 2004).

An important evidence of B cells involvement comes from the successful application of anti-CD20 molecules (i.e. rituximab) in MS treatment, that determine the complete depletion of CD20+ B cells and the reduction of RRMS patients experiencing relapses (Khademi M et al., 2011).

1.1.4. Symptoms

The primary cause of MS clinical manifestations is the demyelination, in which the damage of the insulating covers of nerves disrupts the ability of neurons to communicate (Compston A and Coles A, 2002). This results in a wide range of symptoms, including mobility restrictions, visual problems, changes in sensation (pain, hypoesthesia, paresthesia), muscle weakness, spasms, fatigue, bladder and bowel difficulties, cognitive and emotional impairment.

Sensory disturbance is one of the first manifestation of the disease, with paresthesias or dysesthesias, ataxia, vertigo. Optic neuritis is also a typical symptom onset, as well as bladder disfunction, which can lead to frequent episodes of incontinence (Hauser SL et al., 2008). Lhermitte's sign, an electrical sensation down the back during neck's flexion, is another classic finding in MS.

With the progress of the disease many physics and psychological symptoms can appear, mainly a potentially disabling fatigue and chronic pain, intimately linked to emotional problems as anxiety and depression (Amtmann D et al., 2015; Alschuler KN et al., 2013).

1.1.5. Clinical course

Due to its variable pattern, with relapses and/or a progressive neurological deterioration, the clinical course of MS has been not exactly described until the study of Lublin and Reingold in 1996 (recently updated by the International Advisory Committee on Clinical Trials of MS, Lublin FD et al., 2014), who classified four different disease courses (Fig. 15): Relapsing Remitting multiple sclerosis (RRMS), Primary Progressive multiple sclerosis (PPMS), Secondary Progressive multiple sclerosis (SPMS) and Progressive Relapsing multiple sclerosis (PRMS) (Lublin FD and Reingold SC, 1996). Today this classification is routinely applied in clinical practice.

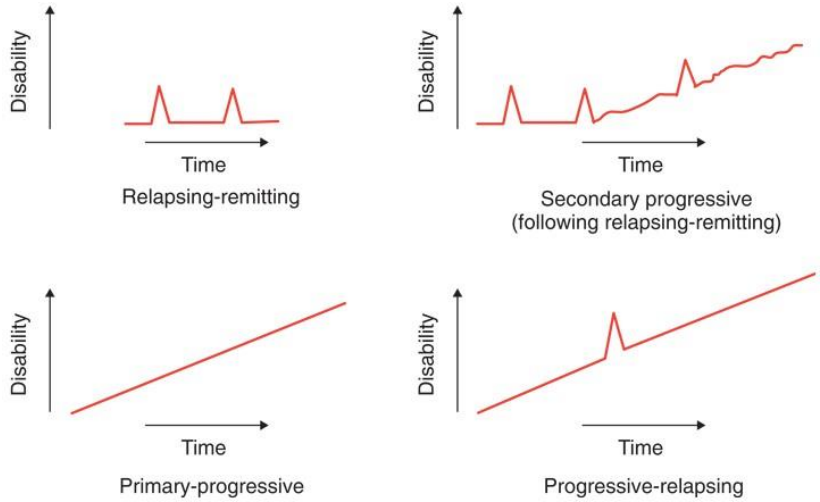

Fig. 15. Illustration of different clinical courses of multiple sclerosis (adaptation from Lublin FD et al., 1996, by Hersh CM and Fox RJ, 2014).

RRMS (80-85% of all MS patients) manifests in acute attacks (also called relapses or

exacerbations) followed by full recovery, that could last months of years, or a residual deficit. Periods between relapses are characterized by a lack of disease progression. RRMS typically occurs in early adulthood and in two decades approximately half of the patients develop SPMS (H. Tremlett, Y. Zhao, and V. Devonshire, "Natural history of secondary-progressive multiple sclerosis," Multiple Sclerosis Journal, vol. 14, no. 3, pp. 314–324, 2008.), which is considered as a long-term outcome of RRSM, characterized by an initial RR form followed by progression of disease with minor remissions or plateaus (Lublin FD and Reingold SC, 1996).

PPMS (10-15% of patients) is characterized by a gradual and continuous neurological decline from onset; the median age of onset for PPMS is 40 years (Koch M et al., 2009). The rarest form of MS (only 5% of patients) is PRSM, characterized by acute relapses separated by a continuous progression of disease.

A certain number of MS patients can be initially diagnosed with clinically isolated syndrome (CIS), whose hallmarks symptoms are optic neuritis, diplopia, bladder and bower dysfunction, ataxia, sensory disfunction (Barten LJ et al., 2010).

MS prognosis may significantly variate: it is usually more unfavorable in patients with optic neuritis, motor involvement and coordination dysfunction rather than patients with visual or sensory symptoms (Barten LJ et al., 2010). The disability level of patients is measured by an Expanded Disability Status Scale (EDSS) that ranges between 0 (no disability) to 10 (death). Anyhow, death due to MS is a quite rare event and life expectants after diagnosis is about 25 years, after that most patients die for other causes (Compston A and Coles A, 2002).

1.1.6. Diagnosis

The clinical evaluation of signs and symptoms, the neuroimaging and laboratory findings contribute to MS diagnosis. McDonald Criteria, dating from 2001 (McDonald WI et al., 2001) and undergone revisions in 2005 (Polman CH et al., 2005), 2010 (Polman CH et al., 2011) and lastly in 2017 (Thompson AJ et al., 2018), include specific guidelines for the diagnostic process, which can be quite complicated for those disease cases that manifest with very nonspecific symptoms. MS diagnosis requires the presence of two or more distinct clinical attacks and two or more inflammatory plaques in myelinated

regions of CNS. The detection of brain and spinal cord lesions by MRI and the analysis of cerebrospinal fluid (CSF) strongly support MS diagnosis. At the time of diagnosis, the disease course must be provisionally indicated and patients must be periodically re-evaluated to update MS phenotype (Thompson AJ et al., 2018).

MRI is the principal technical tool to make a diagnosis of MS. It allows to detect brain and spinal cord lesions and to follow their development and space dissemination during time (Traboulsee AL et al., 2006). The operating principle of MRI is the nuclear magnetic resonance (NMR), a physical phenomenon in which nuclei can absorb and emit an electromagnetic radiation in a magnetic field. The resulting image is constructed by two main parameters, the longitudinal relaxation time (T1) and the transverse relaxation time (T2). T1 “black holes” are hypointense lesions typical of MS patients and indicate severe demyelination and axonal loss. T2-weighted hyperintense lesions ("bright spots") are the prior indication of lesions number, edema and inflammation and patient's disease burden (Katdare A and Ursekar M, 2015).

T2-weighted lesions evaluation can be usefully complemented with gadolinium enhancement and spinal imaging (Miller DH et al., 1998). Gadolinium (Gd) is a chemical agent able to cross the damaged BBB in MS patients. Gd-enhanced MRI scan gives information about the age and the activity of MS lesions and the correlation between a lesion and clinical symptoms, with the eventual detection of "silent" lesions. The ability of Gd to deposit in regions rich of water, e. g. brain lesions, allows the realignment time of magnetization vector of water protons, giving brighter MRI images that reveal CNS damage and spinal cord injury as hyperintense areas. Further contrast agents include myeloperoxidase activity measure in inflamed tissue (Gray E et al., 2008), superparamagnetic iron oxide nanoparticles (SPIONs) (Mahmoudi M et al., 2011) and the contrast agent Gadofluorine M, which selectively accumulates in degenerated nerve fibers and appears on T1-weighted images (Wessig C et al., 2007; Wuerfel E et al., 2010).

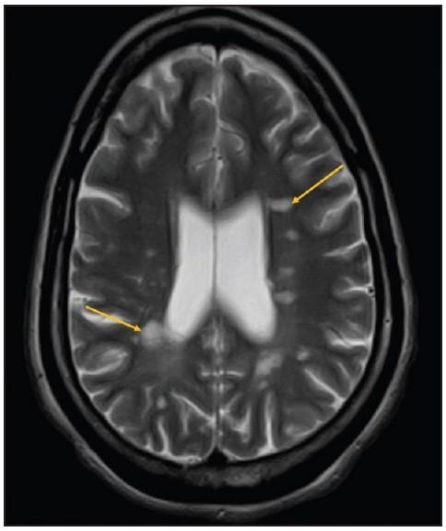

Fig. 16. Brain MRI of an MS patient. Axial T2 image shows hyperintense lesions (yellow arrows) in the periventricular location along bilateral lateral ventricles (Katdare A and Ursekar M, 2015).

The application of MRI confirmed the presence of cortical lesions in MS patients also at early stages, especially in progressive MS forms (Vrenken H et al., 2006). In these patients, cortical lesions are more extended and numerous and their presence, together with cortical atrophy, has been linked to cognitive deficits (Calabrese M et al., 2009).

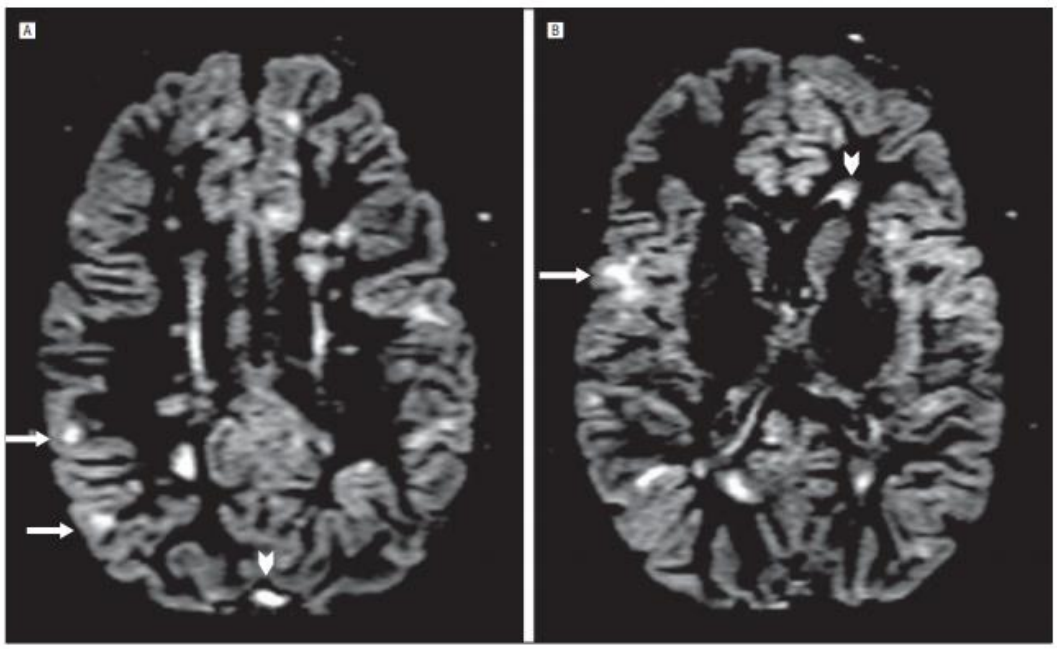

Fig. 17. MRI detection of cortical lesions from 2 MS patients. (A) and (B) report MRI on cortical lesions (arrows) in two RRMS patients. Arrowheads indicate artifacts in (A) and CSF effusion in the periventricular white matter in (B) (Calabrese M et al., 2009).

Despite MRI has notably improved MS diagnosis and understanding, the differential diagnosis with other CNS diseases represents a major challenge. Accumulated findings reported the presence of perivenular lesions in the brain, also called the "central vein sign" (CVS), that are detectable by MRI specifically in MS patients (Sati P et al., 2016; Maggi P et al., 2018). CVS, in fact, appears in a significantly higher percentage of MS patients compared to other neurological disorders (Sinnecker T et al., 2012; Solomon AJ et al., 2015).

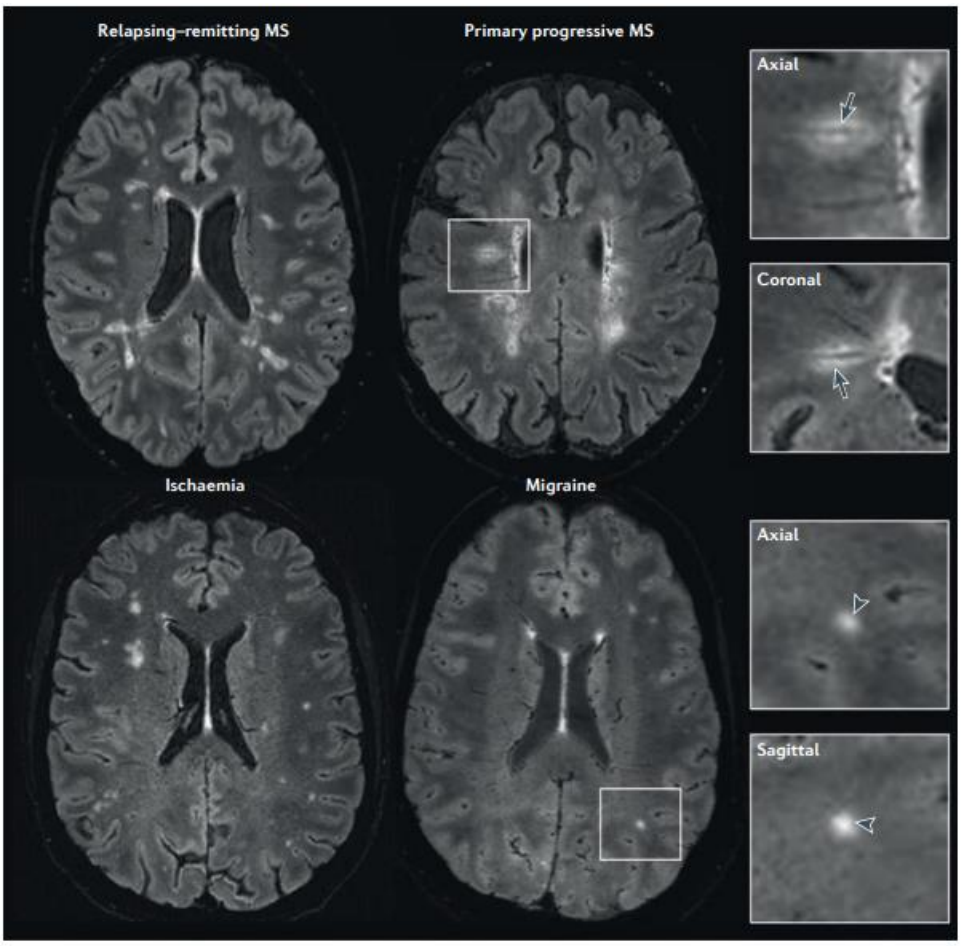

Fig. 18. MRI detection of central vein sign in MS lesions. Figure reports 3T FLAIR* (combined T2*-weighted MRI and fluid-attenuated inversion recovery) MRI detection of brain in one patient with RRMS, one with PPMS, one with ischemia and one with migraine. The dark veins are present centrally in the lesions of MS patients, but not in ischemia and migraine patients. Arrows in magnified panels indicate lesions (Sati P et al., 2016).

An important tool in MS diagnosis is the analysis of CSF, collected from the patients by lumbar puncture. In MS patients, CSF is typically clear and colorless and shows a normal protein and cell counts, even in the acute episodes of the disease. What may be significative in terms of diagnosis are the increased levels of Ig, resulting in the presence

of OCBs, detected by the electrophoresis of CSF immunoglobulins (Lowenthal A et al., 1960; Domingues RB et al., 2017). Immunoglobulin G (IgG) OCBs are found in more than 90% of MS patient, so they are strongly supportive to the diagnosis, and they are usually present in the CSF, but not in serum, where IgG is polyclonal (Weber MS et al., 2011; Winger RC and Zamvil SS, 2016). The maturation of plasma cells from B cells, found as expanded and activated both in CNS lesions and in CSF, contribute to the development of OCBs (Cepok S et al., 2006). The presence of antibodies correlates with the complement activation and the demyelination (Cepok S et al., 2005; Weber MS et al., 2011) and their involvement in the disease is confirmed; some antigens suggested as possible targets might MBP or MOG, as well as infectious agents of oligodendrocyte precursors.

Finally, the evaluation of the response of the brain to electrical stimulation can help to confirm the diagnosis of MS. The slowed nervous conduction due to demyelination is detected by the evoked potential (EP) tests, that consist in the examination of visual and sensory evoked potentials (Walsh P et al., 2005).

1.1.7. Treatments

The landscape of MS treatments has widely expanded in the last decade, although there is no definitive cure for the disease. The main strategies of the current therapies point to relieve symptoms, to stop the progression of disability and to reduce the number of relapses.

The routine approach to handle acute attacks consists in the administration of high doses (500-1000 mg) of intravenous corticosteroids, e. g. methylprednisolone, for 3-5 days. These treatments have been demonstrated to be effective in the short-term, but do not significantly impact on the long-term recovery (Myhr KM and Mellgren SI, 2009). In the advanced stages of the disease, the immune cells infiltrating CNS perpetuate the myelin damage leading to irreversible axonal loss, so the primary target of the long-term therapies is to limit the immune-inflammatory processes that contribute to demyelination and to neuronal degradation (Haines JD et al., 2011). For these purposes, several disease-modifying therapies (DMTs) have been approved by the US Food and Drug Administration (FDA) and the European Medicines Agency (EMA). These treatments reduce the immune-mediated inflammatory process in CNS and lead to an

improvement in clinical and radiologic outcomes; to date, 13 approved DMTs are currently available to treat RRMS worldwide (Pardo G and Jones DE, 2017) and each one targets a different immune pathway and has a different mechanism of action.

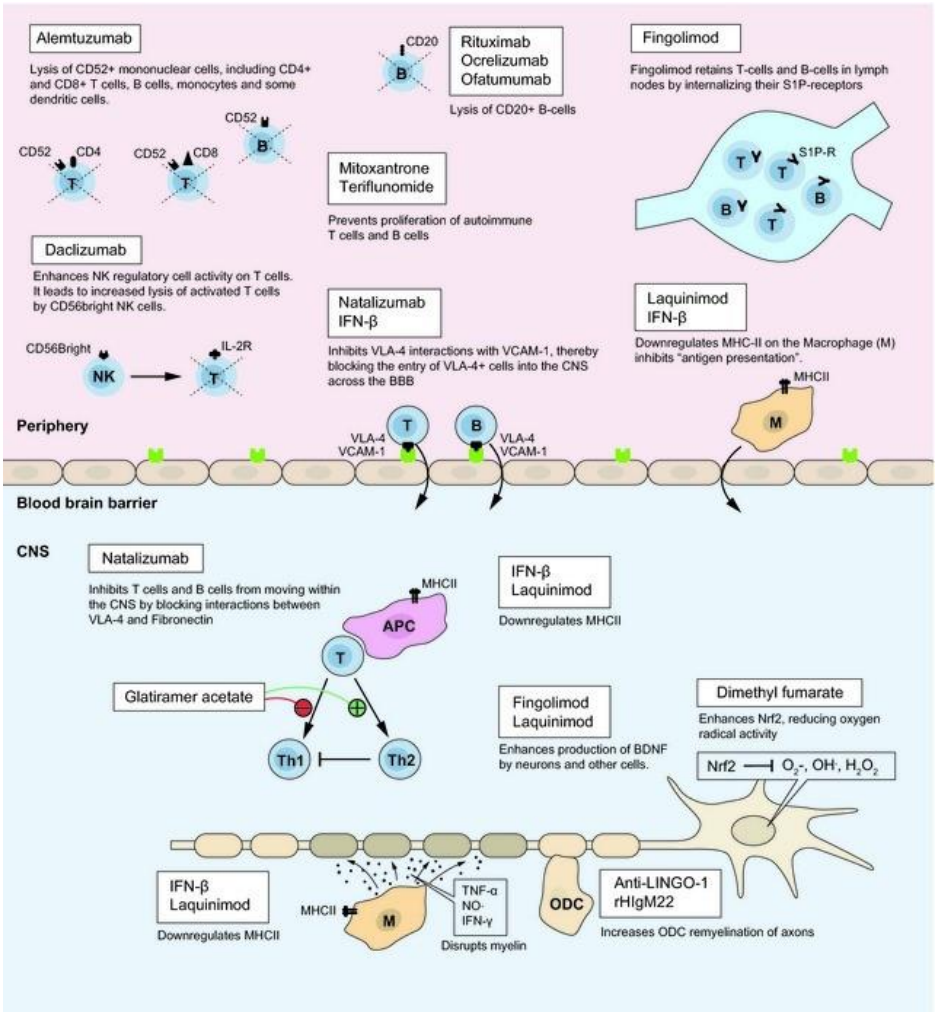

Fig. 19. Illustrated scheme of the sites of therapeutic action of DMTs relatively to MS pathogenesis (Cross AH and Naismith RT, 2014).

Injectable DMTs include β interferons (β-IFNs) and Glatiramer acetate (GA), used in MS treatments over two decades. β-IFNs is administered by subcutaneous or intramuscular injection. Its mechanism of action is still not well known, but it may act reducing T cell adhesion and entrance in CNS across the BBB (Wee Yong V et al., 1998; Compston A and Coles A, 2008). GA is an immunomodulator drug composed of 4 amino-acids (glutamic acid, lysine, alanine and tyrosine) designed to simulate MBP, in order to divert the attack of myelin-autoreactive cells. Also, GA induces a shift from Th1 towards Th2, contributing

to an amelioration of the disease (Arnon R and Aharoni R, 2004).

Fingolimod is an immunomodulating drug approved by the FDA (2010) and EMA (2011) as the first oral DMT for RRMS. It binds the sphingosine-1-phosphate receptor (S1PR) on the surface of naïve and activated lymphocytes, leading to their retention within lymph nodes and preventing their migration towards CNS (Brinkmann V et al., 2010). Notwithstanding its therapeutic potential, patients under Fingolimod must be continuously monitored, because of the eventual side effects (Cohen JA and Chun J, 2011).

Dimethyl fumarate (DMF) is an immunomodulatory drug, orally administered in RRMS patients. The mechanism of action of DMF is not clear, but it has been demonstrated to reduce the progression of disability in patients, probably due to its capacity to enhance endogenous mechanisms that limit oxidative stress (Gold R et al., 2012).

Azathioprine (AZA) is another possible treatment for MS patients who experience frequent relapses. It is an immunosuppressive drug applied to treat different autoimmune disorders; it is a purine synthesis inhibitor, blocking DNA and RNA synthesis with the consequent decreased production of immune cells (Casetta I et al., 2007).

Finally, monoclonal antibodies (mAbs), characterized by high biological potency and selectivity of action (Fontoura P, 2010), represent an interesting and effective alternative from traditional MS treatments.

1.1.7.1. Monoclonal antibodies for MS treatment

The first monoclonal antibody was produced in 1975 by Köhler and Milstein (Köhler G and Milstein C, 1975); later, several mAbs have been approved by FDA in oncology, gastroenterology and transplant rejection prevention (Rommer PS et al., 2014), until the first application in MS treatment with the humanized mAb Natalizumab in 2006.

Monoclonal antibodies are monovalent antibodies deriving from a single B cell clone and therefore able to bind to the same epitope. One of the ways to produce mAbs is the hybridoma technique (Köhler G and Milstein C, 1975), consisting in the fusion of B cells with immortal myeloma cell line lacking the hypoxanthine-guanine-phosphoribosyl transferase (HGPRT) gene. The result of this fusion is the hybridoma cells (or

"hybridomas"), that inherited immortality from the myeloma cells and selective-resistance from the B cells, becoming the only cell population able to survive *in vitro* in a selective medium containing hypoxanthine-aminopterin-thymidine (HAT). After the selection, each clone is separated by dilution into different culture wells. Then, the secreted antibodies from the different clones can be assayed for their ability to bind to the antigen and stored for future use. During time, the efficacy of mAbs has gradually improved, especially with the genetically engineering of the Fc region, that increased the mAbs bioavailability (Wang W et al., 2008), for example by treating the antibody fragments with polyethylene glycol (PEG) to increase mAbs plasma half-life (Kuo TT et al., 2011). mAbs have a specific nomenclature (International Nonproprietary Names (INNs), 1997; United States Adopted Names (USAN) Council, 2007) recently revised in 2017 (World Health Organization (WHO), 2017). The stem -mab is official for monoclonal antibodies. The substem preceding the stem is referred to the animal source of the antibody (-o- for mouse; -e- for hamsters, -i- for primates and -a- for rats). Regarding the composition of antibodies, the nomenclature is the following: -xi- for chimeric antibodies (where the constant region is replaced with the human form); -zu- for humanized antibodies in which the variable regions is substituted; -xizu- for partly chimeric and partly humanized antibodies; -u- for purely human antibodies; -axo- for trifunctional antibodies, where rat/mouse hybrid antibodies are engineered with binding sites for two different antigens (Lordick F et al., 2008). Furthermore, the antibody's target is also indicated in its name: examples are "-lim-" which is referred to immune system (i.e. Natalizumab or Daclizumab) or "-tum" for miscellaneous (i.e. Rituximab or Alemtuzumab).

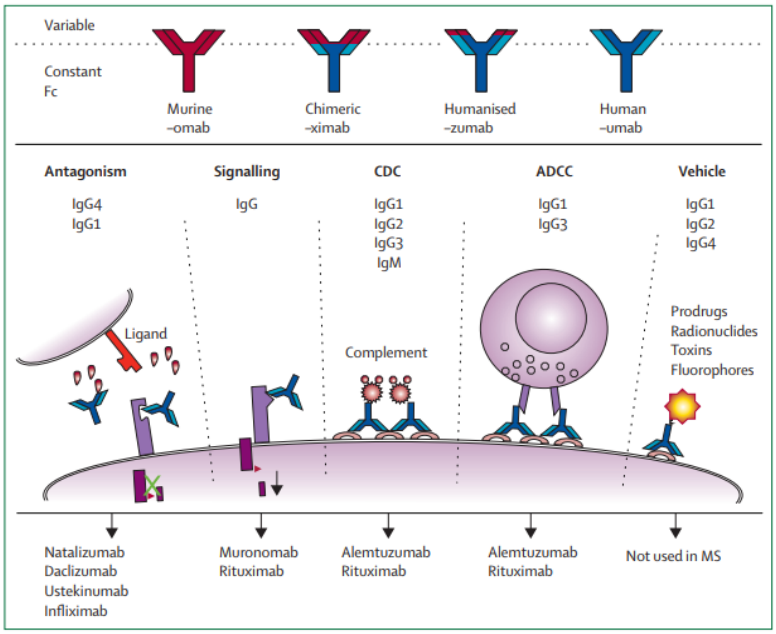

Fig. 20. Example of mAbs tested for MS treatment with their possible effector functions (Lutterotti A and Martin R, 2008).

To date, several mAbs are approved as successful MS treatment:

- Alemtuzumab (Campath®, MabCampath®, Lemtrada®) is a humanized mAb directed against CD52, a glycoprotein expressed on the surface of mature lymphocytes, but not on lymphoid stem cells. This mAb has been definitively approved by FDA for MS treatment in 2014, but is also used in other diseases (e.g. chronic lymphocytic leukemia: CLL). Alemtuzumab causes the depletion of CD52+ cells by Antibody-Dependent Cell-Mediated Cytotoxicity (ADCC) and Complement Dependent Cytotoxicity (CDC), leading to a marked leucopenia (Lutterotti A and Martin R, 2008). Intriguingly, this lymphocytes depletion is not associated with an increased risk of infections (Simpson BS and Coles AJ, 2007). RRMS patients treated with Alemtuzumab showed a reduction in relapses and an improvement in disability (Coles AJ, 2007); however, it may cause several side effects, such as pyrexia, headache, malaise and rash (Lutterotti A and Martin R, 2008).

- Rituximab (Rituxan®) is a chimeric mAb which binds the protein CD20, expressed by B lymphocytes, leading to cell apoptosis by ADCC and CDC (Waubant E, 2008). Its use is approved for non-Hodgkin's lymphoma, rheumatoid arthritis (RA), CLL and other diseases, whereas in MS it is used off-label to treat difficult cases (Tony HP et al., 2011). MS patients tested with Rituximab in a Phase II trials had a reduction in Gd-enhancing lesions (Naismith RT et al., 2010) and a delayed disease progression (Hawker K et al., 2009). Potential side effects of Rituximab include severe infusion reactions, nausea,

headache and urinary and respiratory tract infections (Bar-Or A et al., 2008).

- Ocrelizumab (Ocrevus®) is a humanized mAb which targets CD20, similarly to rituximab, leading to a depletion of B cells and of CD20+ T cells (that are 5% of total blood T cells) (Palanichamy A et al., 2014). It has been approved by FDA for MS in 2017. Ocrelizumab showed beneficial effects in RRMS and PPMS patients (Montalban X et al., 2017). Despite the promising results, further Phase IV clinical trials are required to state if the mAb is safe and effective.

Lastly, one of most effective mAbs and also the first one approved by FDA for MS treatment is Natalizumab (ref. par. 4), which has been also an interesting object of debate about its effects on immune cells balance and T-cell receptor.

1.2. T-cell receptor

1.2.1. Structure and function

TCR is the molecule expressed on the surface of T lymphocytes, responsible of the recognition of the antigen bound to MHC molecules. The structure of TCR is heterodimeric, consisting in two protein chains, mostly (95% in humans) an α and a β chain ($\alpha\beta$ TCR) or, in a minority (5% in humans) a γ and δ chains ($\gamma\delta$ TCR). Chains α and β are encoded by TRA and TRB genes, while γ and δ chains are encoded by TRG and TRD. TCR is anchored to the plasmatic membrane and is associated with two accessory molecules, the invariant CD3 and ζ-chain, that form the TCR complex.

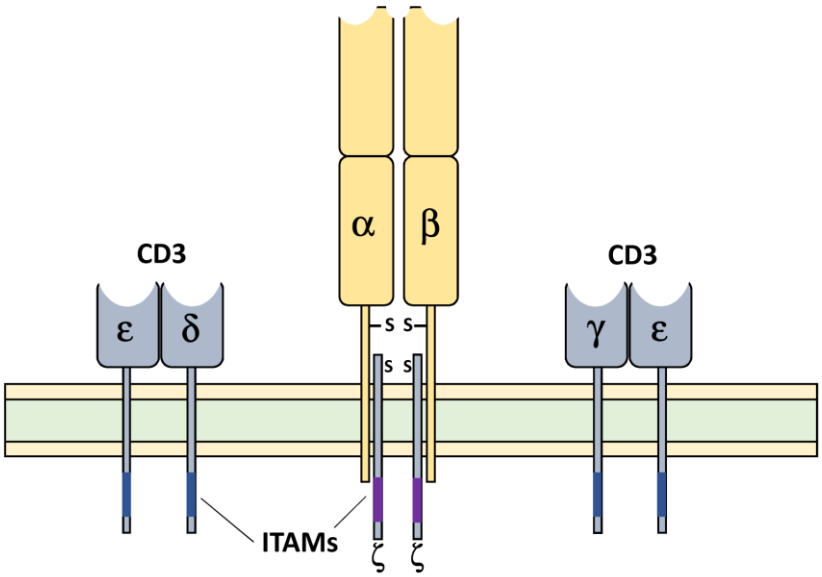

Fig. 21. Schematic illustration of TCR complex. TCR is composed by an αβ or a γδ chain complex, an intracellular portion composed of the Immunoreceptor tyrosine-based activation motif (ITAM) and an extracellular portion to detect peptide antigens presented by MHC complex.

The cluster of differentiation 3 (CD3) is a co-receptor involved in lymphocytes activation and belongs to immunoglobulin superfamily. It is a protein complex formed, in mammals, by a CD3γ chain, a CD3δ chain and two CD3ε chains. CD3 contains aspartate residues, that are negatively charged and allow the association to the cell membrane, which is positively charged. ζ chain is also inserted in the plasmatic membrane, but it protrudes mostly in the intracellular space. Both CD3 and ζ chains contain a conserved motif on their intracellular tails, which is called Immunoreceptor tyrosine-based activation motif (ITAM), essential for TCR signaling. ζ chain contains 3 ITAM motifs. The phosphorylation of the ITAM determines the binding of CD3 with the zeta associated protein 70 (ZAP70), a kinase that initiates the signaling cascade of T cell. The other two principal TCR co-receptors are CD4 (Th cells) and CD8 (CTL).

Each TCR chain is composed by two extracellular regions: the variable (V) and constant (C) domains. The variable domain of α and β chain has three hypervariable regions, the complementarity determining regions (CDRs): CDR1, CDR2 and CDR3, that are non-consecutively arranged on the amino acid sequence of both the 2 variable domains of TCR (for a total of 6 CDRs for receptor). The first two (CDR1 and CDR2) are fully encoded in the genome, while the third (CDR3) is generated somatically, indeed its

notably great variability lays at the basis for the ability of TCR to recognize a great variety of antigens (Lemke H, 2018).

The constant domain of the TCR is composed by a short sequence with a cysteine residue that forms disulfide bonds, linking the two chains.

1.2.2. T-cell receptor V(D)J recombination

TCR results from V(D)J recombination, a process that takes place during the early stages of T maturation, in thymus or bone marrow respectively, and it results in the highly diverse repertoire of Igs and TCR. V(D)J rearrangement is a unique mechanism of somatic recombination and a fundamental feature of adaptive immune system. This mechanism allows to potentially create between 10^{15} and 10^{20} TCR clonotypes, where a clonotype is a population of T cells carrying the same TCR (Nikolich-Zugich J et al., 2004), and a high TCR diversity has been associated with an effective control of viral infections and other pathogens, which is the fundament of a competent immune system (Laydon DJ et al., 2015).

TCR is composed by an α-chain and a β-chain and its genes are similar to Igs, containing multiple V, D and J gene segments for β-chain and V and J for α-chain.

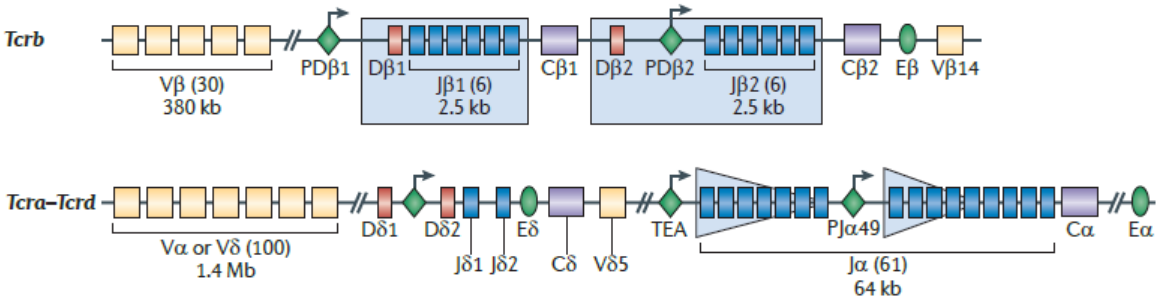

Fig. 22. TCR genes. The T-cell receptor β-chain (Tcrb) and Tcra–Tcrd loci (adapted from Schatz DG and Ji Y, 2011).

V(D)J recombination is a complex mechanism that involves several molecular "actors", which the key ones are: the recombination activating genes 1 and 2 (RAG1, RAG2), the terminal deoxynucleotidyl transferase (TdT), the Artemis nuclease and the non-homologous end joining (NHEJ) DNA repair factors.

RAG recombinases initiate the process. RAG1 and RAG2 contain important regulatory domains and are mainly responsible of DNA binding and cleavage (Schatz DG and Ji Y,

2011). They form a complex which recognizes and binds the DNA at specific sequences, the recombination signal sequences (RSSs). These sequences flank the V, D and J gene segments and consist in conserved heptamers and nonamers (CACAGTG and ACAAAAACC, respectively) separated by a space region of 12 or 23 base pairs (12 and 23RSS).

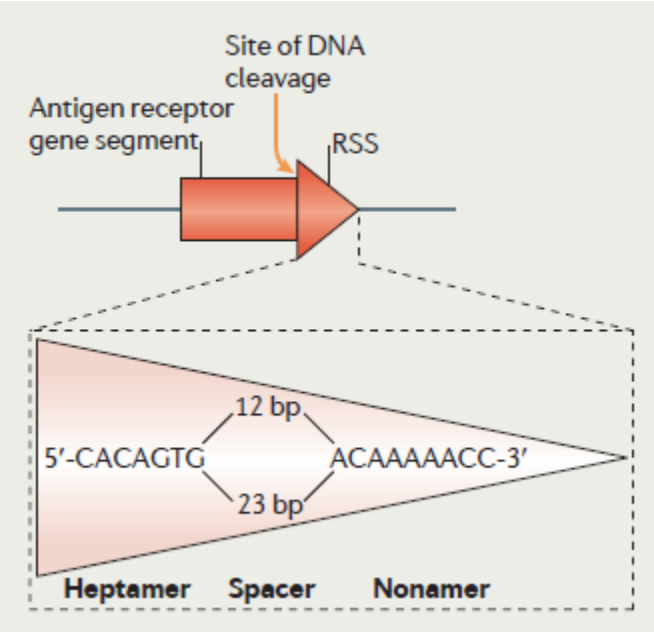

Fig. 23. The recombination signal sequence. RSS is adjacent to antigen receptor gene segment and contains the heptamer and the nonamer, separated by a conserved spacer region of 12 or 23 base pairs. The nonamer acts anchoring the RAG proteins to the DNA, whereas the heptamer enhances this binding and specifies the site of DNA cleavage (Schatz DG and Ji Y, 2011).

Recombination preferentially occurs between a 12 and a 23RSS, a mechanism called the "12/23 rule" (van Gent DC et al., 1996). First, the RAG complex binds to one RSS, generating a signal which is necessary to capture the second RSS and forming the so called synaptic or paired complex (Mundy CL et al., 2002). The next step is DNA cleavage: RAG introduces a single strand nick between the heptamer and the gene segment, generating a 3' hydroxyl group and a 5' phosphate group on the same strand. The 3' hydroxyl group attacks the other strand creating a DNA double strand break or "hairpin". Another group of proteins, the high-mobility group protein B1 and B2 (HMGB1, HMGB2), have been observed as contributing to DNA cleavage *in vitro*, but their role has yet to be proven *in vivo* (Swanson PC, 2004).

A DNA-dependent protein kinase, DNA-PK, binds to each broken DNA end and recruits other proteins such as Artemis, the main one involved in the opening of the coding end

hairpins (Ma Y et al., 2005). This step is so crucial for V(D)J recombination that Artemis-deficient mice develop a severe combined immunodeficiency (SCID) associated with defects in opening and joining V(D)J coding hairpins (Rooney S et al., 2002).

In most cases, hairpins are "off-center" opened, resulting in extra bases remaining on one strand that are palindromic (P) nucleotides. Then, RAG proteins cooperate with NHEJ DNA repair factor to rejoin the DNA ends, that undergo a random non-templated (N) nucleotide addition by TdT and nucleotide loss before being joined.

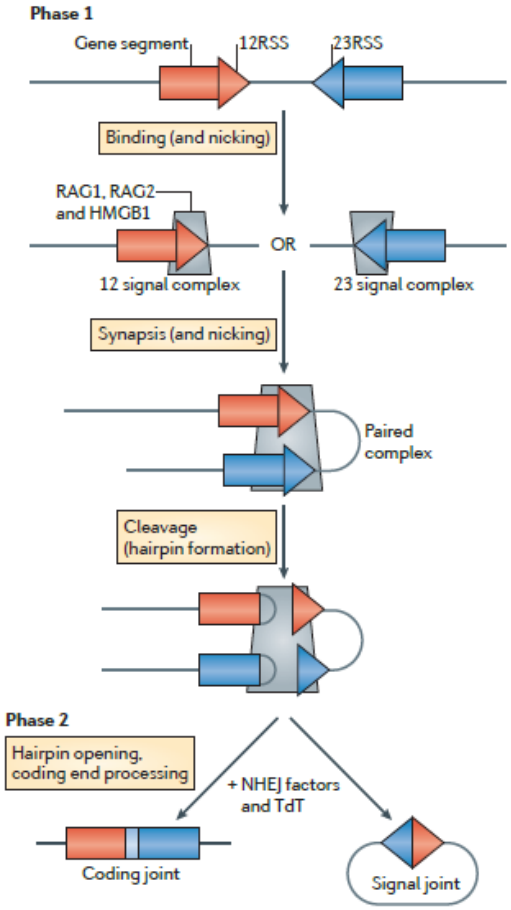

Fig. 24. V(D)J recombination steps grouped in two phases. Phase 1: DNA cleavage by RAG complex with the formation of hairpin. Phase 2: hairpin opening and nucleotides addition (adapted from Schatz DG and Ji Y, 2011).

In the process of TCR generation, first the β-chain is formed by the D-to-J recombination, in which Dβ1 or Dβ2 gene segment joins one of six Jβ1 segments (Abbas AKK, 2015). This event is followed with Vβ-to-DβJβ rearrangement. The α-chain recombination is driven by V-to-J rearrangement like Ig light chains, with the formation of a VJ complex and then the addition of the constant chain gene.

Since V(D)J recombination is a complex molecular event, its main regulation mechanism

resides in chromatin state (Schatz DG and Ji Y, 2011): the permissive or repressive chromatin structure can affect the phase of DNA cleavage. It has been observed that wrapping an RSS around a nucleosome inhibits the DNA binding or cleavage by RAG proteins (McBlane F and Boyes J, 2000; Kwon J et al., 2000). On the other hand, the removal of N-terminal histone tails by specific protease (Golding A et al., 1999) or the action of ATP-dependent chromatin remodeling complexes, e. g. the SWI-SNF ATPase complex, allows DNA cleavage by RAG (Kwon J et al., 2000). The presence of transcriptional control elements, such as enhancers and promotors, has a primary role in RSSs accessibility for recombination. Histone acetyltransferases (HATs), histone methylases and chromatin remodeling complexes, promote histone modifications and RNA polymerase II activity (Li B et al., 2007). The proposed mechanisms involved in RSSs accessibility are mainly three: histone acetylation, which weakens the association between histones and DNA (Shogren-Knaak M et al., 2006), the chromatin remodeling, which liberates RSSs from nucleosome (Zhang Y et al., 2006), and the transcriptional elongation by RNA polymerase II through RSSs (Zhang Y et al., 2006). Moreover, the recombining locus must be far from repressive chromatin compartments, such as the pericentric heterochromatin, and must undergo a structural alteration (compaction or looping) to make possible the separation between gene segments and then their encounter during rearrangement (Jhunjhunwala S et al., 2009).

1.2.3. Methods of investigation of the T-cell receptor

1.2.3.1. CDR3 spectratyping and flow cytometry

The variability and high-responsiveness of the adaptive immune system of vertebrates lies in the highly diverse recombination process that constitutes the individual TCR repertoire. For this reason, the investigation of the TCR repertoire on a sequence level allows us to gain insight in the characteristics of our immune system: immunotolerance, post-treatment immune reconstitution, disease pathogenesis, T-cell contribution in disease development and progress and immune senescence are only few examples of topics that can be explored through the analysis of the TCR repertoire. Most of the published literature on TCR focuses on the CDR3 region, because of its high variability

and antigen-specificity.

The first studies on the TCR repertoire were performed by the "spectratyping" technology, which gives information about the CDR3 length distribution within a functional TCRBV family from a complex cell population. Briefly, the analysis begins from complementary DNA (cDNA) obtained and amplified by several rounds of polymerase chain reaction (PCR) on messenger RNA (mRNA) isolated from a given cell population. In order to amplify the CDR3 region, the technology takes advantage of a set of nested fluorescently labelled primers that are specific for several TCRBV families. Finally, the PCR products are visualized on denaturing polyacrylamide sequencing gel. Results appear as a gaussian distribution of peaks of different areas, depending on the CDR3 length distribution in the observed TCRBV families; the areas of peaks can be analyzed quantitatively with an appropriated, automated DNA sequencing software (Currier JR and Robinson MA, 2001). Since different cell clones are represented by different sequences, the CDR3 length distribution can be considered as a measure of the TCR repertoire diversity (Kepler T et al., 2005). However, even though spectratyping gives good-quality information about the pattern of distribution and the size of CDR3 sequences within a certain TCRBV family, it does not provide any data about the sequence. Furthermore, it is hard to determine how much the results are representative of the entire examined T-cell repertoire (Ciupe SM et al., 2013).

Despite limited, spectratyping analysis allowed the first investigations of the murine (Pannetier C et al., 1993) and human TCR repertoire (Gorski J et al., 1994). To date, spectratyping is not used anymore for the analysis of big and complex TCR-sequence datasets, but it can still be a complement in diagnostic and clinical studies to identify TCR restrictions and to characterize complex T-cell populations from biological specimens.

Later, TCR repertoire has been analyzed by flow cytometry, using TCRBV-specific fluorescent monoclonal antibodies. This methodology helps to determine the oligo- or polyclonality of a cell population and has been used as support to the diagnosis and the understanding of hematological diseases such as leukemias, EBV-induced mononucleosis or HIV infection (Beck RC et al., 2003). Similarly to spectratyping, flow cytometry on TCR provides information only on the Vβ usage of the analyzed T-cell population. Furthermore, the interpretation of results may be challenging, since some

TCR repertoire variations might go undetected and the Vβ usage within a certain T-cell population, especially in low-frequency-expressed TCRVB families, could be underestimated (van der Geest KS et al., 2015).

1.2.3.2. Next-generation sequencing and computational immunology

The study of the TCR repertoire has been completely revolutionized with the advent of Next-Generation Sequencing (NGS) or High-Throughput Sequencing (HTS), commercially launched in 2005. NGS is based on the massive parallel sequencing by using platforms suited to obtain from 1 million to 43 billion short reads per run. The main difference from Sanger sequencing, indeed, is that the last one provides the electrophoretic separation of products from only individual sequencing reactions (Voelkerding KV et al., 2009).

The most common NGS platforms are Roche 454 and Illumina. The two platforms are generally comparable, with some differences in performance and technical aspects. Roche 454 is based on the utilization of ATP sulfurylase and luciferase (pyrosequencing): every time the enzyme DNA polymerase incorporates a nucleotide, a pyrophosphate is released, generating an amount of light which is proportional to the number of incorporated nucleotides. Furthermore, Roche 454 usually provides higher read lengths (400 bases for Roche 454 GS FLX versus 36 bases for Illumina Genome Analyzer) and has a shorter sequencing run time (10 hours for Roche 454 GS FLX, 2.5 days for Illumina Genome Analyzer), but Illumina can provide 1.5 Gb of total bases for run versus 500 Mb of Roche 454 (Voelkerding KV et al., 2009; Luo C et al., 2012). Furthermore, Roche 454 utilizes spherical microbeads for the sequencing process: each DNA fragment is ligated to a bead and undergoes PCR amplification.

On the other hand, Illumina is based on reversible dye-terminators, that identify single bases when they are introduced into DNA strands. The first step is the "tagmentation", in which transposases cut DNA into short segments called "tags". Then, adapters, primer bindings sites and terminal sites are added at the strand ends. The "bridge amplification" phase is performed into an acrylamide-coated glass flow cell, where each flow cell has oligonucleotides that hold the DNA strands. DNA polymerase creates the complementary strands and the original ones are washed away from the flow cell, then a forward strand (which will be identical to the first one) is made from the reversed one.

Then each single strand is clonally amplified several times. At the end, the flow cell is washed and only the forward strands are left. By using primers, polymerase and reversible terminators, fluorescently tagged nucleotides are added to strands and, finally, the machine records the added base.

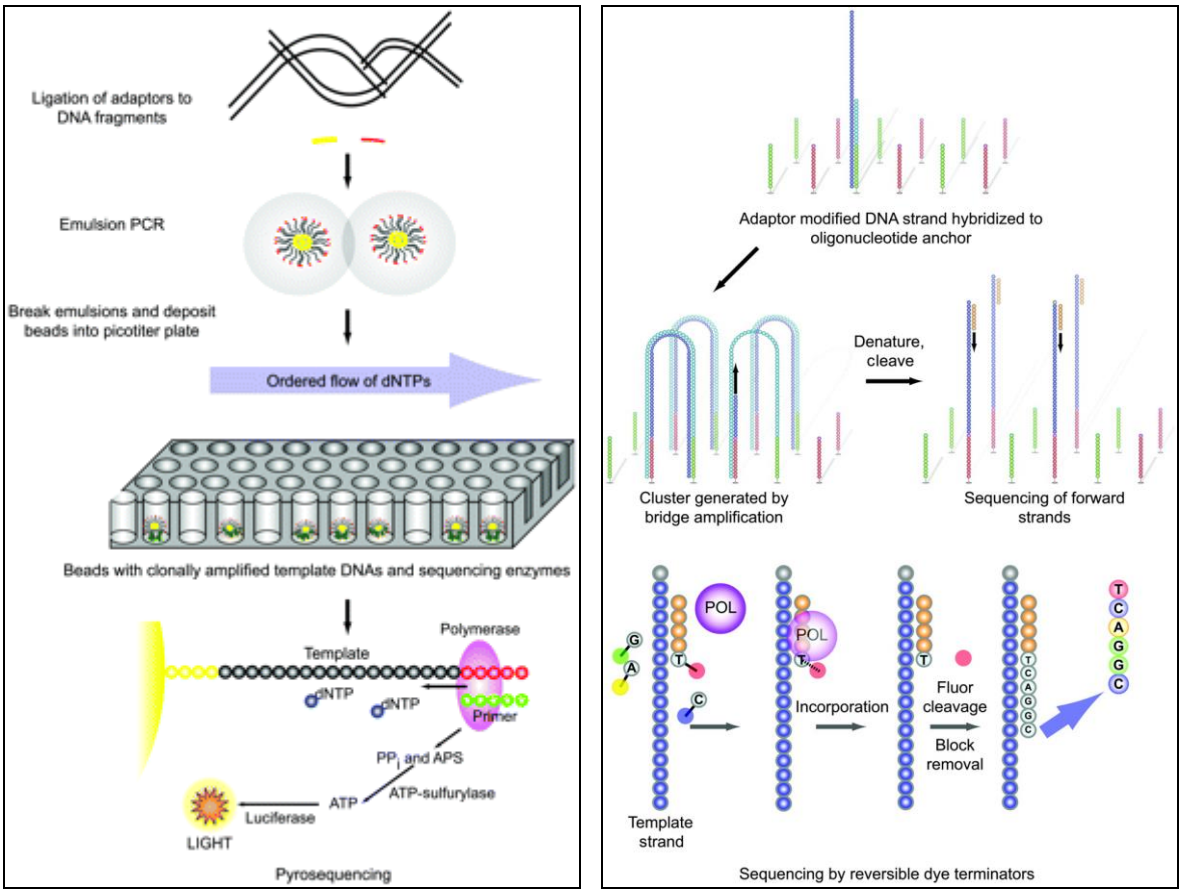

Fig. 25. Roche 454 and Illumina. Illustrated scheme of Roche 454 (left) and Illumina (right) sequencing technology (Voelkerding KV et al., 2009).

With the advent of NGS, the amount and the complexity of sequencing data has increased rapidly, along with the urge to adopt the right method of investigation in order to cover a deeper and more complex sequencing depth.

Computational immunology and Machine Learning (ML), based on the development of statistical models that are applied through the computer systems, enabled the analysis of high-dimensional sequencing data. ML aims to identify recurrent and/or specific patterns in TCR/BCR repertoires, in order to characterize the data and to detect features that differ or are shared across repertoires and, in general, to make possible the use of molecular data for the explanation of biological phenomenon through a rigorous and

specific statistical approach.

Greiff V et al. from 2015 reported an exhaustive review of the main bioinformatic and statistical methodologies that have been applied to the analysis of immune repertoires (Greiff V et al., 2015). As reviewed by authors, the main challenges encountered in the application of ML to the study of immune repertoires are: (i) the minimization of errors; (ii) the definition of clonality and (iii) the data visualization.

To minimize errors (i), the use of unique molecular identifiers (UMIs) or barcodes, that are degenerated and highly diverse nucleotides that tag DNA or RNA during library preparation, is very useful for error correction. Also the switch from Illumina MiSeq to HiSeq platform and increasing RNA input from ng to μg (Greiff V et al., 2015) have greatly improved the process of repertoires sequencing. Furthermore, a frequent problem during the characterization of a repertoire is the underestimation of its diversity, mainly due to sample size variation and PCR errors. As reviewed in Miho E et al., several groups suggested the use of diversity index estimators to overcome this problem (Miho E et al., 2018): Laydon DJ et al. elaborated a method called "DivE" to estimate the total repertoire size through the evaluation of species richness composition within a dataset (Laydon DJ et al., 2015). Kaplinsky J and Arnaout R developed a maximum likelihood (ML) algorithm called "Recon" (that stays for "reconstruction of estimated clones from observed maximum"), which can estimate species richness and also the global diversity within a repertoire (Kaplinsky J and Arnaout R, 2016).

The concept of clonality (ii) is a fundamental point when discussing the interpretation of HTS data. In fact, while it is broadly accepted in immunology that a population of identical immune cells is clonal, the definition of what a "clone" is when analyzing CDR3 sequences from a certain repertoire is hard to state, given the fact that errors can occur during several steps of the process (PCR, library preparation…), leading to redundant results or missing others. To date, a "clonotype" is considered as the result of clustering sequences with high CDR3 homology and V/J gene usage (Hershberg U and Prak ETL, 2015). The diversity in a set of clonotypes can be calculated by appropriated diversity indices, that provide a parameterization of repertoires making possible a comparison between different datasets (Miho E et al., 2018). The Hill-Diversity equation is generally used to calculate the diversity (^{q}D) of a repertoire based on Species Richness (SR):

$$^{q}D = \left(\sum_{i=1}^{SR} f_i^{q}\right)^{\frac{1}{1-q}},$$

where f_i is the frequency of the *i*th clone in a given TCR dataset (ref. Materials and methods, par. 8.11.2).

Shannon-Entropy, which provides the measurement of the grade of entropy, or diversity, based on the sequence-composition in a repertoire:

$$\text{Shannon-Entropy} = -\Sigma\, f_i\, log\, f_i,$$

where f_i is the frequency of the *i*th clone in a given TCR dataset. More recently, Shannon-Evenness, instead of Shannon-Entropy, has been proposed as a reliable measure of TCR diversity, and is calculated as follows:

$$\text{Shannon-Evenness} = exp(-\Sigma\, f_i\, log\, f_i)/SR$$

Shannon-Evenness is the quotient of the exponential of the Shannon entropy and SR (Greiff V et al., 2017). Shannon-Evenness, rather than Shannon-Entropy, simplifies the comparison of the diversity between different repertoires because its value is normalized in a range between 0 and 1: Shannon-Evenness is 1 if all clones in a repertoire have the same frequency or it converges to 0 if very few clones dominate in the repertoire.

Finally, the data visualization (iii) has made huge progresses in the last years, mainly thanks to ML. Venn diagrams were firstly adopted to represent sequence overlap between repertoires and public clones (Jackson KJ et al., 2014; Krzywinski M et al., 2009). However, this representation does not consent to visualize the overlap with a high number (>10) of datasets.

A major step in HTS data visualization has been made with the elaboration of clone "networks". A clone network consists of connections between similar and/or identical clones within a repertoire, when connections (or "edges") are made between clones differing for a certain number (in most cases only 1) of amino acids. Clone networks provide an overview of the repertoire architecture in healthy individuals or during disease and/or treatment, capturing the antigen recognition breadth and the abundance of clones within a repertoire. To date, clone networks can be built using several dedicated R packages such as igraph (Csardi G and Nepusz T) and the Cytoscape software (Shannon P et al., 2003).

Repertoire architecture can be also investigated on a subsequence level. The study of Bürckert J-P et al. reports an interesting method of gene expression analysis, called

DESeq2, that helped to identify overrepresented CDR3 sequences in different groups of immunized rats that match with previously documented sequences associated with tetanus toxoid and measles (Bürckert JP et al., 2017). A further methodology to analyze subsequences composition across repertoires consists in the decomposition of sequences in "k-mers", that are amino acid subsequences of length "k" (see Materials and methods, ref. par. 8.11.3). This kind of analysis is a promising tool to identify common patterns in sequence rearrangement across different repertoires and to build sequence prediction profiles. In 2017, Greiff V et al. developed a ML approach based on CDR3 sequence decomposition into k-mers of length 3 (k=3), that enabled them to predict whether a clone was public or private with 80% accuracy in both humans and mice repertoire (Greiff V et al., 2017). In the same year, Apeltsin L et al. reported an algorithm (the "Haystack Heuristic") able to detect disease-associated motifs from immune repertoires discriminating between healthy and disease individuals (Apeltsin L et al., 2017). All these findings suggest that ML represents a valid tool to the study of immune repertoires, that may be able to shed light on unrevealed features of the immune system in both health and disease.

1.2.4. The investigation of the T-cell receptor repertoire in disease

Once established how the TCR is generated and how T cells are selected after the interaction with MHC molecules, researchers raised the hypothesis that the molecular characterization of TCR through the sequencing of the CDR3 region during disease may address important insights about the pathogenesis of diseases.

In cancer, the analysis of how the TCR repertoire variates between affected and healthy people helped to elucidate what is the role of the adaptive immune system in such diseases characterized by a pathogenesis that is not exclusively immunological. In particular, the individuation of specific and shared sequences in the TCR repertoires of patients, for example, may support the identification of possible biomarkers to diagnosis a disease or to predict the clinical outcome of a disease and/or a treatment, which is in fact one of the main aims of the bioinformatic investigation of the TCR repertoire.

In this direction, some very recent studies characterized the TCR repertoire in cancer. A

2019 study on TCR repertoire of tumor-infiltrating lymphocytes (TIL) in primary pancreatic cancer reported an extensive sequence overlap between TCR repertoires of TIL from different regions of the same tumor in 5 patients, showing that this overlap was not found with the same extent in the peripheral blood (Cui C et al., 2019). In the same year, Simnica D et al. reported a TCR repertoire investigation in more than 300 individuals, including healthy and cancer (hematological or solid) patients, showing that cancer patients were characterized by a less diverse TCR repertoire compared to healthy individuals; furthermore, they found that the TCR repertoire underwent a process of reconstitution after chemotherapy (Simnica D et al., 2019). These results match with other findings in several types of cancer: Liu YY et al. found a less diverse TCR repertoire in advanced lung cancer patients that reflected a worse immune status compared to healthy controls (Liu YY et al. 2019) and Cui JH et al. detected a substantial difference in TCR repertoire diversity between patients with cervical cancer and healthy women, with a lower diversity in affected patients (Cui JH et al., 2018).

On the same line, the sequencing of the TCR repertoire in autoimmune diseases showed a biased TCR rearrangement, linked to an altered balance in immunotolerance, and disease-specific, abnormal characteristics of the TCR repertoire that were not found in healthy individuals. In Systemic Lupus Erythematosus (SLE), an autoimmune, rheumatological and systemic disease, there are some contradictory results: Yu J et al. found a narrowed TCR repertoire, reflecting a skewed capacity of the TCR in recognizing antigens (Yu J et al., 2017), whereas another study did not report any significant variation in the TCR repertoire in SLE patients (Thapa DR et al., 2015). Nevertheless, some findings indicate a biased TCR rearrangement in SLE, with some dominant, recurrent TCR sequences in several patients, suggesting that those sequences may have a role in SLE pathogenesis (Sui W et al. 2015).

TCR repertoire has been studied also in other autoimmune diseases, such as Rheumatoid Arthritis (RA), Type 1 Diabetes Mellitus (T1DM), Crohn's disease (CD), ulcerative colitis (UC) and MS. In RA, where the immune system attacks self-antigens associated to the synovium, several studies indicated a skewed TCR repertoire in patients and a high overlap between TCR sequences within the joints and in the peripheral blood, which may suggest that the abnormal expansion of some T-cell clones could depend on the response to some specific autoantigens within the synovium (Klarenbeek PL et al., 2012; Chini L et al., 2002). Similar findings were reported for

T1DM, where a narrowed TCR repertoire with some islet tissue-specific clones were found (Marrero I et al., 2013). A recent, interesting HTS study in type 1 diabetes reported a shortened CDR3 sequence in the TCR repertoire of patients, that authors suggest may be linked to the development autoreactive T-cell clones that escape the selection in the thymus, increasing the risk to develop the disease (Gomez-Tourino I et al., 2017).
In autoimmune disorders of the intestine there are some interesting findings: a high TCR repertoire diversity was found in UC patients, while a reduced one in the intestine of CD patients (Günaltay S et al., 2017; Doorenspleet ME et al., 2017), but the link with the pathogenesis of these diseases is still not clear and further insights in larger cohorts are required.

In MS, the TCR repertoire was first investigated by spectratyping, detecting a skewed TCR repertoire in terms of CDR3 length distribution within different TRVB families (Laplaud DA et al., 2004) and the TCR clonal expansion in CD8 T-cell clones in brain lesions (Babbe H et al., 2000) as well as in CSF and blood (Skulina C et al., 2004). Nevertheless, most of our knowledge about the TCR repertoire characterization in MS owes much to the advent of HTS, that provided a detailed sequence analysis of the TCR repertoire in brain lesions, CSF and peripheral blood of patients. The main recent findings include the study of Lossius A et al., who characterized the TCR repertoire and the EBV-reactivity in CSF and blood of MS patients compared to patients with other inflammatory neurological diseases (OINDs). Authors detected expanded T-cell clones in both compartments, although they differed between CSF and blood. Furthermore, EBV-reactive TCR sequences in CD8 cells were enriched in CSF of MS patients compared to the control group (Lossius A et al., 2014). In a study from 2015, Salou M et al. found predominant CD8 T-cell clones shared between CSF, brain lesions and peripheral blood of 3 MS patients (Salou M et al., 2015).
In 2018, Planas R et al. identified some shared and clonally expanded TCR sequences among white matter lesions and peripheral blood of MS patients, especially in the CD8 cell compartment (Planas R et al., 2018) In the same year, Jelcic I et al. detected an autoproliferative T-cell subpopulation in peripheral CD4 Th1 cells of MS patients that may sustain B cell survival through T-B interaction in the pathogenesis of the disease; furthermore, authors also indicated a protein, RAS guanyl-releasing protein 2

(RASGRP2), expressed in the brain of patients, as a possible antigen target of this population (Jelcic I et al., 2018). Recently, a comparison between the TCR repertoire of MS patients and patients with a chronic neurological disorder, the HTLV-I-associated myelopathy/tropical spastic paraparesis (HAM/TSP), showed that MS patients were characterized by a higher TCR repertoire diversity compared to HAM/TSP and, interestingly, a cluster of sequences was exclusively shared within a subgroup of MS patients, suggesting the presence of a molecular signature that specifically characterizes MS (Alves Sousa AP et al., 2019).

Taken together, these results highlight how complex MS is, with a pathogenesis which involves many different cell types and a high variability across individuals, and that the investigation of the TCR repertoire represents a promising tool to gain insight the different aspects of the disease that, to date, remain elusive.

1.3. Natalizumab

1.3.1. Definition and history

Natalizumab (Tysabri®, Biogen Idec, Cambridge, MA, USA) is a humanized monoclonal antibody directed against the integrin α4β1 (also known as Very Late Antigen 4: VLA-4 or CD49d) and is the first mAb in a class of DMTs that are selective adhesion molecule (SAM) inhibitors (Léger OJ et al., 1997).

After the approval in 2004 by FDA, Natalizumab was withdrawn by Biogen Idec and Elan from the US market because three patients developed a rare and dangerous neurological disease, the progressive multifocal leukoencephalopathy (PML) (ref. par. 4.5), while treated with Natalizumab in combination with IFN-β-1a (Chaudhuri A, 2006). Subsequently, Natalizumab was reviewed as safe and returned to the US market in 2006. Despite further documented cases of PML in the following years, the drug was not withdrawn again because its clinical benefits outweigh the risks. However, the monoclonal antibody is not a first-line choice, but a second-line drug for patients who failed other treatments, e. g. IFN and glatiramer acetate (Brandstadter R and Katz Sand I, 2017). To date, Natalizumab is approved for RRMS treatment.

1.3.2. Mechanism of action

The α4β1 integrin VLA-4 (or CD49d) is an adhesion molecule expressed at high levels on the surface of all leukocytes except neutrophils (Elices MJ et al., 1990). VLA-4 interacts with the vascular cell adhesion molecule-1 (VCAM-1) expressed by the endothelial cells on the lumen of blood vessels at active MS lesions level (Carlos TM et al 1990). This interaction is necessary for leukocyte adhesion and migration across the BBB into the CNS (Lobb RR and Hemler ME, 1994). Natalizumab binds to α4β1 integrin blocking the interaction with VCAM-1 and, consequently, the migration of immune cells into the CNS, preventing the formation of lesions (Rudick and Sandrock 2004).

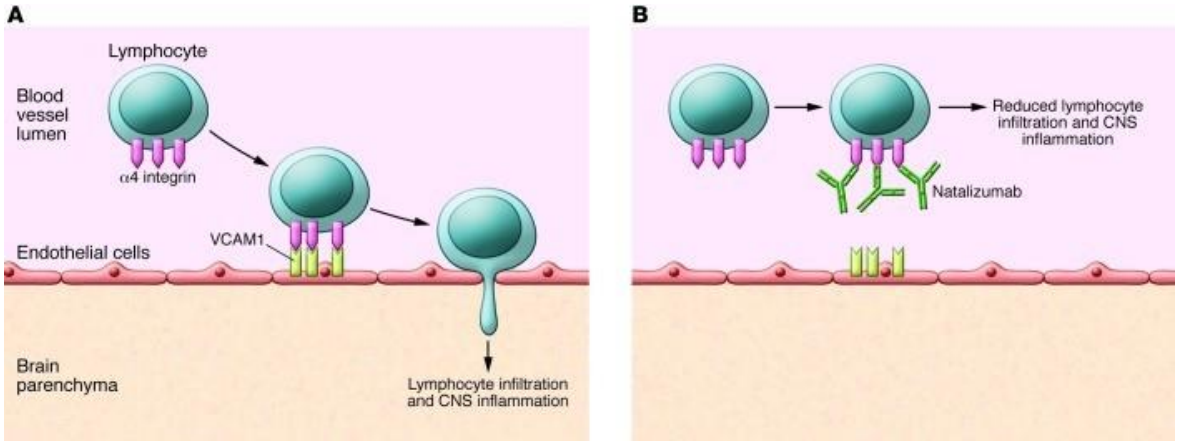

Fig. 26. Mechanism of action of Natalizumab. (A) α4 integrin binds to VCAM1 and gives lymphocytes access to the CNS. (B) Natalizumab blocks binding of lymphocytes to VCAM-1 preventing lymphocyte entry into the CNS (Steinman L, 2015).

The whole process of VLA-4 blocking by Natalizumab is not yet fully clear. The inhibition of T cells migration into CNS is confirmed by multiple evidences that report an increase in peripheral T lymphocytes count (Kivisäkk P et al., 2009; Iannetta M et al., 2016) and a downregulation of CD49d on T cells surface (Kimura K et al., 2016; Iannetta M et al., 2016); the proposed mechanism behind those effects could be the VLA-4 internalization and degradation within the cell. Also, the observed increase in cytokines production after a prolonged administration of Natalizumab suggests that the monoclonal antibody exerts effects on cell signaling (Benkert TF et al., 2012).

1.3.3. Preclinical and clinical studies

The successful *in vivo* administration of α4β1 antibodies in EAE mice, resulting in the reduction of clinical signs and inflammation (Yednock TA et al., 1992), paved the way towards the development of humanized antibodies directed against adhesion molecules. An early clinical trial in 1996-1998 on 35 patients reported a significant reduction in the number of lesions after 12 weeks of Natalizumab therapy (Tubridy N et al., 1999). Few years later, Miller DH et al. performed a placebo-controlled and double-blinded study on 70 MS patients, reporting a decrease of 90% in new active lesions compared to placebo after 6 months of Natalizumab (3 or 6 mg/kg) (Miller DH et al., 2003). In the phase III trial by The Natalizumab Safety and Efficacy in Relapsing-Remitting Multiple Sclerosis (AFFIRM), treated RRMS patients (n=942) showed a decrease of 67% in relapse rate and a reduction of 50% in the accumulation of disability (Polman CH et al., 2006). Concerning MRI evidences, Natalizumab reduced the number of T2-hyperintense lesions by 83%, gadolinium-enhancing lesions by 92% and T1-hypointense lesions by 76% (Miller DH et al., 2007). Natalizumab demonstrated to be effective on RRMS also in combination with other treatments such as IFN-β-1a, reducing the number of lesions over a 2-year trial (Radue EW et al., 2010). Given the effectiveness of the therapy in RRMS, the Clinical Study of the Efficacy of Natalizumab on Reducing Disability Progression in Participants With Secondary Progressive Multiple Sclerosis (ASCEND in SPMS) trial was performed on 439 SPMS patients treated with 300 mg of Natalizumab once a month for up to 96 weeks (Steiner D, 2016). Unfortunately, there was no significant difference between treated patients and placebo group after 2 years of therapy; to date, Natalizumab is still considered not effective for SPMS treatment.

1.3.4. Adverse effects

Natalizumab is administered at a dose of 300 mg, intravenously, every 4 weeks. The most common side effects are nausea, headache, pharyngitis, urinary tract infections, myalgia, depression, diarrhea (Biogen, 2016). The AFFIRM study reports a 5% of patients experiencing hypersensitivity reactions and a 0.8% of severe reactions (i.e. anaphylactic shock) (Philips J et al., 2006). Some viral infections (*H. zoster, H. simplex*) may be slightly more frequent during treatment (Ransohoff R, 2007). To date, the main

dangerous adverse effect due to the monoclonal antibody is represented by PML, which could be potentially fatal.

1.3.5. Progressive Multifocal Leukoencephalopathy

The first 3 cases of PML under Natalizumab were reported in 2005, followed first by the withdrawn of the drug (Kleinschmidt-DeMasters BK and Tyler KL, 2005; Yousry TA, et al., 2006), then by a reintroduction after a safety long-term report by Tysabri Global Observational Program in Safety Study (TYGRIS-US).

PML is a neurological disorder caused by the reactivation of the John Cunningham virus (JCV), that damages the white matter multifocally leading to oligodendrocytes death (Kean JM et al., 2009). Despite 50%-70% of the population encounters JCV during lifetime with no clinical consequences (Ferenczy MW et al., 2012), in some people the virus develops neurotropism and causes PML in concomitance with a condition of immunosuppression (Mancuso R et al., 2012): during Natalizumab, the sequestration of T cells in periphery could lead to an impaired immunosurveillance within CNS promoting viral reactivation, but the mechanism is still under debate (Warnke C et al., 2010). MRI analysis in PML patients reveals subcortical lesions commonly in the frontal lobe (48%) followed by the occipital (20%), the parietal (12%), the temporal (10%) and cerebellum (10%) (Richert N et al., 2012). The most common clinical signs are seizures, cognitive deterioration, impairment in speech and visual and psychiatric manifestations. The risk to develop PML is strongly connected to JCV positivity and, moreover, it is higher in men compared to women and increases with age (Bloomgren G et al., 2012). From clinical studies, the overall risk to develop PML was calculated of 3.87 cases per 1000 JCV-positive patients that underwent immunosuppressive treatments before Natalizumab, with a greatest risk after more than 2 years of treatment (Bozic C et al., 2012). Given the bad prognosis of PML, Natalizumab patients must be periodically checked for the presence of serum anti-JCV antibodies or JCV activity in blood, urine or CSF by JCV-DNA PCR detection. Usually, JCV tests are repeated every 6 months, accompanied by MRI at least once a year in JCV-negative patients and every 6 months in case of JCV-positivity (Brandstadter R and Katz Sand I, 2017). The occurrence of JCV positivity requires the interruption of Natalizumab, warding off the risk of PML but, unfortunately, exposing the patient to a possible bad MS relapse (Tan I et al., 2011).

1.3.6. Immune-reconstitution Inflammatory Syndrome

In patients developing PML, Natalizumab discontinuation is necessary. The cessation of the therapy rehabilitates the autoreactive cells to migrate into the CNS, leading to a phenomenon called Immune-reconstitution Inflammatory Syndrome (IRIS), that consists in a reactivation of the disease that could be even worse than the pre-treatment condition (Sorensen PS et al., 2014). MS relapses appear in few months after Natalizumab interruption, with a peak at 4-7 months (O'Connor PW et al., 2011). Many possible solutions have been proposed to avoid IRIS, e. g. the administration of corticosteroids as a bridge-treatment after the monoclonal antibody cessation but, to date, there is still no agreement about the issue. Recently, the successful application of the autologous hematopoietic stem cell transplantation (AHSCT) to previously Natalizumab-treated RRMS patients has been proposed as a possible strategy to overcome this problem (Mariottini A et al., 2018).

1.4. Autologous hematopoietic stem cell transplantation

1.4.1. Definition and history

The hematopoietic stem cell transplantation (HSCT) was firstly applied as a treatment for hematopoietic system disorders, i.e. hematologic malignancies, until its successful test for autoimmune diseases and metabolic disorders (Henig I and Zuckerman T, 2014). The first bone marrow transfusion was performed on a patient affected with aplastic anemia in 1939 (Osgood EE et al., 1939). Two types of HSCT are: the allogeneic transplant, where the patient receives the infusion of stem cells derived from HLA-matching donor, and the AHSCT, based on using the patient's own stem cells, with the main advantage of no needing to identify a potential donor and a lower probability to develop graft-versus-host disease (GVHD). After phase II and III trials, AHSCT has been approved for RRMS treatment.

1.4.2. Procedure and mechanism of action

AHSCT consists in four steps: 1) mobilization, 2) harvesting, 3) ablative conditioning and 4) transplantation. During the mobilization, the patient is administered with granulocyte colony-stimulating factor (G-CSF) and cyclophosphamide (2-4 g/m^2) to facilitate the aspiration of CD34+ HSCs from the posterior iliac crests of bone marrow (BM) under anesthesia (Saccardi R and Gualandi F, 2008). In the second step, HSCs are harvested from peripheral blood by leukapheresis. Then, the ablation of immune system (or phase of "conditioning regimen") is achieved by high-dose chemotherapy or chemoradiotherapy, bringing to a transient BM aplasia. In this phase, patients are usually treated with chemotherapeutic agents such as BEAM (a combination of bis-chloroethyl nitrosourea (BCNU), etoposide, cytosine arabinoside (ARA-C) and melphalan) and antithymocyte globulin (ATG) to deplete T cells. Finally, HSCs previously cryopreserved and stored are intravenously infused to the patient. During the post-transplantation recovery, antibiotic and antiviral prophylaxis protects the patients from infections. Mobilization, harvesting and conditioning usually cover the first 2-4 weeks of the process; the post-transplantation phase can last 2-3 weeks (Muraro PA et al., 2017).

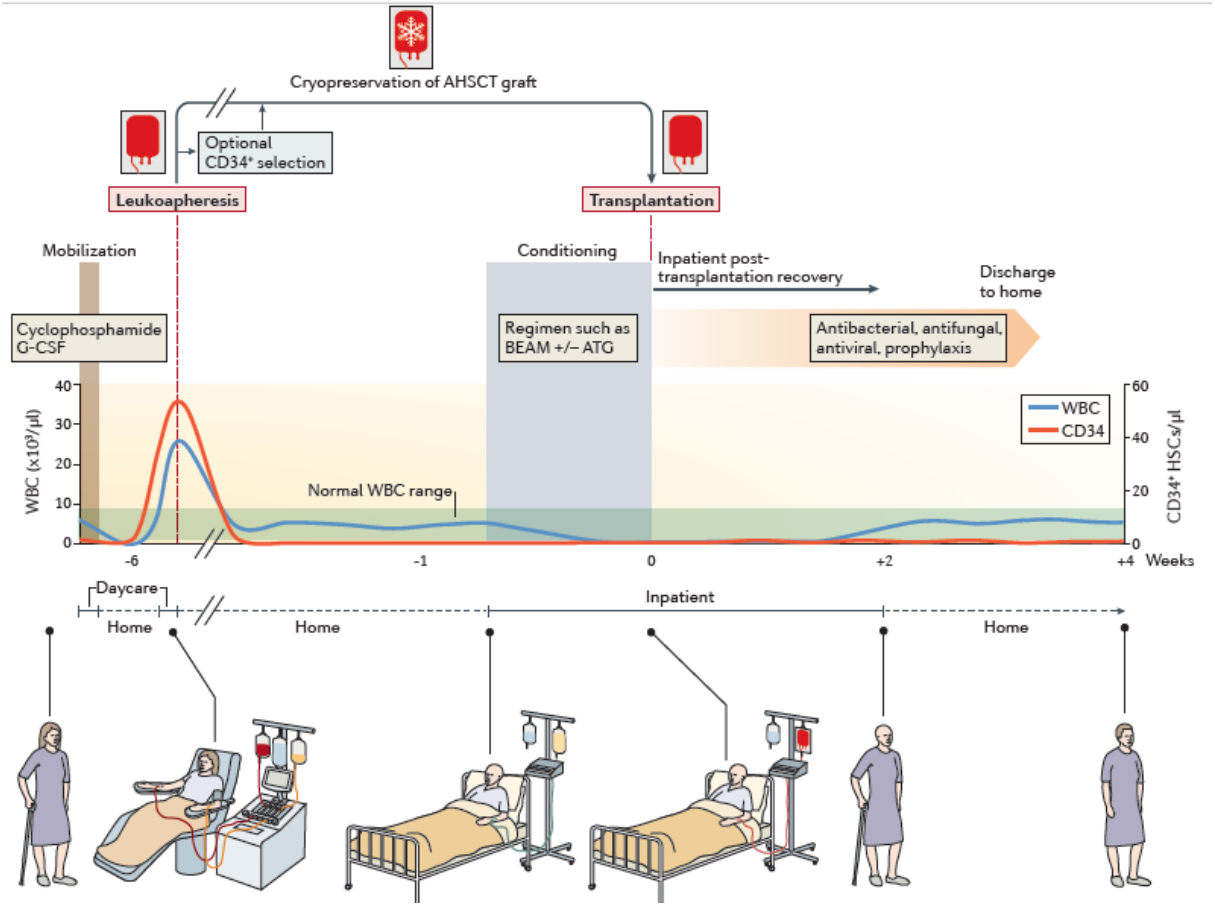

Fig. 27. AHSCT procedure. Figure reports a schematic illustration of AHSCT procedure (Muraro PA et al., 2017). The first phase is the mobilization of CD34+ HSCs with G-CSF and cyclophosphamide, followed by leukapheresis. The conditioning regimen (BEAM, ATG etc.) leads to the ablation of immune cells. Then, patient's own stem cells are re-infused to repopulate the immune system. Finally, the patient goes through the post-transplantation recovery under antibiotic and antiviral prophylaxis. The whole procedure takes approximately 4 weeks.

AHSCT acts depleting autoreactive cells and repopulating the immune system of the patient from stem cells with a reset of the immune system and the restoration of immunotolerance. The process of reconstitution is gradual: natural killer (NK) cells, CD8 T cells and B cells are the first that repopulate the immune system (6 months from the transplantation), followed by CD4 T cells, whose development requires up to 2 years (Saccardi R et al., 2005). Immune ablation induces lymphopenia-induced cell proliferation: in the first 1-2 years after the transplantation, thymopoiesis produces new T cells that undergo TCR rearrangement and, in parallel, naïve B cells are restored (Muraro PA et al., 2017). After 2 years from AHSCT, also gene expression of tolerance is normalized; furthermore, it has been described an increased expression of regulatory factors such as FOXP3 and FOXO1 (Arruda LCM et al., 2015).

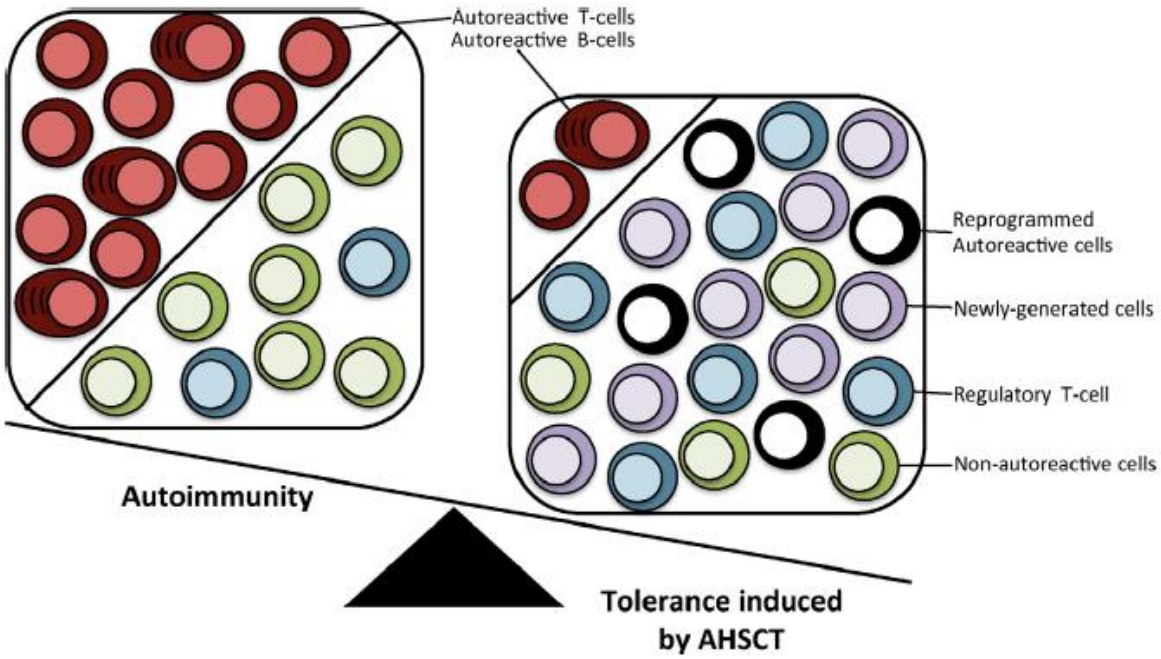

Fig. 28. Proposed mechanism for immunotolerance reconstitution after AHSCT. AHSCT leads to the depletion of autoreactive T and B cells, reprogramming of the autoimmune and pro-inflammatory profile together with the generation of new thymic-derived naïve cells and the expansion of regulatory T lymphocytes (Arruda LCM et al., 2016).

1.4.3. Preclinical and clinical studies

HSCT was tested on animals with "spontaneous" (genetic etiology) or "induced" (by adjuvants) autoimmune disorders, showing that normal mice could develop the disease when transferred with BM transplantation from mice with both forms of autoimmune diseases, and particularly quickly when sustained by a genetic background (Denman AM et al., 1969; Morton JI and Siegel BV, 1974). Further studies confirmed this effect performing allogeneic or autologous HSCT in animal models of several autoimmune diseases, such as experimental allergic encephalomyelitis and myasthenia gravis (Knaan-Shanzer S et al., 1991).

The largest study on MS patients is the EBMT-CIBMTR (European Group for Blood and Marrow Transplantation-Center for International Blood & Marrow Transplant Research) study, with 281 patients receiving AHSCT for different forms of MS in the period 1995-2006 (Muraro PA et al., 2015). This study showed that half of patients survived to the treatment and, during the first 1 year after the transplantation, 52% of RRMS and 31% of patients with progressive MS experienced neurological improvements.

In a phase II trial of 3 years, the HALT-MS study tested AHSCT in 24 RRMS patients (Nash RA et al., 2015): after 3 years, 86.3% of patients were free from relapses and 90.9% did not experience any worsening disability; moreover, young age and RRMS diagnosis were demonstrated as supportive of a good treatment-outcome. Another large study included 123 RRMS and 28 SPMS (Burt RK et al., 2015) and reported a proportion of relapse-free patients of 80% (4 years after AHSCT), with the improvement of disability in 64% of RRMS. In parallel, a significant improvement in EDSS was documented. To date, about 800 MS patients have been successfully treated with AHSCT (Sormani MP et al., 2017).

1.4.4. Adverse effects

The risk to develop adverse effects after AHSCT is mainly linked to the intensity of the conditioning regimen (type and dose of the chemotherapeutic agents), along with comorbidities and age of the patient (Muraro PA et al., 2017). Today, to minimize that risk, a low-intensity regimen is preferred. Nevertheless, secondary to the immunosuppression, it is possible to develop infections, fever, viral reactivations and neurological toxicity (Saccardi R et al., 2006). Further adverse effects are frequent urinary infections, the Uhtoff phenomenon, limb spasticity, alopecia and amenorrhea (Atkins H and Freedman M, 2009). Concerning late adverse effects (months or years after the transplantation), two EBMT Registry analyses report an incidence of secondary autoimmune diseases of 3.6% and 6.4% (Saccardi R et al., 2006; Daikeler T et al., 2011), while a study by the CIBMTR reports a 3.2% of patients developing malignancies (Muraro PA et al., 2017).

Concerning post-transplant mortality, on 281 MS patients Saccardi R et al. documented a treatment-related mortality lower than 2.8% and a positive correlation between a higher risk of death and a higher EDSS score (Saccardi R et al, 2006). Recent meta-analyses reported a post-AHSCT mortality of 2.1% (764 patients, 15 different studies) (Sormani MP et al., 2017) and 3.58% (732 patients, 18 different studies) (Ge F et al., 2019).

1.5. Impact of MS treatments on T-cell subpopulations and T-cell receptor

MS treatments impact on T-cell subpopulations and TCR in different ways, depending on their mechanism of actions. Fingolimod, that retains T cells within lymph nodes, determines a reduction of the total lymphocytes count in the periphery, especially of CCR7+ naïve and memory T cells; these effects manifest in the early phases of treatment (within 1 month) (Teniente-Serra A et al., 2016). Intriguingly, in the same paper, Teniente-Serra A et al. documented an increased percentage of late CD4 Tem cells in responder patients compared to non-responder. Contrarily, naïve, memory and regulatory T lymphocytes that not recirculate between lymphoid tissues and blood are less affected in total counts (Hunter SF et al., 2016) and were found increased in number after 12 months of Fingolimod (Claes N et al., 2014). Fingolimod also interferes with TCR-dependent T cells activation, reducing the release of IL-2 and IFN-γ from activated T cells (Baer L et al., 2018). Furthermore, MS patients showed the presence of TCR restrictions, that were already present at pre-treatment, increased after 12 months of treatment (Chiarini M et al., 2015).

Dimethyl fumarate was tested in MS patients for its effects on CD4 and CD8 memory cells after 6 months of therapy (Gross CC et al., 2015). Fewer CD4 and CD8 cells were found, together with a reduction of Th1 cells and an increase of Th2 and Treg, while Th17 remained unaltered. In the light of these results, the authors suggested that the benefit that patients experienced from DMF therapy may depend on a predominance in Th1 cells. On the other hand, not much is known about the effect of DMF on TCR signaling or molecular repertoire.

In 2008, Korporal M et al. demonstrated that in RRMS patients peripheral naïve Tregs were upregulated after 3 and 6 months of IFN-β-1a, along with a reduction of memory Tregs, that contributed to improve disease progression (Korporal M et al., 2008). Few years later, an analysis of T-cell subpopulations frequency in two groups of RRMS patients after 6 and 12 months of IFN-β-1a or glatiramer acetate reported an increased frequency of naïve cells, along with a decrease of memory cells after both treatments, but especially of Tcm after 6 and 12 months of GA (Praksova P et al., 2012). With these observations, the authors suggested that the beneficial effects of these two treatments in MS patients may lie in their immunomodulatory action on circulating T lymphocytes.

Less is known about the impact of IFN-β-1a and GA on TCR.

Alemtuzumab, acting as agonist of CD52 expressed on B cells surface, shows effects on innate immune cells, suggested by the authors as connected to long-term effectiveness of the treatment: after 6 months, the monoclonal antibody causes CD52+ cells depletion, decrease of circulating plasmacytoid and conventional DCs and expansion of $CD56^{bright}$ NK cells (Gross CC et al., 2016). Some interesting data about the effect of Alemtuzumab on TCR are available so far: in a pilot study, Rezvany MR et al. reported the increase of CDR3 restrictions in peripheral T cells after Alemtuzumab treatment in 5 patients with B-cell chronic lymphocytic leukaemia (Rezvany MR et al., 2006). More recently, Ruck et al. described 3 RRMS patients developing vitiligo after 14, 18 and 52 months of Alemtuzumab (Ruck T et al., 2018). These patients had CD8 T cell infiltration in the depigmented skin areas and a reduced TCR repertoire diversity in CD8 compartment. In the light of this, the authors speculate that the impaired TCR repertoire might be connected to the development of vitiligo after Alemtuzumab administration.

Concerning anti-CD20 treatments, Rituximab's effects on immune cell balance has been explored especially in rheumatoid arthritis: Leandro MJ described that Rituximab successfully depletes most of the circulating CD20+ B cells during the first 3 months of treatment and that, in the following 8 months, B cells compartment undergoes repopulation with an increase of immature B cells (Leandro MJ, 2013). However, knowledge about the effect of Rituximab on T cells and TCR in MS patients is still lacking. Interesting data are documented about the effects of Natalizumab and AHSCT on T-cell subpopulation balance and TCR repertoire, providing insights about the individual response to therapy and treatments mechanism of action.

1.5.1. Reconstitution of T cells and T-cell receptor repertoire after AHSCT

As mentioned above, AHSCT resets the immune system providing its renewal. This implies an intensified thymic output, confirmed either by the observation of the functional reactivation, the volume enlargement of the thymus after the transplantation (Arruda LCM et al., 2016) and the increase of circulating T-cell receptor excision circles (TRECs), circular DNA molecules produced by TCR gene rearrangement and marker of

thymic output, that have been demonstrated to double in frequency at 2 years post-AHSCT (Arruda LCM et al., 2016; Muraro PA et al., 2005).

After the transplantation, cells involved in innate immunity repopulate over weeks, while the reconstitution of adaptive immune cells requires years (Lutter L et al., 2018). Regarding T cells, naïve and Tem cells decrease while Tcm increase over the first 3 months after AHSCT (Arruda LCM et al., 2016). The regeneration of CD8 occurs faster (6-12 months after AHSCT), while CD4 are fully renewed after 2 years or more (Muraro PA et al., 2005; Lutter L et al., 2018). In parallel, T-cells gene expression normalizes within 1 year for CD8 and is comparable with pre-transplantation whereas, for CD4, it completely changes after AHSCT (de Paula Sousa A et al., 2015).

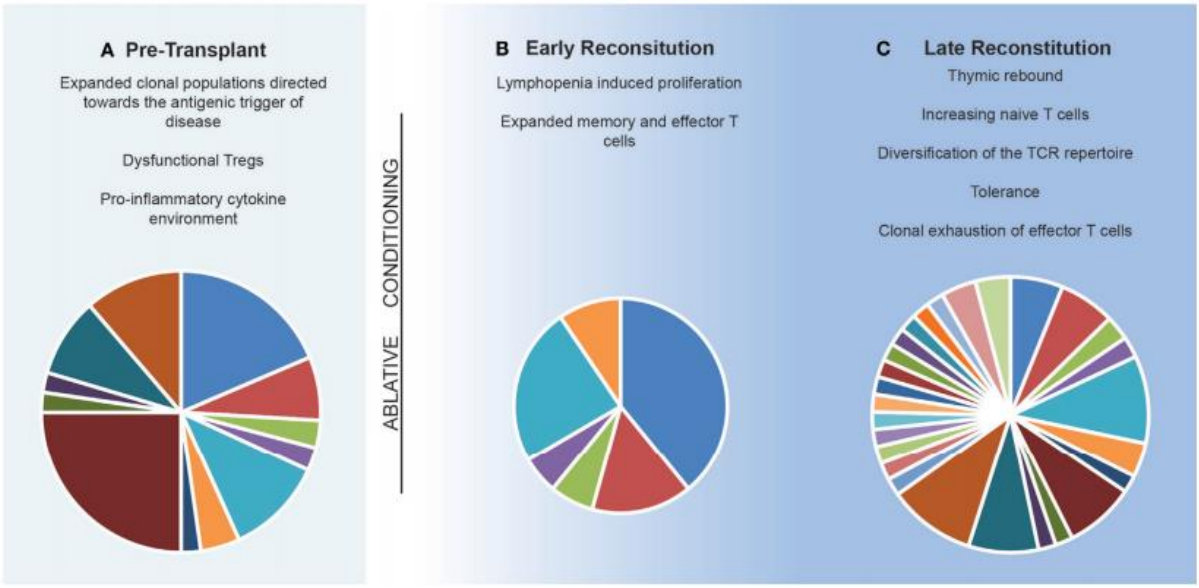

Fig. 29. Schematic illustration of immune reconstitution after AHSCT. A) Pre-transplant environment: clonal expansions of few T cell populations; B) Reconstitution of immune system with early regeneration of CD8 memory cells; C) Late reconstitution including thymic rebound, increase of naïve T cells and restoration of immunotolerance (Massey JC et al., 2018).

About Treg, contradictory evidences are documented: some studies address a post-AHSCT increase of these cells, while others report no variation (Arruda LCM et al., 2018; Lutter L et al., 2018). However, it has been observed the post-transplant upregulation of immunoregulatory molecules e. g. the cytotoxic T lymphocyte-associated protein 4 (CTLA-4) on Treg surface of MS and diabetes mellitus (DM type 1) patients, along with an increased production of IL-10, even if these results did not positively correlate with the clinical outcome (Arruda LCM et al., 2016; Ye L et al., 2017).

The reconstitution of the immune system and the restoration of immune tolerance

following AHSCT pass through a reassessment of the TCR repertoire that is, as mentioned above, intimately dependent on the post-transplant increase of thymic activity.

In systemic sclerosis (SSc), an autoimmune disease characterized by the accumulation of collagen in the connective tissue, the TCR repertoire of 10 patients became more diverse 6 months after AHSCT compared to baseline and more similar to healthy individuals (Farge D et al., 2017). A greater TCR-repertoire clonality has been documented in the mucosal T cell compartment of 16 patients with Crohn's disease (CD), along with the improvement of patients clinical condition (Le Bourhis L et al., 2017).

Muraro et al. have made an extensive investigation of TCR repertoire reconstitution after AHSCT in MS patients. In 2014, they performed high-throughput sequencing (HTS) of TCRβ chain in 24 MS patients before and two months and one year after AHSCT (Muraro PA et al., 2014). They found that, despite an initial skewed TCR repertoire, CD4 cells were characterized by a completely renewed TCR repertoire after one year: indeed, compared to baseline, CD4 clones were new in a proportion of a median of 81.52%. On the contrary, the proportion of new CD8 clones after one year from AHSCT was a median value of 45.32%, so almost half compared to the proportion of new CD4 clones. Furthermore, the authors observed a more diverse TCR repertoire in responder patients compared to non-responders 2 months after AHSCT; such difference disappeared after one year.

Those results have been fundamental to begin to discuss whether the investigation of TCR repertoire changes after a treatment that reassesses the immune system may be helpful, in the future, to understand and to putatively predict the clinical outcome of patients.

1.5.2. Redistribution of T cells and T-cell receptor repertoire after Natalizumab

To date, our knowledge about how Natalizumab impacts the TCR repertoire in MS is very limited. The main published study about this topic dates to 2013, when Warnke C et al. investigated the TCR repertoire through spectratyping in CSF and blood of 59 MS patients treated with Natalizumab. Authors identified the presence of TCR restrictions in CSF and not in the peripheral blood of MS patients, that they suggest that may be linked

to an impaired immunosurveillance within the CNS and, consequently, to the higher risk of PML. However, due to the limits of the methodology, there is no information on a sequence level.

Of note, a recent study performed by HTS investigated the impact of Natalizumab on the TCR repertoire in the treatment of Rasmussen encephalitis (RE) (Schneider-Hohendorf T et al., 2016), a rare neurological disease, particularly common among children, mediated by T lymphocytes (more likely CD8) and characterized by unilateral inflammation of the cerebral cortex (Varadkar S et al., 2014). Nevertheless, authors did not find any significant result after 5 months of Natalizumab treatment on the TCR repertoire of RE patients.

2. Aim of the study

Despite the progress that has been made thanks to HTS in the study of the TCR repertoire in MS and the increasingly deeper computational methods of analysis of TCR databases, there is still much to address. First, we lack of a large, comprehensive TCR database in MS under treatments. Second, the contribution of different T-cell subpopulations and their TCR repertoire in the pathogenesis of the disease and in treatments outcome is still not enough investigated. Furthermore, since bioinformatic analysis of TCR databases is a developing field, we lack of a broadly accepted statistical approach in the analysis of the TCR repertoire.

The present study aimed to perform a high-dimensional longitudinal investigation of the TCR repertoire variation in T-cell subpopulations of RRMS patients before and after the most effective immunomodulatory treatments, in order to correlate TCR variation and state of the disease identifying treatment-specific molecular traces in the TCR repertoire of patients. Therefore, the CDR3 amino acid (CDR3-a.a.) sequence of the TCR Vβ gene was sequenced by an Illumina MiSeq platform (iRepertoire Inc., Alabama, USA) from the mRNA isolated from sorted peripheral T-cell subpopulations from 15 RRMS patients before (t0, baseline) and after 24 months (t24) of two successful RRMS treatments, Natalizumab and AHSCT. In parallel, patients were also evaluated for serum cytokines levels at t0 and t24. Finally, the same analyses were performed on CSF of 4 incoming MS patients and their paired peripheral memory T-cell subpopulations.

This study provided the largest TCR database of RRMS patients under treatment so far, for a total of 180 repertoires and more than 55 million of CDR3-a.a. sequences. The TCR repertoires were deeply investigated by bioinformatic analysis through the choice of quantitative (number of sorted cells, total sequences or “reads”, unique sequences or “clones”, Shannon-Evenness, clonal persistence over treatment) and qualitative (repertoire architecture, sub-sequence composition, public sequences across samples and with published TCR databases) parameters.

3. Material and methods

3.1. Patients

All patients included in the study were enrolled at the Clinic of the Second Division of Neurology, Careggi University Hospital, Florence, Italy. The diagnosis of RRMS was performed according to McDonald criteria (McDonald WI et al., 2001). During treatments (AHSCT; Natalizumab), patients were followed monthly and evaluated collecting clinical, MRI and laboratory data. A third group of patients undergone lumbar puncture for CSF analysis at the time of diagnosis was included in the study. Patient characteristics are summarized in Tab. 1, Tab. 2 and Tab. 3.

3.1.1. AHSCT patients enrollment

Patients affected by MS and resistant to conventional therapies were included in the AHSCT program of the Hematology Unit of Careggi University Hospital, Florence, Italy. All signed informed consent was approved by the Local Ethical Committee (prat. 467/11). For all patients, MRI, clinical and laboratory data (IgG index and oligoclonal IgG bands) were performed. Patients recruited for AHSCT had the following characteristics:
- MS diagnosed according to the McDonald criteria;
- age between 18 and 55 years;
- EDSS = 1-6,5;
- Relapsing-Remitting MS form, with MRI activity and/or clinical worsening of the disability despite treatment, in the previous 6 months;
- refractory to treatment with Natalizumab or impossibility to perform this therapy due to allergic reaction to the drugs or presence of neutralizing antibodies.

3.1.2. Transplantation procedure

Peripheral blood stem cells (PBSCs) from patients were mobilized by Cyclophosphamide (4 g/sqm) and Filgrastim (5 mcg/Kg from). Cells were collected by continuous flow leukapheresis (2 whole body blood volumes) when circulating CD34+ cells exceed 20/mcl of whole blood. 3-8x10^6 CD34+ cells/Kg were collected and stored in liquid nitrogen. Conditioning regimen included Carmustine (300 mg/sqm/day), Cytosine

Arabinoside (ARA-C) (200 mg/sqm/day), Etoposide (200 mg/sqm/day) and Melphalan (BEAM) (140 mg/sqm/day) for 3 consecutive days. Rabbit anti-T globulin (ATG, Thymoglobuline™) was administered at day +1 and +2 at a total dosage of 7.5 mg/Kg. During the Reduced Intensity Conditioning (RIC) phase, Cyclophosphamide (50 mg/Kg/day) and ATG (2.5 mg/Kg) were administered at +2 and +6 and at +2 and +4 respectively. Biological samples from RRMS patients before (t0) and 24 months (t24) after AHSCT were collected at the Hematology Unit, Careggi University Hospital, Florence, Italy. Antibiotic and antiviral prophylaxis were administered during the phase of aplasia according to Hematology Unit practice. At t0, immunosuppressive treatments were stopped at least 1 month before sample collection.

3.1.3. Natalizumab patients enrollment

All Natalizumab patients were enrolled at the 2nd Neurological Clinic of the Careggi University Hospital (Florence, Italy) and were diagnosed as RRMS following reviewed McDonald criteria. Local Ethical Committee approval was obtained for the study and all patients signed informed consent (#CEAVC12745). Patients included were previously treated 12 months with Copaxone/IFN-β, as first line therapy. All patients showed aggressive form of MS (patients that failed the first line therapy and with high disease activity: 2 relapses in the last year of therapy or 1 relapse with no complete recovery and up to 9 lesions T2 in MRI or one Gadolinium positive, or rapidly evolving patients: 2 or more relapses in one year and 1 or more Gd+ lesions or with a significative increment of T2 lesions). All samples of the study had the following characteristics:

- age between 18-60 years;
- EDSS score between 0-5.5.

Inclusion and Exclusion criteria are described in detail in SURPASS study (ClinicalTrials.gov Identifier: NCT01058005). Presence of antibodies anti JCV and anti-Natalizumab in serum was evaluated in the whole sample.

3.1.4. Cerebrospinal fluid patients enrollment

CSF samples were obtained from incoming patients undergoing the diagnostic lumbar puncture and enrolled at Neurological Clinic (University of Florence, Italy). All patients signed informed consent and Local Ethical Committee authorized the study (#2014/003601). Recruited patients had the following characteristics:

- age between 18 and 55 years;
- no immunomodulatory therapy since at least 6 months;
- no immune-suppressive therapy since at least 12 months;
- no corticosteroid administration in the previous month.

Exclusion criteria:

- cognitive decline preventing informed consent release;
- concomitant diseases that may interact with disease course or with sample processing (i.e. neoplasms or infections as hepatitis and HIV) or induce any risk for the patient;
- pregnancy or breastfeeding.

Recruited patients were clinically assessed every 6 months. All patient material was encoded to avoid identification of individual's name or identity during material processing.

3.2. Samples collection

3.2.1. Peripheral blood mononuclear cells collection

Whole peripheral blood (PB) has been collected in heparin containing tubes. Mononuclear cells (MNCs) were collected by density gradient centrifugation using Pancoll (density: 1.077 g/ml; PAN-Biotech) at 1500 rpm, RT, for 30 min within 6 hours from blood collection. MNCs were cryopreserved in 10% dimethyl sulfoxide (DMSO) in aliquots containing $20x10^6$ cells and stored in liquid nitrogen freezer until used.

3.2.2. Serum samples collection

Serum samples were collected according to the same time schedule and in the same vein puncture as performed for PB collection. For each time point, 10 ml of blood were drawn

in serum-separated tubes (SST). Serum was separated from clotted blood by centrifugation at 3000 rpm for 10 min, RT, then aliquoted and stored in -80°C freezer until used.

3.2.3. Classical samples phenotypic characterization

Immunophenotype was analysed as routine from fresh whole blood upon erythrocyte lysis (BD Lysis buffer, BD Bioscences) by labelling cells with the following panel of fluorescent monoclonal antibodies: anti-CD45RA FITC (Clone: HI30), anti-CD3 PE (Clone: UCHT1), anti-CD4 APC (Clone: OKT4), anti-CD8 APC-Cy7 (Clone: SK1), anti-CD19 PerCP (Clone: SJ25C1), anti-CD16 APC (Clone: 3G8), anti-CD56 PerCP Cy5.5 (Clone: B159), anti-HLA-DR HV450 (Clone: L243) (all from BD Bioscences). Cells were analysed by FACSCanto II flow cytometer (BD Bioscence).

3.2.4. Phenotypical analysis of activated memory T cells

Frozen PBMCs from Natalizumab patients were analyzed by flow cytometry to monitor the absolute cell counts of activated memory T-cell subpopulations. Cells were stained with the following antibodies: anti-CD4 APC (Clone: OKT4, eBioscence), anti-CD8 APC-Cy7 (Clone: SK1), anti-CCR7 PE (Clone: 3D12, eBioscence), anti-CD45RO PE-Cy5 (Clone: UCHL1, eBioscence), anti-CD25 FITC (Clone: P4A10, eBioscence).

3.2.5. Cerebrospinal fluid collection

CSF from each patient was collected by lumbar puncture. The spinal tap was carried out using a Sprotte type 19 or 20 G conical elliptic shaped spinal atraumatic needle (Pajuk, Germany), inserted through a 4 cm long, cutting tip needle as intruder needle. The volume of the samples was 10-15 ml for patient. CSF samples were analyzed immediately after lumbar puncture for cell counts, quantitative (IgM and IgG indices) and qualitative (oligoclonal bands) analysis of intrathecal Ig synthesis, and albumin quotient as indicator of the BBB status using standard methods. Samples containing at least 10000 cells were included in the study and centrifuged at 800 rpm for 15 min, RT. CSF cells were destined to RNA isolation, as described below. CSF supernatants were

collected and frozen at -80 °C. At the same time an equal number of paired PBMCs were destined to RNA extraction as CSF cells. Serum was also collected and stored at -80°C. Exclusion criteria: CSF samples containing <10x10^4 mononuclear cells and/or >10 red blood cells/μL.

3.3. Immunophenotype of MS patients cerebrospinal fluid

CSF were characterized for the percentage of Tem and Tcm CD4 and CD8 cells immediately after collection. CSF cells were divided in two tubes and labelled 20 min, RT, in the dark, with the following antibodies: one tube with anti-CD4 APC (Clone: OKT4, eBioscence), anti-CCR7 PE (Clone: G043H7, BioLegend) and anti-CD45RO PE-Cy5 (Clone: UCHL1, eBioscence) and the other tube with anti-CD8 FITC (Clone: OKT8, eBioscence), anti-CCR7 PE and anti-CD45RO PE-Cy5. The percentage of Tem and Tcm CD4 and CD8 cells was then evaluated by flow cytometry (CyFlow Space, Sysmex Partec).

3.4. HLA II genotyping

All patients were typed for HLA class II by Sequence Specific Primers PCR (PCR-SSP) technique using the AllSet+™ Gold SSP Low-Resolution kit (One Lambda).

3.5. Cytokine and chemokine evaluation

Serum of Natalizumab and AHSCT patients were analyzed for the presence of a panel of 17 cytokines and chemokines (IFNγ, IL4, IL1α, IL1β, IL2, IL6, IL8, IL10, IL12p40, IL12p70, IL17, IL23, TNFα, GM-CSF, CXCL10, CXCL13, MMP9) by Luminex technology, using Milliplex assay (Merck Millipore) and Bioplex device (Biorad).

Luminex technology allows a quantitative analysis of an elevated number (within 100) of different biomolecules contained in small volumes (ranging from 15 to 50 μl). The technology provides the utilization of magnetic microspheres (characterized by a diameter of 5,6 μm) conjugated to an antibody which is specific for the analyte to

quantify. Each microsphere is also conjugated to 2 fluorochromes that emit in two different regions of the visible spectrum, one in the red and the other in the infrared spectrum. The combination of these colors, each one present in 10 different gradations, products a hundred of different tones of red and infrared. Each resulting intensity of fluorescence univocally defines a precise population of microspheres, called "class". By the moment that each microsphere class is conjugated with a primary antibody (capture antibody) directed to the analyte to quantify, it is possible to identify the analyte based on the fluorescence emitted by the microsphere. A further fluorophore (reporter), which emits in the green spectrum when excited, provides a quantification of the analyte bound to the antibody. This fluorophore (i.e. phycoerythrin) is conjugated to streptavidin, a protein with high affinity to the biotin bound to the secondary antibody (detection antibody).

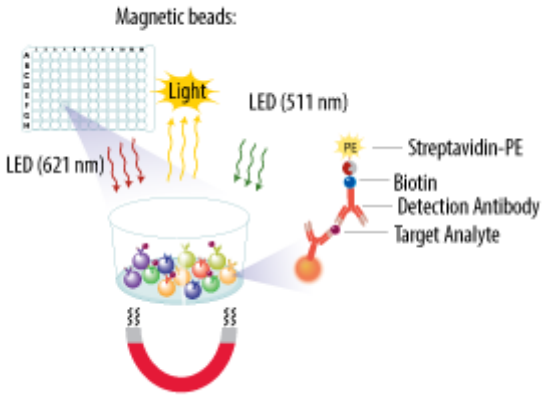

Fig. 30. Luminex technology scheme. The technology provides the utilitation of magnetic microsphere conjugated to an antibody specific for the analyte to quantify. Each microsphere is conjugated also to 2 fluorochromes which emit in two different regions of the visible spectrum (one in the red and the other in the infrared spectrum).

The assay execution provides the following steps:

- adding of a combination of different microspheres in a 96-well plate with flat bottom, followed by washing with a buffer solution using a magnet under the plate to keep the microspheres in the wells;
- adding of samples containing the analytes to quantify and washing with buffer solution;

- adding of a secondary antibody conjugated to biotin, which binds the analyte in a different site from the one recognized by the antibody conjugated to the microsphere, then washing as previously described;
- adding of streptavidin conjugated to a third fluorophor and washing;
- resuspension of the microspheres in a reading buffer.

In the reading instrument, the microspheres are aspired by a capillary needle and passed one by one through a reading chamber, where they are hit by two different laser: the first (classification laser) excites the 2 fluorochromes that identify the microspheres class and consequently the analyte bound to the antibody; the second (laser reporter) excites the fluorophore bound to the secondary antibody, allowing the analyte quantification.

3.6. CD3+ cells isolation

CD3+ cells were isolated from at least $25x10^6$ PBMCs of Natalizumab, AHSCT and paired PBMCs of CSF patients. PBMCs were thawed in defrosting medium (10% FCS in DPBS), centrifuged at 1300 rpm, RT, for 10 min, then counted and used for T cell isolation by negative immunomagnetic depletion using the Pan T Cell Isolation Kit human (Miltenyi Biotec), consisting in a Pan Cell Biotin-Antibody Cocktail and a Pan T Cell MicroBead Cocktail that provide the retention of the unwanted cell fraction (CD3 negative cells) and the elution of the CD3-positive cells fraction through the LS column placed on a suitable MACS Separator (Miltenyi Biotec). Finally, CD3+ isolated cells were washed once in MACS buffer (PBS 1X with 0.5% bovine serum albumin (BSA) and 2mM ethylenediaminetetraacetic acid (EDTA)) at 1500 rpm, RT, for 5 minutes, then resuspended in RPMI 1640 medium and counted. Mean CD3+ cells value per sample: $4x10^6$ (±2.2).

3.7. Sorting of T-cell subpopulations

3.7.1. AHSCT patients

CD3+ cells were washed once in MACS buffer (PBS 1X with 0.5% bovine serum albumin (BSA) and 2mM ethylenediaminetetraacetic acid [EDTA]) at 1500 rpm, RT, for 5

minutes, then resuspended in RPMI 1640 medium and counted. To identify naïve and memory CD4 and CD8 T lymphocytes, CD3+ cells were labelled in one tube for 20 min, RT, in the dark, with the following fluorescent antibodies: anti-CD4 APC (Clone: OKT4), anti-CD8 PE Cy7 (Clone: RPA-T8), anti-CD45RA FITC (Clone: HI100), all from eBioscience. T-cell subpopulations were sorted by FACSAria II flow cytometer (BD Bioscience).

Fluorescence-activated cell sorting (FACS) is a specific type of flow cytometry, that consents to quantitatively record fluorescent signals from individual cells and to physically separate cells based on prefixed characteristics.

To detect signals, cell surface proteins are labelled with a target-specific antibody associated with a fluorescent molecule. The cell suspension enters in a flowing stream of liquid, which consents to separate cells relatively to their diameter. A laser beam allows to monitor cells flow, which consists in droplets containing single cells with a positive or a negative charge. The laser hits each cell producing a fluorescent signal that depends on the antibody used for cell labelling. Then, each droplet flows towards a different container leading to the sorting of different cell populations.

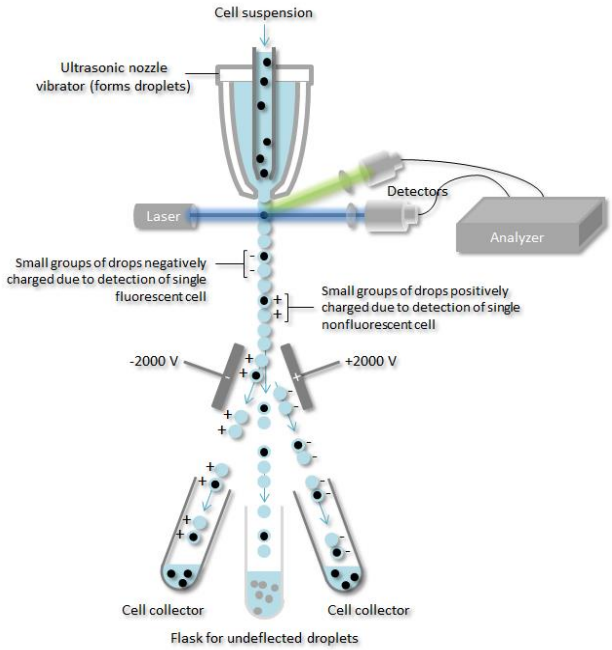

Fig. 31. Flow cytometry and cell sorting. Illustration source**:** http://www.sinobiological.com/flow-cytometry-fcm-facs-fluorescence-activated-cell-sorting-facs.html.

3.7.2. Natalizumab patients

Purified CD3+ cells were washed and counted as described above. To identify naïve, EM, CM CD4 and CD8 and Temra CD8 T lymphocytes, cells were divided in two tubes and labelled for 20 min, RT, in the dark, with the following fluorescent antibodies: one tube with anti-CD4 APC (Clone: OKT4), anti-CD45RA FITC (Clone: HI100), anti-CCR7 PE (Clone: 3D12); the other one with anti-CD8 PE Cy7 (Clone: RPA-T8), anti-CD45RA FITC (Clone: HI100), anti-CCR7 PE (Clone: 3D12). All the antibodies are from eBioscience. T-cell subpopulations were sorted by FACSAria II flow cytometer (BD Bioscience).

3.7.3. Cerebrospinal fluid patients

Purified CD3+ cells from paired PBMCs of CSF patients at the time of diagnosis (t0) were washed and counted as described above. To identify EM and CM CD4 and CD8 T lymphocytes, CD3+ cells from PBMCs were divided in two tubes and labelled for 20 min, RT, in the dark, with the following fluorescent antibodies: one tube with anti-CD4 APC (Clone: OKT4), anti-CD45RA FITC (Clone: HI100), anti-CCR7 PE (Clone: 3D12); the other one with anti-CD8 PE Cy7 (Clone: RPA-T8), anti-CD45RA FITC (Clone: HI100), anti-CCR7 PE (Clone: 3D12). All the antibodies are from eBioscience. T-cell subpopulations were sorted by FACSAria II flow cytometer (BD Bioscience).

3.8. RNA isolation

RNA was isolated immediately after sorting by using the RNeasy Plus Micro Kit (Qiagen), according to manufacturer's protocol, from PBMCs of the three groups of patients and from the whole CSF cell samples of CSF patients. RNA purity was assessed by NanoDrop ND-1000 spectrophotometer (EuroClone) evaluating the 260/280 nm absorbance. RNA concentration (pg/μl), rRNA ratio [28s/18s] and RNA Integrity Number (RIN) were assessed using the RNA 6000 Pico Kit (Agilent), according to the manufacturer's recommendations, and analyzed by Agilent BioAnalyzer 2100.

3.9. T-cell receptor library generation

TCR Vβ chain libraries were prepared using a multiplex PCR technology, the patented tem-PCR (for target enriched multiplex PCR technology; Fig. 32), where nested primers were designed for every target to be co-amplified (Fo: Forward outside; Fi: Forward inside; Ro: Reverse outside; Ri: Reverse inside) in the multiplex assay. The inside primers for all the targets share the same tag sequence which will bind to a pair of "Superprimers" (FS: Forward superprimer; RS: Reverse superprimer). Nested primers and superprimers are in the same reaction together.

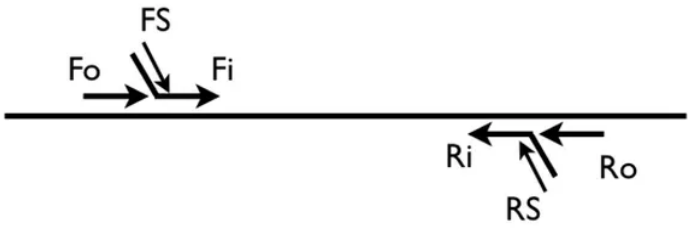

Fo: Forward outside; Fi: Forward inside; FS: Forward superprimer;
Ri: Reverse inside; Ro: Reverse outside; RS: Reverse superprimer.

Fig. 32. The tem-PCR technology. Nester primers (Fo, Fi, Ro and Ri), designed for every target to be co-amplified, share the same tag sequence, which will bind to a pair of Superprimers (FS and RS). http://www.irepertoire.com/technology.

Two rounds of PCR were carried out; in the first one high concentration of the nested primers was used, in the second-round fresh communal primers (recognizing the shared tag sequence already introduced during the first round of amplification) and enzymes were added.

3.10. Next-Generation Sequencing

Amplified libraries, after purification, were sequenced by MiSeq Illumina platform, using 250 PER (paired-end read) primers, that cover from within the first framework region through the C-region (Fig. 33). The term "paired-end" read (PER) refers to the reading of both the forward and reverse template strands of the same receptor sequence during sequencing. The overall read length of the sequence can be increased by using the sequence read from both strands (with some overlap between both reads to increase

confidence in the paired-read). The human Illumina MiSeq 250 PER primers and all Roche 454 primers cover from within the first framework region through the C-region.

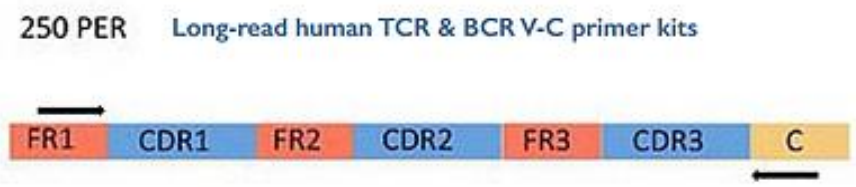

Fig. 33. 250 PER (paired-end read) primers. The human Illumina MiSeq 250 PER primers cover from within the first framework region through the C-region. Picture from: http://www.irepertoire.com/technology.

A software offered by iRepertoire, iRweb, allowed to perform some basic analysis, as the determination of V- & J-gene combinations in relation to frequency, the individuation of all called CDRs for a given peptide sequence, the calculation of shared CDR3 across samples, the determination of percentage use of V and J genes within the sample.

3.11. Statistical analysis

3.11.1. Repertoire data analysis

Statistical analysis of TCR Vβ sequence data was performed using the statistical programming environment R (R Core Team, Austria) and GraphPad Prism v.6 (GraphPad Inc.). Graphs in R were generated by the packages ggplot2 (Hadley W, 2016), ggpubr (Kassambara A), igraph (Csardi G and Nepusz T) and ComplexHeatmap (Gu Z et al., 2016). Hierarchical clustering of evenness profiles was performed based on correlation-based distance and visualized by heatmaps using the NMF R package (Gaujoux R and Seoighe C, 2010). Repertoire architecture networks were made using Cytoscape (Shannon P et al., 2003). Each network has been constructed based on the 10,000 highest frequency clones (that account in each repertoire for at least 90% of the reads) and is based on Levenshtein distance of 1 (CDR3s-a.a. are connected when they differ maximally of 1 amino acid [a.a.]) (Miho E et al., 2018; Greiff V et al., 2015). Statistical analyses were performed with non-parametric tests or One-way ANOVA where appropriated. Statistical significance was considered when $p<0.05$.

3.11.2. Shannon-Evenness and clonal expansion profiles

Shannon-Evenness and clonal expansion profiles were calculated as previously established by Greiff V et al., 2017. Briefly, the Shannon-Evenness is defined as the quotient of the exponential of the Shannon entropy and Species Richness (SR: number of unique CDR3s in a given TCR dataset).

$$\text{Shannon-Entropy} = -\Sigma\, f_i\, log\, f_i,$$

where f_i is the frequency of the *i*th clone in a given TCR dataset.

$$\text{Shannon-Evenness} = exp(-\Sigma\, f_i\, log\, f_i)/SR$$

Shannon-Evenness is 1 if all clones in a repertoire have the same frequency (an "even" repertoire), or it converges to 0 if very few clones dominate in the repertoire (a "polarized" repertoire). That is, if very few clones have very high frequency and a lot of clones have very low frequency.

Clonal expansion profiles (also called Evenness profiles) represent Hill-diversity profiles scaled by the repertoire Species Richness (SR). Hill diversity profiles are defined as:

$$^{q}D = \left(\sum_{i=1}^{SR} f_i^{q}\right)^{\frac{1}{1-q}},$$

where f_i is the frequency of the *i*th clone in a given TCR dataset. Clonal expansion profiles are then defined as ^{q}D/SR, where q ranging from 0 to 10 with a step size of 0.2. The parameter *q* determines the importance of high frequency clones in the determination of the q-parameterized evenness; the higher q, the more higher frequency clones are weighted (Greiff V et al., 2015).

3.11.3. k-mer decomposition analysis

All amino acid CDR3s from each patient TCR repertoire were deconstructed into overlapping sub-sequences ("k-mers") of length 3 (k=3) using the tokenizers R package

(Mullen AL et al., 2018). Then, all k-mers were condensed into a k-mer frequency distribution providing each k-mer's frequency across all CDR3s of a given repertoire. Finally, k-mer frequency distributions were correlated across repertoires using Pearson correlation and visualized using hierarchical clustering and heatmap as described above.

3.11.4. Definition and quantification of clonal persistence

A clone is defined as V-J-CDRβ3 (amino acid sequence). Pairwise clonal persistence between repertoires A and B is calculated as:

$$\text{Clonal persistence}(A,B) = \frac{A \cap B}{mean(|A|,|B|)} ,$$

where A ∩ B is the absolute number of persisting clones and |A| signifies the number of clones in repertoire A. The clonal persistence was calculated over treatment (t0–t24) within each patient.

3.11.5. Private and public clones

A clone was considered private when present only in one sample and public when shared at least twice across samples.

3.11.6. Cytokine and chemokine data analysis

Statistical analysis of cytokine and chemokine levels at t0 and t24 within or among the two groups of patients was performed by non-parametric Wilcoxon test using R software (R Core Team, Austria). Statistical significance where considered when $p \leq 0.05$.

4. Results

4.1. Natalizumab and AHSCT

4.1.2. Patients characteristics and clinical follow-up

To date, 13/15 patients are still followed at the Second Division of Neurology, Careggi University Hospital in Florence, Italy. Natalizumab and ASHCT patients characteristics are reported in Tab. 1 and Tab. 2, respectively.

Among AHSCT patients, only one (MS032) experienced a relapse at t24 from AHSCT. Of note, MS032 has a family history of MS and interrupted the standard protocol of conditioning chemotherapy to minimize infection risk, subsequently to positivity to a multi-resistant strain of *Klebsiella pneumoniae*. Specifically, MS032 received BCNU, VP-16 and Ara-c as 1st, 2nd and 3rd conditioning drugs respectively, whereas the other patients received BEAM, following the standard AHSCT protocol. The patient P received melphalan as 1st conditioning drug and BCNU as 2nd and 3rd conditioning drug because of a BCNU-related anaphylactic shock.

MS020, MS029, MS032 and MS034 were treated with Natalizumab before transplantation and MS029 is the only one that interrupted Natalizumab treatment after the development of antibodies against JCV. Among Natalizumab patients, Ty20, Ty21 and Ty25 experienced MS relapses during treatment, whereas MRI brain inflammatory activity (defined as new MRI T2 lesions or Gd-enhancing lesions) was present in patient Ty29. Ty12, Ty17, Ty21, Ty25 and Ty26 suspended the treatment because of JCV-positivity. None of the Natalizumab-treated patients had anti-Natalizumab antibodies. Anti-JCV antibodies were present in all patients except for Ty20. During NTZ, Ty26 had an ischemic stroke and Ty30 developed depression and was lost at the follow-up; no other concomitant disease has been reported. During washout after Natalizumab, Ty12, Ty20, Ty25 and Ty26 had relapses. Ty21 suspended NTZ for JCV+ and ineffectiveness of treatment.

Table 1. Clinical characteristics of Natalizumab patients

N. of patients	8
Gender (F:M)	8:0
Age average (min-max)	39,5 (28-45)
Age at treatment initiation average (min-max)	38,5 (21-39)
Type of MS	RRMS
Disease duration average (min-max)	14,3 (8-21)
EDSS T0-T24 average (min-max T0; min-max T24)	3-2,1 (1,5-4,5; 1-3,5)
N. of patients with relapses before Natalizumab (AIFA criteria A:B)[#A]	8/8 (5:3)
N. of patients positive for anti-JCV Abs[A]	7/8
N. of patients with relapses[B]	3/8
N. of patients with disease activity (MRI)[B]	2/8
N. of patients developing anti-Natalizumab Abs[B]	1/8
N. of patients with washout relapses	4/8
Therapy:	
IFN-beta	6/8
Copaxone	1/8
Azathioprine	3/8
No therapies	1/8

#A= patients that failed the first line therapy, with high disease activity: 2 relapses in the last year of therapy, or 1 relapse with not complete recovery and up to 9 lesions T2 in MRI or one Gd+ lesions

#B= rapidly evolving patients, with 2 or more relapses in one year and 1 or more Gd+ lesions/a significative increment of T2

[A]at the first Natalizumab administration

[B]during Natalizumab therapy

Table 2. Clinical characteristics of AHSCT patients

N. of patients	7
Gender F:M	7:0
Age average (min-max)	39,9 (31-47)
Age at treatment initiation average (min-max)	32,7 (21-47)
Type of MS	RRMS
Disease duration average (min-max)	19,7 (13-38)
EDSS before AHSCT average (min-max)	4,9 (2,5-6,5)
EDSS after AHSCT average (min-max)	4,4 (1,5-6,5)
N. of patients with relapses before AHSCT[A]	6/7
N. of patients with disease progression before AHSCT[A]	0/7
N. of patients with relapses after AHSCT[B]	1/7
N. of patients with disease progression after AHSCT[B]	0/7
Therapy:	
Natalizumab	4/7
Cyclophosphamide	3/7
Copaxone	2/7
Azathioprine	2/7
IFN-beta	4/7
Mitoxantrone	2/7
No therapies	0/7

[A]during the 2 years before the transplant; [B]during the 2 years after the transplant

4.1.3. Immunophenotypic characterization of peripheral blood from Natalizumab patients

Immunophenotypes were analyzed by flow cytometry on fresh blood samples of 16 Natalizumab patients, of whom 5/16 were then included in the TCR sequencing experiments. Phenotypic analyses were performed at baseline (t0) and at 6, 12 and 24 months of treatment (t6, t12, t24) and included the evaluation of percentage and absolute cell count of total T, B, NK, lymphokine-activated killer (LAK) cells and CD4/CD8 ratio.

Results showed a significant ($p<0.05$; $p<0.01$; $p<0.001$) increase of the absolute cell number of all examined populations over time, without altering the CD4/CD8 ratio (Fig. 34).

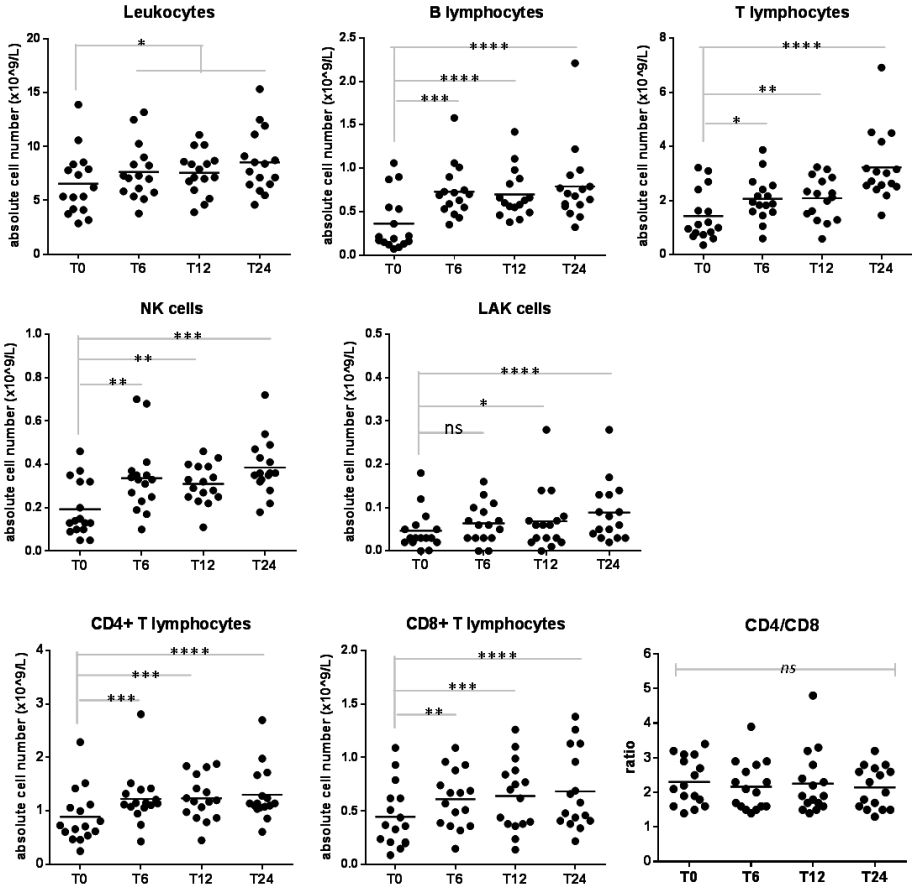

Fig. 34. Absolute cell counts of circulating lymphocytes in patients under Natalizumab. Graphs report the percentage and absolute cell count of total T, B, NK, lymphokine-activated killer (LAK) cells and the ratio between CD4 and CD8 T cells at baseline (t0) and after 6, 12 or 24 (t6, t12, t24) months of Natalizumab treatment. Mean±SEM is reported. Statistical significance was determined by One-way ANOVA followed by post-hoc Tukey test (*p<0.05; **p<0.01; ***p<0.001; ns= not significant).

Then, from frozen PBMCs of 8/16 Natalizumab patients, the absolute cell counts of sorted T-cell subpopulations (naïve, EM, CM CD4 and CD8 and Temra CD8) and activated memory T-cell subpopulations (EM and CM CD4 and CD8 and Temra CD8) were evaluated at t0, t6, t12 and t24 of Natalizumab treatment.

Results showed a significant ($p<0.05$) increase of CM CD4 and a significant ($p<0.05$) decrease of EM CD4 T-cell absolute cell count at t24 compared to t0. Activated EM CD4 absolute cell count was significantly ($p<0.05$) decreased at t24 compared to t0 as well. A trend towards an increase of naïve and CM CD8 absolute cell counts at t24 compared to t0 was observed, although the variation was not statistically significant (Fig. 35).

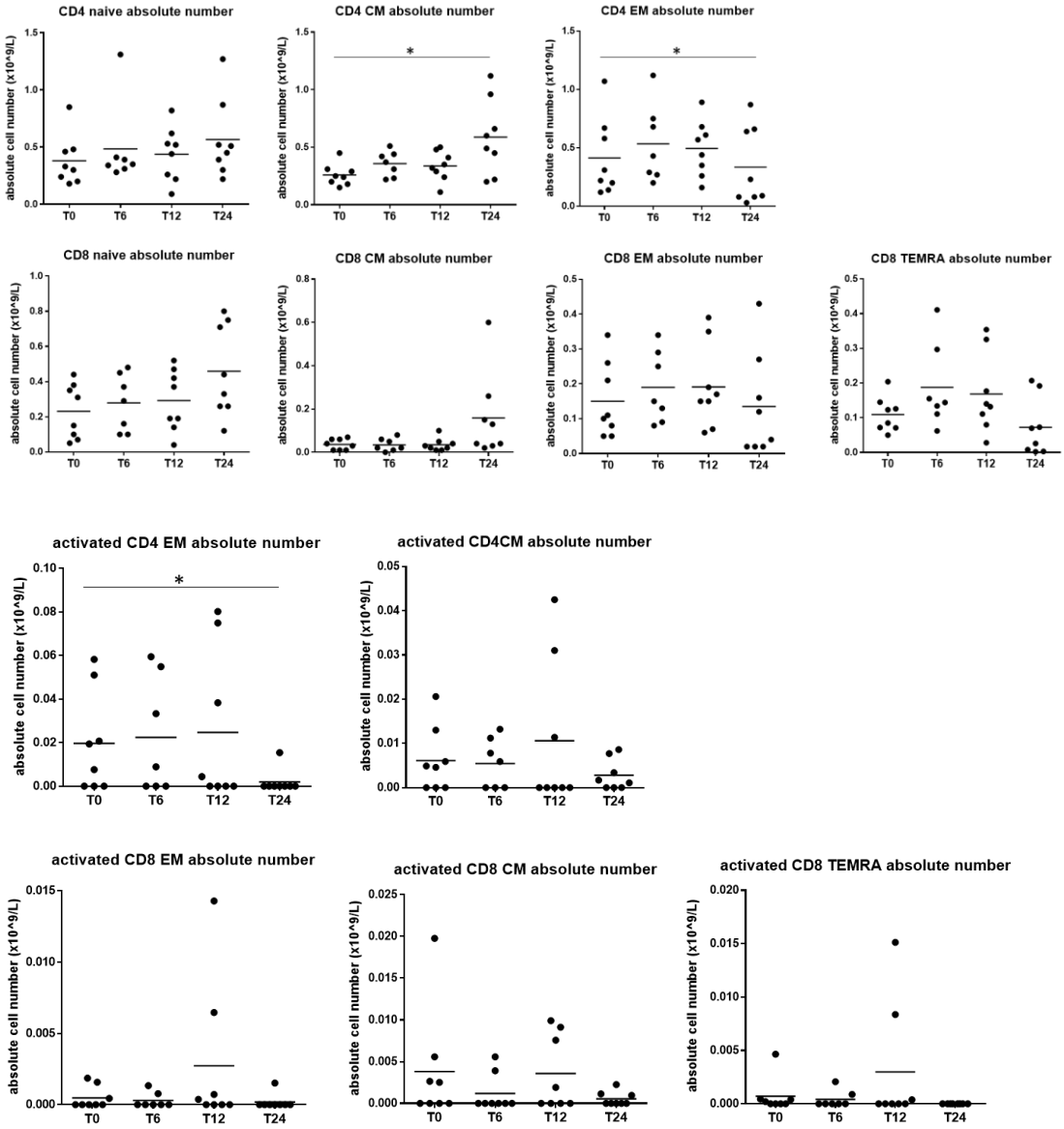

Fig. 35. Absolute cell counts of T-cell subpopulations and activated memory T-cell subpopulations in patients under Natalizumab. Graphs show the absolute cell counts of sorted T-cell subpopulations and activated memory T-cell subpopulations in 8 Natalizumab patients at t0, t6, t12 and t24. CD45RO+CCR7- = EM T cells; CD45RO+CCR7+ = CM T cells; CD25+ = activated T cells. Statistical significance was determined by non-parametric Mann Whitney test (*p<0.05).

4.1.4. Data acquisition: experimental workflow

The TCRβ gene from T-cell subpopulations (naïve, EM, CM CD4 and CD8 and Temra CD8 for Natalizumab patients; naïve and memory CD4 and CD8 for AHSCT patients) of 15 RRMS patients, of which 8 Natalizumab and 7 AHSCT, was sequenced. T-cell subpopulations were sorted from PBMCs at t0 and t24, obtaining a total number of 57,330,057 reads (total sequences) and 1,500,769 V-CDR3-J amino acid (a.a.) clones (or unique sequences). The experimental workflow is reported in Fig. 36.

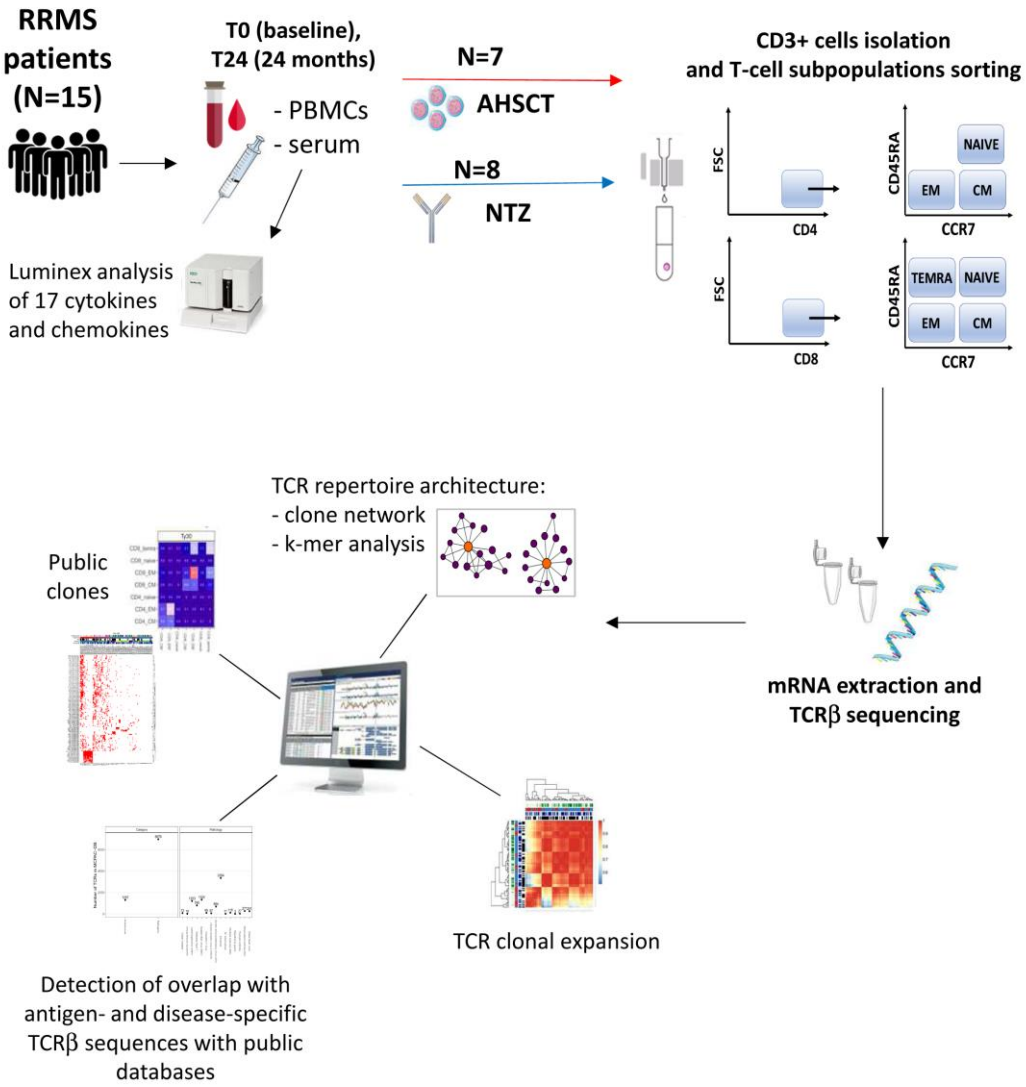

Fig. 36. Experimental workflow. PBMCs and serum were collected from RRMS patients (N=15) before (t0) and after 24 months (t24) AHSCT (N=7) or Natalizumab ("NTZ"; N=8). Serum samples were analyzed for the presence of cytokines and chemokines. CD3+ cells were isolated from PBMCs and T-cell subpopulations (naïve, EM, CM CD4 and CD8 and Temra CD8 from Natalizumab patients; naïve and memory CD4 and CD8 from AHSCT patients) were isolated. From total mRNA, TCRβ chain (TCRβ) sequencing was performed by iRepertoire Inc., Alabama, USA. High-dimensional TCRβ data analyses included repertoire sequencing statistics, repertoire architecture, clonal expansion distribution, sequence similarity, clonal persistence across time points, and comparison with public TCRβ databases.

4.1.5. T-cell subpopulation sorting: gating strategy

For each Natalizumab patients, 7 T-cell subpopulations were sorted by FACSAria II flow cytometer as already mentioned (see Methods) at t0 and t24 timepoints, for a total of 14 cell tubes/patient. For each AHSCT patient, 4 T-cell subpopulations were sorted at t0 and t24, for a total of 8 cell tubes/patient. The gating strategy from one representative patient (Ty12, CD4 t0) is reported in Fig. 37.

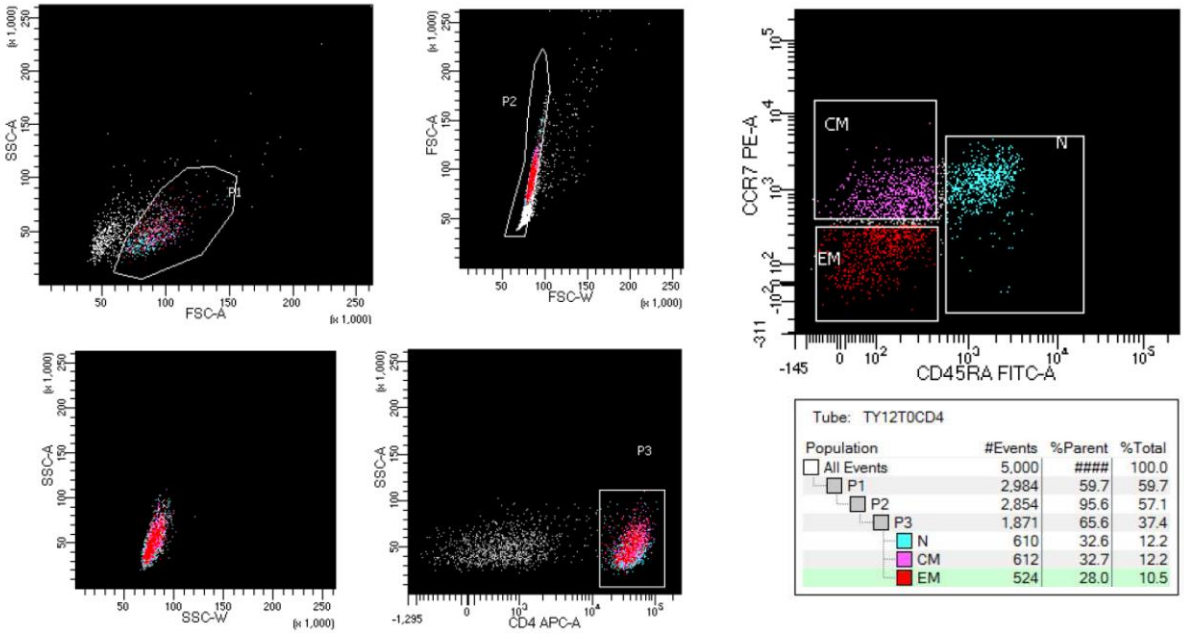

Fig. 37 Gating strategy for T-cell subpopulations sorting by flow cytometry. Panel reports an example of gating from one representative patient (Ty12, CD4 t0) for T-cell subpopulations sorting by FACSAria II flow cytometry. The morphological gate P1 includes all T cells on the total of events (first row, left dot plot). T cells were furtherly selected by P2 gate, excluding doublets and triplets (first row, middle dot plot). T-cell subpopulations gates (first row, third dot plot) include CM (CCR7+CD45RA-), EM (CCR7-CD45RA-) and naïve (CCR7+CD45RA+) CD4 cells. All CD4 cells are included in gate P3 (second row, left dot plot).

4.1.6. Data quality and repertoire statistics

To confirm the quality of our dataset, excluding under- or oversampling in the sequencing depth, it was calculated the Pearson correlation coefficient (r) between several quantitative parameters: the number of reads (#Reads), clones (#Clones) and the Shannon-Evenness versus the number of sorted cells; #Reads versus #Clones and Shannon-Evenness and, finally, Shannon-Evenness versus #Clones.

The Pearson correlation coefficient (r) resulted negative (r<0.5) in almost all the comparisons and in both groups of patients, indicating that the number of clones did not increase with the number of reads, representing a sufficient sequencing depth (Fig. 38). A moderate correlation (0.5<r<0.7) was found between #Clones and cell numbers (r=0.57 for AHSCT; r=0.54 for Natalizumab) and between Shannon-Evenness and #Clones (r=0.69 for AHSCT; r=0.76 for Natalizumab).

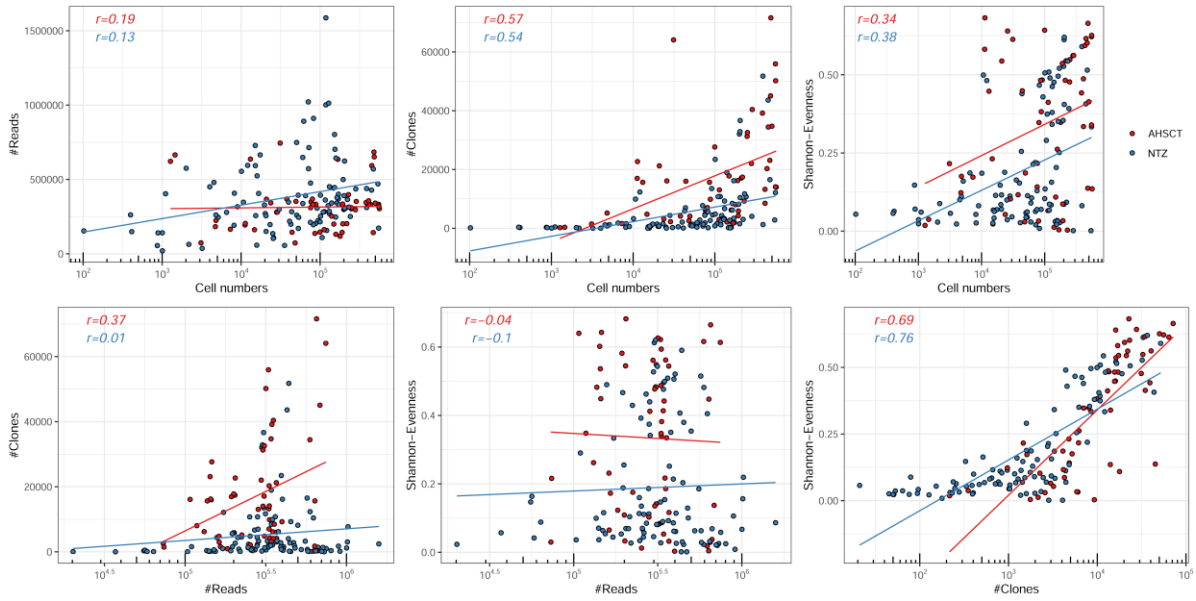

Fig. 38. Repertoire statistics correlation. Graphs report the Pearson correlation coefficient (r) calculated between various quantitative TCR repertoire parameters in RRMS patients. In all graphs, blue dots represent NTZ patients and red dots represent AHSCT patients. The correlations are reported as follows: reads number (#Reads) versus cell numbers (first row, left graph); clones number (#Clones) versus cell numbers (first row, middle graph); Shannon-Evenness versus cell numbers (first row, right graph); #Clones versus #Reads (second row, left graph); Shannon-Evenness versus #Reads (second row, middle graph); Shannon-Evenness versus #Clones (second row, right graph). Correlation values for the two groups of patients are reported on the upper left of each graph.

Next, the variation of the number of cells, reads, clones and Shannon-Evenness (see Methods for a definition of Shannon-Evenness) was evaluated by T-cell subpopulation at t0 and t24 across treatments (Fig. 39). Results showed a significantly ($p<0.05$) decreased Shannon-Evenness (closer to 0: few clones dominate) in CD8 naïve cells from t0 (Shannon-Evenness mean value = 0.3) to t24 (Shannon-Evenness mean value = 0.12) in Natalizumab patients compared to AHSCT, as well as a significant ($p<0.01$) reduction in the number of clones (t0≈8700, t24≈2000).

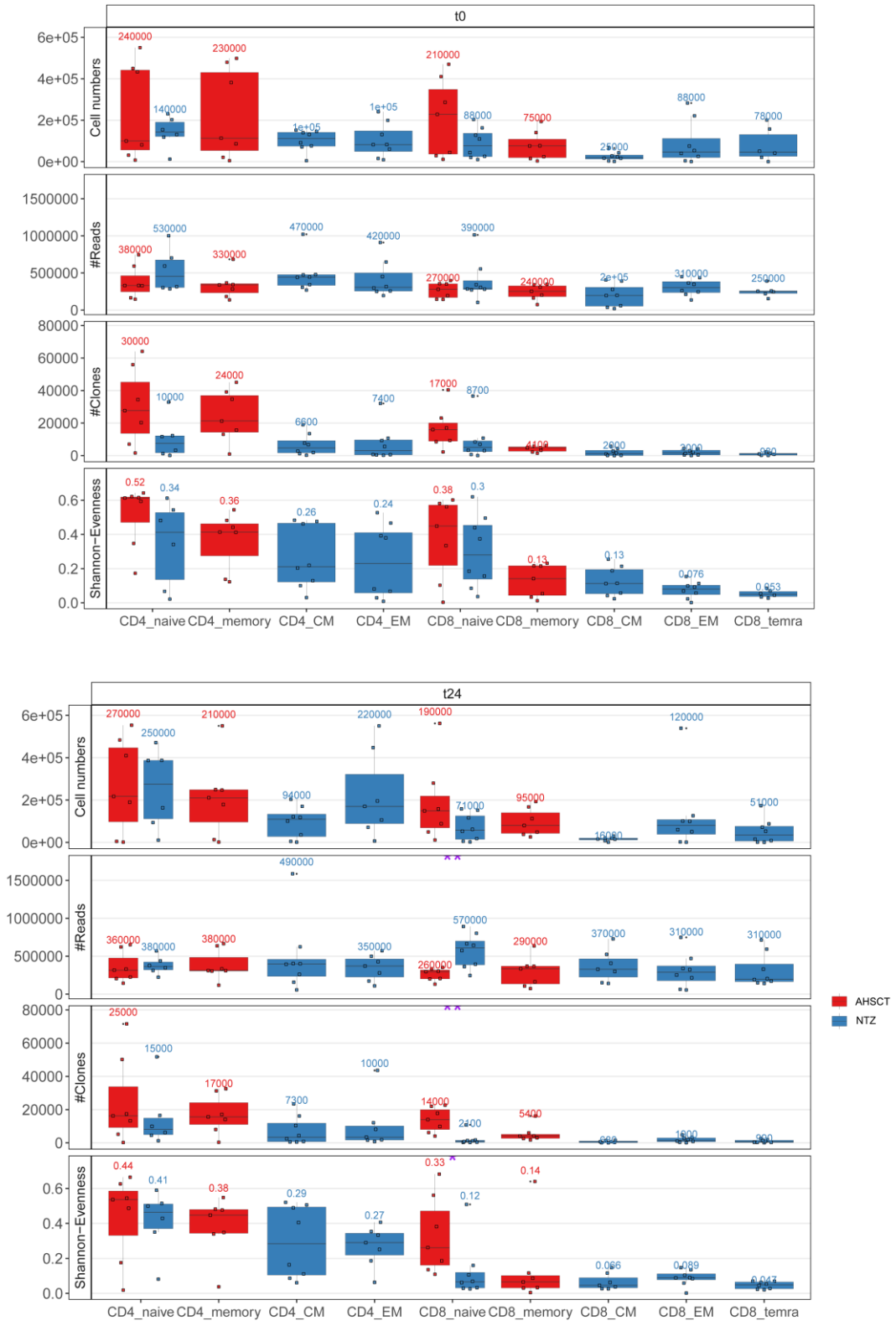

Fig. 39. Clonal statistics in the two groups of patients across timepoints. Cell number, #Reads, #Clones (*y*-axis: absolute values) and Shannon-Evenness of T-cell subpopulations in NTZ (blue) and AHSCT (red) patients at t0 (upper panel) and t24 (lower panel). Mean values are shown for each T-cell subpopulation. Statistical significance was determined by Wilcoxon test (*p<0.05; **p<0.01).

4.1.7. Individuality of the T-cell receptor repertoire variation

Repertoire statistics was evaluated on an individual basis for Natalizumab (Ty12, Ty17, Ty20, Ty21, Ty25, Ty26, Ty29, Ty30) and AHSCT (MS002, MS003, MS020, MS029, MS032, MS034, P) patients, in all T-cell subpopulations at t0 and t24 (Fig. 40). Results did not show any treatment-specific, common molecular trace across patients: no specific trends emerged and each patient showed its own TCR repertoire variation.

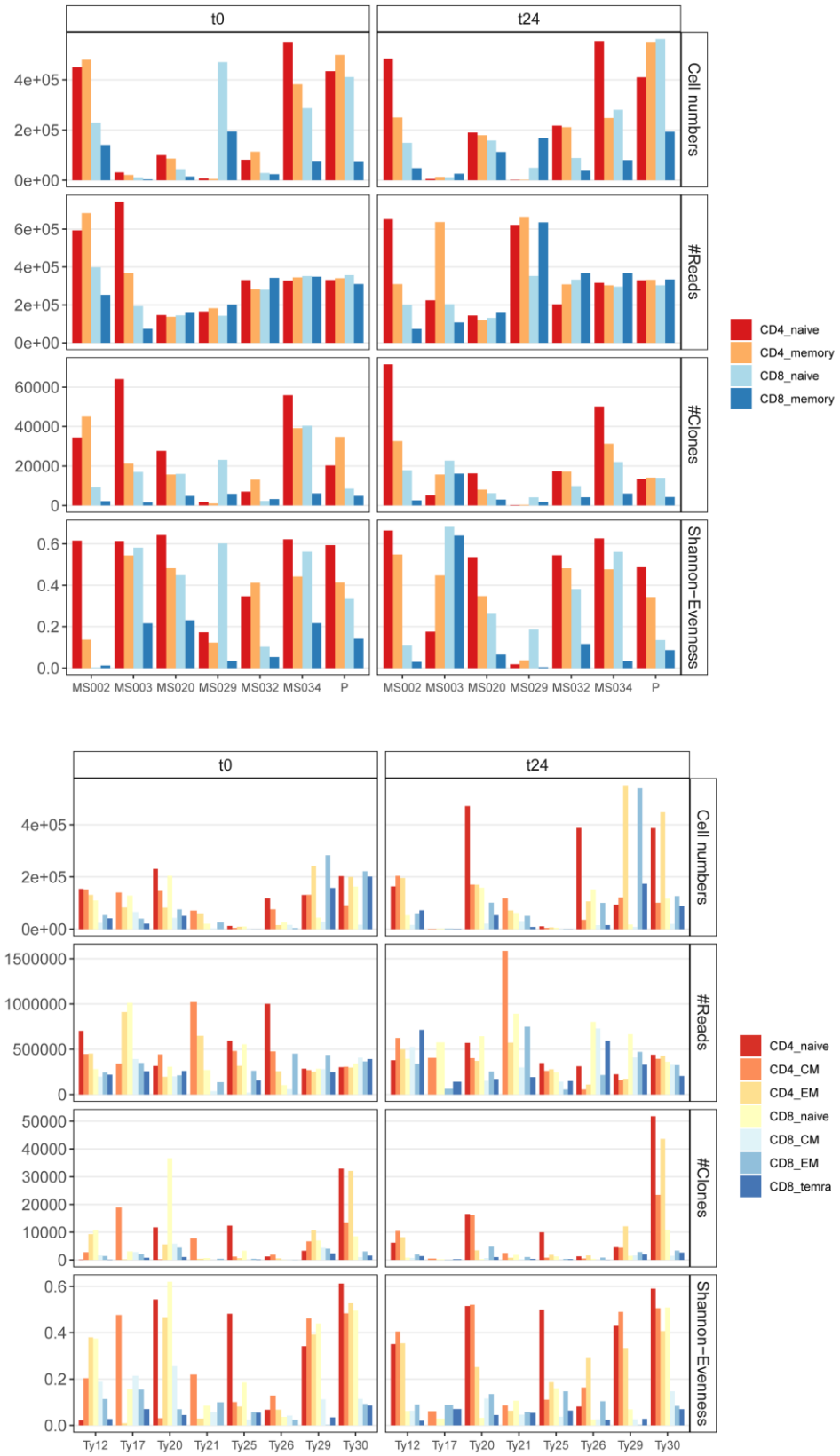

Fig. 40. Individual TCR repertoire dynamics. Cell numbers, number of reads (#Reads), number of clones (#Clones) (y-axis: absolute values) and Shannon-Evenness reported patient by patient for T-cell subpopulations of AHSCT (upper graph) and NTZ (lower graph) patients at t0 (left panel in each graph) and t24 (right panel in each graph). Each bar represents a T-cell subpopulation.

4.1.8. State of the T-cell receptor repertoire clonal expansion

Since the differences in the TCR repertoire variation across timepoints were difficult to detect on an individual basis, the global state of the TCR repertoire clonal expansion was investigated using previously established Hill-based evenness profiles (Greiff V et al., 2015). Hill evenness profiles have been developed in mathematical ecology and allow a fine-grained comparison of clonal expansion across patient TCR repertoires.

Findings showed that the clonal expansion state differed among the two groups of patients for both CD4 and CD8 T-cell subpopulations based on treatment (Fig. 41A). In the light of the documented association of MS susceptibility with the HLA class II haplotype DRB1*1501 (Ballerini C et al., 2004), the clonal expansion variation by HLA-DRB1*1501 type of patients (-/+) was also evaluated. Interestingly, results report a global effect of HLA class II on the entire CD4 T-cell compartment, including both naïve and memory cells (Fig. 41B). No difference in clonal expansion was detected between timepoints.

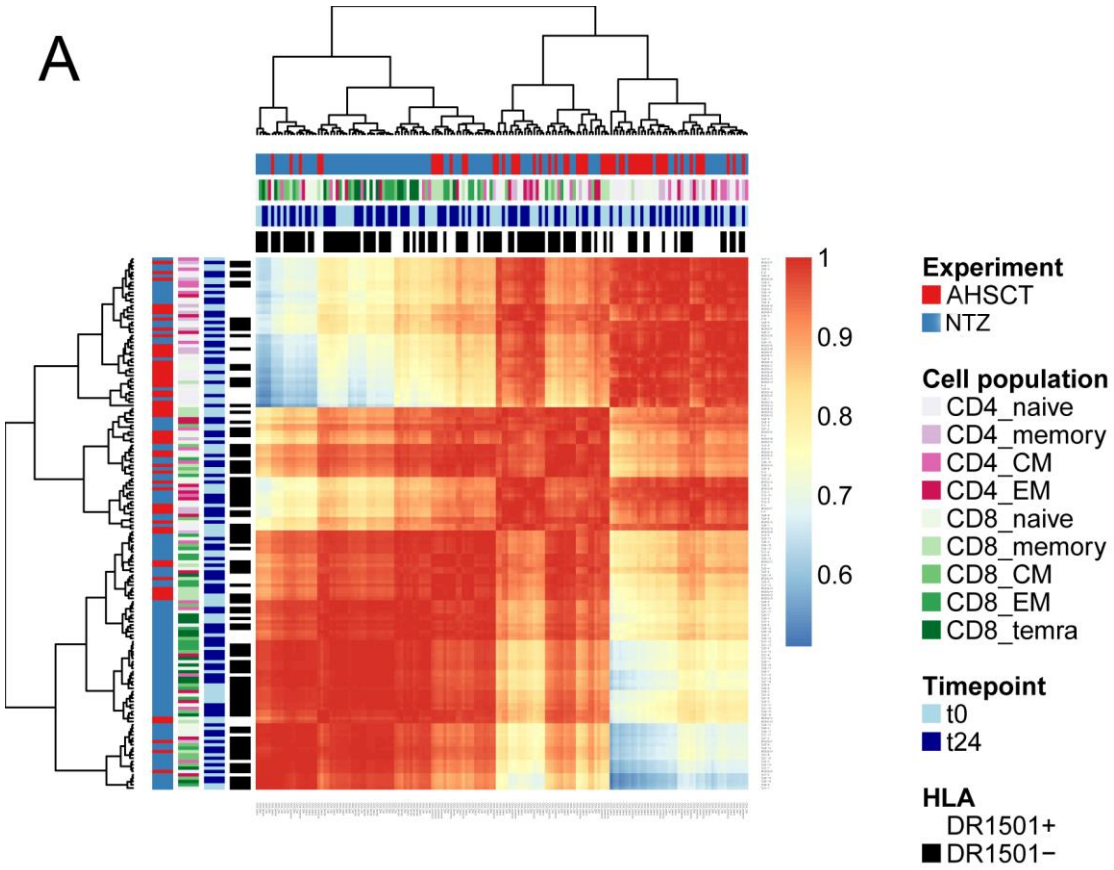
A
1
0.9
0.8
0.7
0.6
Experiment
AHSCT
NTZ
Cell population
CD4_naive
CD4_memory
CD4_CM
CD4_EM
CD8_naive
CD8_memory
CD8_CM
CD8_EM
CD8_temra
Timepoint
t0
t24
HLA
DR1501+
DR1501−

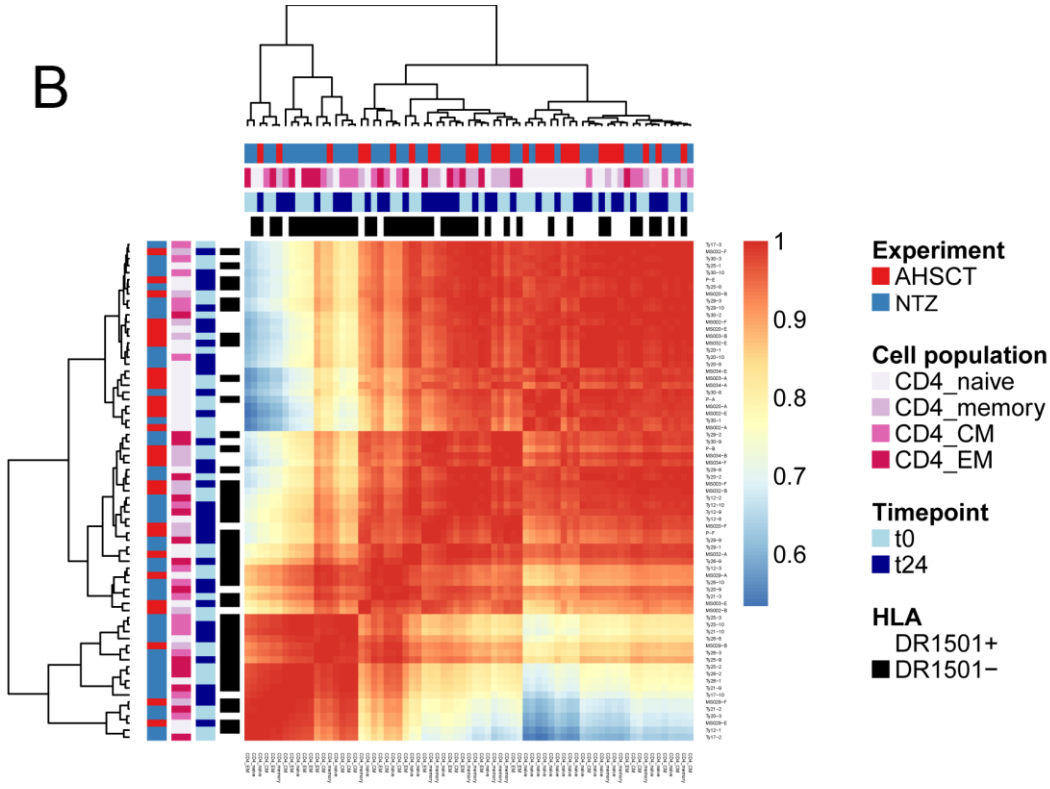
B
1
0.9
0.8
0.7
0.6
Experiment
AHSCT
NTZ
Cell population
CD4_naive
CD4_memory
CD4_CM
CD4_EM
Timepoint
t0
t24
HLA
DR1501+
DR1501−

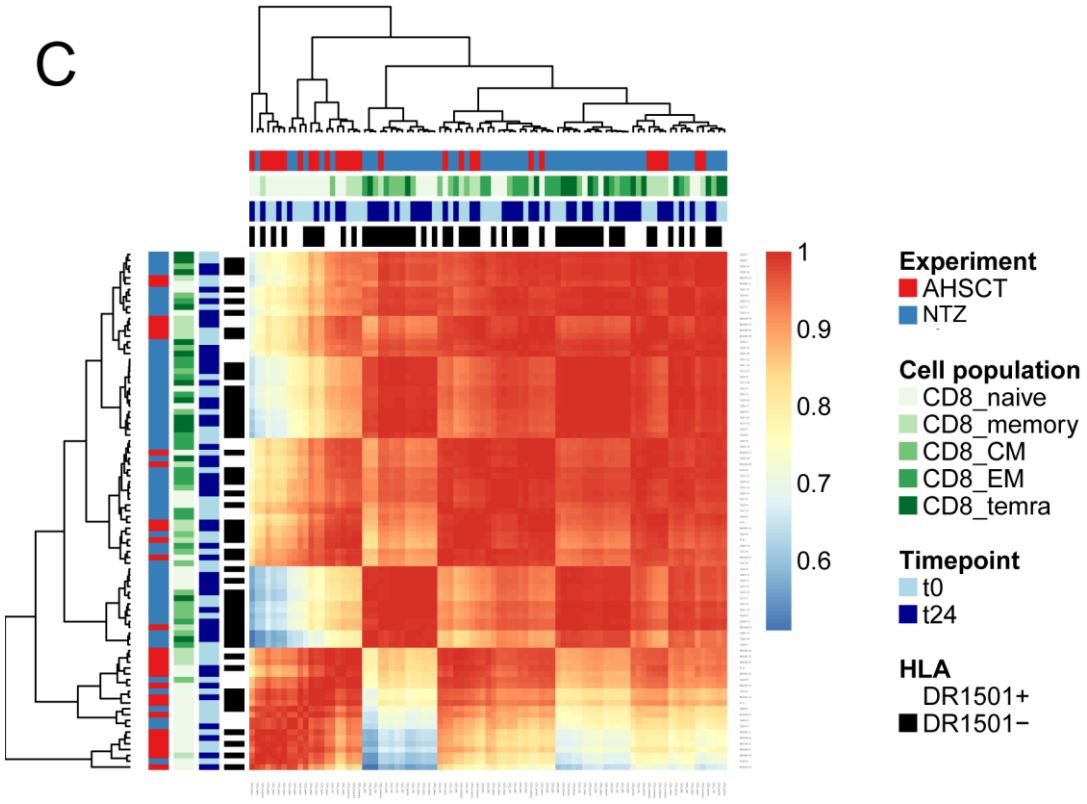

Fig. 41. Global state of TCR clonal expansion in NTZ and AHSCT patients. Heatmap of the Pearson correlation of all evenness profiles (or state of clonal expansion) visualized by all T-cell subpopulations (A) or only by CD4 (B) or CD8 (C). In each heatmap, color bars indicate treatment (AHSCT in red, NTZ in blue), T-cell subpopulation (different shades of pink or green are reported for CD4 or CD8 subpopulations, respectively), timepoint (t0-t24 in light and dark blue, respectively) and HLA class II of patients when DR1501+ (white) or DR1501- (black). The heatmap x-axis labels indicate T-cell subpopulation and the y-axis labels indicate sample name. Hierarchical clustering of evenness profiles was performed using correlation-based distance.

4.1.9. Clonal persistence over treatments

In order to quantify how many TCRβ clones were still in the peripheral blood after Natalizumab and AHSCT, the clonal persistence from t0 to t24 was calculated (see Methods). Fig. 42 reports the clonal persistence as a percentage and scaled by color for all Natalizumab and AHSCT patients. Results showed that the CD4 and CD8 memory compartment has a generally higher clonal persistence compared to the naive compartment. In Natalizumab patients, the percentage of persistent clones across timepoints is higher in CD4 (0.1-18.5%) and CD8 (0.4- 35.8%) memory subpopulations compared to AHSCT patients (0.2-9.6% and 2.2-15.7% in CD4 and CD8 memory cells, respectively). However, some exceptions are present: patient MS032, who received a different conditioning chemotherapy during transplantation compared to the other patients, showed the highest observed percentage of clonal persistence of all AHSCT patients (15.7% in CD8 memory and 9.6% in CD4 memory), whereas in the Natalizumab group Ty17, 391 Ty21 and Ty25 (of whom Ty21 and Ty25 experienced a relapse during treatment) differed from the other Natalizumab patients by showing no or very low clonal persistence in most cell subpopulations.

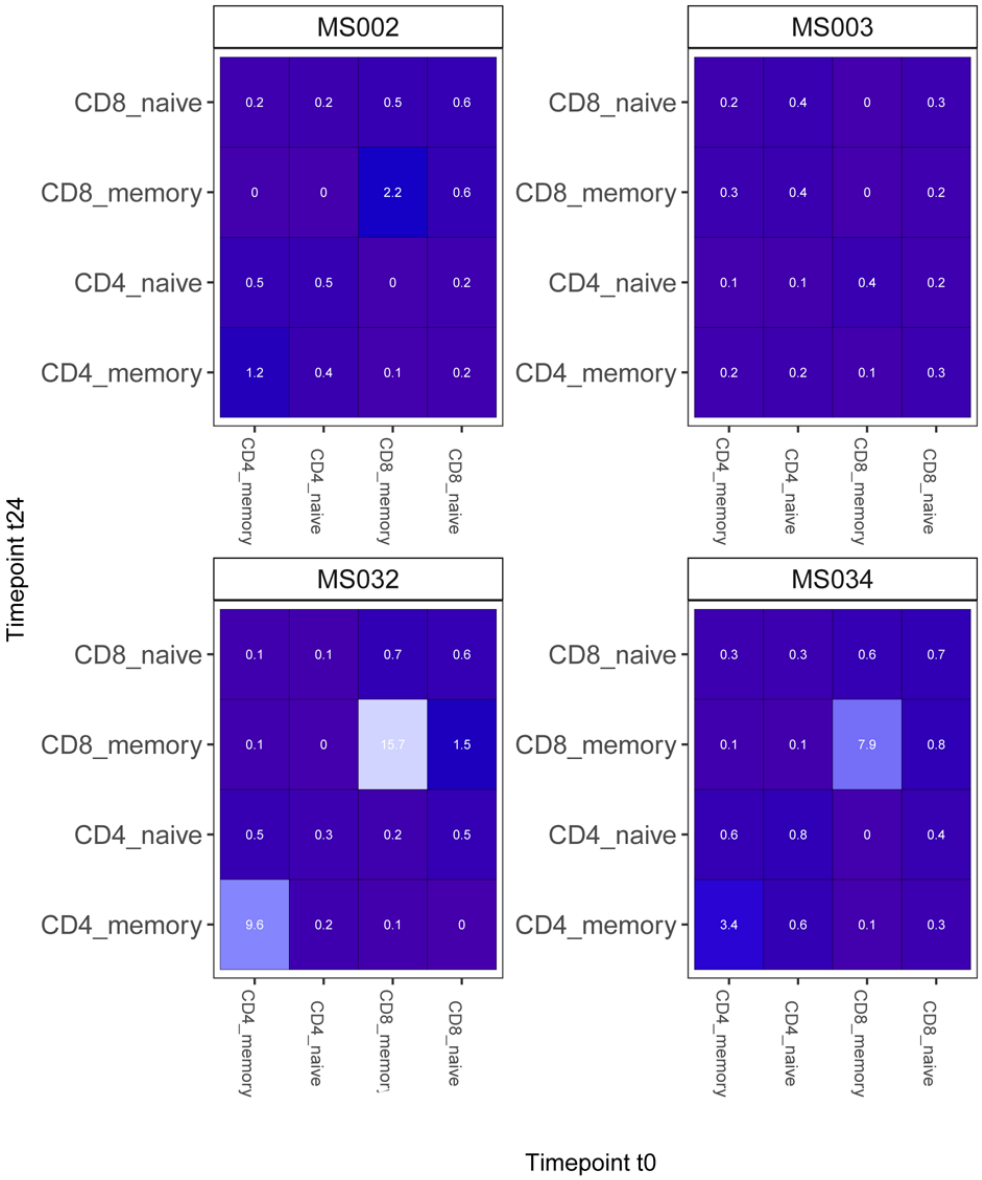
MS002
CD8_naive
CD8_memory
CD4_naive
CD4_memory
0.2 0.2 0.5 0.6
0 0 2.2 0.6
0.5 0.5 0 0.2
1.2 0.4 0.1 0.2
CD4_memory
CD4_naive
CD8_memory
CD8_naive
MS003
0.2 0.4 0 0.3
0.3 0.4 0 0.2
0.1 0.1 0.4 0.2
0.2 0.2 0.1 0.3
MS032
0.1 0.1 0.7 0.6
0.1 0 15.7 1.5
0.5 0.3 0.2 0.5
9.6 0.2 0.1 0
MS034
0.3 0.3 0.6 0.7
0.1 0.1 7.9 0.8
0.6 0.8 0 0.4
3.4 0.6 0.1 0.3
Timepoint t24
Timepoint t0

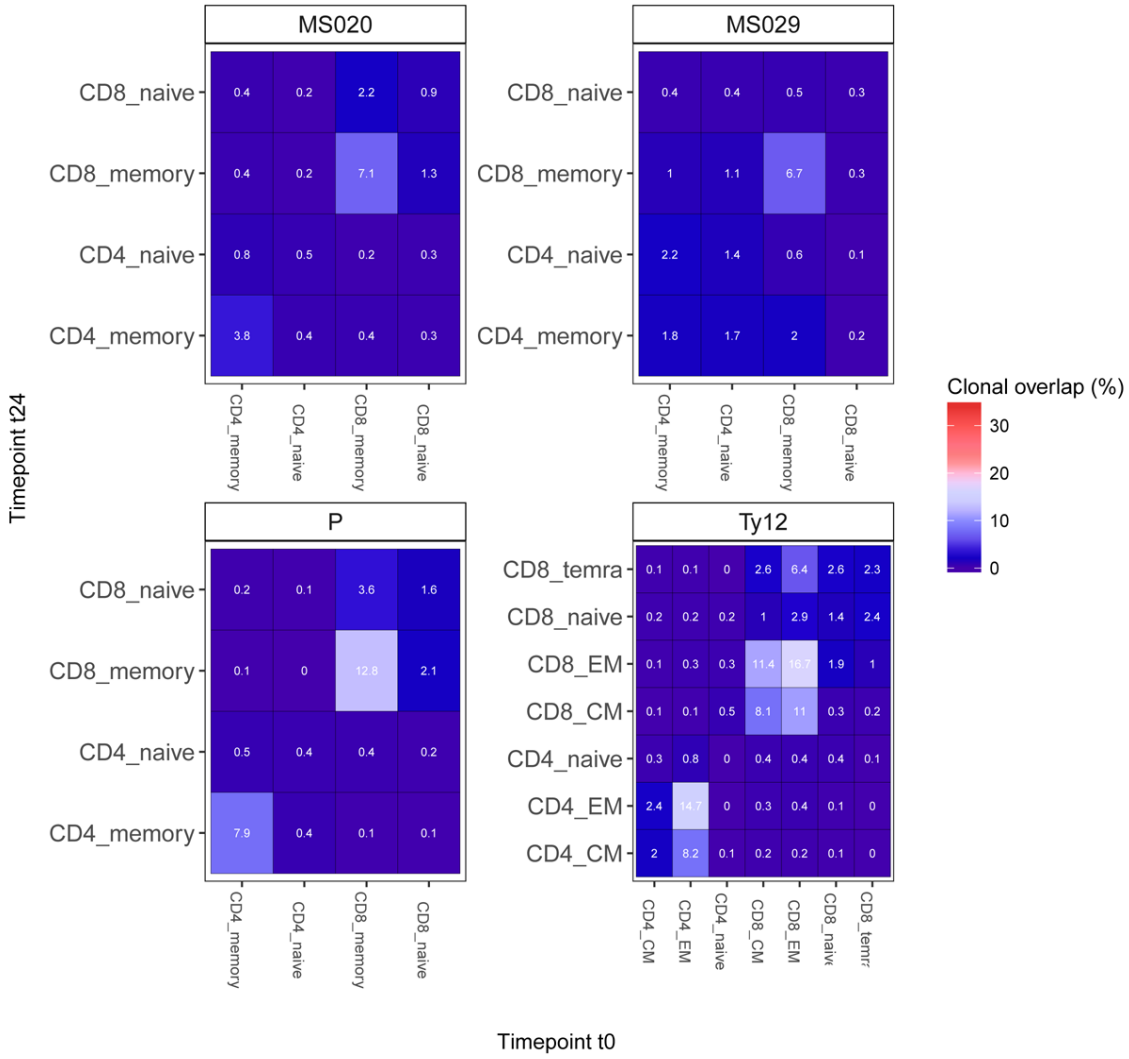
MS020
CD8_naive
CD8_memory
CD4_naive
CD4_memory
0.4 0.2 2.2 0.9
0.4 0.2 7.1 1.3
0.8 0.5 0.2 0.3
3.8 0.4 0.4 0.3
CD4_memory CD4_naive CD8_memory CD8_naive
MS029
CD8_naive
CD8_memory
CD4_naive
CD4_memory
0.4 0.4 0.5 0.3
1 1.1 6.7 0.3
2.2 1.4 0.6 0.1
1.8 1.7 2 0.2
CD4_memory CD4_naive CD8_memory CD8_naive
P
CD8_naive
CD8_memory
CD4_naive
CD4_memory
0.2 0.1 3.6 1.6
0.1 0 12.8 2.1
0.5 0.4 0.4 0.2
7.9 0.4 0.1 0.1
CD4_memory CD4_naive CD8_memory CD8_naive
Ty12
CD8_temra
CD8_naive
CD8_EM
CD8_CM
CD4_naive
CD4_EM
CD4_CM
0.1 0.1 0 2.6 6.4 2.6 2.3
0.2 0.2 0.2 1 2.9 1.4 2.4
0.1 0.3 0.3 11.4 16.7 1.9 1
0.1 0.1 0.5 8.1 11 0.3 0.2
0.3 0.8 0 0.4 0.4 0.4 0.1
2.4 14.7 0 0.3 0.4 0.1 0
2 8.2 0.1 0.2 0.2 0.1 0
CD4_CM CD4_EM CD4_naive CD8_CM CD8_EM CD8_naive CD8_temra
Timepoint t24
Timepoint t0
Clonal overlap (%)
30
20
10
0

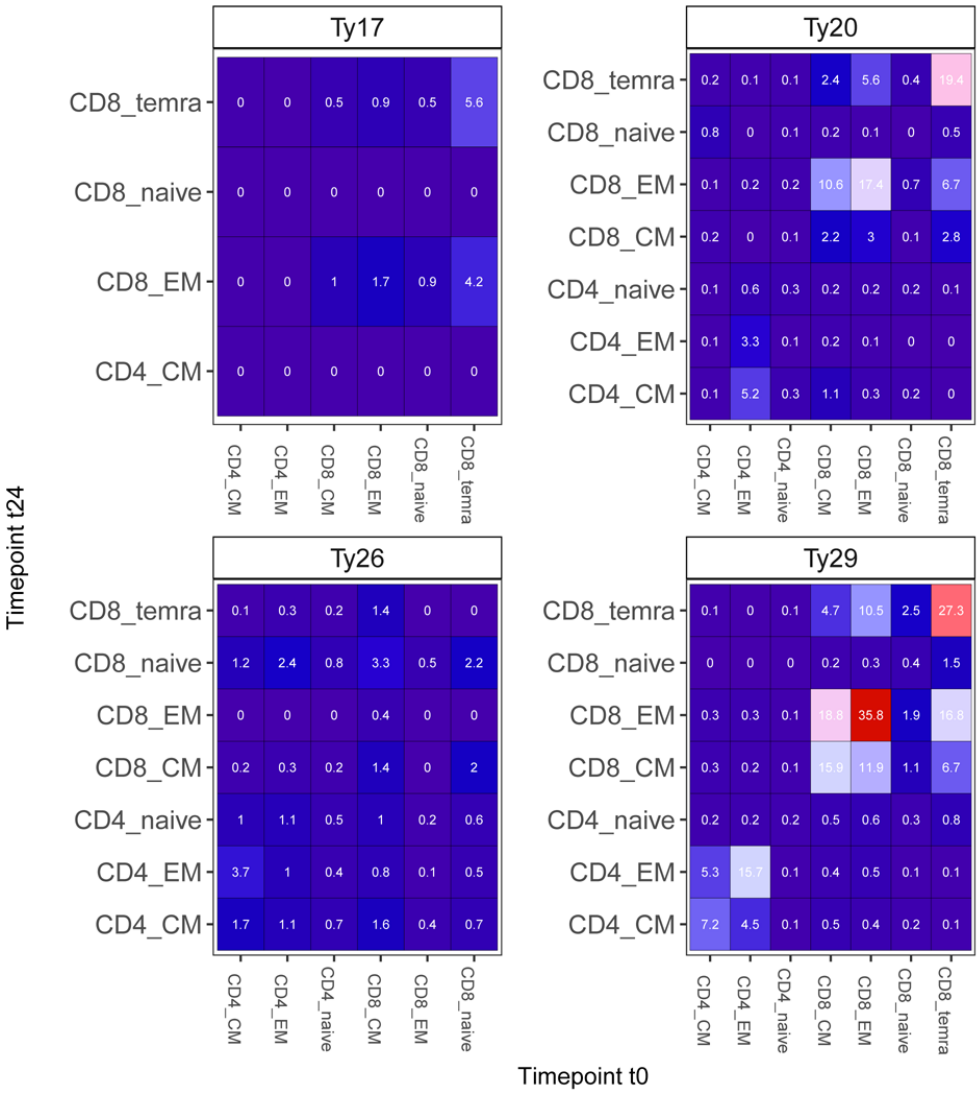
Ty17
CD8_temra 0 0 0.5 0.9 0.5 5.6
CD8_naive 0 0 0 0 0 0
CD8_EM 0 0 1 1.7 0.9 4.2
CD4_CM 0 0 0 0 0 0
CD4_CM CD4_EM CD8_CM CD8_EM CD8_naive CD8_temra
Ty20
CD8_temra 0.2 0.1 0.1 2.4 5.6 0.4 19.4
CD8_naive 0.8 0 0.1 0.2 0.1 0 0.5
CD8_EM 0.1 0.2 0.2 10.6 17.4 0.7 6.7
CD8_CM 0.2 0 0.1 2.2 3 0.1 2.8
CD4_naive 0.1 0.6 0.3 0.2 0.2 0.2 0.1
CD4_EM 0.1 3.3 0.1 0.2 0.1 0 0
CD4_CM 0.1 5.2 0.3 1.1 0.3 0.2 0
CD4_CM CD4_EM CD4_naive CD8_CM CD8_EM CD8_naive CD8_temra
Ty26
CD8_temra 0.1 0.3 0.2 1.4 0 0
CD8_naive 1.2 2.4 0.8 3.3 0.5 2.2
CD8_EM 0 0 0 0.4 0 0
CD8_CM 0.2 0.3 0.2 1.4 0 2
CD4_naive 1 1.1 0.5 1 0.2 0.6
CD4_EM 3.7 1 0.4 0.8 0.1 0.5
CD4_CM 1.7 1.1 0.7 1.6 0.4 0.7
CD4_CM CD4_EM CD4_naive CD8_CM CD8_EM CD8_naive
Ty29
CD8_temra 0.1 0 0.1 4.7 10.5 2.5 27.3
CD8_naive 0 0 0 0.2 0.3 0.4 1.5
CD8_EM 0.3 0.3 0.1 18.8 35.8 1.9 16.8
CD8_CM 0.3 0.2 0.1 15.9 11.9 1.1 6.7
CD4_naive 0.2 0.2 0.2 0.5 0.6 0.3 0.8
CD4_EM 5.3 15.7 0.1 0.4 0.5 0.1 0.1
CD4_CM 7.2 4.5 0.1 0.5 0.4 0.2 0.1
CD4_CM CD4_EM CD4_naive CD8_CM CD8_EM CD8_naive CD8_temra
Timepoint t24
Timepoint t0

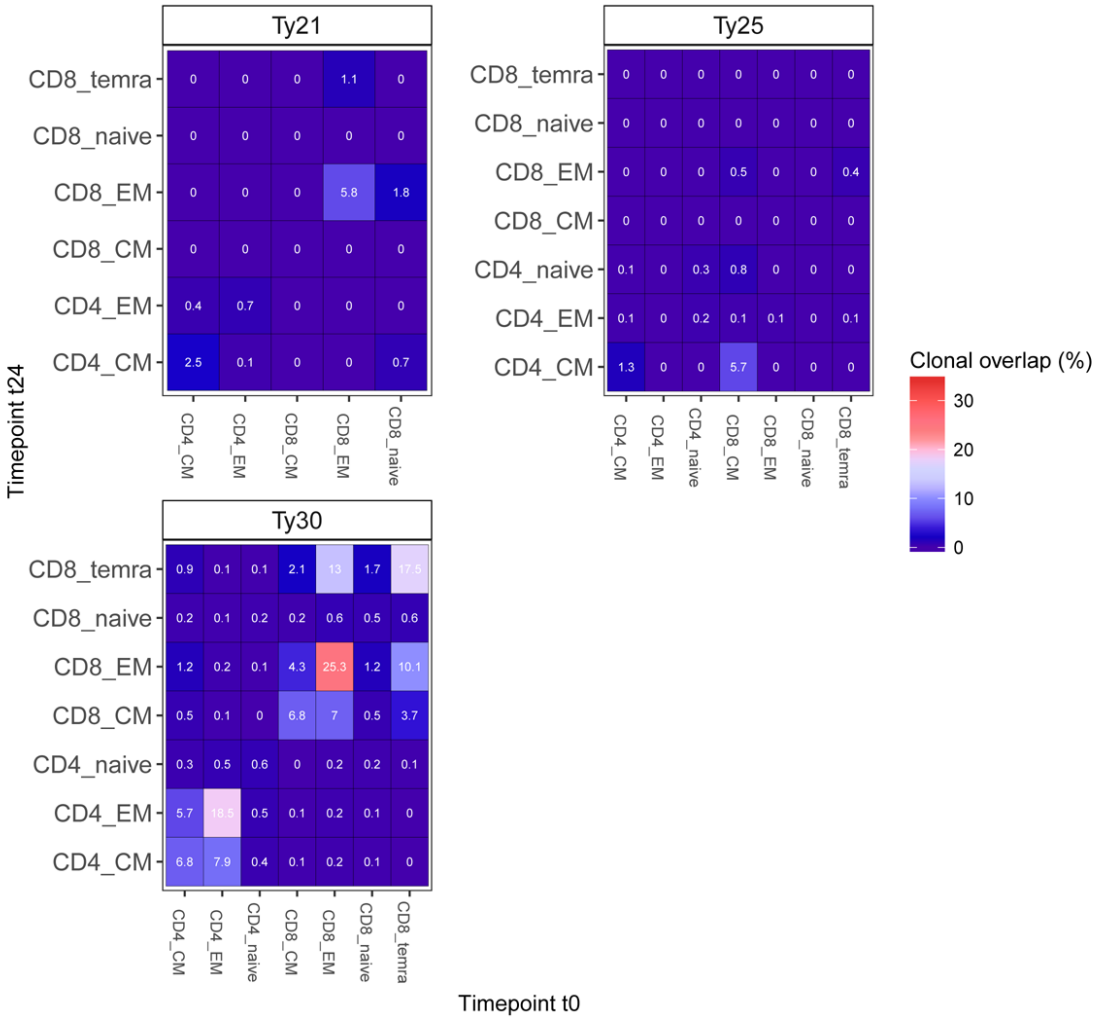

Fig. 42. Clonal persistence across timepoints in Natalizumab and AHSCT patients. Percentage of clonal persistence (overlap) from t0 to t24 is reported for all T-cell subpopulations of AHSCT (MS002, MS003, MS020, MS029, MS032, MS034 and P) and NTZ (Ty12, Ty17, Ty20, Ty21, Ty25, Ty26, Ty29, Ty30) patients.

4.1.10. Public clones across patients over treatments

The percentage of public clones shared across all Natalizumab and AHSCT patients was next investigated. A clone was defined as public when shared among at least two patient repertoires.

Results showed (Fig. 43) a significantly ($p<0.01$) lower absolute number of public clones in CD8 naïve cells of Natalizumab compared to AHSCT at t24.

When investigating those clones that are highly shared across repertoires, a group of clones exclusively shared among AHSCT patients was found in both CD4 and CD8 cell subpopulations (Fig. 44A, B). The percentage of highly-shared public clones was found to be significantly ($p<0.05$) higher in CD4 and in CD8 ($p<0.01$) naïve cells of AHSCT patients compared to Natalizumab at t0 and at t24, respectively (Fig. 44C).

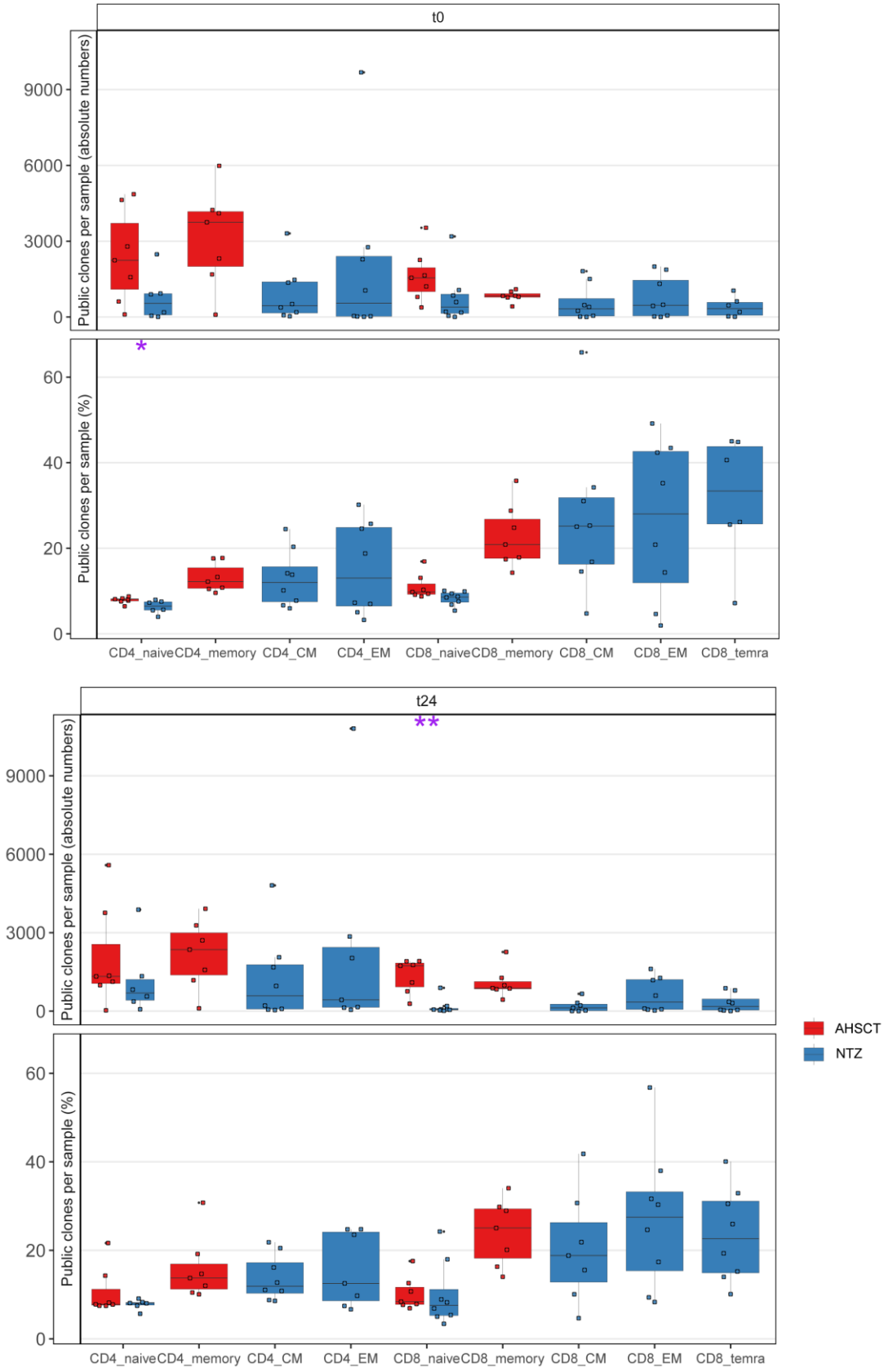

Fig. 43. Public clones statistics in Natalizumab and AHSCT patients. Public clones per sample shown by T-cell subpopulation as absolute number (upper panel in each graph) or as a percentage (lower panel in each graph) in AHSCT (in red) and NTZ (in blue) patients at t0 (upper graph) or t24 (lower graph).

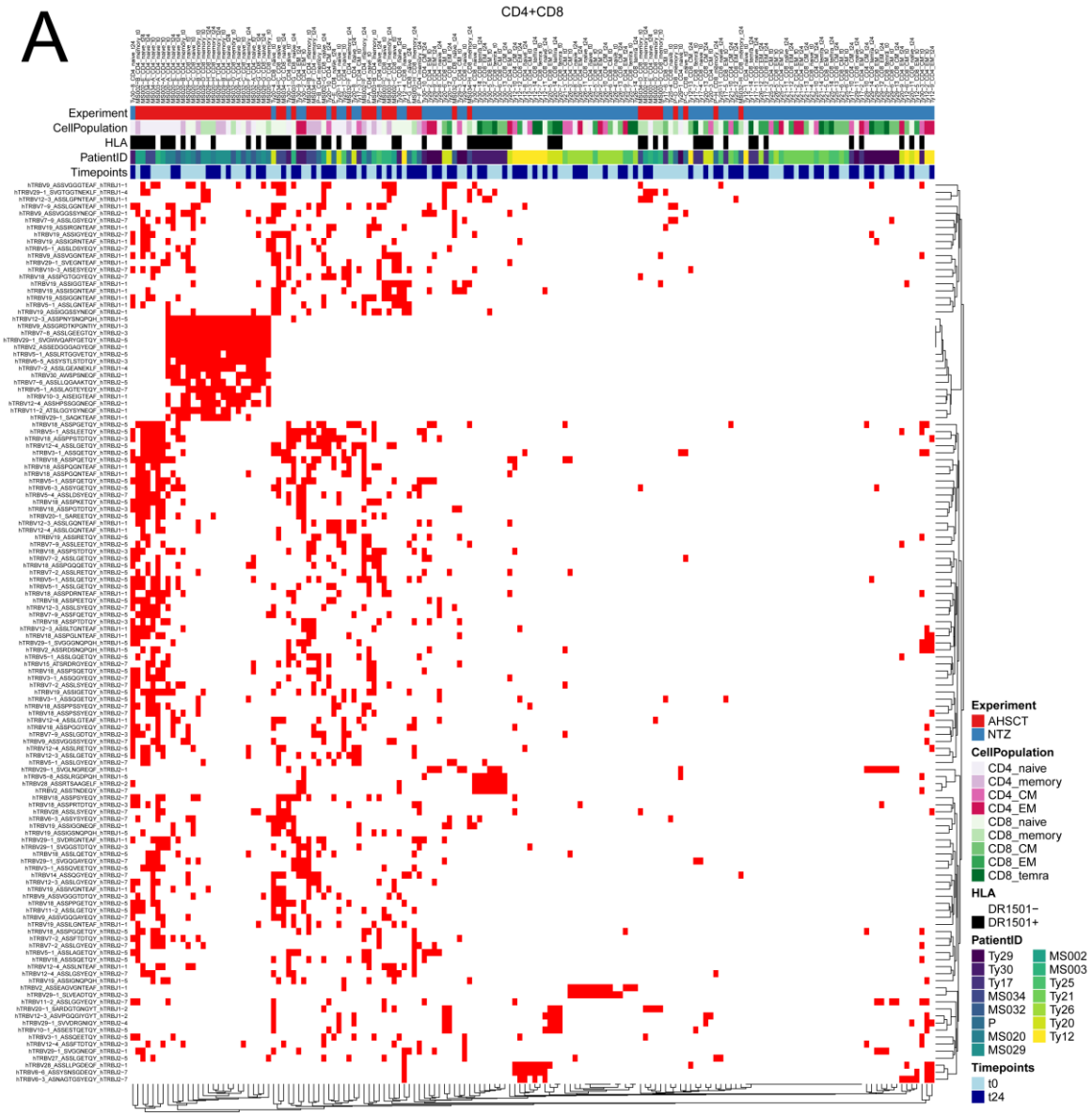
A
CD4+CD8
Experiment
CellPopulation
HLA
PatientID
Timepoints
Experiment
AHSCT
NTZ
CellPopulation
CD4_naive
CD4_memory
CD4_CM
CD4_EM
CD8_naive
CD8_memory
CD8_CM
CD8_EM
CD8_temra
HLA
DR1501−
DR1501+
PatientID
Ty29
Ty30
Ty17
MS034
MS032
P
MS020
MS029
MS002
MS003
Ty25
Ty21
Ty26
Ty20
Ty12
Timepoints
t0
t24

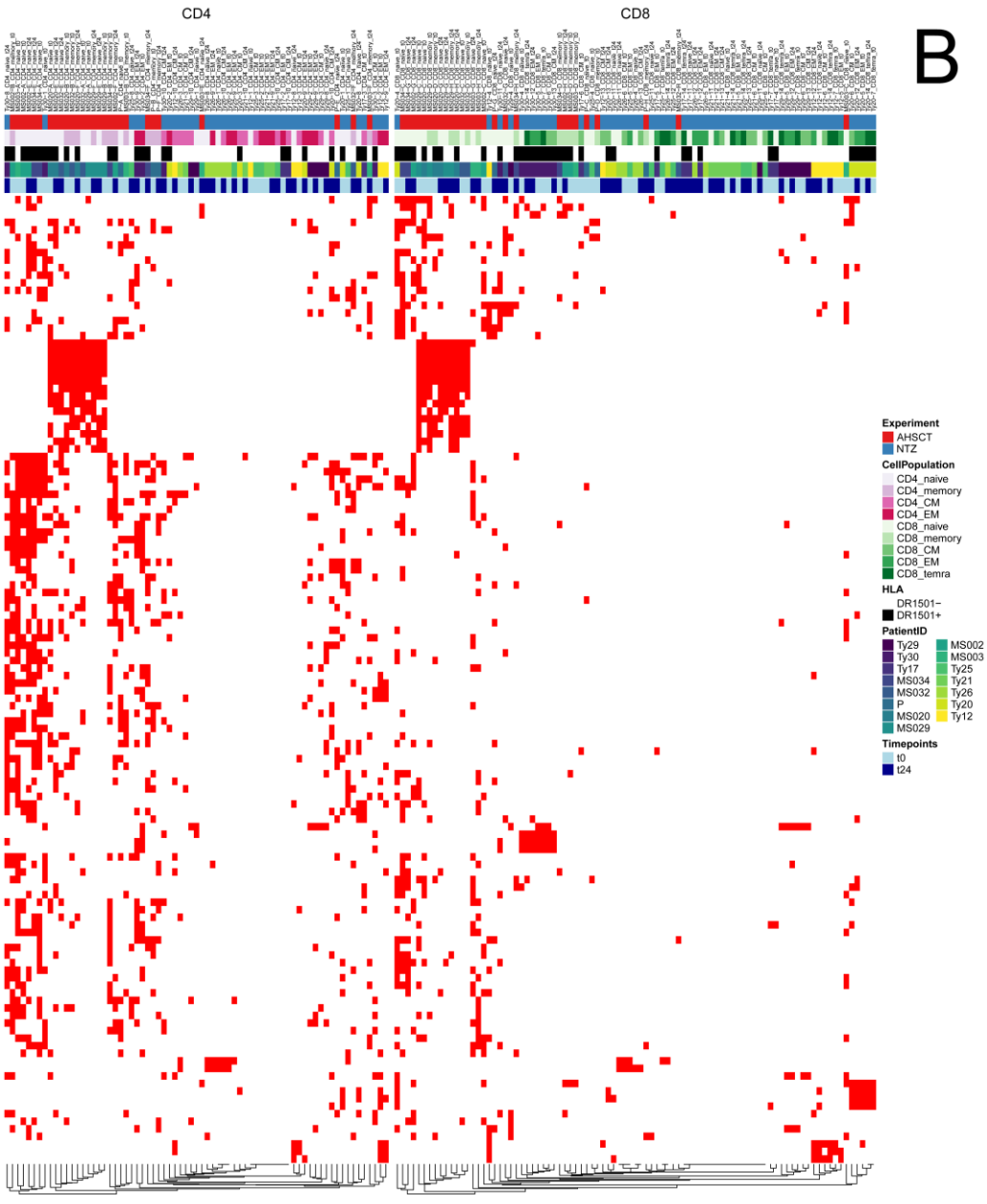
CD4
CD8
B
Experiment
AHSCT
NTZ
CellPopulation
CD4_naive
CD4_memory
CD4_CM
CD4_EM
CD8_naive
CD8_memory
CD8_CM
CD8_EM
CD8_temra
HLA
DR1501−
DR1501+
PatientID
Ty29
Ty30
Ty17
MS034
MS032
P
MS020
MS029
MS002
MS003
Ty25
Ty21
Ty26
Ty20
Ty12
Timepoints
t0
t24

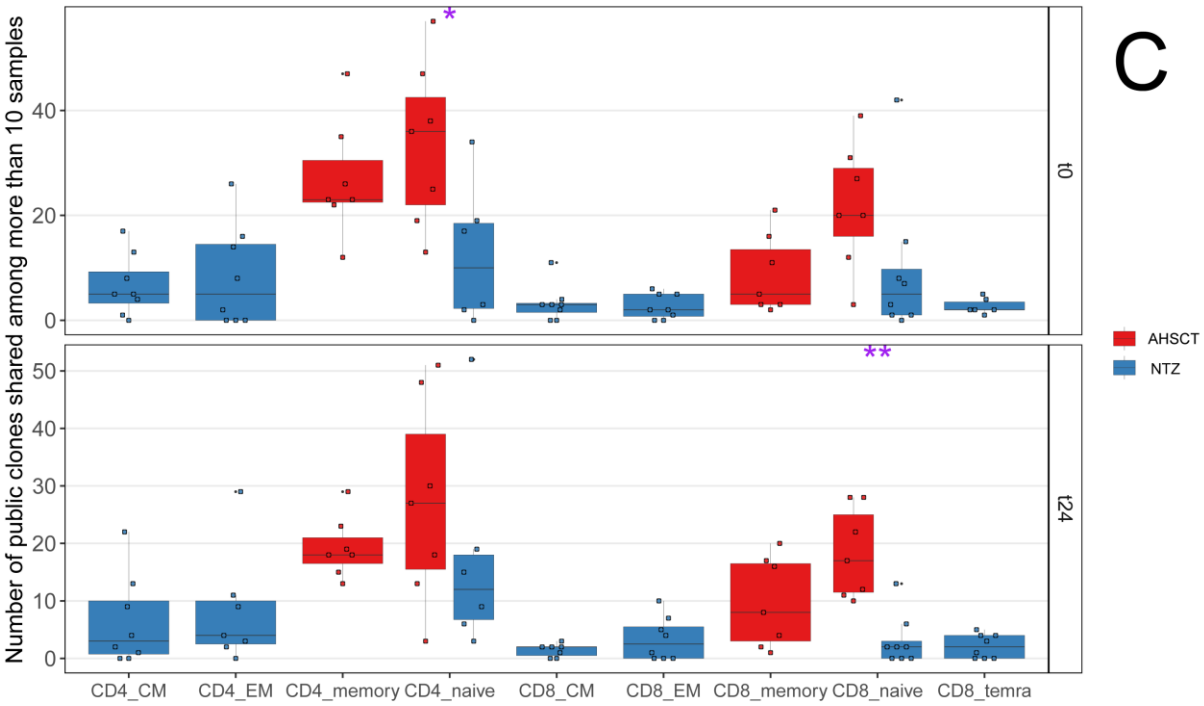

Fig. 44. Graphical representation and statistics of the highly shared public clones in the two groups of patients. TCR clones shared among more than 10 samples visualized by treatment (AHSCT in red, NTZ in blue) in all T-cell subpopulation (A) or in only CD4 or only CD8 (B). CD4 or CD8 subpopulations are reported in different shades of pink or green, respectively. Results are also shown by patient ID, timepoint (t0-t24 in light and dark blue, respectively) and by HLA class II of patients when DR1501+ (white) or DR1501- (black). TCR clones are reported on the left and sample name on the top of the heatmaps. C) Statistics of public clones shared among more than 10 samples (as shown in (A) in the two groups of patients (AHSCT in red, NTZ in blue) shown by T-cell subpopulation at t0 (upper panel) and t24 (lower panel). Statistical significance was determined by Wilcoxon test (*p<0.05).

4.1.11. Architecture of the T-cell receptor repertoire across treatments

The clonal architecture of a TCR repertoire represents the sequence similarity of its composing immune receptor sequences. Therefore, the repertoire architecture is a direct correlate of antigen recognition breadth: when all TCR sequences are similar to each other, the recognition breadth is poor; in contrast, if sequences are more dissimilar, a larger space of the antigenome is covered. In this study, the TCR repertoire architecture was evaluated in each patient before and after Natalizumab or AHSCT, to evaluate the impact of treatments on the TCR repertoire architecture reconstitution. To explore the repertoire architecture in the two groups of patients, clone network and subsequence (k-mer) decomposition analysis were evaluated (see Methods). For the analysis of clone network, the sequence similarity of all sequences was determined by recording for each CDR3 whether is differed in maximally one amino acid from the other CDR3s of TCR repertoire (Miho E et al., 2019; Madi A et al., 2017). In fact, changes of 1 single a.a. may reflect clones with similar antigen binding profile (Dash P et al., 2017). The sequence similarity was measured as a degree of similarity, which is the number of a CDR3 sequence connections. The degree distribution then enumerates the number of CDR3s with an identical degree.

Results showed that AHSCT repertoires have many more clones with degree 0 (no similar clones in the repertoire) compared to Natalizumab repertoires (Fig. 45). This was both true for CD4 and CD8 subpopulations (Fig. 45A). In CD4 subpopulations, the additional clustering by HLA DRB1*1501 was found (Fig. 45B). Of interest, differences in clonal connectivity were mostly located in the private part of TCR repertoires. Public clones showed fewer unconnected clones. Furthermore, the connectivity of public and private clones percentage increased in Natalizumab compared to AHSCT at t24 as evidenced by a significant ($p<0.01$) increase in CD8 naïve compartment connectivity from t0 to t24 (Fig. 46C).

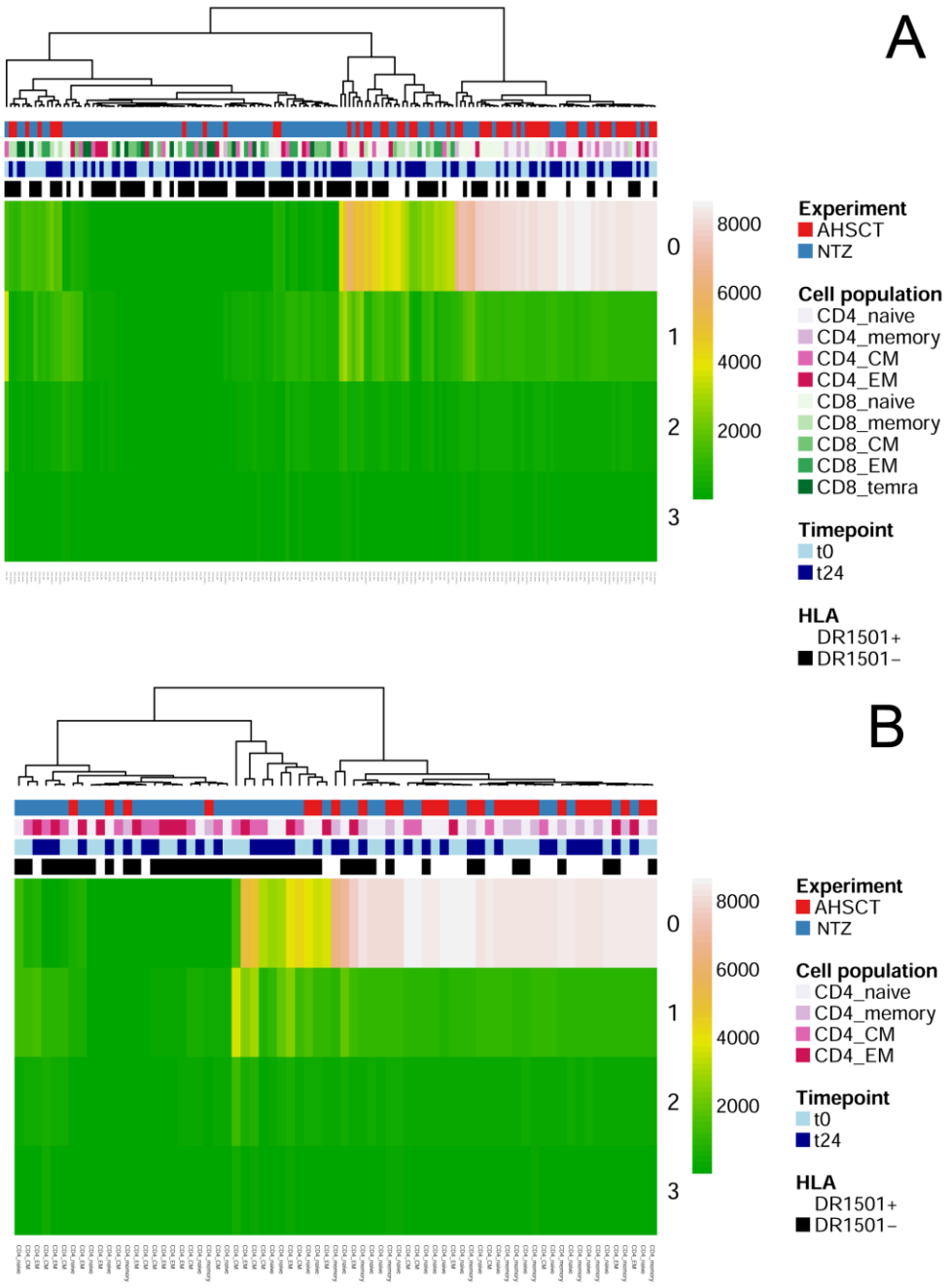

Fig. 45. Degree of CDR3-sequence similarity in TCR repertoires of Natalizumab and AHSCT patients. Heatmaps of the degree distribution of private and public clones of all T-cell subpopulations (A) or of only CD4 (B). The degree of a clone is the number of clones that is similar to (Levenshtein distance [LD] of 1: 1 amino acid [a.a.] change apart). Bars indicate treatment (AHSCT in red, NTZ in blue), T-cell subpopulation, timepoint and HLA class II of patients when DR1501+ (white) or DR1501- (black). The heatmap x-axis labels indicate T-cell subpopulation and the y-axis labels indicate clones degree from 0 (no clones similar to a clone) to 3 (3 clones similar to a given clone). Hierarchical clustering was based on Euclidean distance.

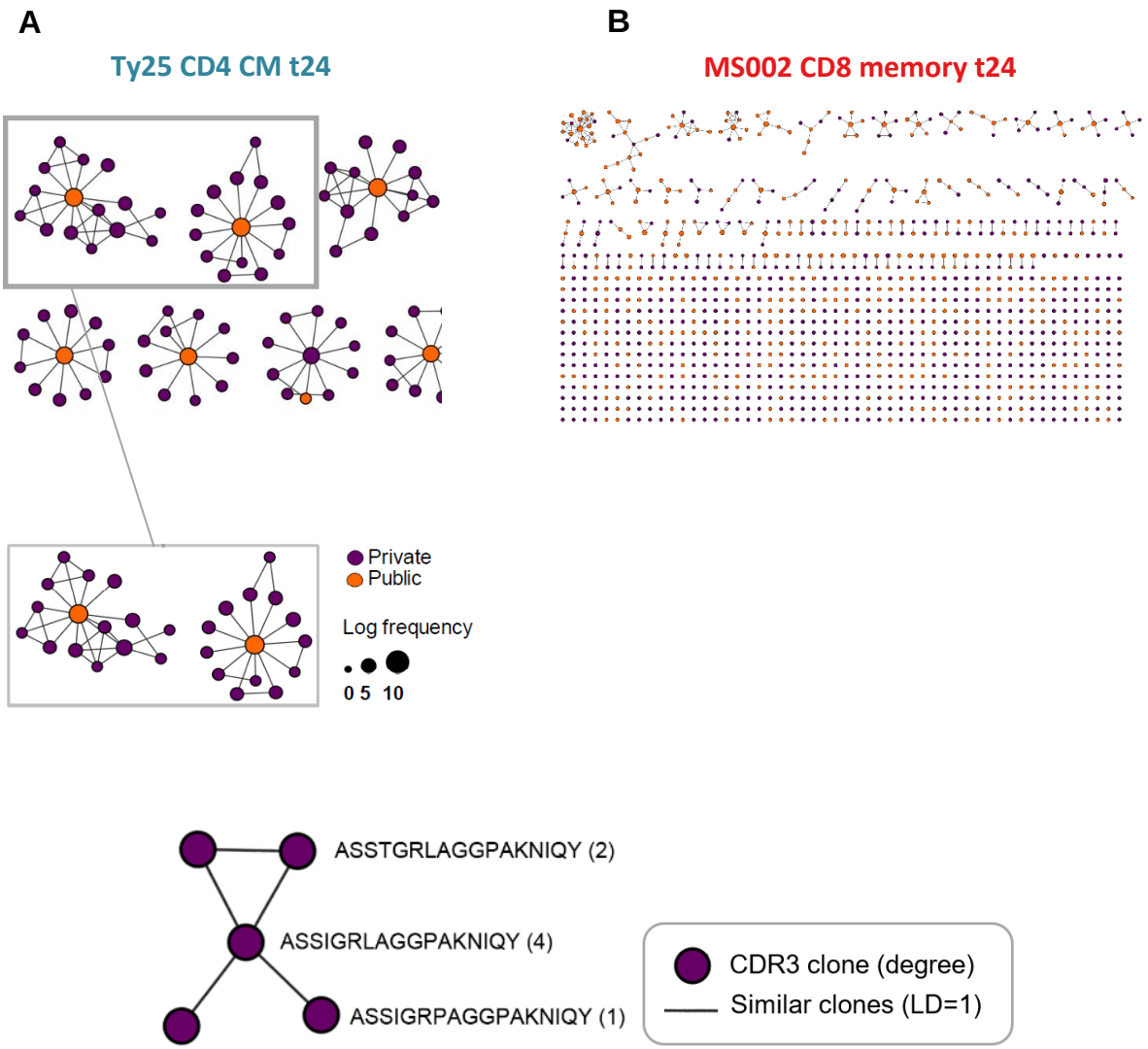
A
Ty25 CD4 CM t24
B
MS002 CD8 memory t24
Private
Public
Log frequency
0 5 10
ASSTGRLAGGPAKNIQY (2)
ASSIGRLAGGPAKNIQY (4)
ASSIGRPAGGPAKNIQY (1)
CDR3 clone (degree)
Similar clones (LD=1)

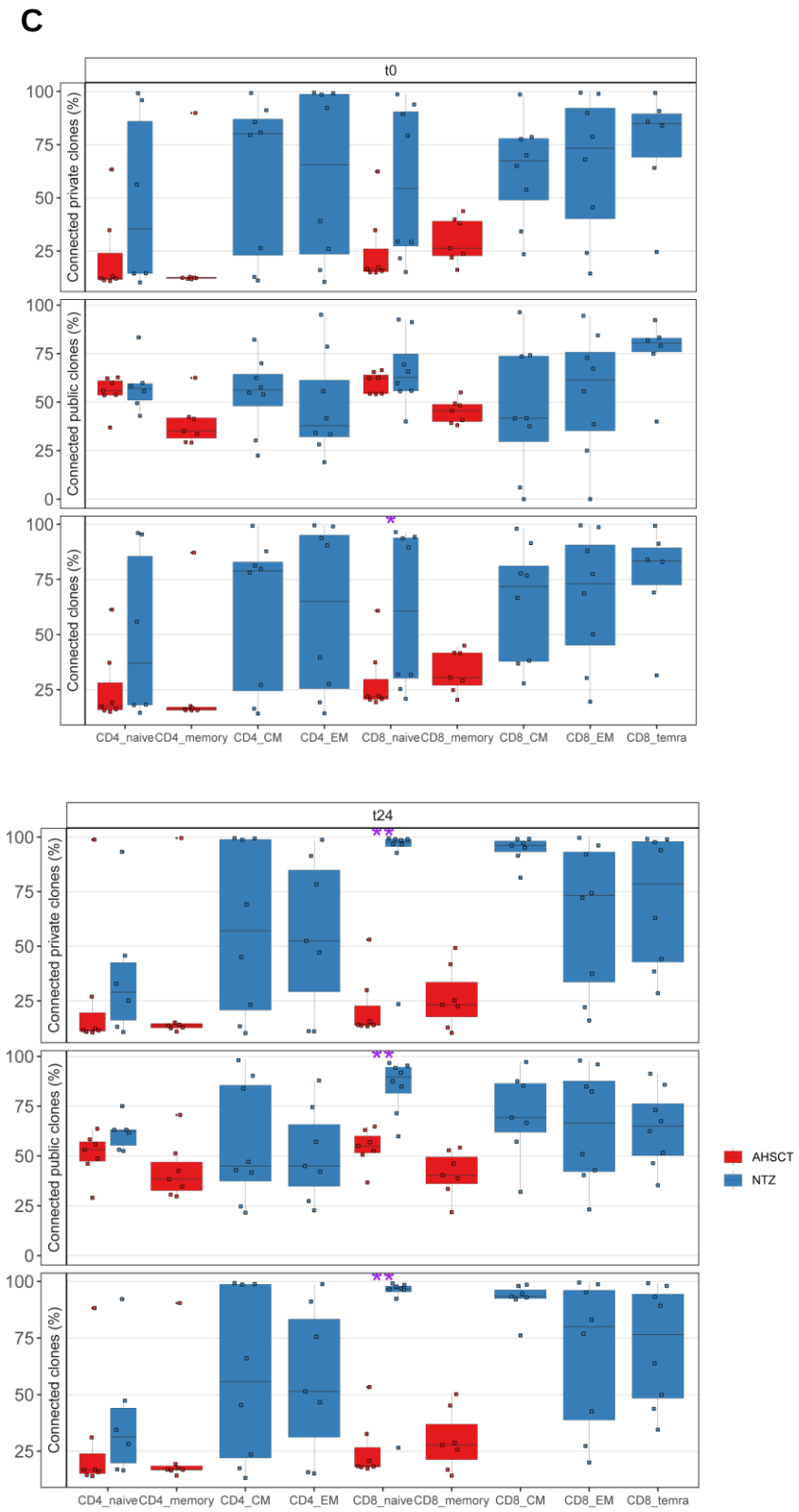

Fig. 46. Clone network representation and statistics in NTZ and AHSCT patients. A, B) Representative TCR repertoire architectures, displayed as clone networks, of the NTZ patient Ty25, CD4 CM cells, t24 and of the AHSCT patient MS002, CD8 memory cells, t24. Each node is an amino acid CDR3 sequence (CDR3-a.a.) and links between nodes connect CDR3s-a.a. based on LD = 1. Node size scales with log clone frequency and node color indicate private (purple) or public (orange) clones (see legend). C) Percentage of connected private (upper panel), public (middle panel) or all (lower panel) clones in T-cell subpopulations of AHSCT (in red) and NTZ (in blue) patients at t0 (left) and t24 (right). Statistical significance was determined by Wilcoxon test (*p<0.05; **p<0.01).

To extend the investigation of TCR repertoire architecture in patients, the similarity of CDR3 subsequence distribution across repertoires was also analyzed (Greiff V et al., 2017). In particular, the TCR sequence similarity was evaluated across Natalizumab treatment or AHSCT, timepoints (from t0 to t24), T-cell subpopulation and haplotype, basing on subsequence length of 3 amino acids (k-mers where k=3 or "3-mers"). All CDR3 sequences of each repertoire were cut into overlapping 3-mers which were then aggregated to calculate the frequency of each 3-mers. 3-mer frequency was analyzed across repertoires by correlation. Results showed that AHSCT patients have a higher TCR subsequence similarity than Natalizumab patients (Fig. 47), indicating higher preservation of repertoire architecture across AHSCT patients.

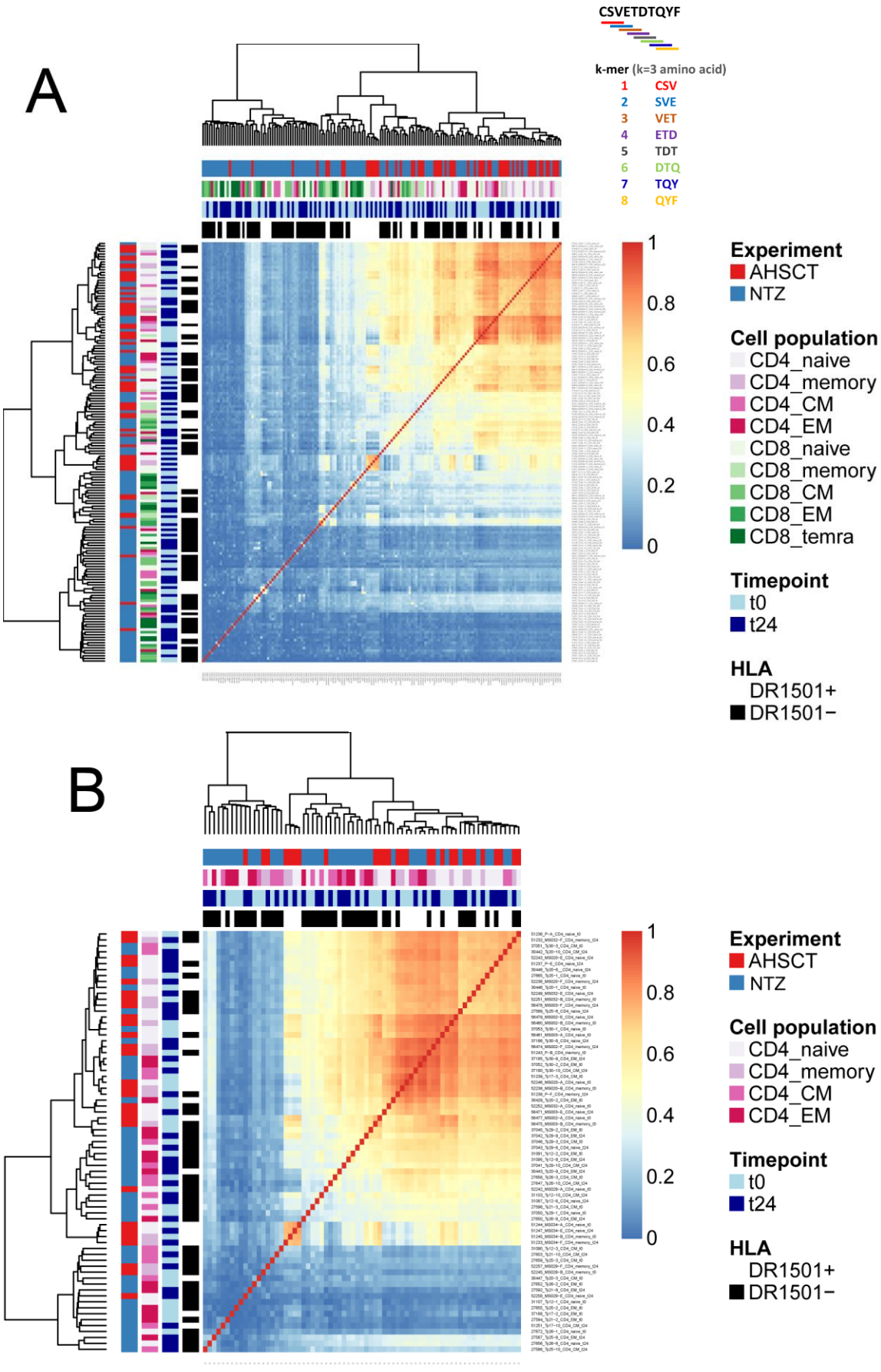
A
CSVETDTQYF
k-mer (k=3 amino acid)
1 CSV
2 SVE
3 VET
4 ETD
5 TDT
6 DTQ
7 TQY
8 QYF
1
0.8
0.6
0.4
0.2
0
Experiment
AHSCT
NTZ
Cell population
CD4_naive
CD4_memory
CD4_CM
CD4_EM
CD8_naive
CD8_memory
CD8_CM
CD8_EM
CD8_temra
Timepoint
t0
t24
HLA
DR1501+
DR1501−
B
1
0.8
0.6
0.4
0.2
0
Experiment
AHSCT
NTZ
Cell population
CD4_naive
CD4_memory
CD4_CM
CD4_EM
Timepoint
t0
t24
HLA
DR1501+
DR1501−

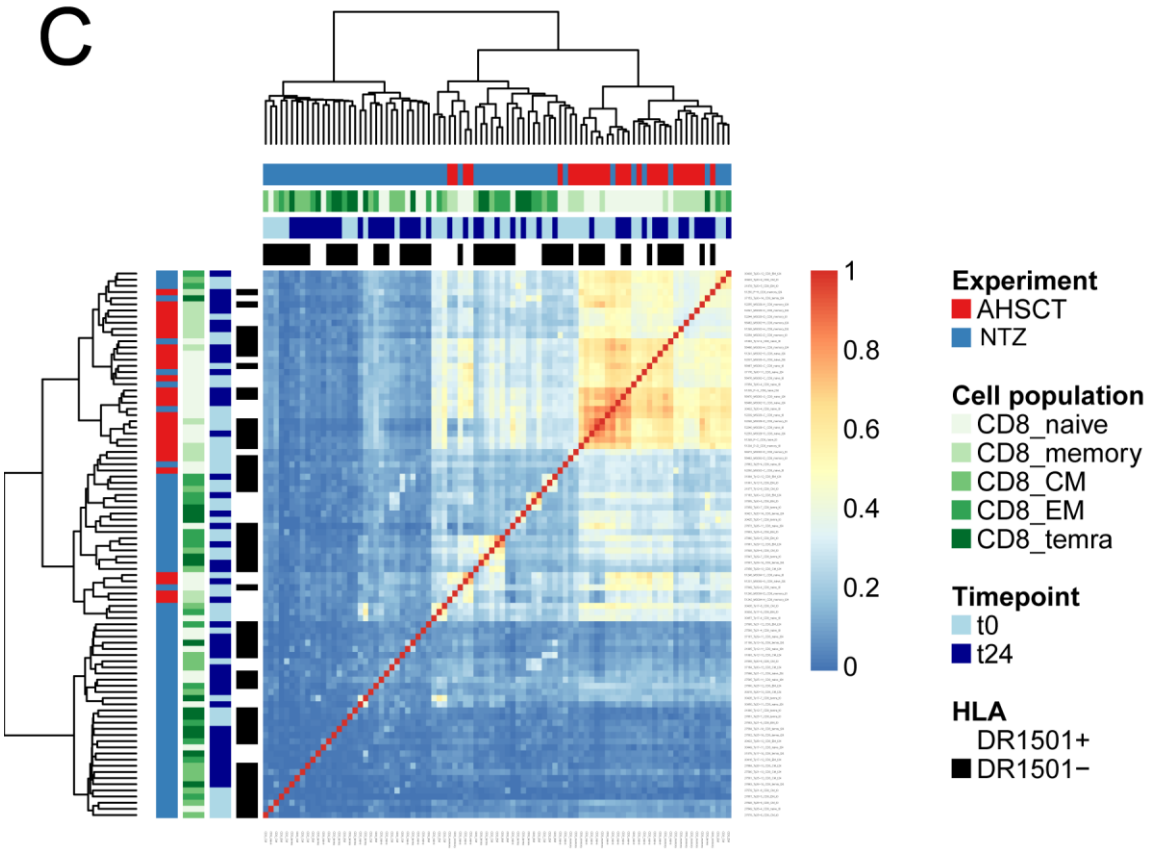

Fig. 47. CDR3 subsequence (k-mers) decomposition of NTZ and AHSCT TCR repertoires. Heatmap of the Pearson correlation of CDR3 k-mer decomposition profiles in all T-cell subpopulations (A) or in only CD4 (B) or CD8 (C) subpopulations. Color bars indicate treatment (AHSCT in red, NTZ in blue), T-cell subpopulation (different shades of pink or green are reported for CD4 or CD8 subpopulations, respectively), timepoint (t0-t24 in light and dark blue, respectively) and HLA class II of patients when DR1501+ (white) or DR1501- (black). The heatmap x-axis labels indicate T-cell subpopulation and the y-axis labels indicate sample name. Hierarchical clustering of evenness profiles was performed on correlation-based distance.

4.1.12. V gene usage variation before and after treatments

V gene usage of patients TCR repertoires was evaluated before and after 24 months of Natalizumab treatment or from AHSCT. Results did not show any variation in V gene usage before and after treatments or across timepoints (Fig. 48).

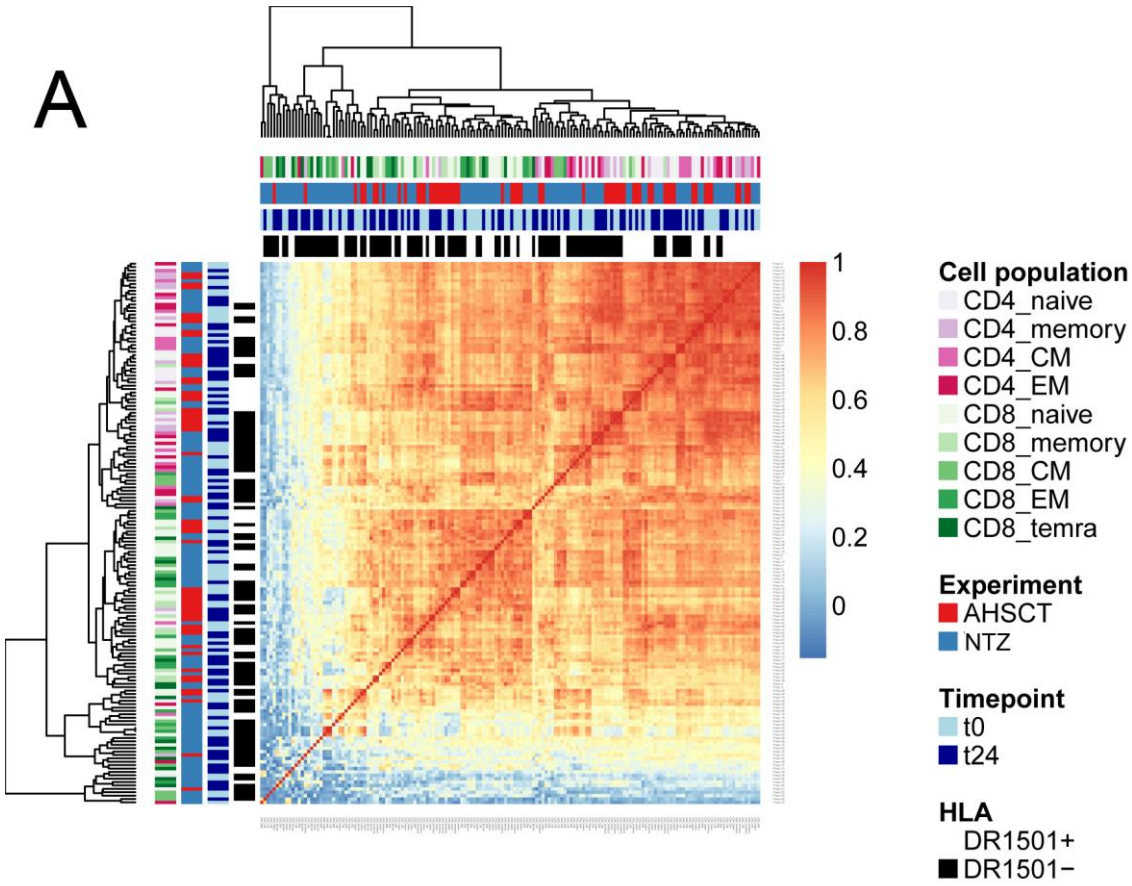

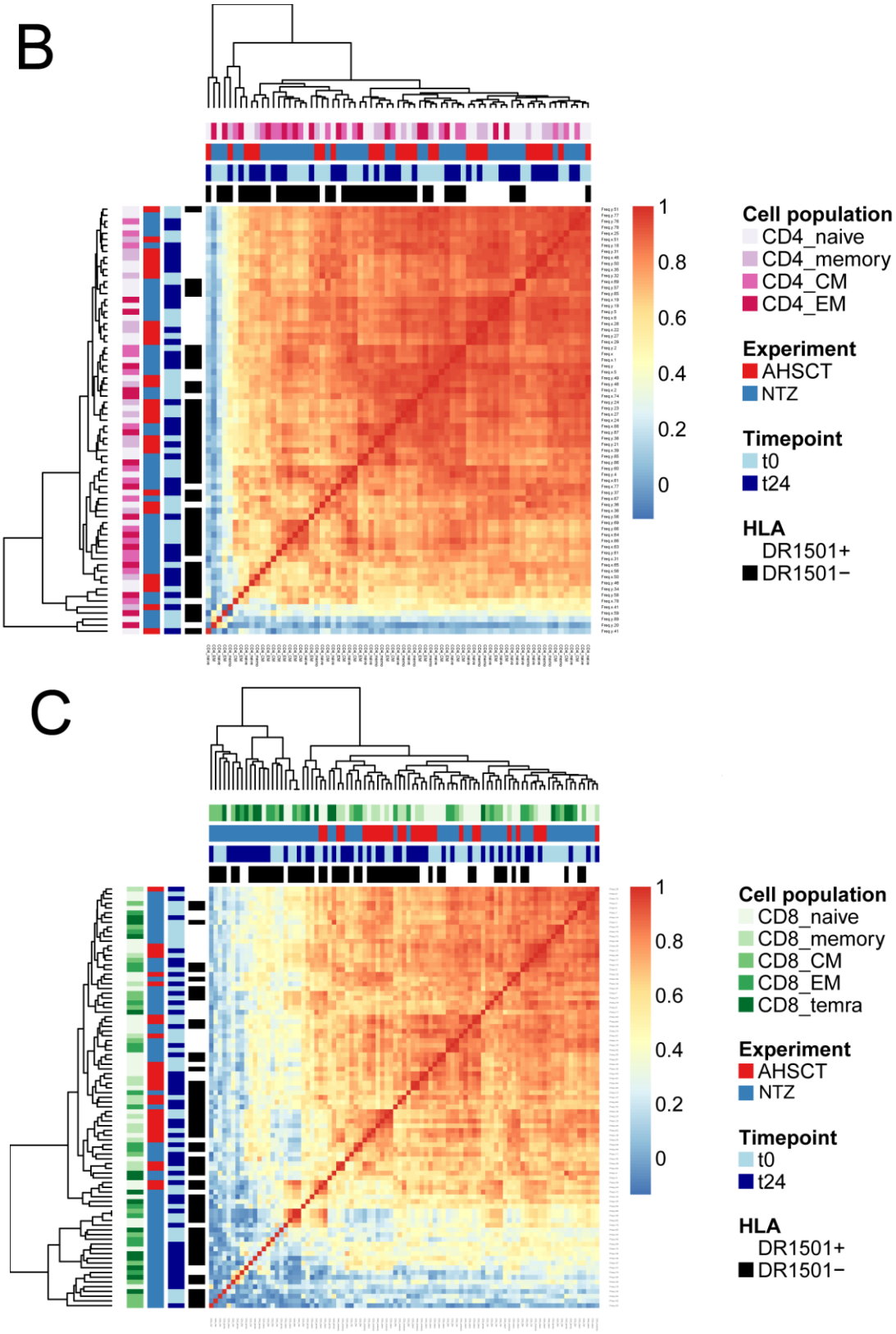

Fig. 48. V gene usage between RRMS treatments and across timepoints. Heatmap of the Pearson correlation of V gene usage. Bars indicate treatment (AHSCT in red, NTZ in blue), CD4 (A) or CD8 (B) T-cell subpopulation, timepoint and HLA class II of patients when DR1501+ (white) or DR1501- (black). The heatmap x-axis labels indicate T-cell subpopulation and the y-axis labels indicate sample name. Hierarchical clustering was performed using correlation-based distance.

4.1.13. Shared sequences with public T-cell receptor databases

Given the suggested association between several viruses, e.g. EBV (Lossius A et al., 2014), with MS risk development and since Natalizumab and AHSCT expose patients to the risk of viral reactivation, the CDR3 sequence overlap between our dataset and three public CDR3 databases was evaluated. The databases are: McPAS-TCR (Tickotsky N et al., 2017), VDJdb (Shugay M et al., 2018) and the TCRβ sequencing dataset from the work of Jelcic I et al. (Jelcic I et al., 2018), who identified a population of proliferative peripheral T cells that share clones with MS lesions (Planas R et al., 2018). McPAS-TCR and VDJdb store TCR clones of known disease association and/or antigen specificity. First, the databases were characterized. At time of download, McPAS-TCR (Fig. 49A) included 1297 sequences putatively associated with autoimmune diseases, 6979 associated with pathogens out of which most are influenza, Cytomegalovirus (CMV), EBV and few MS-associated (118). VDJdb (Fig. 49B), including a total of 2459 human-associated sequences, stored several viral-associated CDR3s, out of which CMV (5776), human immunodeficiency viruses-1 (HIV-1) (2637) and EBV (1825)-associated CDR3s are the most represented. The Jelcic I et al.-dataset (Fig. 49C) reported information on patient origin (MS1 and MS2), CD4/CD8 memory cells, peripheral or brain-infiltrating cells and auto-proliferative or non auto-proliferative cells as previously described by authors (Jelcic I et al., 2018). The highest number of CDR3s (60449) was identified among the non-proliferative PBMCs of patient MS2.

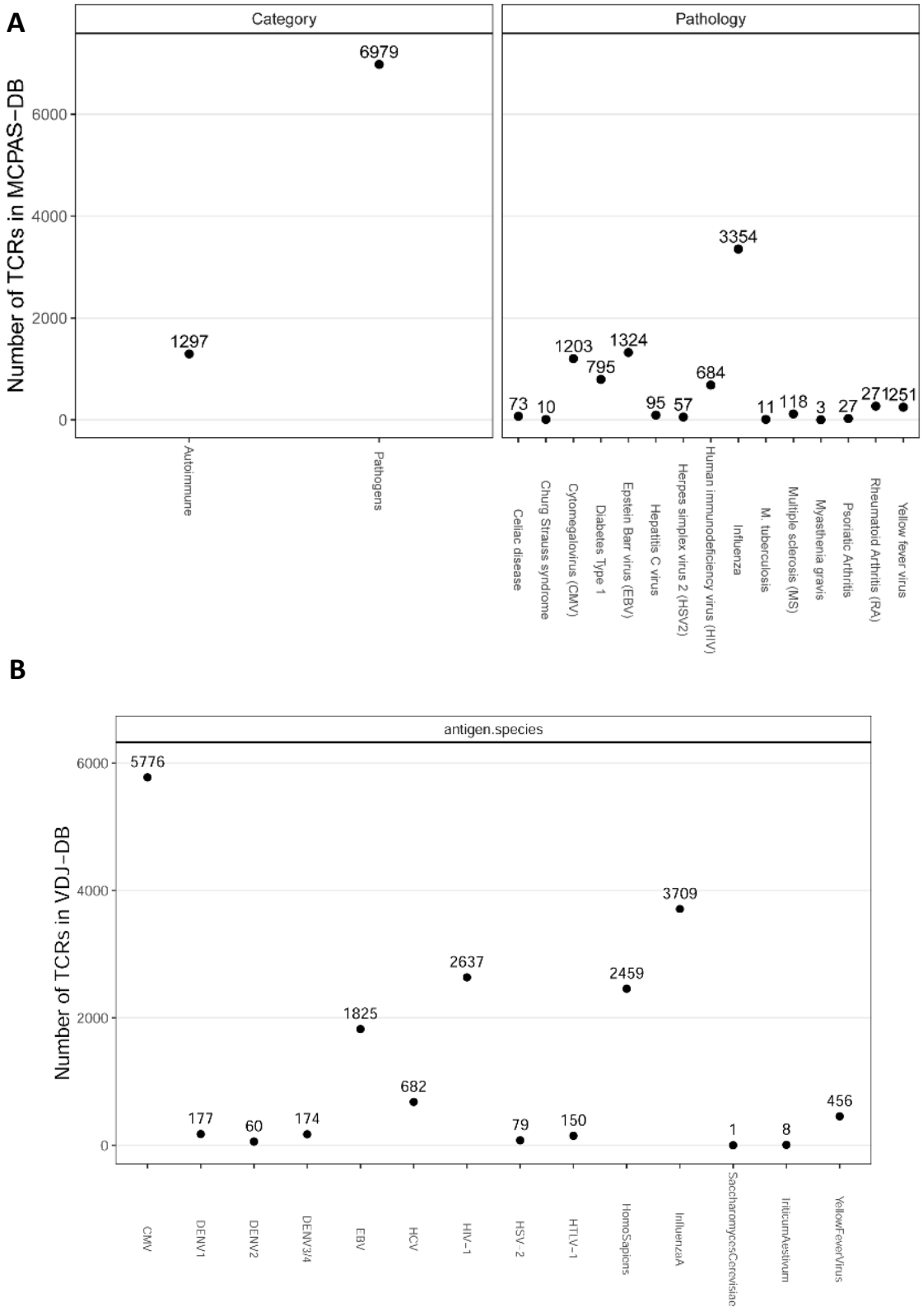
A
Category
Pathology
Number of TCRs in MCPAS−DB
0
2000
4000
6000
6979
1297
73
10
1203
795
1324
95
57
684
3354
11
118
3
27
271
251
Autoimmune
Pathogens
Celiac disease
Churg Strauss syndrome
Cytomegalovirus (CMV)
Diabetes Type 1
Epstein Barr virus (EBV)
Hepatitis C virus
Herpes simplex virus 2 (HSV2)
Human immunodeficiency virus (HIV)
Influenza
M. tuberculosis
Multiple sclerosis (MS)
Myasthenia gravis
Psoriatic Arthritis
Rheumatoid Arthritis (RA)
Yellow fever virus
B
antigen.species
Number of TCRs in VDJ−DB
0
2000
4000
6000
5776
177
60
174
1825
682
2637
79
150
2459
3709
1
8
456
CMV
DENV1
DENV2
DENV3/4
EBV
HCV
HIV−1
HSV−2
HTLV−1
HomoSapiens
InfluenzaA
SaccharomycesCerevisiae
TriticumAestivum
YellowFeverVirus

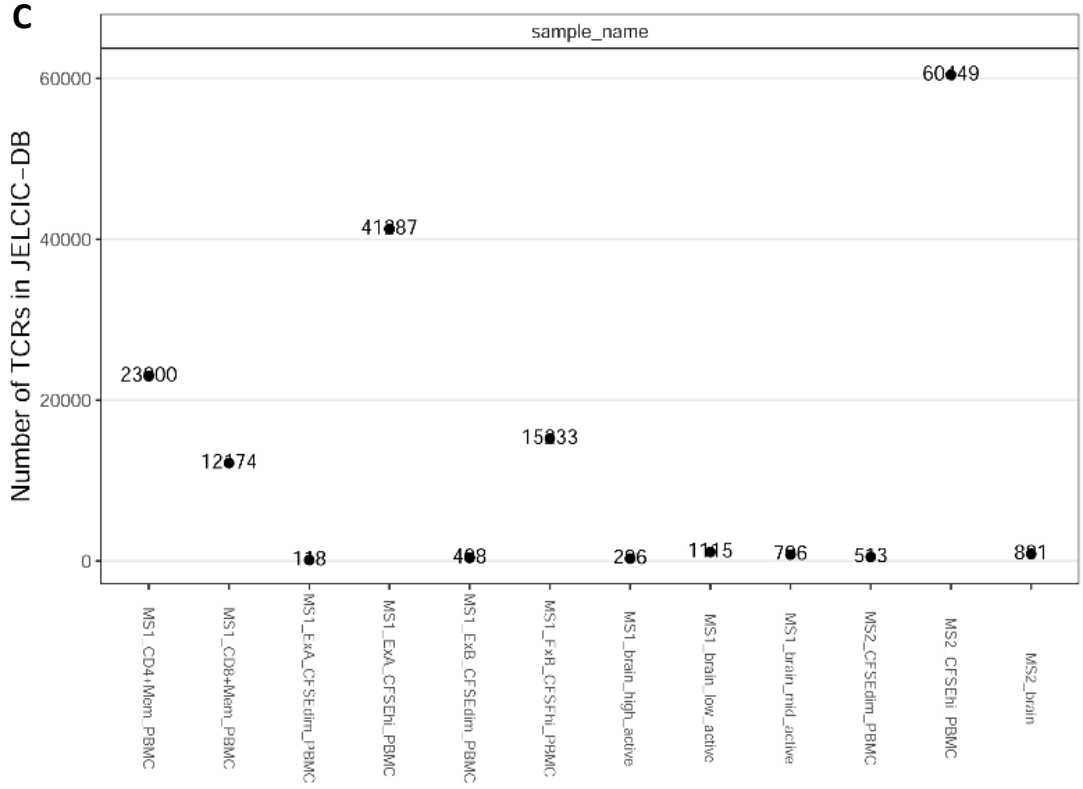

Fig. 49. Characterization of McPAS-TCR, VDJdb and Jelcic I et al. datasets. (A) TCRs number of McPas-TCR database is reported by disease category, including autoimmune and pathogens (left panel) or by specific pathology (right panel). (B) TCRs number of VDJdb is reported by antigen species. (C) Number of TCRs found in Jelcic et al. MS dataset is reported by sample name (4). CFSE: Carboxyfluorescein Diacetate Succinimidyl Ester.

The percentage of overlapping CDR3-a.a. sequences between RRMS repertoires and all the examined databases (McPAS-TCR, VDJdb and Jelcic I et al., fig. 50A-C) resulted significantly ($p<0.01$) lower in CD8 naïve cells of Natalizumab patients compared to AHSCT at t24.

A

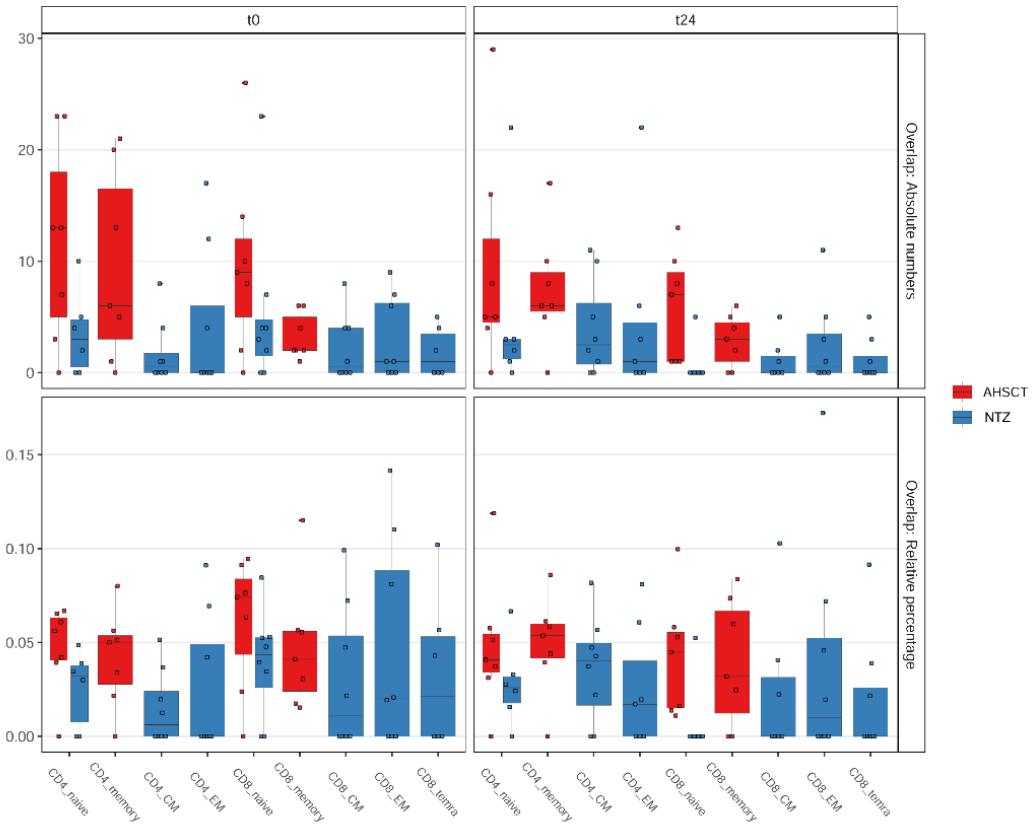

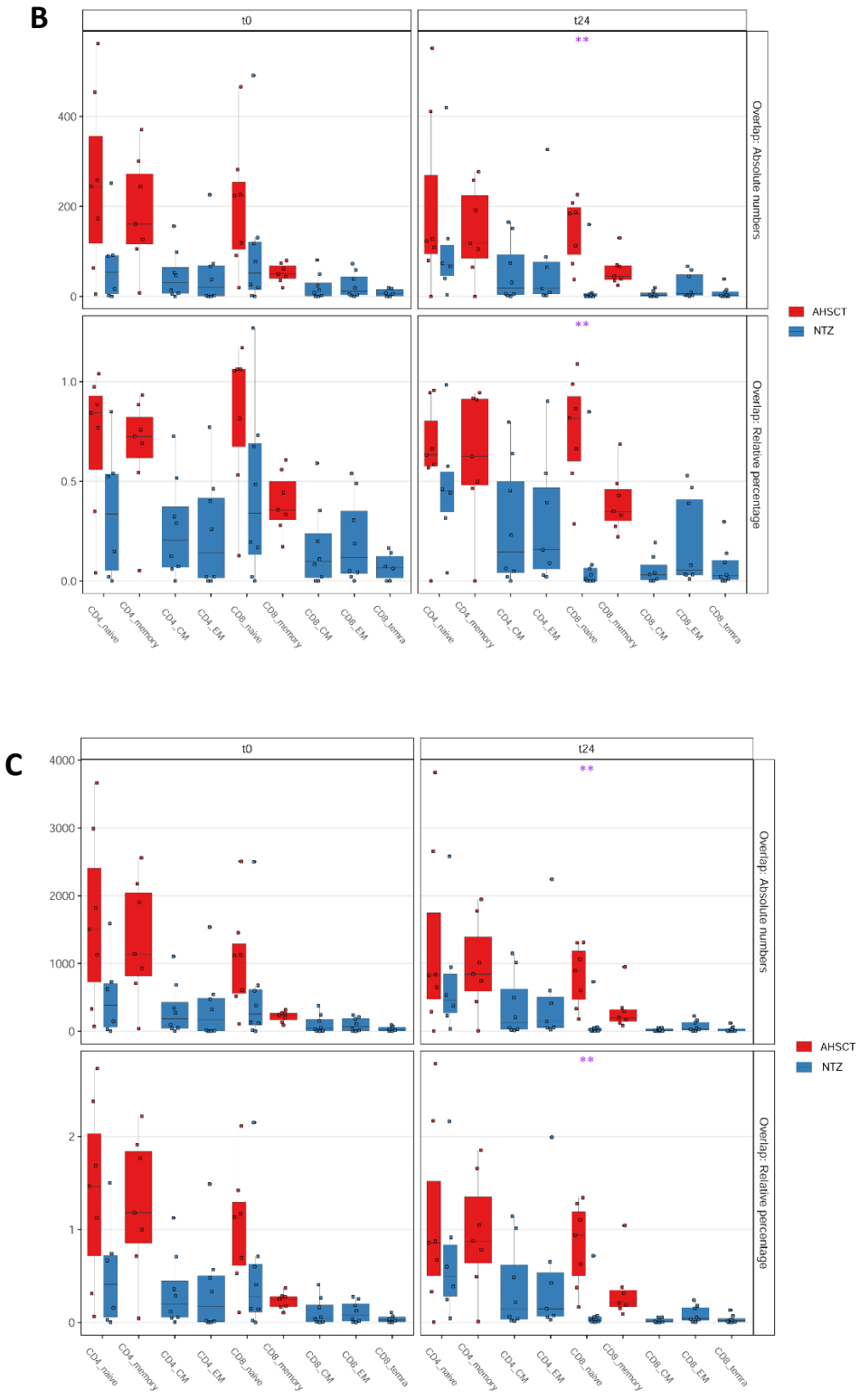

Fig. 50. Shared sequences between RRMS cohorts and public TCR databases. CDR3 sequence overlap with McPAS-TCR (A), VDJdb (B) and TCRß sequencing databases of two MS patients from Jelcic et al. (4) (C). CDR3 sequence overlap is reported as absolute number (upper panel in each graph) or relative percentage (lower panel in each graph) between AHSCT (in red) and NTZ (in blue) patients at t0 (left panel in each graph) and at t24 (right panel in each graph), shown by T-cell subpopulations. Statistical significance was determined by the Wilcoxon test (*p<0.05; **p<0.01).

Furthermore, comparing RRMS repertoires by disease-type with McPAS-TCR (Fig. 51A) or by antigen-species with VDJdb (Fig. 51B), the major overlap was identified with sequences classified as viral-infection associated rather than autoimmunity-associated. Specifically, the overlap was higher with EBV- and CMV-associated sequences (Fig. 51A, B) and, for VDJdb, also with Influenza A virus (Fig. 51B).

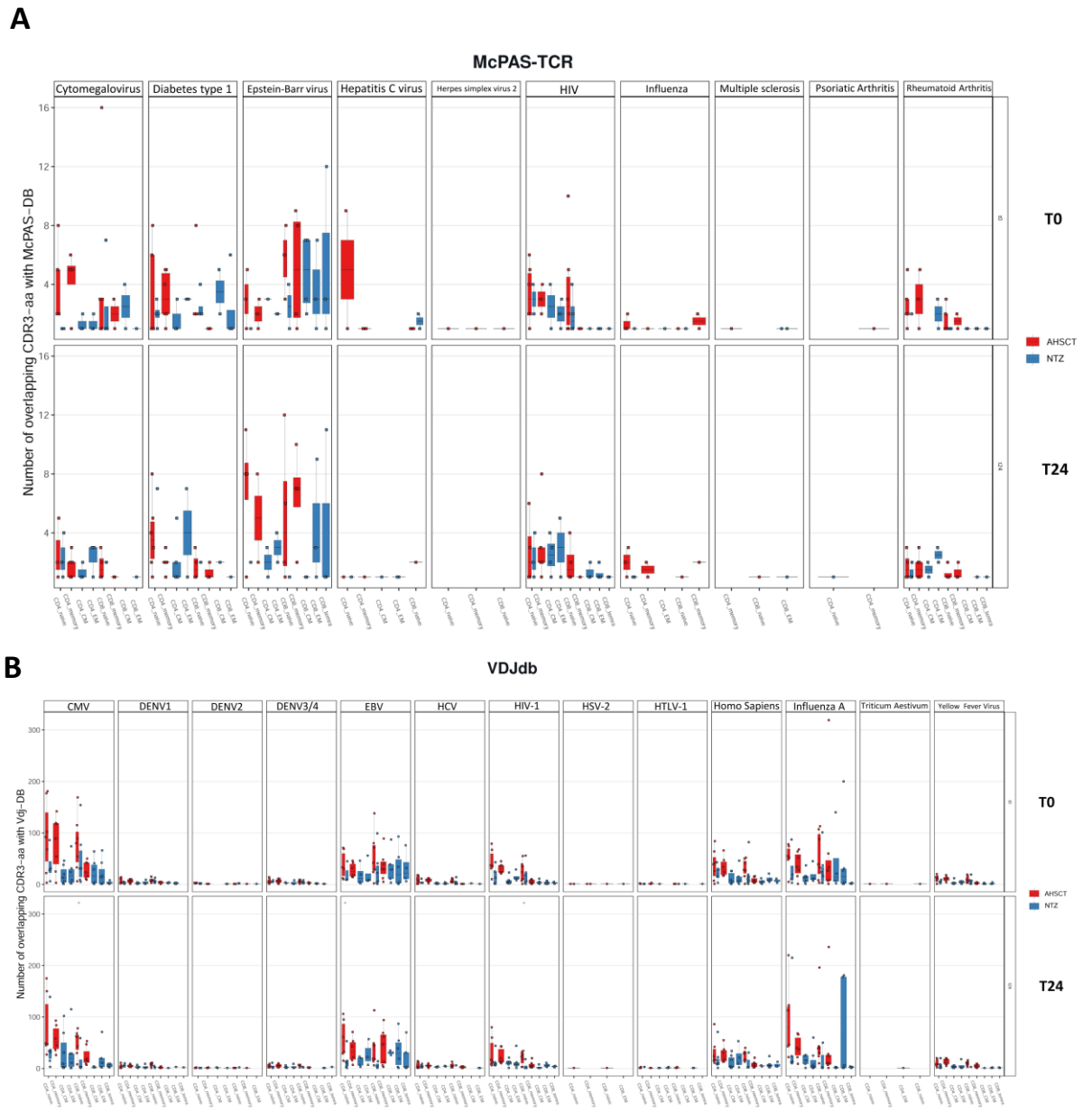

Fig. 51. Shared sequences between RRMS cohorts and public TCR databases by disease-type. The absolute number of overlapping CDR3 sequences between McPAS-TCR (A) or VDJdb (B) TCR databases and AHSCT (in red) or NTZ (in blue) patients at t0 (upper panel in each graph) and at t24 (lower panel in each graph) shown by disease-type. On the x-axis, from left to right, T-cell subpopulations are reported as follows: CD4 naïve, CD4 memory, CD4 CM, CD4 EM, CD8 naïve, CD8 memory, CD8 CM, CD8 EM, CD8 Temra. Statistical significance was determined by Wilcoxon test.

4.1.14. Serum cytokines evaluation in RRMS cohorts

Since alterations in cytokines production may govern T-cell differentiation, we evaluated the inflammatory profile in Natalizumab and AHSCT patients before and after treatments.

Among all the cytokines and chemokines measured in serum, findings show that TNFα is significantly ($p<0.01$) lower in Natalizumab t0, while at t24 it is significantly increased in Natalizumab patients ($p<0.05$) compared to AHSCT (Fig. 52). These results indicate an increase in TNFα production in Natalizumab versus a stable production in AHSCT. On the contrary, recall chemokines CXCL10 and CXCL13 are significantly ($p<0.05$) increased at t24 in AHSCT patients compared to Natalizumab.

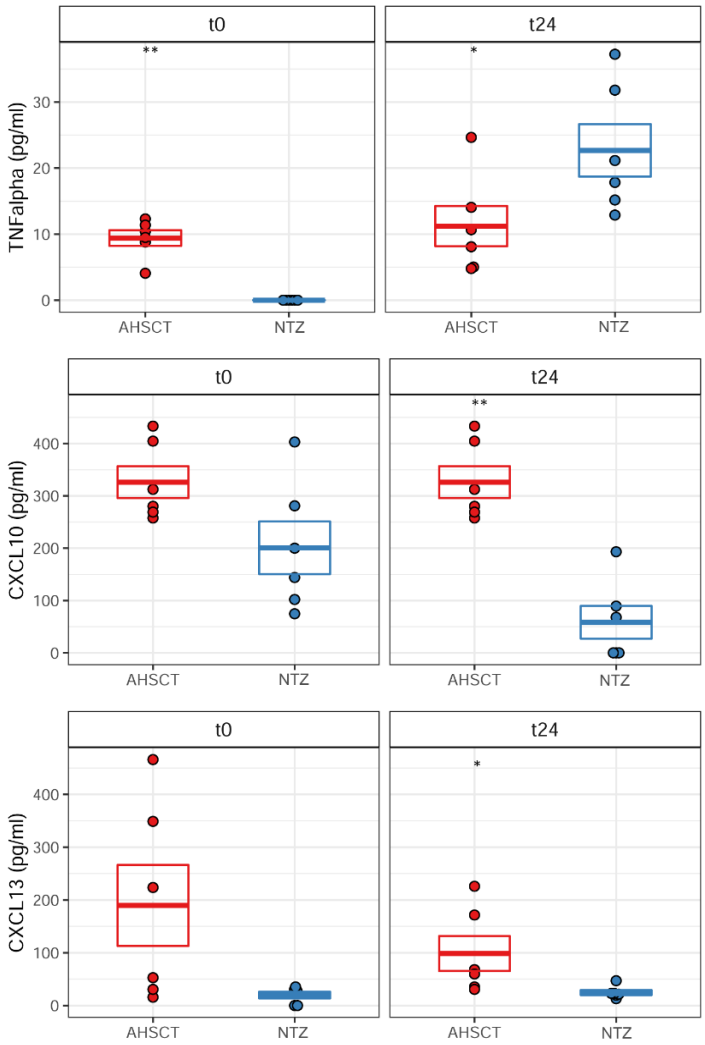

Fig. 52. Serum cytokine levels in AHSCT and NTZ patients. Panel reports, from the top to the bottom, TNFα, CXCL10 and CXCL13 levels (pg/ml) in serum samples of AHSCT (in red) and NTZ (in blue) patients at t0 (left graphs) and at t24 (right graphs). Each dot is a patient. Mean±SEM is reported. Statistical significance was determined by Wilcoxon test (*p<0.05; **p<0.01).

4.2. Cerebrospinal fluid patients

4.2.1. Patients characteristics and clinical follow-up

The 4 patients included in the study (CSF2, CSF3, CSF4, CSF5) undergone CSF collection at the time of diagnosis (t0). All patients were confirmed with RRMS diagnosis except for one patient (CSF2), whom diagnosis switched from RRMS to PPMS. The first symptoms of MS included uncertain walk (1/4), diplopia (2/4) and lower limb dysaesthesia (1/4). CSF2 patient has familiarity with MS (2 cousins). All patients showed the presence of OCBs except one (CSF5). All patients except for one (CSF4) had a disease relapse after the lumbar puncture. CSF4 was the only patient who had Gd+ lesions at both the first and the second MRI. CSF patients characteristics are summarized in Tab. 3.

Table 3. Clinical characteristics of CSF patients

N. of patients	4
Gender F:M	2:2
Age at diagnosis average (min-max)	34,5 (19-46)
Type of MS	3 RR, 1 PP
Disease duration (years) average (min-max)	3 (2-4)
CFS n. of cells/µl average (min-max)	3,5 (2-6)
BBB[A] damage (N. of positive patients/tot)	0/4
IgG index alteration (N. of positive patients/tot)	4/4
OCB[B] (N. of positive patients/tot)	3/4
N. of patients with pre-lumbar puncture relapse	3/4
N. of patients with post-lumbar puncture relapse	3/4
Therapy:	
Dimethyl fumarate[C]	3/4
IFN-beta[D]	2/4
Azathriopine	1/4
No therapies	0/4
Corticosteroids[E]	1/4

[A]blood-brain barrier; [B]oligoclonal bands; [C]1/4 patient switched to IFN-beta because of ineffectiveness of the first therapy; [D]1/4 patient switched to Azathriopine because of drug intolerance; [E]pre-lumbar puncture administration

4.2.2. Immunophenotype of cerebrospinal fluid of MS patients

First, 20 incoming MS patients were immunophenotypically characterized by flow cytometry (see Methods) for the percentage of Tem and Tcm cells within their CSF samples, collected at the diagnosis. Gating strategy is reported in Fig. 53A. Among these 20 patients, 2 were then selected for TCR sequencing experiments. Results showed that the total lymphomonocytes population of CSF included a significantly ($p<0.05$) higher percentage of CD4 cells compared to CD8 and a significantly ($p<0.0001$) higher percentage of Tem compared to Tcm cells (Fig. 53B). Most of these Tem cells were CD4 EM (median=38.2%) rather than CD8 EM (median=8.47%), while the percentages of total Tcm cells in CSF samples were so low (median=0.46%) that discriminating between CD4 and CD8 was challenging (data not shown).

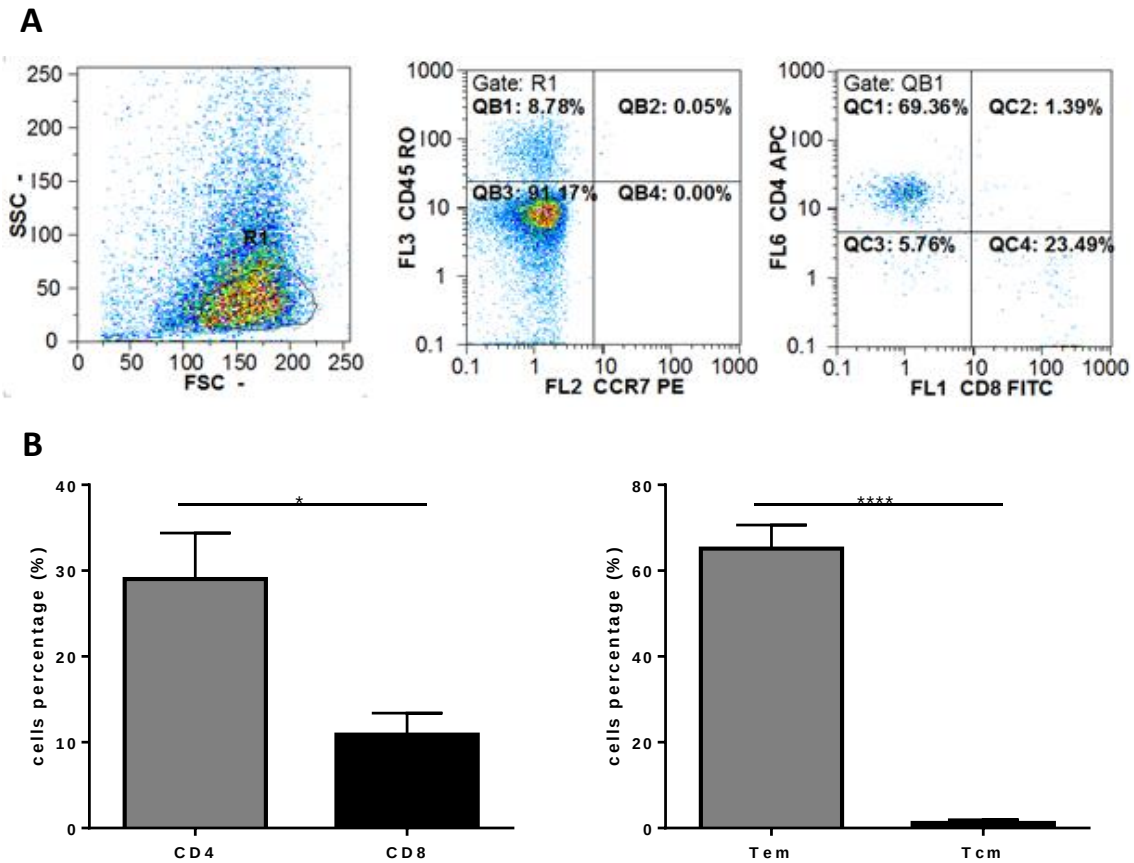

Fig. 53. Immunophenotype of MS patients CSF. A) Flow cytometry gating strategy to select CD4 and CD8 EM and CM cells. Figure reports the analysis performed on CSF of one representative incoming MSs patient. Gate R1 morphologically includes T lymphocytes (left dot plot). Gate QB1 includes Tem (CD45RO+CCR7-) and gate QB2 includes Tcm (CD45RO+CCR7+) (middle dot plot). Dot plot on the right reports the percentages of CD4 and CD8 cells within the gate QB1, that collects Tem cells. B) Graph reports the percentage (%) of CD4 and CD8 cells (left graph) and of Tem (CD45RO+CCR7-) and Tcm (CD45RO+CCR7+) cells (right graph) on the total population of lymphomonocytes from the CSF of 20 MS patients enrolled at the diagnosis. Mean±SEM is reported. Statistical significance was determined by non-parametric Mann-Whitney test (*$p<0.05$; ****$p<0.0001$).

4.2.3. Data acquisition and repertoire statistics

The TCRβ gene from memory T-cell subpopulations (EM and CM CD4 and CD8) or from the whole CSF cell population of 4 incoming MS patients was sequenced. T-cell subpopulations were sorted from PBMCs collected at the time of diagnosis (t0), obtaining a total number of 4,395,408 reads (total sequences) and 153,040 V-CDR3-J a.a. clones (or unique sequences). For each CSF patients, 4 sorted T-cell subpopulations and CSF were obtained, for a total of 5 tubes/patient. Gating strategy for T-cell subpopulations sorting was the same as mentioned for AHSCT and Natalizumab patients (Fig. 37). The experimental workflow is reported in Fig. 54.

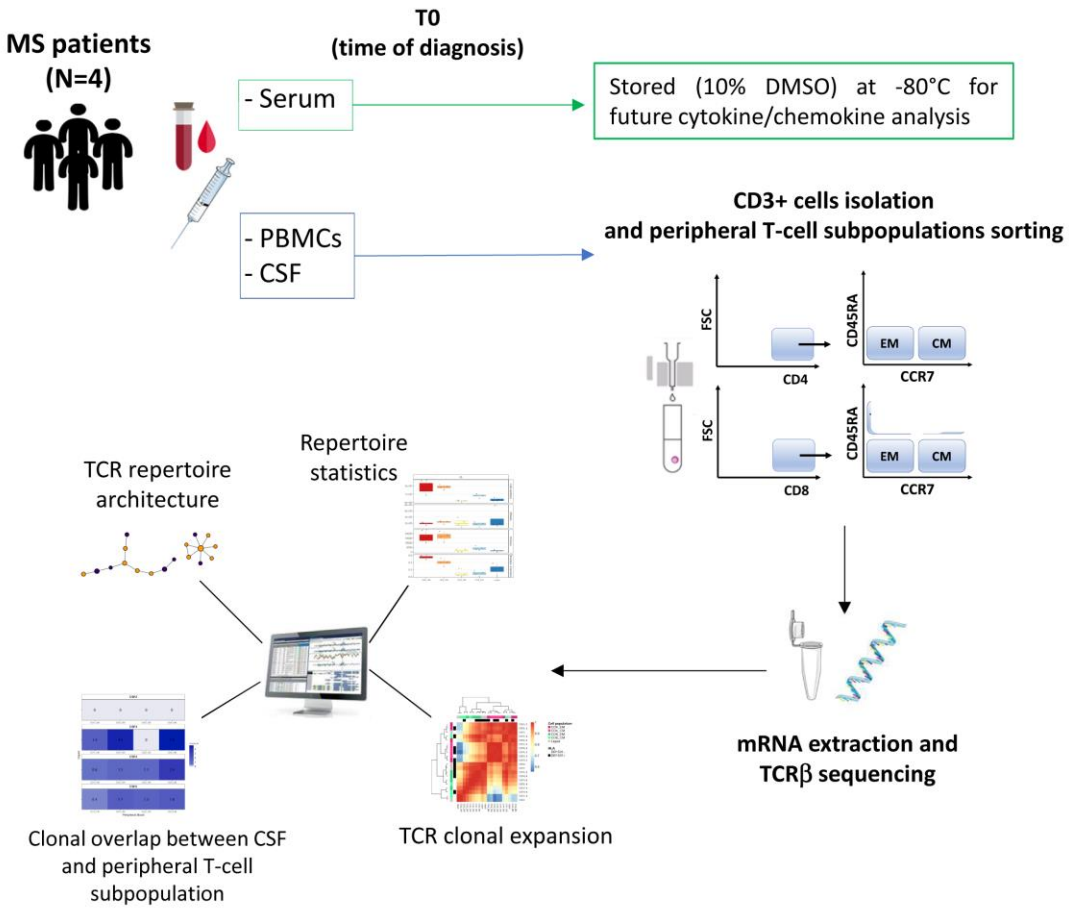

Fig. 54. Experimental workflow. From 4 patients (CSF2, CSF3, CSF4, CSF5), PBMCs, serum and CSF (or "liquor" in the figure) were collected. Serum samples were stored in 10% dimethyl sulfoxide (DMSO) for future analysis of cytokines and chemokines. CD3+ T cells were isolated from the whole CSF cell population and paired PBMCs of each patient. From peripheral CD3+ cells, memory T-cell subpopulations (EM and CM CD4 and CD8) were sorted. Subsequently, from total mRNA TCRβ sequencing was performed by iRepertoire Inc., Alabama, USA. High-dimensional TCRβ data analyses included: repertoire statistics, clonal overlap between CSF and paired PBMCs, TCR repertoire architecture, sequence overlap with public TCR databases.

To confirm the quality of our dataset as already mentioned for Natalizumab and AHSCT, it was calculated the Pearson correlation coefficient (r) between Shannon-Evenness and reads number (#Reads) and between #Reads and clones numbers (#Clones) (Fig. 55). For both comparisons, the Pearson correlation resulted negative (Shannon-Evenness versus #Reads: -0.27; #Reads versus #Clones number: r=-0.13), indicating a good sequencing depth.

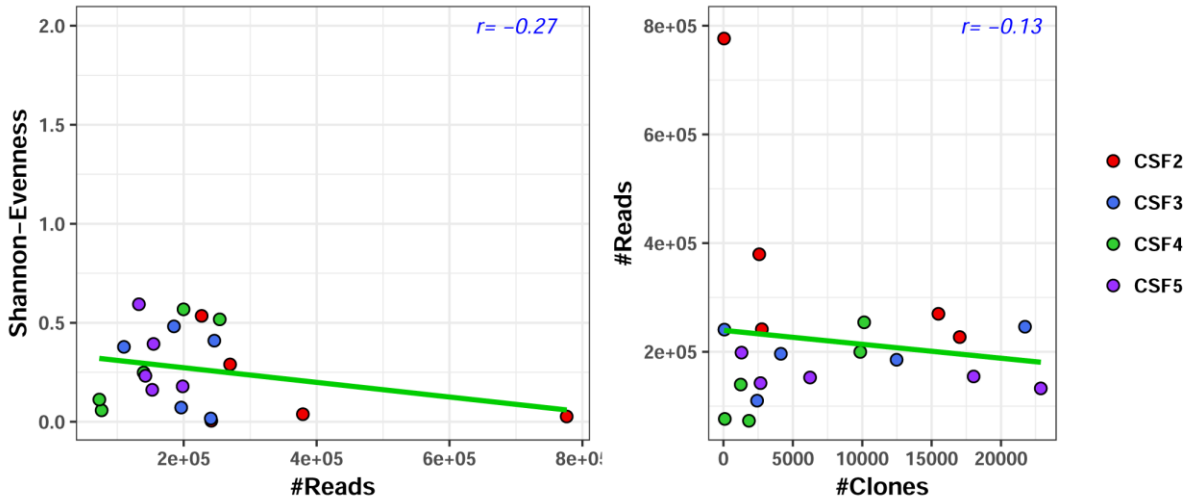

Fig. 55. Data quality assessment in CSF patients. Pearson correlation coefficient (r) between Shannon-Evenness and reads number (#Reads) (left graph) and #Reads versus clones number (#Clones) (right graph) in CSF patients. Each dot represents a different patient. Pearson correlation coefficient (r) value is reported in the upper right of both graphs.

Next, the variation of the number of cells, reads, clones and Shannon-Evenness was evaluated by T-cell subpopulation (Fig. 56). Results showed a significantly ($p<0.05$) higher cell numbers and #Clones in CD4 CM and EM compared to CD8 CM and CSF and a significantly ($p<0.05$) higher Shannon-Evenness in CD4 CM and EM compared to CD8 CM and also in CD4 CM compared to CSF. No significant differences in the number of reads among peripheral T-cell subpopulations and CSF repertoires were found.

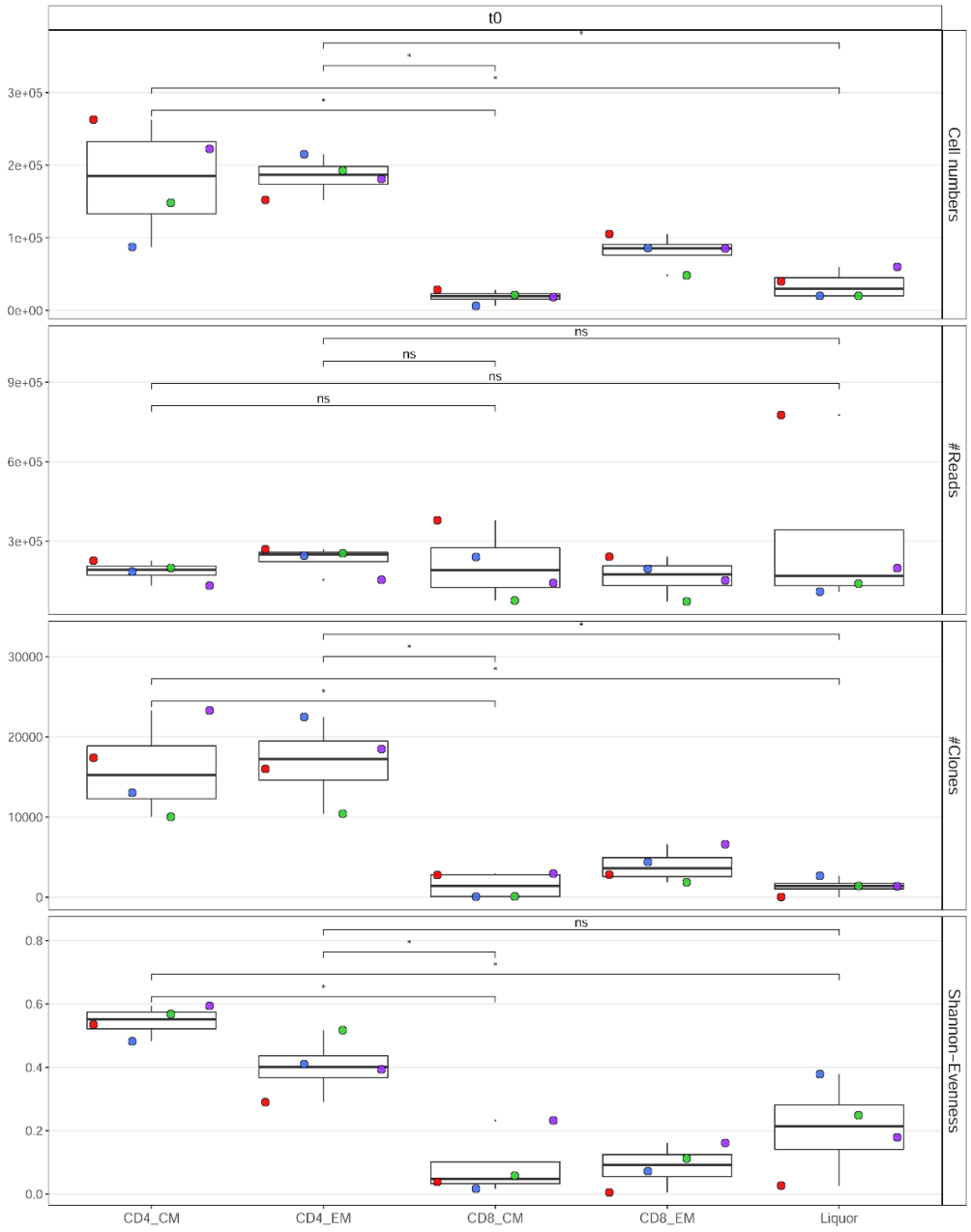

Fig. 56. Repertoire statistics in CSF patients. Graph reports, from the top to the bottom, cell numbers, #Reads, #Clones and Shannon-Evenness in peripheral memory T-cell subpopulations (CD4 CM, CD4 EM, CD8 CM, CD8 EM) and in the CSF (liquor=CSF) of patients at t0. Mean values are shown for each T-cell subpopulation. Statistical significance was determined by non-parametric Kruskal-Wallis test (*$p<0.05$).

4.2.4. Visualization of T-cell receptor repertoires sequence composition and frequency in cerebrospinal fluid of patients

The service iRepertoire (iRepertoire Inc.) offers an online platform, iRweb, for basic bioinformatic analysis and visualization of data. iRweb allows to visualize TCR repertoires as small tree maps based on sequence composition and frequency, where each color rectangle is a CDR3-a.a. sequence and the size of the rectangles is proportional to the frequency of the sequences. The tree maps come along with a top 10 of more represented sequences.

Results showed that whereas 3/4 patients are characterized by a generally highly variable TCR repertoire composition in terms of total and unique (or distinct) CDR3 sequences, one patient, CSF2, shows the predominance of one sequence, CASSLLPGDEQF, that appears in the CSF of this patient 766784 times (=copy number) (Fig. 57). Of note, CSF2 is the only patient who received a final diagnosis of PPMS.

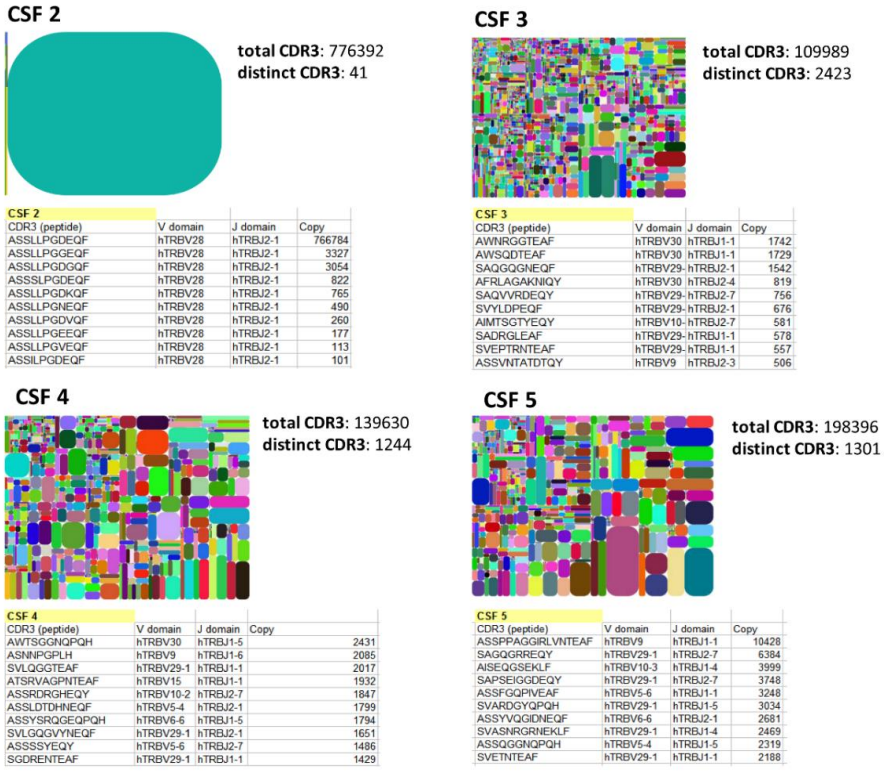

CSF 2

CDR3 (peptide)	V domain	J domain	Copy
ASSLLPGDEQF	hTRBV28	hTRBJ2-1	766784
ASSLLPGGEQF	hTRBV28	hTRBJ2-1	3327
ASSLLPGDGQF	hTRBV28	hTRBJ2-1	3054
ASSSLPGDEQF	hTRBV28	hTRBJ2-1	822
ASSLLPGDKQF	hTRBV28	hTRBJ2-1	765
ASSLLPGNEQF	hTRBV28	hTRBJ2-1	490
ASSLLPGDVQF	hTRBV28	hTRBJ2-1	260
ASSLLPGEEQF	hTRBV28	hTRBJ2-1	177
ASSLLPGVEQF	hTRBV28	hTRBJ2-1	113
ASSILPGDEQF	hTRBV28	hTRBJ2-1	101

CSF 3

CDR3 (peptide)	V domain	J domain	Copy
AWNRGGTEAF	hTRBV30	hTRBJ1-1	1742
AWSQDTEAF	hTRBV30	hTRBJ1-1	1729
SAQGQGNEQF	hTRBV29-	hTRBJ2-1	1542
AFRLAGAKNIQY	hTRBV30	hTRBJ2-4	819
SAQVVRDEQY	hTRBV29-	hTRBJ2-7	756
SVYLDPEQF	hTRBV29-	hTRBJ2-1	676
AIMTSGTYEQY	hTRBV10-	hTRBJ2-7	581
SADRGLEAF	hTRBV29-	hTRBJ1-1	578
SVEPTRNTEAF	hTRBV29-	hTRBJ1-1	557
ASSVNTATDTQY	hTRBV9	hTRBJ2-3	506

CSF 4

CDR3 (peptide)	V domain	J domain	Copy
AWTSGGNQPQH	hTRBV30	hTRBJ1-5	2431
ASNNPGPLH	hTRBV9	hTRBJ1-6	2085
SVLQGGTEAF	hTRBV29-1	hTRBJ1-1	2017
ATSRVAGPNTEAF	hTRBV15	hTRBJ1-1	1932
ASSRDRGHEQY	hTRBV10-2	hTRBJ2-7	1847
ASSLDTDHNEQF	hTRBV5-4	hTRBJ2-1	1799
ASSYSRQGEQPQH	hTRBV6-6	hTRBJ1-5	1794
SVLGQGVYNEQF	hTRBV29-1	hTRBJ2-1	1651
ASSSSYEQY	hTRBV5-6	hTRBJ2-7	1486
SGDRENTEAF	hTRBV29-1	hTRBJ1-1	1429

CSF 5

CDR3 (peptide)	V domain	J domain	Copy
ASSPPAGGIRLVNTEAF	hTRBV9	hTRBJ1-1	10428
SAGQGRREQY	hTRBV29-1	hTRBJ2-7	6384
AISEQGSEKLF	hTRBV10-3	hTRBJ1-4	3999
SAPSEIGGDEQY	hTRBV29-1	hTRBJ2-7	3748
ASSFGQPIVEAF	hTRBV5-6	hTRBJ1-1	3248
SVARDGYQPQH	hTRBV29-1	hTRBJ1-5	3034
ASSYVQGIDNEQF	hTRBV6-6	hTRBJ2-1	2681
SVASNRGRNEKLF	hTRBV29-1	hTRBJ1-4	2469
ASSQGGNQPQH	hTRBV5-4	hTRBJ1-5	2319
SVETNTEAF	hTRBV29-1	hTRBJ1-1	2188

Fig. 57. Visualization of TCR repertoires in the CSF of incoming MS patients. Figure reports an overview of the CDR3 composition of CSF-TCR repertoires (CSF2, CSF3, CSF4, CSF5) visualized as tree maps by iRweb platform (iRepertoire, Inc.). Each colored rectangle in the tree maps represents a unique CDR3 sequence and the size of the rectangle depends on the sequence's frequency. A top 10 list of the more represented CDR3 sequences is reported below each tree map.

4.2.5. Individual variability of repertoire statistics

Repertoire statistics was evaluated on an individual basis in all CSF patients (CSF2, CSF3, CSF4, CSF5), in all memory T-cell subpopulations and CSF at t0 (Fig. 58). Results showed a trend towards a higher Shannon-Evenness in memory CD4 cells compared to memory CD8 compartment and, interestingly, a higher variability across patients in the Shannon-Evenness of CSF repertoires.

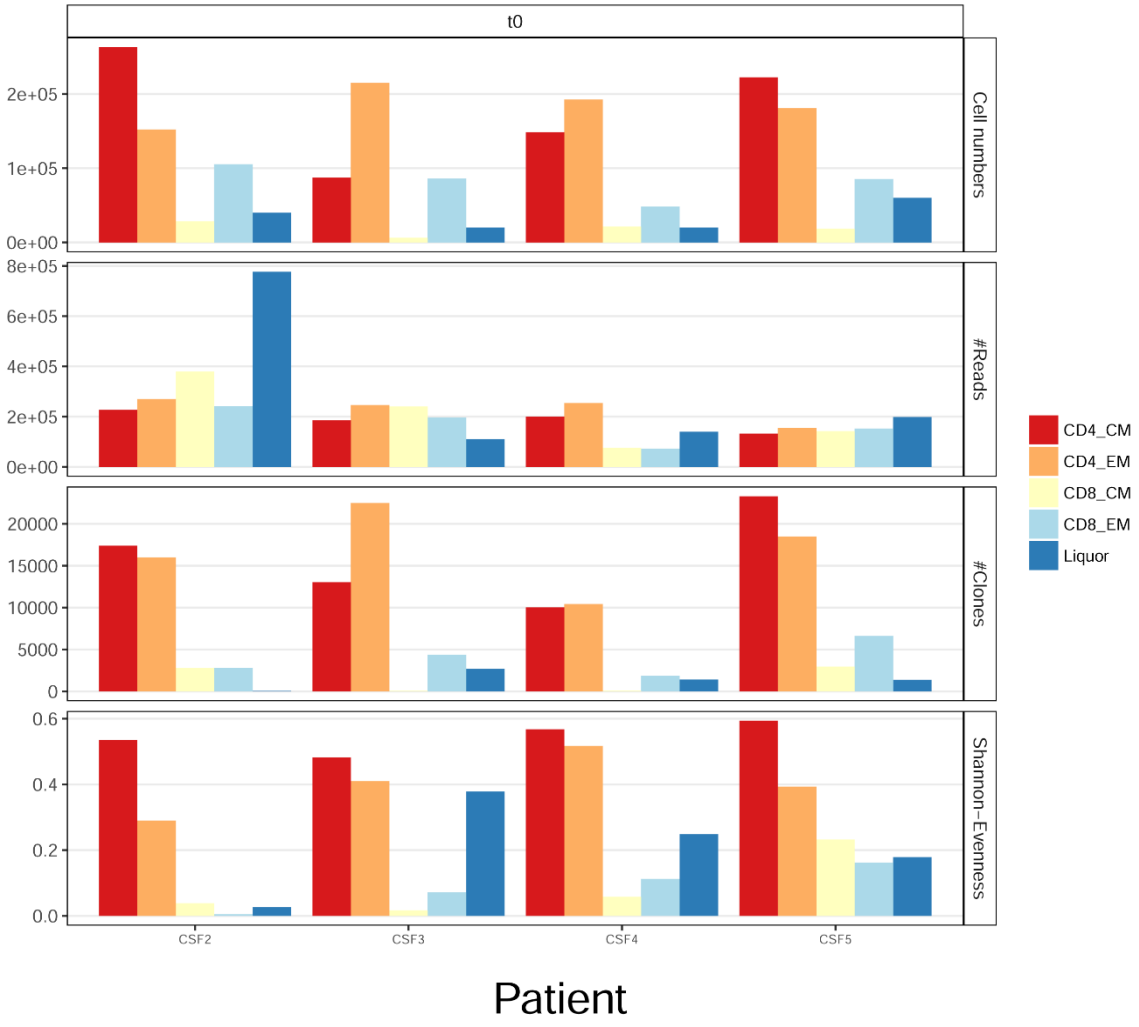

Fig. 58. Repertoire statistics patient by patient. Cell numbers, #Reads, #Clones and Shannon-Evenness are reported by T-cell subpopulation and CSF for each patient (CSF2, CSF3, CSF4, CSF5). Each bar represents a T-cell subpopulation.

4.2.6. Clonal overlap between cerebrospinal fluid and periphery

The percentage of a.a. clones, or unique sequences, shared between CSF and peripheral memory T-cell subpopulations was evaluated for each CSF patient (Fig. 59). Results showed a generally higher clonal overlap between CSF and CD8 EM cells (1.8-4.8%), followed by the overlap between CSF and CD4 EM (1.1-4.5), CD4 CM (0.4-1.5) and CD8 CM (0-1.3). Patient CSF2, who has very few unique sequences in the CSF (41 a.a. clones) and a clonal expansion, showed no overlap with paired peripheral T-cell subpopulations. The higher clonal overlap percentage was observed between CSF and CD8 EM cells of the patient CSF3 (4.8%).

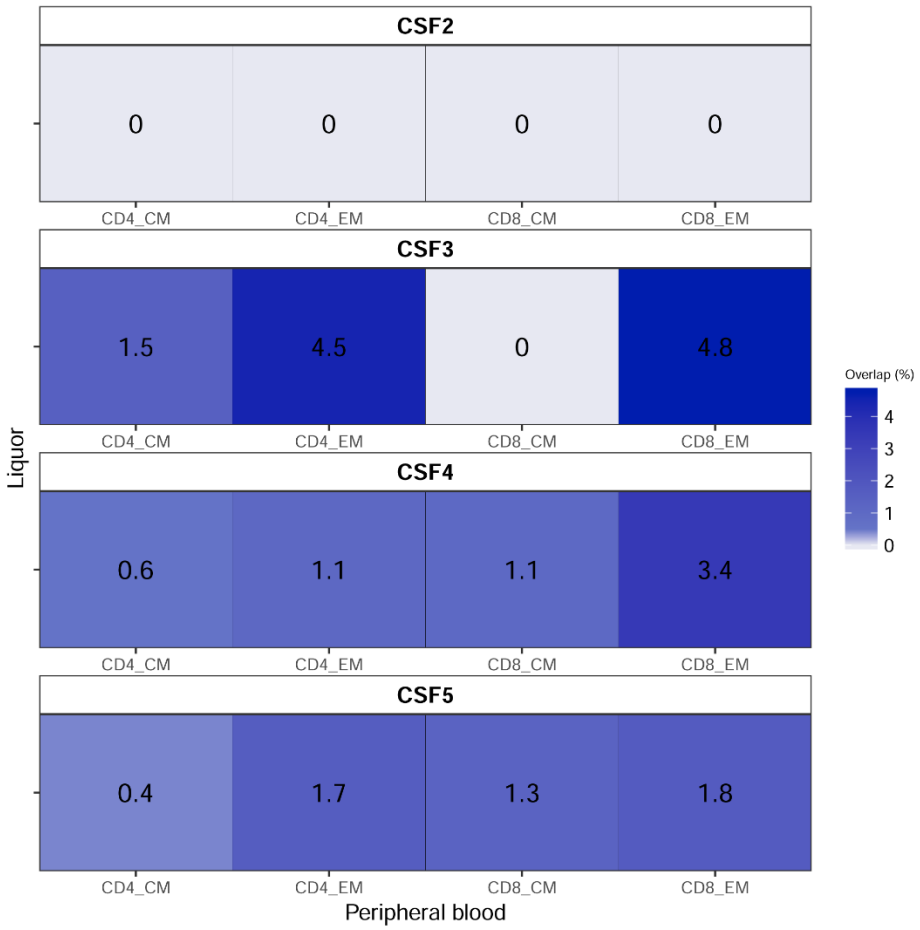

Fig. 59. Clonal overlap between CSF and peripheral blood cell populations of MS patients. Figure reports the percentage of overlapping clones (a.a. unique sequences), scaled by color, between TCR repertoires of CSF (y-axis, "Liquor") and peripheral T-cell subpopulations (x-axis) for each patient.

4.1.7. Architecture of the T-cell receptor repertoire in CSF patients

To investigate how the TCR repertoire of CSF and peripheral T-cell subpopulations of CSF patients appeared as a clone network and whether there was a difference between the two compartments, clone networks of CSF patients TCR repertoires and paired statistics were analyzed as already mentioned for Natalizumab and AHSCT patients. Results showed that the percentage of both private and public clones with connections is similar across peripheral T-cell subpopulations and there are no significant differences among memory CD4 and CD8 subpopulations and CSF (Fig. 60C). Nevertheless, CSF TCR repertoires are generally more variable in terms of connected clones compared to paired peripheral cell populations.

Interestingly, the patient CSF2 showed a TCR repertoire characterized by a low number of clones (41) highly connected between each other (Fig. 60B). The difference can be particularly appreciated in the comparison with another CSF TCR repertoire (patient CSF3; Fig. 60A), that is characterized by a higher number of total clones and less connections. Of note, CSF2 is the only PPMS of the cohort.

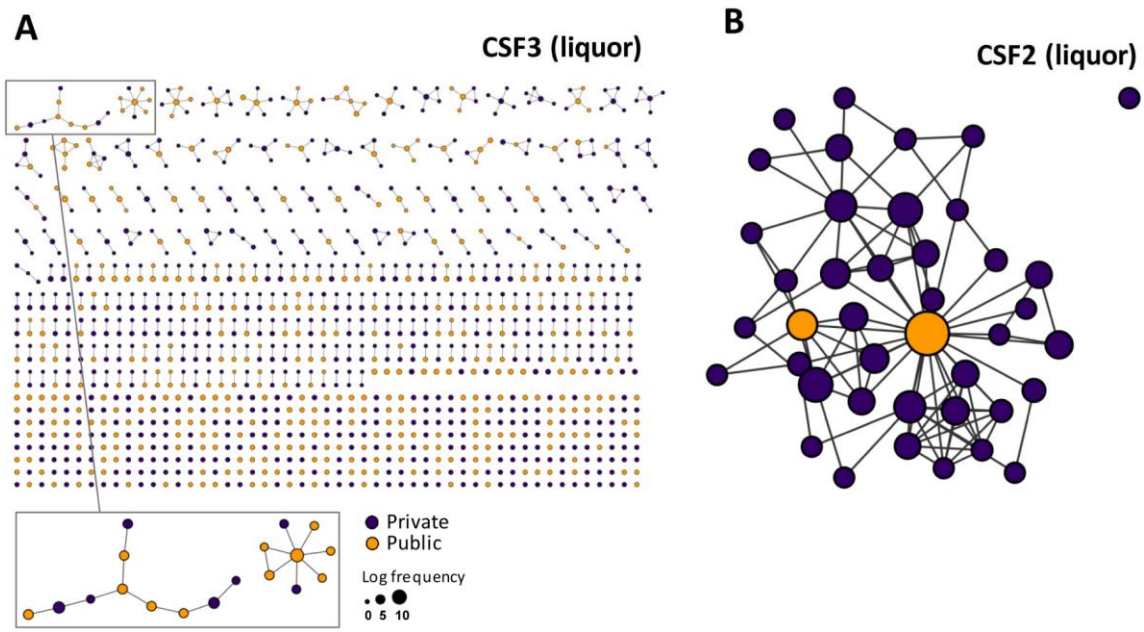

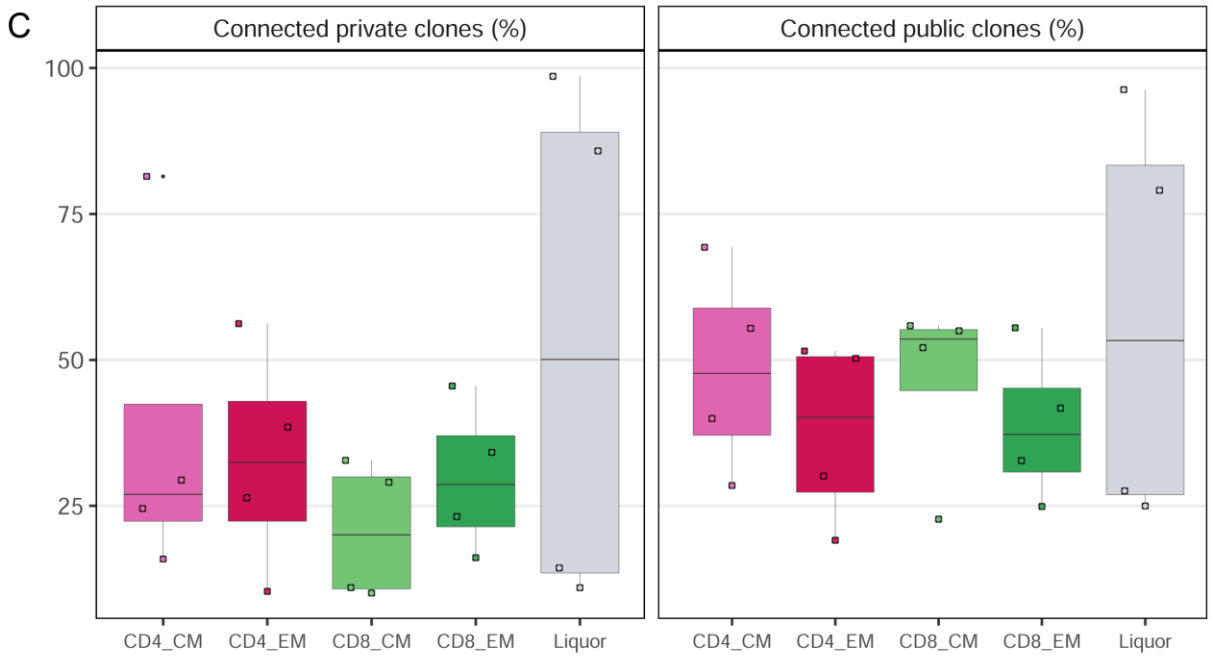

Fig. 60. Clone networks visualization in CSF patients and statistics. (A, B) Representative TCR repertoire architectures, displayed as clone networks, of the CSF of CSF3 and CSF2 patients. Each node is an amino acid CDR3 sequence (CDR3-a.a.) and links between nodes connect CDR3s-a.a. based on Levenhstein distance of 1 (LD = 1). Node size scales with log clone frequency and node color indicate private (dark blue) or public (yellow) clones (see legend). (C) Percentage of connected private (left panel), public (right panel) clones in T-cell subpopulations of CSF patients.

4.1.8. Shared sequences with public T-cell receptor databases

As already reported for Natalizumab and AHSCT groups, the CDR3 sequences overlap was evaluated between our CSF dataset and the public CDR3 databases McPAS-TCR (Tickotsky N et al., 2017) and VDJdb (Shugay M et al., 2018), characterized in Fig. 49A, B. Results were much similar in both comparisons with McPAS-TCR and VDJdb databases, with a significantly ($p<0.05$) higher overlap, as absolute number or percentage, in peripheral CD4 CM and EM subpopulations compared to CD8 CM and EM and CSF of all CSF patients (Fig. 61). The overlap is particularly low in CSF TCR repertoires, that therefore are more private than the peripheral cell compartments.

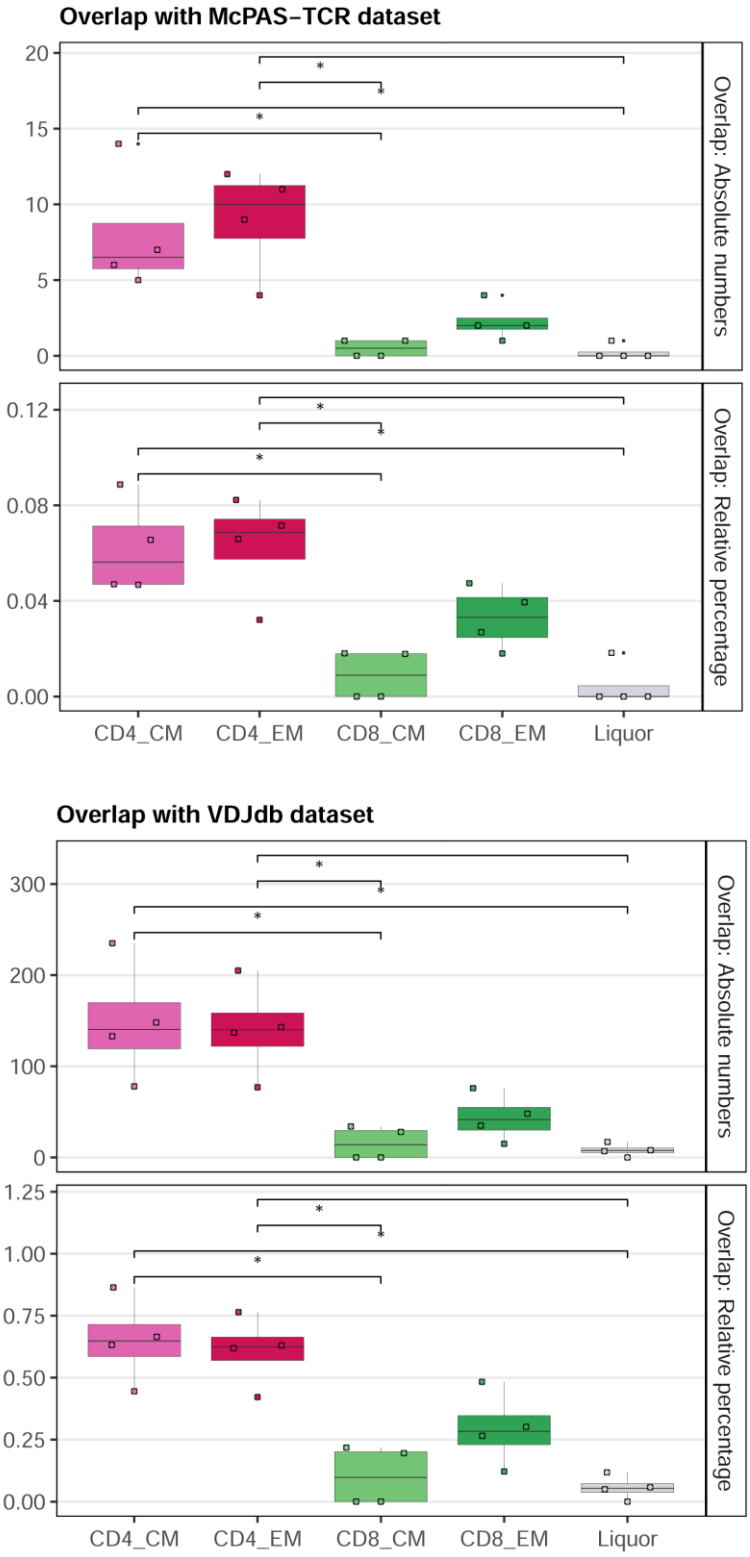

Fig. 61. Sequence overlap between CSF dataset and public TCR databases. Graphs report the sequence overlap between our CSF patients and two public TCR databases: McPAS-TCR (upper graph) and VDJdb (lower graph). The overlap is reported as absolute number (upper panel in each graph) or as percentage (lower panel in each graph) in both cases. T-cell subpopulations are reported on x-axis. Each dot represents a patient. Mean values are shown for each T-cell subpopulation. Statistical significance was determined by non-parametric Kruskal-Wallis test (*p<0.05).

The CDR3-a.a. sequence overlap with McPAS-TCR by disease-type (Fig. 62A) is higher for pathogens compared to autoimmune diseases and, within the pathogens category, the overlap is significantly ($p<0.05$) higher in EM and CM CD4 cells compared to memory CD8 cells and CSF TCR repertoires. The overlap with VDJdb visualized by antigen-species (Fig. 62B) is significantly ($p<0.05$) higher in memory CD4 cells compared to memory CD8 cells and CSF with CDR3-a.a. sequences associated to Homo Sapiens epitopes and CMV, EBV and Influenza A viruses. Globally, TCR repertoires of CSF share less sequence compared to peripheral memory T-cell subpopulations with public databases.

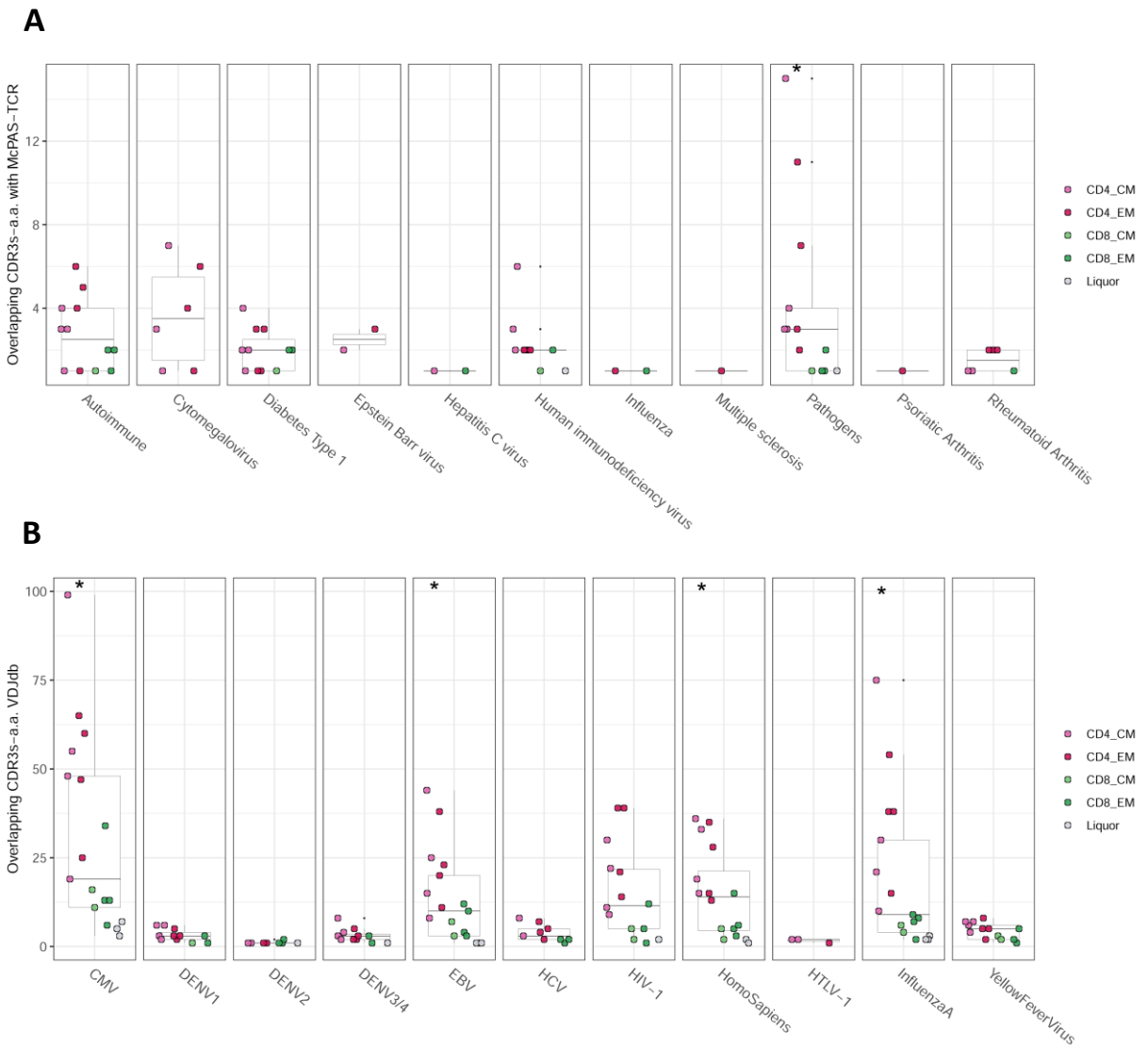

Fig. 62. Shared sequences between RRMS cohorts and public TCR databases by disease-type. The absolute number of overlapping CDR3 sequences between McPAS-TCR (A) or VDJdb (B) TCR databases and CSF patients shown by disease-type. Statistical significance was determined by Wilcoxon test (*$p<0.05$).

5. Discussion

The present study investigated how Natalizumab and AHSCT, two successful immunomodulatory treatments for RRMS, longitudinally impacted the adaptive immune system and the TCR repertoire in RRMS patients. Through a rigorous and methodical statistical approach, the bioinformatic analysis of our data allowed to detect treatment-specific molecular traces in the TCR repertoire from peripheral T-cell subpopulations of 15 RRMS patients, before and after 24 months of immunomodulatory treatments.
Since there is no single, universally accepted method to analyze TCR sequencing data, our choice to describe the molecular features of the TCR repertoire of patients based on quantitative (number of sorted cells, reads, clones, Shannon-Evenness and clonal persistence) and qualitative (repertoire architecture and public clones across patients) parameters was successful, allowing to obtain clear and consistent results.

First, Natalizumab patients were immunophenotypically evaluated for absolute cell count of T-cell subpopulations before and after 6, 12 and 24 months of treatment. Results showed an increase in the count of all immune cells, as expected due to the mechanism of action of Natalizumab, that blocks T cells in the peripheral blood (Fig. 34); specifically, it was observed a significant increase of CM CD4 cells and a significant decrease of EM CD4 cells at t24 compared to t0.
The first step of sequencing data analysis was the quality assessment, through the calculation of the Pearson correlation coefficient (r) calculated between some of the TCR repertoire quantitative parameters in Natalizumab and AHSCT patients: number of reads, number of clones, number of sorted cells and Shannon-Evenness (Fig. 38). The Pearson correlation resulted negative in almost all comparisons, with a slight correlation between clones number and cell numbers and Shannon-Evenness and clones number; however, it was found a negative Pearson correlation between the number of clones and the number of reads in both groups of patients. In fact, in a reliable TCR repertoire, the number of reads, or total sequences, and the number of clones, or unique sequences, are supposed to be two independent variables that do not flow together. Next, the variation of quantitative parameters (number of sorted cells, clones, reads and Shannon-Evenness) of TCR repertoires was evaluated over treatments. Results showed a significantly less diverse TCR repertoire in CD8 naïve cells of Natalizumab patients

compared to AHSCT at t24 (Fig. 39). In previous literature, any significant effect of Natalizumab on CD8 naïve cells was reported (Schneider-Hohendorf T et al., 2016). In this case, it is possible that the reduced TCR diversity of CD8 naïve cells may reflect decreased immune protection, also considering the capability of Natalizumab to reduce immune surveillance through the modulation of immune cell populations (Kaufmann M et al., 2018). Furthermore, the restricted TCR repertoire in this subpopulation may depend on antigen-specific triggering and/or the persistence of a state of inflammation, as sustained by the increased serum level of TNFα from t0 to t24 in Natalizumab compared to AHSCT (Fig. 52).

The variation of TCR repertoire statistics was challenging to quantify on an individual basis, showing no common pattern across patients when evaluated patient by patient (Fig. 40); therefore, the global state of the TCR clonal expansion based on different variables (cell population, treatment, timepoint, HLA) was investigated. Results showed that TCR clonal expansion differed by treatment (Fig. 41A). Furthermore, given the role of the HLA-DRB1*1501 in MS susceptibility (Jelcic I et al., 2018; Ballerini C et al., 2004), it was interesting to detect the impact of HLA-DRB1*1501 on CD4 clonal expansion (Fig. 41B).

Quantitative parameters included the evaluation of clonal persistence, that measures the percentage of clones that are still in the peripheral blood of patients after treatments. The clonal persistence differed by treatment: Natalizumab patients showed a clonal persistence in CD4 and CD8 subpopulations to a higher extent compared to AHSCT, where clonal persistence was slightly pronounced only in memory CD8 cells, whereas the other subpopulations resulted widely renewed (Fig. 42). This result is comparable with previous findings from the study of Muraro PA et al., who reported a higher renewal in the CD4 cell compartment compared to CD8 (unsorted) in RRMS patients one year after AHSCT (Muraro PA et al., 2014).

Nevertheless, there are some exceptions among our patients. The AHSCT patient MS032 showed the highest percentage of clonal persistence from t0 to t24 among all transplanted patients. This patient interrupted the standard protocol of conditioning chemotherapy for safety reasons and underwent a milder conditioning regimen; furthermore, MS032 experienced a disease relapse at t24. Among Natalizumab, where the periphery is enriched by pathogenic clones due to drug's mechanism of action, clonal persistence is generally higher compared to AHSCT patients, except for Ty17, Ty21 and

Ty25, whom 2/3 (Ty21 and Ty25) had a relapse during treatment. Interestingly, Muraro PA et al. documented a lower TCR repertoire diversity in AHSCT non-responder patients compared to responders (Muraro PA. et al., 2014), suggesting a link between TCR repertoire degree of reconstitution and treatment outcome. In light of these results, it is possible to speculate that the evaluation of clonal persistence may contribute to predict the patient outcome to treatment in the future.

The repertoire architecture was next evaluated. It qualitatively describes the TCR repertoire organization and structure based on similarity between amino acid CDR3 sequences. The concept is that T-cell clones with similar CDR3 sequences may have been selected by a common force, such as such as V(D)J recombination, thymic selection, antigen encounter and, in this case, immunomodulatory treatment (Miho E et al., 2019; Greiff V et al., 2017). The TCR repertoire architecture in our patients was also evaluated on a sub-sequence level, decomposing a.a. sequences in sub-sequences of length "k" called "k-mers". In both analyses, the repertoire architecture differed by treatment. A greater percentage of connected private and public clones was found at t24 in CD8 naïve T cells of Natalizumab compared to AHSCT (Fig. 45C). Of note, clone networks were constructed including a top of 10,000 frequency-based clones, that accounts for the 90% of all 180 repertoires. This choice was made because in complex diseases such as MS, where the antigen is unknown, it is not possible to state that high-frequency clones are surely linked to MS pathogenesis compared to low-frequency clones, therefore the selection of a top of a random number of clones could not be meaningful.

In k-mers analysis, a higher similarity on a sub-sequence level was found among AHSCT patients compared to Natalizumab (Fig. 46). Since k-mers distribution reflects the process of insertion/deletion of single amino acid during the V(D)J recombination that leads to TCR generation, this similarity may depend on the fact that AHSCT patients underwent the same post-transplant protocol, remaining at least one month in a sterile chamber, sharing the same nutritional restrictions and the same antimicrobial therapies. The V-gene usage did not show any variation over cell population, treatment, timepoints or HLA (Fig. 48).

As a further qualitative parameter, the CDR3-a.a. sequence overlap between our database and publicly available TCR databases (McPAS-TCR, VDJdb and the database from the study of Jelcic I et al., 2018) was evaluated. A statistically significant difference was found between AHSCT and Natalizumab patients in CD8 naïve cells at t24: in this

subpopulation, the percentage of shared sequences with public TCR databases was significantly lower at t24 in Natalizumab compared to AHSCT (Fig. 49). This result, together with the decreased Shannon-Evenness (Fig. 39), the higher sequence similarity (Fig. 45-47) and the lower number of public clones (Fig. 44) after 24 months of Natalizumab indicates a restricted TCR repertoire of CD8 naïve cells in this group of patients. This may depend on a mild impact of Natalizumab on VLA-4 expression on the surface of naïve cells compared to memory subpopulations, as previously documented (Iannetta M et al., 2016), with the consequence of an increased thymic retention of this cell population (Sawada M et al., 1992).

Moreover, the majority of sequences shared with McPAS-TCR and VDJdb was virus-associated and only few of them were classified as associated with autoimmune diseases (Fig. 51); of note, virus-associated sequences are more abundant than autoimmune-associated ones and this could have affected this result.

Finally, an opposite trend in cytokines and chemokines level was found between Natalizumab and AHSCT patients over treatment (Fig. 52). Specifically, TNFα was significantly higher in Natalizumab patients compared to AHSCT at t24, whereas CXCL10 and CXCL13 were significantly higher in AHSCT patients compared to Natalizumab at t24. Not much is known, from literature, about recall chemokines after AHSCT; on the other hand, it is known that Natalizumab determines an increase in pro-inflammatory cytokines in periphery (Khademi M et al., 2009). However, the levels of other pro-inflammatory cytokines, such as IFNγ, were not significantly increased in our patients after 24 months of Natalizumab. This result could depend on the fact that, in some cases, IFNγ and other pro-inflammatory cytokines are too low to be detectable in the serum and, furthermore, the presence of autoantibodies directed against cytokines, as reported in literature in MS patients, could affect their detection (Cappellano G et al., 2012).

It is worth mentioning that our results do not suggest that previous first-line treatments of patients impacted the TCR repertoire, since these treatments were randomly distributed in the two cohorts and variate intra- and inter- patient groups.

In summary, repertoire sequencing statistics evaluated longitudinally patient by patient suggest that, even though it was possible to distinguish the two treatments describing the TCR repertoire dynamics, each patient has its own repertoire and shows an individual treatment response (Fig. 40). However, when investigating multiple different

aspects of repertoire diversity, results showed that clonal expansion (Fig. 41), clonal persistence (Fig. 42), public clones number (Fig. 43, Fig. 44) and repertoire architecture (Fig. 45, Fig. 46) differentiate readily between treatment groups. Specifically, for Natalizumab there is a trend toward a status a less diverse TCR repertoire, that is significantly different from transplanted patients in CD8 naïve cells, whereas in AHSCT there is an almost complete TCR repertoire reconstitution in all the observed T-cell subpopulations.

The same bioinformatic analyses were performed on TCR repertoire of CSF and paired memory T-cell subpopulations from a third group of 4 incoming MS patients. The immunophenotypic analysis performed by flow cytometry on the CSF of previously collected 20 MS patients (Fig. 53) showed that most of the T cells present within the CSF of incoming patients are CD4 EM. Specifically, the total percentage of CD4 cells are significantly more abundant than CD8 cells and Tem cells are significantly higher compared to Tcm cells. This is in contrast with previous findings, that reported a majority of CD4 CM cells in the composition of CSF from MS patients (Kivisäkk P et al., 2003; van Nierop GP et al., 2017).

The negative Pearson correlation coefficient between Shannon-Evenness and reads and between reads and clones number ensured the good quality of data (Fig. 55).

Repertoire statistics showed a significant difference between peripheral memory (EM and CM) CD4 cells, peripheral memory CD8 cells and CSF: memory CD4 cells are characterized by a significantly higher number of sorted cells, clones and Shannon-Evenness compared to memory CD8 cells and CSF repertoires (Fig. 56). Of note, the significant difference in the number of clones, that are the unique sequences, and not in the number of reads, that are the total sequences, reflects a difference that lies specifically in the clonality of the peripheral memory subpopulations and it is presumably not biased by the number of total sequences. The difference in the Shannon-Evenness value reflects a higher diversity in the TCR repertoire of memory CD4 cells. Repertoire statistics visualized patient by patient showed a trend in a higher number of clones and Shannon-Evenness values in memory CD4 cells compared to CD8 and CSF, that are more variable across patients (Fig. 58).

The clonal overlap was then evaluated between the CSF compartment and paired peripheral memory T-cell subpopulations in each patient (Fig. 58). Generally, the higher clonal overlap was found between CD8 EM cells and CSF (1.8-4.8%) compared to CD4

EM (1.1-4.5%) and CM subpopulations (0.4-1.5% between CD4 CM and CSF and 0-1.3% between CD8 CM and CSF), that may be linked with results from the previously mentioned phenotypic analysis of CSF from 20 MS patients (Fig. 59), that showed an enrichment of Tem cells compared to Tcm in this compartment.

The highest overlap between periphery and CSF was found between CD4 and CD8 EM cells and CSF (4.5% and 4.8%, respectively) of patient CSF3, whereas the lowest clonal overlap was found in patient CSF2, who does not share any clone between the CSF and the peripheral memory T compartment. Of note, this patient is the only one who was diagnosed with PPMS, whereas the other three were confirmed with RRMS; furthermore, in the CSF of patient CSF2 (that is characterized by only 41 total unique sequences) it was observed the presence of a CDR3-a.a. sequence (CASSLLPGDEQF) that strongly predominates, in terms of frequency, on the other ones (766784 number of copies) (Fig. 57). To mention, the overlap between periphery and CSF of our patients is generally lower compared to previous studies (Lossius A et al., 2014), but such difference may lie in the low number of patients (N=4) included in our study.

As already described for Natalizumab and AHSCT patients, the percentage of sequences shared between TCR repertoires of CSF patients and McPAS-TCR and VDJdb was evaluated. Results showed a significantly higher overlap between peripheral EM and CM CD4 cells compared to EM and CM CD8 cells and CSF (Fig. 61). When considering the disease type in McPAS-TCR (Fig. 62A) or the antigen-species in VDJdb (Fig. 62B), memory CD4 cells showed a significantly higher sequence overlap with virus-associated CDR3 sequences compared to memory CD8 cells and CSF, in particular with CMV, EBV and Influenza A classified in VDJdb database (Fig. 62B).

In general, these results showed that TCR repertoires of CSF are more private and more variable across patients in terms of repertoire statistics (Fig. 56, Fig. 58) and of shared clones with public databases (Fig. 61, Fig. 62), whereas memory CD4 cells are characterized by a more diverse and more public TCR repertoire.

Patient CSF2, who was finally diagnosed with PPMS, was characterized by a highly prominent CDR3-a.a. sequence (CASSLLPGDEQF) in his CSF. In the biggest study on TCR repertoire in CSF of MS patients, including a total of 10 patients (Lossius A et al., 2014), a similar profile in TCR repertoires of patients CSF was not reported. Furthermore, the sequence CASSLLPGDEQF is not classified in any of the public TCR databases examined

in this study. It would be worthwhile to investigate whether the presence of this expanded sequence may correlate with clinical characteristics of patient.

In conclusion, this study demonstrated that the bioinformatic analysis of a big amount of sequencing data, such as our RRMS database (180 TCR repertoires), requires rigorous statistics through the choice of quantitative and qualitative parameters to analyze, in order to perform a consistent comparison between different TCR repertoires. Despite our results showed that is possible to find a link between molecular and clinical data, more insights are required, and the bioinformatic analyses workflow that was adopted in this study could be successfully replicated for similar data. First, it would be worthwhile, in the future, to enlarge the cohorts, including more Natalizumab and AHSCT patients and treatment-naïve incoming MS patients, and also to extend the analysis to other T-cell subpopulations, such as Tregs. Furthermore, this study highlighted on the necessity to find a consensus, within the scientific community, on the way of analyzing TCR sequencing data, in order to make possible a reliable comparison across different studies.

6. Bibliography

1. Abbas AKK. Cellular and Molecular Immunology. *ELSEVIER* 2015; **8e**: p. 192.

2. Abromson-Leeman SR and Cantor H. Specificity of T cell clones for antigen and autologous major histocompatibility complex products determines specificity for foreign major histocompatibility complex products. *J Exp Med* 1983; **158**: 428–437.

3. Alonso A and Hernán MA. Temporal trends in the incidence of multiple sclerosis: a systematic review. *Neurology* 2008 Jul 8; **71**(2): 129-35.

4. Alschuler KN, Ph.D., Ehde DM, Ph.D., Jensen MP, Ph.D. Co-Occurring Depression and Pain in Multiple Sclerosis. *Phys Med Rehabil Clin N Am* 2013 Nov; **24**(4): 10.

5. Alves Sousa AP, Johnson KR, Ohayon J, Zhu J, Muraro PA, Jacobson S. Comprehensive Analysis of TCR-β Repertoire in Patients with Neurological Immune-mediated Disorders. *Sci Rep* 2019 Jan 23; **9**(1): 344.

6. AMA (USAN) Monoclonal antibodies. United States Adopted Names. 2007-08-07. Retrieved 2007-08-15.

7. Amtmann D, PhD, Askew RL, Ph.D, MPH, Kim J, Ph.D, Chung H, Ph.D, Ehde DM, Ph.D, Bombardier CH, Ph.D, Kraft GH, MD, Jones SM, PhD, Johnson KL, PhD. Pain affects depression through anxiety, fatigue and sleep in Multiple Sclerosis. *Rehabil Psychol* 2015 Feb; **60**(1): 81–90.

8. Angelini DF, Serafini B, Piras E, Severa M, Coccia EM, Rosicarelli B, Ruggieri S, Gasperini C, Buttari F, Centonze D, Mechelli R, Salvetti M, Borsellino G, Aloisi F, Battistini L. Increased CD8+ T cell response to Epstein-Barr virus lytic antigens in the active phase of multiple sclerosis. *PLoS Pathog* 2013; **9**(4): e1003220.

9. Apeltsin L, Wang S, von Büdingen HC, Sirota M. A Haystack Heuristic for Autoimmune Disease Biomarker Discovery Using Next-Gen Immune Repertoire Sequencing Data. Sci Rep 2017; 7(1): 5338.

10. Arnon R and Aharoni R. Mechanism of action of glatiramer acetate in multiple sclerosis and its potential for the development of new applications. *Proc Natl Acad Sci USA* 2004 Oct 5; **101 (**Suppl 2): 14593-8.

11. Arruda LCM, de Azevedo JTC, de Oliveira GLV, Scortegagna GT, Rodrigues ES, Palma PVB, Brum DG, Guerreiro CT, Marques VD, Barreira AA, Covas DT, Simões BP, Voltarelli JC, Oliveira MC, Malmegrim KCR. Immunological correlates of favorable long-term clinical outcome in multiple sclerosis patients after autologous hematopoietic stem cell transplantation. *Clin Immunol* 2016 Aug; **169**: 47-57.

12. Arruda LCM, Lorenzi JC, Sousa AP, Zanette DL, Palma PV, Panepucci RA, Brum DS, Barreira AA, Covas DT, Simões BP, Silva WA Jr, Oliveira MC, Malmegrim KC. Autologous hematopoietic SCT normalizes miR-16, -155 and -142-3p expression in multiple sclerosis patients. *Bone Marrow Transplant* 2015 Mar; **50**(3): 380-9.

13. Arruda LCM, Malmegrim KCR, Lima-Júnior JR, Clave E, Dias JBE, Moraes DA, Douay C, Fournier I,NMoins-Teisserenc H, Alberdi AJ, Covas DT, Simões BP, Lansiaux P, Toubert A, Oliveira MC. Immune rebound associates with a favorable clinical response to autologous HSCT in systemic sclerosis patients. *Blood Adv* 2018 Jan 23; **2**(2): 126–141.

14. Atkins H and Freedman M. Immune ablation followed by autologous hematopoietic stem cell transplantation for the treatment of poor prognosis multiple sclerosis. *Methods Mol Biol* 2009; **549**: 231–246.

15. Atlas of Multiple Sclerosis, World Health Organization and Multiple Sclerosis International Federation. 2013.

16. Babbe H, Roers A, Waisman A, Lassmann H, Goebels N, Hohlfeld R, Friese M, Schröder R, Deckert M, Schmidt S, Ravid R, Rajewsky K. Clonal expansions of CD8(+) T cells dominate the T cell infiltrate in active multiple sclerosis lesions as shown by micromanipulation and single cell polymerase chain reaction. *J Exp Med* 2000 Aug 7; **192**(3): 393-404.

17. Baer L, Colon-Moran W, Bhattarai N. Characterization of the effects of immunomodulatory drug fingolimod (FTY720) on human T cell receptor signaling pathways. *Sci Rep* 2018; **8**: 10910.

18. Balint B, Haas J, Schwarz A, Jarius S, Furwentsches A, Engelhardt K, Bussmann C, Ebinger F, Fritzsching B, Paul F, Seidel U, Vlaho S, Huppke P, Gartner J, Wildemann B. T-cell homeostasis in pediatric multiple sclerosis: old cells in young patients. *Neurology* 2013; **81**: 784–792.

19. Ballerini C, Guerini FR, Rombolà G, Rosati E, Massacesi L, Ferrante P, Caputo D, Talamanca LF, Naldi P, Liguori M, Alizadeh M, Momigliano-Richiardi P, D'Alfonso

S. HLA-multiple sclerosis association in continental Italy and correlation with disease prevalence in Europe. *J Neuroimmunol* 2004 May; **150**(1-2): 178-85.

20. Barten LJ, Allington DR, Procacci KA, Rivey MP. New approaches in the management of multiple sclerosis. *Drug Des Devel Ther* 2010 Nov 24; **4**: 343-66.

21. Beck RC, Stahl S, O'Keefe CL, Maciejewski JP, Theil KS, His ED: Detection of mature T-cell leukemias by flow cytometry using anti-T-cell receptor B antibodies. *Am J Clin Pathol* 2003; **120**: 785–794.

22. Benkert TF, Dietz L, Hartmann EM, Leich E, Rosenwald A, Serfling E, Buttmann M, Berberich-Siebelt F. Natalizumab exerts direct signaling capacity and supports a pro-inflammatory phenotype in some patients with multiple sclerosis. *PLoS One* 2012; **7**(12): e52208.

23. Biogen. Tysabri (natalizumab) injection, for intravenous use. Full prescribing information. Revised May 2016. Available from: www.tysabri.com/prescribinginfo.

24. Bloomgren G, Richman S, Hotermans C, Subramanyam M, Goelz S, Natarajan A, Lee S, Plavina T, Scanlon JV, Sandrock A, Bozic C. Risk of natalizumab-associated progressive multifocal leukoencephalopathy. *N Engl J Med* 2012; **366**: 1870-1880.

25. Bozic C, Richman S, Plavina T, Natarajan A, Scanlon J, Subramanyam M, Sandrock A, Bloomgren G. Anti-JCV Antibody prevalence in patients with relapsing multiple sclerosis receiving or considering treatment with natalizumab: baseline results of STRATIFY-2 (S41.002). *Neurology* 2012; **78**(1 Supplement): S41.002.

26. Brandstadter R and Katz Sand I. The use of natalizumab for multiple sclerosis. *Neuropsychiatr Dis Treat* 2017 Jun 28; **13**: 1691-1702.

27. Brenchley JM, Karandikar NJ, Betts MR, Ambrozak DR, Hill BJ, Crotty LE, Casazza JP, Kuruppu J, Migueles SA, Connors M, Roederer M, Douek DC, Koup RA. Expression of CD57 defines replicative senescence and antigen-induced apoptotic death of CD8+ T cells. *Blood* 2003 Apr 1; **101**(7): 2711-20.

28. Brinkmann V, Billich A, Baumruker T, Heining P, Schmouder R, Francis G, Aradhye S, Burtin P. Fingolimod (FTY720): discovery and development of an oral drug to treat multiple sclerosis. *Nat Rev Drug Discov* 2010 Nov; **9**(11): 883-97.

29. Bromley SK, Mempel TR, Luster AD. Orchestrating the orchestrators: chemokines in control of T cell traffic. *Nat Immunol* 2008; **9**: 970–980.

30. Broux B, Markovic-Plese S, Stinissen P, Hellings N. Pathogenic features of CD4(+)CD28(-) T cells in immune disorders. *Trends Mol Med* 2012; **18**: 446–53.

31. Bürckert JP, Dubois ARSX, Faison WJ, Farinelle S, Charpentier E, Sinner R, Wienecke-Baldacchino A, Muller CP. Functionally Convergent B Cell Receptor Sequences in Transgenic Rats Expressing a Human B Cell Repertoire in Response to Tetanus Toxoid and Measles Antigens. *Front Immunol* 2017; **8**: 1834.

32. Burt RK, Balabanov R, Han X, Sharrack B, Morgan A, Quigley K, Yaung K, Helenowski IB, Jovanovic B, Spahovic D, Arnautovic I, Lee DC, Benefield BC, Futterer S, Oliveira MC, Burman J. Association of nonmyeloablative hematopoietic stem cell transplantation with neurological disability in patients with relapsing-remitting multiple sclerosis. *JAMA* 2015 Jan 20; **313**(3): 275-84.

33. Caballero A, Alvés-León S, Papais-Alvarenga R, Fernández O, Navarro G, Alonso A. DQB1*0602 confers genetic susceptibility to multiple sclerosis in Afro-Brazilians. *Tissue Antigens* 1999 Nov; **54**(5): 524-6.

34. Calabrese M, Agosta F, Rinaldi F, Mattisi I, Grossi P, Favaretto A, Atzori M, Bernardi V, Barachino L, Rinaldi L, Perini P, Gallo P, Filippi M. Cortical lesions and atrophy associated with cognitive impairment in relapsing-remitting multiple sclerosis. *Arch Neurol* 2009 Sep; **66**(9): 1144-50.

35. Cappellano G, Orilieri E, Woldetsadik AD, Boggio E, Soluri MF, Comi C, Sblattero D, Chiocchetti A, Dianzani U. Anti-cytokine Autoantibodies in Autoimmune Diseases. *Am J Clin Exp Immunol* 2012; **1**(2): 136-146.

36. Carlos TM, Schwartz BR, Kovach NL, Yee E, Rosa M, Osborn L, Chi-Rosso G, Newman B, Lobb R, Harlan JM. Vascular cell adhesion molecule-1 mediates lymphocyte adherence to cytokine-activated cultured human endothelial cells. *Blood* 1990 Sep 1; **76**(5): 965-70.

37. Casetta I, Iuliano G, Filippini G. Azathioprine for multiple sclerosis. Cochrane *Database Syst Rev* 2007 Oct 17; **(4)**: CD003982.

38. Cepok S, Rosche B, Grummel V, Vogel F, Zhou D, Sayn J, Sommer N, Hartung HP, Hemmer B. Short-lived plasma blasts are the main B cell effector subset during the course of multiple sclerosis. *Brain* 2005 Jul; **128**(Pt 7): 1667-76.

39. Cepok S, von Geldern G, Grummel V, Hochgesand S, Celik H, Hartung H, Hemmer B. Accumulation of class switched IgD-IgM- memory B cells in the cerebrospinal fluid during neuroinflammation. *J Neuroimmunol* 2006 Nov; **180**(1-2): 33-9.

40. Charcot JM. Lectures on the Diseases of the Nervous System. London: The New Sydenham Society; Lecture VI. Disseminated Sclerosis. *Pathological Anatomy* 1887; pp. 157–181.

41. Chaudhuri Abhijit. Drugs. Lessons for clinical trials from natalizumab in multiple sclerosis. *BMJ* 2006 Feb 18; **332**(7538): 416–419.

42. Chiarini M, Sottini A, Bertoli D, Serana F, Caimi L, Rasia S, Capra R, Imberti L. Newly produced T and B lymphocytes and T-cell receptor repertoire diversity are reduced in peripheral blood of fingolimod-treated multiple sclerosis patients. *Mult Scler*. 2015 May;**21**(6):726-34.

43. Chini L, Bardare M, Cancrini C, Angelini F, Mancia L, Cortis E, Finocchi A, Riccardi C, Rossi P. Evidence of clonotypic pattern of T-cell repertoire in synovial fluid of children with juvenile rheumatoid arthritis at the onset of the disease. *Scand J Immunol* 2002 Nov; **56**(5): 512-7.

44. Ciupe SM, Devlin BH, Markert ML, Kepler TB. Quantification of total T-cell receptor diversity by flow cytometry and spectratyping. *BMC Immunol* 2013 Aug 6; **14**:35.

45. Claes N, Dhaeze T, Fraussen J, Broux B, Van Wijmeersch B, Stinissen P, Hupperts R, Hellings N, Somers V. Compositional changes of B and T cell subtypes during fingolimod treatment in multiple sclerosis patients: a 12-month follow-up study. *PLoS One* 2014 Oct 31; **9**(10): e111115.

46. Cocco E, Meloni A, Murru MR, Corongiu D, Tranquilli S, Fadda E, Murru R, Schirru L, Secci MA, Costa G, Asunis I, Cuccu S, Fenu G, Lorefice L, Carboni N, Mura G, Rosatelli MC, Marrosu MG. Vitamin D responsive elements within the HLA-DRB1 promoter region in Sardinian multiple sclerosis associated alleles. *PLoS One* 2012; **7**(7): e41678.

47. Cohen JA and Chun J. Mechanisms of fingolimod's efficacy and adverse effects in multiple sclerosis. *Ann Neurol* 2011 May; **69**(5): 759-77.

48. Coles AJ. Alemtuzumab improved multiple sclerosis functional composite scores and delayed time to first relapse at 2-year interim analysis compared to

subcutaneous interferon beta-1a. *Multiple Sclerosis* 2007; **13**: S166.

49. Compston A and Coles A. Multiple sclerosis. *Lancet* 2002 Apr 6; **359(**9313): 1221-31.

50. Compston A and Coles A. Multiple sclerosis. *Lancet* 2008 Oct 25; **372**(9648): 1502-17.
51. Correale J and Farez M. Association between parasite infection and immune responses in multiple sclerosis. *Ann Neurol* 2007; **61**: 97–108.

52. Coulter SN, Rose TM, Schultz ER, Bennett JL, Garber RL, Chang M, Shad PA, Stewart PM, Nowinski RC, Brown JP, Burmer GC. Plaque-associated expression of human herpesvirus 6 in multiple sclerosis*. Proc Natl Acad Sci U S A* 1995 Aug 1; **92**(16): 7440-4.

53. Correale J, Ysrraelit MC, Gaitán MI. Immunomodulatory effects of Vitamin D in multiple sclerosis. *Brain* 2009 May; **132**(Pt 5): 1146-60.

54. Cree BA, Rioux JD, McCauley JL, Gourraud PA, Goyette P, McElroy J, De Jager P, Santaniello A, Vyse TJ, Gregersen PK, Mirel D, Hafler DA, Haines JL, Pericak-Vance MA, Compston A, Sawcer SJ, Oksenberg JR, Hauser SL; IMAGEN; IMSGC. A major histocompatibility Class I locus contributes to multiple sclerosis susceptibility independently from HLA-DRB1*15:01. *PloS one* 2010; **5**(6): e11296.

55. Cross AH and Naismith RT. Established and novel disease-modifying treatments in multiple sclerosis. *J Intern Med* 2014 Apr; **275**(4): 350-63.

56. Croxford JL, Anger HA, Miller SD. Viral delivery of an epitope from Haemophilus influenzae induces central nervous system autoimmune disease by molecular mimicry. *J Immunol* 2005 Jan 15; **174**(2): 907-17.

57. Csardi G and Nepusz T. The igraph software package for complex network research, InterJournal, Complex Systems 1695. http://igraph.org.

58. Cui JH, Lin KR, Yuan SH, Jin YB, Chen XP, Su XK, Jiang J, Pan YM, Mao SL, Mao XF, Luo W. TCR Repertoire as a Novel Indicator for Immune Monitoring and Prognosis Assessment of Patients With Cervical Cancer. *Front Immunol* 2018; **9**:2729.

59. Cui C, Tian X, Wu J, Zhang C, Tan Q, Guan X, Dong B, Zhao M, Lu Z, Hao C. T cell receptor β-chain repertoire analysis of tumor-infiltrating lymphocytes in pancreatic cancer. *Cancer Sci* 2019; **110**(1): 61-71.

60. Currier JR, Robinson MA. Spectratype/immunoscope analysis of the expressed TCR repertoire. *Curr Protoc Immunol* 2001 May; **Chapter 10**: Unit 10.28.

61. Dhaeze T, Peelen E, Hombrouck A, Peeters L, Van Wijmeersch B, Lemkens N, Lemkens P, Somers V, Lucas S, Broux B, Stinissen P, Hellings N. Circulating Follicular Regulatory T Cells Are Defective in Multiple Sclerosis. *J Immunol* 2015 Aug 1; **195**(3): 832-40.

62. Daikeler T, Labopin M, Di Gioia M, Abinun M, Alexander T, Miniati I, Gualandi F, Fassas A, Martin T, Schwarze CP, Wulffraat N, Buch M, Sampol A, Carreras E, Dubois B, Gruhn B, Güngör T, Pohlreich D, Schuerwegh A, Snarski E, Snowden J, Veys P, Fasth A, Lenhoff S, Messina C, Voswinkel J, Badoglio M, Henes J, Launay D, Tyndall A, Gluckman E, Farge D; EBMT Autoimmune Disease Working Party. Secondary autoimmune diseases occurring after HSCT for an autoimmune disease: a retrospective study of the EBMT Autoimmune Disease Working Party. *Blood* 2011; **118**: 1693–1698

63. Danikowski KM, Jayaramam S, Prabhakar BS. Regulatory T cells in multiple sclerosis and myasthenia gravis. *J Neuroinflammation* 2017; **14**: 117.

64. Dash P, Fiore-Gartland AJ, Hertz T, Wang GC, Sharma S, Souquette A, Crawford JC, Clemens EB, Nguyen THO, Kedzierska K, La Gruta NL, Bradley P, Thomas PG. 2017. 682 Quantifiable predictive features define epitope-specific T cell receptor repertoires. Nature 2017; **547**: 89–93; Glanville J, Huang H, Nau A, Hatton O, Wagar LE, Rubelt F, Ji X, Han A, Krams SM, Pettus C, Haas N, Lindestam Arlehamn CS, Sette A, Boyd SD, Scriba TJ, Martinez OM, Davis MM. Identifying specificity groups in the T cell receptor repertoire. Nature 2017; **547**: 94–98.

65. Dendrou CA, Fugger L, Friese MA. Immunopathology of multiple sclerosis. *Nat Rev Immunol* 2015 Sep 15; **15**(9): 545-58.

66. Denman AM, Russell AS, Denman EJ. Adoptive transfer of the diseases of New Zealand black mice to normal mice strains. *Clin Exp Immunol* 1969; **5**(6): 567–95.

67. de Paula Sousa A, Malmegrim KC, Panepucci RA, Brum DS, Barreira AA, Carlos Dos Santos A, Araújo AG, Covas DT, Oliveira MC, Moraes DA, Pieroni F, Barros GM, Simões BP, Nicholas R, Burt RK, Voltarelli JC, Muraro PA. Autologous haematopoietic stem cell transplantation reduces abnormalities in the expression of immune genes in multiple sclerosis. *Clin Sci (Lond)* 2015 Jan; **128**(2): 111-20.

68. Domingues RB, Fernandes GBP, Leite FBVM, Tilbery CP, Thomaz RB, Silva GS, Mangueira CLP, Soares CAS. The cerebrospinal fluid in multiple sclerosis: far beyond the bands. *Einstein (Sao Paulo)* 2017 Jan-Mar; **15**(1): 100-104.

69. Doorenspleet ME, Westera L, Peters CP, Hakvoort TBM, Esveldt RE, Vogels E, van Kampen AHC, Baas F, Buskens C, Bemelman WA, D'Haens G, Ponsioen CY, Te Velde AA, de Vries N, van den Brink GR. Profoundly Expanded T-cell Clones in the Inflamed and Uninflamed Intestine of Patients With Crohn's Disease. *J Crohns Colitis* 2017; **11**(7): 831-839.

70. Duddy ME, Alter A, Bar-Or A. Distinct profiles of human B cell effector cytokines: A role in immune regulation? *J Immunol* 2004; **172**: 3422–3427.

71. Elices MJ, Osborn L, Takada Y, Crouse C, Luhowskyj S, Hemler ME, Lobb RR. VCAM-1 on activated endothelium interacts with the leukocyte integrin VLA-4 at a site distinct from the VLA-4/fibronectin binding site. *Cell* 1990 Feb 23; **60**(4): 577-84.

72. Engelhardt B and Ransohoff RM. The ins and outs of T lymphocyte trafficking to the CNS: anatomical sites and molecular mechanisms. *Trends Immunol* 2005; **26**: 485–495.

73. Engelhardt B, Wolburg-Buchholz K, Wolburg H. Involvement of the choroid plexus in central nervous system inflammation. *Microsc Res Tech* 2001; **52**: 112–129.

74. Farge D, Arruda LC, Brigant F, Clave E, Douay C, Marjanovic Z, Deligny C, Maki G, Gluckman E, Toubert A, Moins-Teisserenc H. Long-term immune reconstitution and T cell repertoire analysis after autologous hematopoietic stem cell transplantation in systemic sclerosis patients. *J Hematol Oncol*. 2017 Jan 19;**10**(1):21.

75. Ferenczy MW, Marshall LJ, Nelson CD, Atwood WJ, Nath A, Khalili K, Major EO. Molecular biology, epidemiology, and pathogenesis of progressive multifocal leukoencephalopathy, the JC virus-induced demyelinating disease of the human brain. *Clin Microbiol Rev* 2012; **25**(3): 471–506.

76. Field J, Shahijanian F, Schibeci S, Australia and New Zealand MS Genetics Consortium (ANZgene), Johnson L, Gresle M, Laverick L, Parnell G, Stewart G, McKay F, Kilpatrick T, Butzkueven H, Booth D. The MS Risk Allele of CD40 Is Associated with Reduced Cell-Membrane Bound Expression in Antigen Presenting Cells: Implications for Gene Function. *PLoS One* 2015 Jun 11; **10**(6):

e0127080.

77. Fogdell-Hahn A, Ligers A, Grønning M, Hillert J, Olerup O. Multiple sclerosis: a modifying influence of HLA class I genes in an HLA class II associated autoimmune disease. *Tissue Antigens* 2000; **55**: 140–8.

78. Ford ML and Evavold BD. Specificity, magnitude, and kinetics of MOG-specific CD8+ T cell responses during experimental autoimmune encephalomyelitis. *Eur J Immunol* 2005; **35**: 76–85.

79. Fontoura P. Monoclonal antibody therapy in multiple sclerosis - Paradigm shifts and emerging challenges. *MAbs* 2010 Nov-Dec; **2**(6): 670–681.

80. Freedman MS, Thompson EJ, Deisenhammer F, Giovannoni G, Grimsley G, Keir G, Ohman S, Racke MK, Sharief M, Sindic CJ, Sellebjerg F, Tourtellotte WW. Recommended standard of cerebrospinal fluid analysis in the diagnosis of multiple sclerosis: a consensus statement. *Arch Neurol* 2005 Jun; **62**(6): 865-70.

81. Fujinami RS and Oldstone MB. Amino acid homology between the encephalitogenic site of myelin basic protein and virus: mechanism for autoimmunity. *Science* 1985 Nov 29; **230**(4729): 1043-5.

82. Fujinami RS, Oldstone MBA, Wroblewska Z, Frankel ME, Koprowski H. Molecular mimicry in virus infection: Crossreaction of measles virus phosphoprotein or of herpes simplex virus protein with human intermediate filaments. *Proc Natl Acad Sci USA* 1983; **80**: 2346–2350.

83. Gaujoux R and Seoighe C. A flexible R package for nonnegative matrix factorization. *BMC Bioinformatic* 2010; **11**:367.

84. Ge F, Lin H, Li Z, Chang T. Efficacy and safety of autologous hematopoietic stem-cell transplantation in multiple sclerosis: a systematic review and meta-analysis. *Neurol Sci* 2019; **40**(3): 479–487.

85. Geginat J, Lanzavecchia A, Sallusto F. Proliferation and differentiation potential of human CD8 memory T-cell subsets in response to antigen or homeostatic cytokines. *Blood* 2003; **101**(11): 4260.

86. Gehad A, Teague JE, Matos TR, Huang V, Yang C, Watanabe R, O'Malley JT, Trimble CL, Kupper TS, Clark RA. A primary role for human central memory cells in tissue immunosurveillance. *Blood Adv* 2018 Feb 13; **2**(3): 292-298.

87. Giovannoni G, Cutter GR, Lunemann J, Martin R, Münz C, Sriram S, Steiner I, Hammerschlag MR, Gaydos CA. Infectious causes of multiple sclerosis. *Lancet Neurol* 2006 Oct; **5**(10): 887-94.

88. Gold R, Kappos L, Arnold DL, Bar-Or A, Giovannoni G, Selmaj K, Tornatore C, Sweetser MT, Yang M, Sheikh SI, Dawson KT; DEFINE Study Investigators. Placebo-controlled phase 3 study of oral BG-12 for relapsing multiple sclerosis. *N Engl J Med* 2012 Sep 20; **367**(12): 1098-107.

89. Golding A, Chandler S, Ballestar E, Wolffe AP, Schlissel MS. Nucleosome structure completely inhibits *in vitro* cleavage by the V(D)J recombinase. *EMBO J* 1999; **18**: 3712–3723.

90. Goodman AD, Mock DJ, Powers JM, Baker JV, Blumberg BM. Human herpesvirus 6 genome and antigen in acute multiple sclerosis lesions. *J Infect Dis* 2003; **187**: 1365–1376.

91. Gorski J, Yassai M, Zhu X., Kissela B, Kissella B., Keever C, Flomenberg N. Circulating T cell repertoire complexity in normal individuals and bone marrow recipients analyzed by CDR3 size spectratyping. Correlation with immune status. *J Immunol* 1994; **152**: 5109–5119.

92. Gomez-Tourino I, Kamra Y, Baptista R, Lorenc A, Peakman M. T cell receptor β-chains display abnormal shortening and repertoire sharing in type 1 diabetes. *Nat Commun* 2017 Nov 27; **8**(1): 1792.

93. Gray E, Thomas TL, Betmouni S, Scolding N, Love S. Elevated myeloperoxidase activity in white matter in multiple sclerosis. *Neurosci Lett* 2008 Oct 24; **444**(2): 195-8.

94. Gregory SG, Schmidt S, Seth P, Oksenberg JR, Hart J, Prokop A, Caillier SJ, Ban M, Goris A, Barcellos LF, Lincoln R, McCauley JL, Sawcer SJ, Compston DA, Dubois B, Hauser SL, Garcia-Blanco MA, Pericak-Vance MA, Haines JL; Multiple Sclerosis Genetics Group. Interleukin 7 receptor alpha chain (IL7R) shows allelic and functional association with multiple sclerosis. *Nat Genet* 2007 Sep; **39**(9): 1083-91.

95. Greiff, V, Bhat P, Cook SC, Menzel U, Kang W, Reddy ST. A bioinformatic framework for immune repertoire diversity profiling enables detection of immunological status. *Genome Med* 2015; **7**: 49.

96. Greiff V, Menzel U, Miho E, Weber C, Riedel R, Cook S, Valai A, Lopes T, Radbruch A, Winkler TH, Reddy ST. Systems Analysis Reveals High Genetic and Antigen-Driven Predetermination of Antibody Repertoires throughout B Cell Development. *Cell Rep* 2017; **19**: 1467–1478.

97. Greiff V, Miho E, Menzel U, Reddy ST. Bioinformatic and Statistical Analysis of Adaptive Immune Repertoires. *Trends Immunol* 2015 Nov; **36**(11): 738-749.

98. Greiff V, Weber CR, Palme J, Bodenhofer U, Miho E, Menzel U, Reddy ST. Learning the High-Dimensional Immunogenomic Features That Predict Public and Private Antibody Repertoires. *J Immunol* 2017; **199**: 2985–2997.

99. Gross CC, Ahmetspahic D, Ruck T, Schulte-Mecklenbeck A, Schwarte K, Jörgens S, Scheu S, Windhagen S, Graefe B, Melzer N, Klotz L, Arolt V, Wiend H, Meuth SG, Alferink J. Alemtuzumab treatment alters circulating innate immune cells in multiple sclerosis. *Neurol Neuroimmunol Neuroinflamm* 2016 Dec; **3**(6): e289.

100. Gross CC, Schulte-Mecklenbeck A, Klinsing S, Posevitz-Fejfár A, Wiendl H, Klotz L. Dimethyl fumarate treatment alters circulating T helper cell subsets in multiple sclerosis. *Neurol Neuroimmunol Neuroinflamm* 2015 Dec 10; **3**(1): e183.

101. Gu Z, Eils R, Schlesner M. Complex heatmaps reveal patterns and correlations in multidimensional genomic data. *Bioinformatics* 2016; **32**(18): 2847–2849.

102. Guidelines on the Use of International Nonproprietary Names (INNs) for Pharmaceutical Substances (PDF). 1997 pp. 27–28. Retrieved 2007-08-15.

103. Günaltay S, Repsilber D, Helenius G, Nyhlin N, Bohr J, Hultgren O, Hultgren Hörnquist E. Oligoclonal T-cell Receptor Repertoire in Colonic Biopsies of Patients with Microscopic Colitis and Ulcerative Colitis. *Inflamm Bowel Dis* 2017; **23**(6): 932-945.

104. Gunn MD, Ngo VN, Ansel KM, Ekland EH, Cyster JG, Williams LT. A B-cell-homing chemokine made in lymphoid follicles activates Burkitt's lymphoma receptor-1. *Nature* 1998; **391**: 799–803.

105. Hadley W. ggplot2: Elegant Graphics for Data Analysis. New York, NY: Springer-Verlag New York; 2016.

106. Haegert DG. Multiple Sclerosis: A Disorder of Altered T-Cell Homeostasis. *Mult Scler Int* 2011; **2011**: 461304.

107. Haines JD, Inglese M, Casaccia P. Axonal damage in multiple sclerosis. *Mt Sinai J Med* 2011 Mar-Apr; **78**(2): 231-43.

108. Han S, Lin YC, Wu T, Salgado AD, Mexhitaj I, Wuest SC, Romm E, Ohayon J, Goldbach-Mansky R, Vanderver A, Marques A, Toro C, Williamson P, Cortese I, Bielekova B. Comprehensive immunophenotyping of cerebrospinal fluid cells in patients with neuroimmunological diseases. *J Immunol* 2014 Mar 15; **192**(6): 2551-63.

109. Harbo HF, Lie BA, Sawcer S, Celius EG, Dai K-Z, Oturai A, et al. Genes in the HLA class I region may contribute to the HLA class II-associated genetic susceptibility to multiple sclerosis. *Tissue Antigens* 2004; **63**: 237–47.

110. Hassan-Smith G, Douglas MR. Epidemiology and diagnosis of multiple sclerosis. *Br J Hosp Med (Lond)* 2011 Oct; **72**(10): M146-51.

111. Hauser SL, Bhan AK, Gilles F, Kemp M, Kerr C, Weiner HL. Immunohistochemical analysis of the cellular infiltrate in multiple sclerosis lesions. *Ann Neurol* 1986; **19**: 578–87.

112. Hawker K, O'Connor P, Freedman MS, Calabresi PA, Antel J, Simon J, Hauser S, Waubant E, Vollmer T, Panitch H, Zhang J, Chin P, Smith CH, OLYMPUS trial group. Rituximab in patients with primary progressive multiple sclerosis: results of a randomized double-blind placebo-controlled multicenter trial. *Ann Neurol* 2009 Oct; **66**(4): 460-71.

113. Hedegaard CJ, Krakauer M, Bendtzen K, Lund H, Sellebjerg F, Nielsen CH. T helper cell type 1 (Th1), Th2 and Th17 responses to myelin basic protein and disease activity in multiple sclerosis. *Immunology* 2008; **125**(2): 161–169.

114. Hemmer B, Vergelli M, Gran B, Ling N, Conlon P, Pinilla C, Houghten R, McFarland HF, Martin R. Predictable TCR antigen recognition based on peptide scans leads to the identification of agonist ligands with no sequence homology. *J Immunol* 1998; **160**: 3631–3636.

115. Henig I and Zuckerman T. Hematopoietic Stem Cell Transplantation—50 Years of Evolution and Future Perspectives. *Rambam Maimonides Med J* 2014 Oct; **5**(4): e0028.

116. Hershberg U and Prak ETL. The analysis of clonal expansions in normal and autoimmune B cell repertoires. *Philos Trans R Soc B* 2015; **370**: 20140239.

117. Hu D, Weiner HL, Ritz J. Identification of Cytolytic CD161(−)CD56(+) Regulatory CD8 T Cells in Human Peripheral Blood. *PLoS One* 2013; **8**: e59545.

118. Hunter SF, Bowen JD, Reder AT. The Direct Effects of Fingolimod in the Central Nervous System: Implications for Relapsing Multiple Sclerosis. *CNS Drugs* 2016 Feb; **30**(2): 135-47.

119. Iannetta M, Zingaropoli MA, Bellizzi A, Morreale M, Pontecorvo S, D'Abramo A, Oliva A, Anzivino E, Lo Menzo S, D'Agostino C, Mastroianni CM, Millefiorini E, Pietropaolo V, Francia A, Vullo V, Ciardi MR. Natalizumab Affects T-Cell Phenotype in Multiple Sclerosis: Implications for JCV Reactivation. *PLoS One* 2016 Aug 3; **11**(8): e0160277.

120. International Multiple Sclerosis Genetics Consortium. The genetic association of variants in CD6, TNFRSF1A and IRF8 to multiple sclerosis: a multicenter case-control study. *PLoS One* 2011 Apr 28; **6**(4): e18813.

121. Jackson KJ, Liu Y, Roskin KM, Glanville J, Hoh RA, Seo K, Marshall EL, Gurley TC, Moody MA, Haynes BF, Walter EB, Liao HX, Albrecht RA, García-Sastre A, Chaparro-Riggers J, Rajpal A, Pons J, Simen BB, Hanczaruk B, Dekker CL, Laserson J, Koller D, Davis MM, Fire AZ, Boyd SD. Human responses to influenza vaccination show seroconversion signatures and convergent antibody rearrangements. *Cell Host Microbe* 2014; **16**(1): 105-14.

122. Jafari N, Broer L, Hoppenbrouwers IA, van Duijn CM, Hintzen RQ. Infectious mononucleosis-linked HLA class I single nucleotide polymorphism is associated with multiple sclerosis. *Mult Scler* 2010; **16**(11): 1303–1307.

123. Jakkula E, Leppä V, Sulonen AM, Varilo T, Kallio S, Kemppinen A, Purcell S, Koivisto K, Tienari P, Sumelahti ML, Elovaara I, Pirttilä T, Reunanen M, Aromaa A, Oturai AB, Søndergaard HB, Harbo HF, Mero IL, Gabriel SB, Mirel DB, Hauser SL, Kappos L, Polman C, De Jager PL, Hafler DA, Daly MJ, Palotie A, Saarela J, Peltonen L. Genomewide association study in a high-risk isolate formultiple sclerosis reveals associated variants in STAT3 gene. *Am J Hum Genet* 2010 Feb 12; **86**(2): 285-91.

124. Jelcic I, Al Nimer F, Wang J, Lentsch V, Planas R, Jelcic I, Madjovski A, Ruhrmann S, Faigle W, Frauenknecht K, Pinilla C, Santos R, Hammer C, Ortiz Y, Opitz L, Grönlund H, Rogler G, Boyman O, Reynolds R, Lutterotti A, Khademi M, Olsson T, Piehl F, Sospedra M, Martin R. Memory B Cells Activate Brain-Homing, Autoreactive CD4+ T Cells in Multiple Sclerosis. *Cell* 2018 Sep 20; **175**(1): 85-

100.e23.

125. Jersild C, Svejgaard A, Fog T. HL-A antigens and multiple sclerosis. *Lancet* 1972 Jun 3; **1**(7762): 1240-1.

126. Jhunjhunwala S, van Zelm MC, Peak MM, Murre C. Chromatin architecture and the generation of antigen receptor diversity. *Cell* 2009; **138**: 435–448.

127. Joseph FG, Hirst CL, Pickersgill TP, Ben-Shlomo Y, Robertson NP, Scolding NJ. CSF oligoclonal band status informs prognosis in multiple sclerosis: a case control study of 100 patients. *J Neurol Neurosurg Psychiatry* 2009; **80**: 292–296.

128. Kang JH, Sheu JJ, Kao S, Lin HC. Increased risk of multiple sclerosis following herpes zoster: a nationwide, population-based study. *J Infect Dis* 2011; **204**: 188–192.

129. Kaplinsky J and Arnaout R. Robust estimates of overall immune-repertoire diversity from high-throughput measurements on samples. *Nat Commun* 2016; **7**: 11881.

130. Kassambara A. ggpubr: "ggplot2" Based Publication Ready Plots. https://rpkgs.datanovia.com/ggpubr/index.html.

131. Katdare A and Ursekar M. Systematic imaging review: Multiple Sclerosis. *Ann Indian Acad Neurol* 2015 Sep; **18**(Suppl 1): S24–S29.

132. Kaufmann M, Haase R, Proschmann U, Ziemssen T, Akgün K. Real-World Lab Data in Natalizumab Treated Multiple Sclerosis Patients Up to 6 Years Long-Term Follow Up. *Front Neurol* 2018 Dec 7; **9**: 1071.

133. Kean JM, Rao S, Wang M, Garcea RL. Seroepidemiology of human polyomaviruses. *PLoS Pathog* 2009 Mar; **5**(3): e1000363.

134. Kebir H, Ifergan I, Alvarez JI, Bernard M, Poirier J, Arbour N, Duquette P, Prat A. Preferential recruitment of interferon-gamma-expressing TH17 cells in multiple sclerosis. *Ann Neurol* 2009 Sep; **66**(3): 390-402.

135. Kepler T, He M, Tomfohr J, Devlin B, Sarzotti M, Markert M: Statistical analysis of antigen receptor spectratype data. *Bioinformatics* 2005; **21**(16): 3394-3400.

136. Khademi M, Bornsen L, Rafatnia F, Andersson M, Brundin L, Piehl F, Sellebjerg F, Olsson T. The effects of natalizumab on inflammatory mediators in multiple

sclerosis: prospects for treatment-sensitive biomarkers. *Eur J Neurol* 2009; **16**(4): 528–536.

137. Khademi M, Kockum I, Andersson ML, Iacobaeus E, Brundin L, Sellebjerg F, Hillert J, Piehl F, Olsson T. Cerebrospinal fluid CXCL13 in multiple sclerosis: a suggestive prognostic marker for the disease course. *Mult Scler* 2011; **17**: 335–343.

138. Kidd D, Barkhof F, McConnell R, Algra PR, Allen IV, Revesz T. Cortical lesions in multiple sclerosis. *Brain* 1999 Jan; **122**(Pt 1): 17-26.

139. Kimura K, Nakamura M, Sato W, Okamoto T, Araki M, Lin Y, Murata M, Takahashi R, Yamamura T. Disrupted balance of T cells under natalizumab treatment in multiple sclerosis. *Neurol Neuroimmunol Neuroinflamm* 2016 Mar 3; **3**(2): e210.

140. Kivisäkk P, Mahad DJ, Callahan MK, Sikora K, Trebst C, Tucky B, Wujek J, Ravid R, Staugaitis SM, Lassmann H, Ransohoff RM. Expression of CCR7 in multiple sclerosis: implications for CNS immunity. *Ann Neurol* 2004 May; **55**(5): 627-38.

141. Kivisäkk P1, Mahad DJ, Callahan MK, Trebst C, Tucky B, Wei T, Wu L, Baekkevold ES, Lassmann H, Staugaitis SM, Campbell JJ, Ransohoff RM. Human cerebrospinal fluid central memory CD4+ T cells: evidence for trafficking through choroid plexus and meninges via P‐selectin. *Proc Natl Acad Sci USA* 2003; **100**: 8389–8394.

142. Kivisäkk P, Healy BC, Viglietta V, Quintana FJ, Hootstein MA, Weiner HL, Khoury SJ. Natalizumab treatment is associated with peripheral sequestration of proinflammatory T cells. *Neurology* 2009 Jun 2; **72**(22): 1922-30.

143. Klarenbeek PL, de Hair MJ, Doorenspleet ME, van Schaik BD, Esveldt RE, van de Sande MG, Cantaert T, Gerlag DM, Baeten D, van Kampen AH, Baas F, Tak PP, de Vries N. Inflamed target tissue provides a specific niche for highly expanded T-cell clones in early human autoimmune disease. *Ann Rheum Dis* 2012 Jun; **71**(6): 1088-93.

144. Klein L, Kyewski B, Allen PM, Hogquist KA. Positive and negative selection of the T cell repertoire: what thymocytes see (and don't see). *Nat Rev Immunol* 2014 Jun; **14**(6): 377-91.

145. Kleinschmidt-DeMasters BK, Tyler KL. Progressive multifocal leukoencephalopathy complicating treatment with natalizumab and interferon beta-1a for multiple sclerosis. *N Engl J Med* 2005; **353**: 369-374.

146. Knaan-Shanzer S, Houben P, Kinwel-Bohre´ EP, van Bekkum DW. Remission induction of adjuvant arthritis in rats by total body irradiation and autologous bone marrow transplantation. *Bone Marrow Transplant* 1991; **8**(5): 333–8.

147. Kobayashi KS and van den Elsen PJ. NLRC5: a key regulator of MHC class I-dependent immune responses. *Nat Rev Immunol* 2012 Dec; **12**(12): 813-20.

148. Kobelt G, Berg J, Lindgren P, Elias WG, Flachenecker P, Freidel M, König N, Limmroth V, Straube E. Costs and quality of life of multiple sclerosis in Germany. *Eur J Health Econ* 2006 Sep 7; Suppl **2**: S34-44.

149. Koch M, Kingwell E, Rieckmann P, Tremlett H. The natural history of primary progressive multiple sclerosis. *Neurology* 2009 Dec 8; **73**(23): 1996-2002.

150. Köhler G and Milstein C. Continuous cultures of fused cells secreting antibody of predefined specificity. *Nature* 1975 Aug 7; **256**(5517): 495-7.

151. Korporal M, Haas J, Balint B, Fritzsching B, Schwarz A, Moeller S, Fritz B, Suri-Payer E, Wildemann B. Interferon beta-induced restoration of regulatory T-cell function in multiple sclerosis is prompted by an increase in newly generated naive regulatory T cells. *Arch Neurol* 2008 Nov; **65**(11): 1434-9.

152. Krzywinski M, Schein J, Birol I, Connors J, Gascoyne R, Horsman D, Jones SJ, Marra MA. Circos: an information aesthetic for comparative genomics. *Genome Res* 2009; **19**: 1639–1645.

153. Kuo TT and Aveson VG. Neonatal fc receptor and IgG-based therapeutics. *mAbs* 2011; **3**(5): 422–430.

154. Kwon J, Morshead KB, Guyon JR, Kingston RE, Oettinger MA. Histone acetylation and hSWI/SNF remodeling act in concert to stimulate V(D)J cleavage of nucleosomal DNA. *Mol Cell* 2000; **6**: 1037–1048.

155. Langrish CL, Chen Y, Blumenschein WM, Mattson J, Basham B, Sedgwick JD, McClanahan T, Kastelein RA, Cua DJ. IL-23 drives a pathogenic T cell population that induces autoimmune inflammation. *J Exp Med* 2005; **201**: 233-240.

156. Laplaud DA, Ruiz C, Wiertlewski S, Brouard S, Berthelot L, Guillet M, Melchior B, Degauque N, Edan G, Brachet P, Damier P, Soulillou JP. Blood T-cell receptor beta chain transcriptome in multiple sclerosis. Characterization of the T cells with altered CDR3 length distribution. *Brain* 2004 May; **127**(Pt 5): 981-95.

157. Laydon DJ, Bangham CR, Asquith B. Estimating T-cell repertoire diversity: limitations of classical estimators and a new approach. *Philos Trans R Soc Lond B Biol Sci* 2015 Aug 19; **370**(1675). pii: 20140291.

158. Leandro MJ. B-cell subpopulations in humans and their differential susceptibility to depletion with anti-CD20 monoclonal antibodies. *Arthritis Res Ther* 2013; **15**(Suppl 1): S3.

159. Le Bourhis L, Corraliza A, Auzolle C, Ricart E, Hawkey C, Lindsay J, Clark M, Rogler G, Satsangui J, Haller D, Panes J, Salas A, Allez M. Resetting of the mucosal T cell repertoire after hematopoietic stem cell transplantation in refractory CD. *Gastroenterology*. 2017; **152**:S613–4.

160. Léger OJ, Yednock TA, Tanner L, Horner HC, Hines DK, Keen S, Saldanha J, Jones ST, Fritz LC, Bendig MM. Humanization of a mouse antibody against human alpha-4 integrin: a potential therapeutic for the treatment of multiple sclerosis. *Hum Antibodies* 1997; **8**: 3-16.

161. Leinikki P, Shekarchi I, Iivanainen M, Taskinen E, Holmes KV, Madden D, Sever JL. Virus antibodies in the cerebrospinal fluid of multiple sclerosis patients detected with ELISA tests. *J Neurol Sci* 1982; **57**: 249–255.

162. Lemke H. Immune Response Regulation by Antigen Receptors' Clone-Specific Nonself Parts. *Front Immunol* 2018; **9**: 1471.

163. Levin LI, Munger KL, Rubertone MV, Peck CA, Lennette ET, Spiegelman D, Ascherio A. Temporal relationship between elevation of Epstein-Barr virus antibody titers and initial onset of neurological symptoms in multiple sclerosis. *JAMA* 2005; **293**: 2496–500.

164. Li B, Carey M, Workman JL. The role of chromatin during transcription. Cell 2007; 128: 707–719.

165. Li Y, Yin Y, Mariuzza RA. Structural and biophysical insights into the role of CD4 and CD8 in T cell activation. *Front Immunol* 2013 Jul 22; **4**: 206.

166. Lincoln JA and Cook SD, An overview of gene-epigenetic-environmental contributions to MS causation. *J Neurol Sci* 2009 Nov 15; **286**(1-2):54-7.

167. Link J, Lorentzen AR, Kockum I, Duvefelt K, Lie BA, Celius EG, Harbo HF, Hillert J, Brynedal B. Two HLA class I genes independently associated with multiple sclerosis. *J Neuroimmunol* 2010; **226**(1–2): 172–176.

168. Liu YY, Yang QF, Yang JS, Cao RB, Liang JY, Liu YT, Zeng YL, Chen S, Xia XF, Zhang K, Liu L. Characteristics and prognostic significance of profiling the peripheral blood T-cell receptor repertoire in patients with advanced lung cancer. *Int J Cancer* 2019 Sep 1; **145**(5): 1423-1431.

169. Lobb RR and Hemler ME. The pathophysiologic role of alpha 4 integrins in vivo. *J Clin Invest* 1994 Nov; **94**(5): 1722-8.

170. Lordick F, Ott K, Weitz J, Jäger D. The evolving role of catumaxomab in gastric cancer. *Expert Opin Biol Ther* 2008 Sep; **8**(9): 1407-15.

171. Lossius A, Johansen JN, Vartdal F, Robins H, Jūratė Šaltytė B, Holmøy T, Olweus J. High-throughput sequencing of TCR repertoires in multiple sclerosis reveals intrathecal enrichment of EBV-reactive CD8+ T cells. *Eur J Immunol* 2014 Nov; **44**(11): 3439-5.

172. Lowenthal A, Vansande M, Karcher D. The differential diagnosis of neurological diseases by fractionating electrophoretically the CSF gamma-globulins. *J Neurochem* 1960 Aug; **6**: 51-6.

173. Lublin FD and Reingold SC. Defining the clinical course of multiple sclerosis: results of an international survey. National Multiple Sclerosis Society (USA) Advisory Committee on Clinical Trials of New Agents in Multiple Sclerosis. *Neurology* 1996 Apr; **46**(4): 907-11.

174. Lublin FD, Reingold SC, Cohen JA, Cutter GR, Sørensen PS, Thompson AJ, Wolinsky JS, Balcer LJ, Banwell B, Barkhof F, Bebo B Jr, Calabresi PA, Clanet M, Comi G, Fox RJ, Freedman MS, Goodman AD, Inglese M, Kappos L, Kieseier BC, Lincoln JA, Lubetzki C, Miller AE, Montalban X, O'Connor PW, Petkau J, Pozzilli C, Rudick RA, Sormani MP, Stüve O, Waubant E, Polman CH. Defining the clinical course of multiple sclerosis: the 2013 revisions. *Neurology* 2014 Jul 15; **83**(3): 278-86.

175. Lucchinetti C, Brück W, Parisi J, Scheithauer B, Rodriguez M, Lassmann H. Heterogeneity of multiple sclerosis lesions: implications for the pathogenesis of

demyelination. *Ann Neurol* 2000 Jun; **47**(6): 707-17.

176. Lucchinetti CF, Popescu BFG, Bunyan RF, Moll NM, Roemer SF, Lassmann H, Brück W, Parisi JE, Scheithauer BW, Giannini C, Weigand SD, Mandrekar J, Ransohoff RM. Inflammatory cortical demyelination in early multiple sclerosis. *N Engl J Med* 2011 Dec 8; **365**: 2188–97

177. Lundmark F, Duvefelt K, Iacobaeus E, Kockum I, Wallström E, Khademi M, Oturai A, Ryder LP, Saarela J, Harbo HF, Celius EG, Salter H, Olsson T, Hillert J. Variation in interleukin 7 receptor alpha chain (IL7R) influences risk of multiple sclerosis. *Nat Genet* 2007 Sep; **39**(9): 1108-13.

178. Luo C, Tsementzi D, Kyrpides N, Read T, Konstantinidis KT. Direct Comparisons of Illumina vs. Roche 454 Sequencing Technologies on the Same Microbial Community DNA Sample. *PLoS One* 2012; **7**(2): e30087.

179. Lutter L, Spierings J, van Rhijn-Brouwer FCC, van Laar JM, van Wijk F. Resetting the T Cell Compartment in Autoimmune Diseases With Autologous Hematopoietic Stem Cell Transplantation: An Update. *Front Immunol* 2018; **9**: 767.

180. Lutterotti A and Martin R. Getting specific: monoclonal antibodies in multiple sclerosis. *Lancet Neurol* 2008 Jun; **7**(6): 538-47.

181. Ma Y, Schwarz K, Lieber MR. The Artemis: DNA-PKcs endonuclease cleaves DNA loops, flaps, and gaps. *DNA Repair (Amst)* 2005 Jul 12; **4**(7): 845-51.

182. Mackay LK, Wynne-Jones E, Freestone D, Pellicci DG, Mielke LA, Newman DM, Braun A, Masson F, Kallies A, Belz GT, Carbone FR. T‐Box transcription factors combine with the cytokines TGF‐β and IL‐15 to control tissue-resident memory T cell fate. *Immunity* 2014; **43**: 1101–1111.

183. Madi A, Poran A, Shifrut E, Reich-Zeliger S, Greenstein E, Zaretsky I, Arnon T, Laethem FV, Singer A, Lu J, Sun PD, Cohen IR, Friedman N. T cell receptor repertoires of mice and humans are clustered in similarity networks around conserved public CDR3 sequences. *eLife* 2017; **6**: e22057.

184. Madsen LS, Andersson EC, Jansson L, Krogsgaard M, Andersen CB, Engberg J, Strominger JL, Svejgaard A, Hjorth JP, Holmdahl R, Wucherpfennig KW, Fugger L. A humanized model for multiple sclerosis using HLA-DR2 and a human T-cell receptor. *Nat Genet* 1999; **23**: 343–347.

185. Maggi P, Absinta M, Grammatico M, Vuolo L, Emmi G, Carlucci G, Spagni G, Barilaro A, Repice AM, Emmi L, Prisco D, Martinelli V, Scotti R, Sadeghi N, Perrotta G, Sati P, Dachy B, Reich DS, Filippi M, Massacesi L. Central vein sign differentiates Multiple Sclerosis from central nervous system inflammatory vasculopathies. *Ann Neurol* 2018 Feb; **83**(2): 283-294.

186. Magliozzi R, Howell O, Vora A, Serafini B, Nicholas R, Puopolo M, Reynolds R, Aloisi F. Meningeal B-cell follicles in secondary progressive multiple sclerosis associate with early onset of disease and severe cortical pathology. *Brain* 2007 Apr; **130**(Pt 4): 1089-104.

187. Mahmoudi M, Sahraian MA, Shokrgozar MA, Laurent S. Superparamagnetic Iron Oxide Nanoparticles: Promises for Diagnosis and Treatment of Multiple Sclerosis. ACS *Chem Neurosci* 2011 Mar 16; **2**(3): 118–140.

188. Mancuso R, Saresella M, Hernis A, Marventano I, Ricci C, Agostini S, Rovaris M, Caputo D, Clerici M. JC virus detection and JC virus-specific immunity in natalizumab-treated multiple sclerosis patients. *J Transl Med* 2012 Dec 11; **10**: 248.

189. Marie P. Lectures on diseases of the spinal cord. London. *The New Sydenham Society* 1895; p: 103.

190. Marion S, Nicol B, Garcia A, Laplaud D. Involvement of CD8+ T Cells in Multiple Sclerosis. *Front Immunol* 2015; **6**: 604.

191. Mariottini A, Innocenti C, Forci B, Magnani E, Mechi C, Barilaro A, Nistri R, Fani A, Saccardi R, Massacesi L, Repice AM. Safety and efficacy of autologous hematopoietic stem-cell transplantation following natalizumab discontinuation in aggressive multiple sclerosis. *Eur J Neurol* 2018 Nov 10.

192. Markovic-Plese S and McFarland HF. Immunopathogenesis of the multiple sclerosis lesion. *Curr Neurol Neurosci Rep* 2001; **1**: 257–62.

193. Marrero I, Hamm DE, Davies JD. High-throughput sequencing of islet-infiltrating memory CD4+ T cells reveals a similar pattern of TCR Vβ usage in prediabetic and diabetic NOD mice. *PLoS One* 2013 Oct 17; **8**(10): e76546.

194. Marrie RA and Wolfson C. Multiple sclerosis and varicella zoster virus infection: a review. *Epidemiol Infect* 2001; **127**: 315–325.

195. Marrosu MG, Murru MR, Costa G, Murru R, Muntoni F, Cucca F. DRB1-DQA1-DQB1 loci and multiple sclerosis predisposition in the Sardinian population. Hum Mol Genet 1998 Aug; **7**(8): 1235-7.

196. Massey JC, Sutton IJ, Ma DDF, Moore JJ. Regenerating Immunotolerance in Multiple Sclerosis with Autologous Hematopoietic Stem Cell Transplant. *Front Immunol* 2018 Mar 12; **9**: 410.

197. Matusevicius D, Kivisäkk P, He B, Kostulas N, Ozenci V, Fredrikson S, Link H. Interleukin-17 mRNA expression in blood and CSF mononuclear cells is augmented in multiple sclerosis. *Multiple Sclerosis* 1999; **5**(2): 101–104.

198. McBlane F and Boyes J. Stimulation of V(D)J recombination by histone acetylation. *Curr Biol* 2000 Apr 20; **10**(8): 483-6.

199. McDonald WI, Compston A, Edan G, Goodkin D, Hartung HP, Lublin FD, McFarland HF, Paty DW, Polman CH, Reingold SC, Sandberg-Wollheim M, Sibley W, Thompson A, van den Noort S, Weinshenker BY, Wolinsky JS. Recommended diagnostic criteria for multiple sclerosis: guidelines from the International Panel on the diagnosis of multiple sclerosis. *Ann Neurol* 2001 Jul; **50**(1): 121-7.

200. Messi M, Giacchetto I, Nagata K, Lanzavecchia A, Natoli G, Sallusto F. Memory and flexibility of cytokine gene expression as separable properties of human TH1 and TH2 lymphocytes. *Nat Immunol* 2003; **4**: 78–86.

201. Miho E., Roškar R, Greiff V, Reddy ST. Large-scale network analysis reveals the sequence space architecture of antibody repertoires. *Nat Commun* 2019; **10**: 1321.

202. Miho E, Yermanos A, Weber CR, Berger CT, Reddy ST, Greiff V. Computational Strategies for Dissecting the High-Dimensional Complexity of Adaptive Immune Repertoires. *Front Immunol* 2018 Feb 21; **9**: 224.

203. Miller DH, Khan OA, Sheremata WA, Blumhardt LD, Rice GP, Libonati MA, Willmer-Hulme AJ, Dalton CM, Miszkiel KA, O'Connor PW; International Natalizumab Multiple Sclerosis Trial Group. A controlled trial of natalizumab for relapsing multiple sclerosis. *N Engl J Med* 2003 Jan 2; **348**(1): 15-23.

204. Miller DH, Soon D, Fernando KT, MacManus DG, Barker GJ, Yousry TA, Fisher E, O'Connor PW, Phillips JT, Polman CH, Kappos L, Hutchinson M, Havrdova E, Lublin FD, Giovannoni G, Wajgt A, Rudick R, Lynn F, Panzara MA, Sandrock AW; AFFIRM Investigators. MRI outcomes in a placebo-controlled trial of natalizumab in relapsing MS. *Neurology* 2007 Apr 24; **68**(17): 1390-401.

205. Milo R and Kahana E. Multiple sclerosis: geoepidemiology, genetics and the environment. Multiple sclerosis: geoepidemiology, genetics and the environment. *Autoimmun Rev* 2010 Mar; **9**(5): A387-94.

206. Montalban X, Hauser SL, Kappos L, Arnold DL, Bar-Or A, Comi G, de Seze J, Giovannoni G, Hartung H, Hemmer B, Lublin F, Rammohan KW, Selmaj K, Traboulsee A, Sauter A, Masterman D, Fontoura P, Belachew S, Garren H, Mairon N, Chin P, Wolinsky JS for the ORATORIO Clinical Investigators. Ocrelizumab versus Placebo in Primary Progressive Multiple Sclerosis. *N Engl J Med* 2017; **376**: 209-220.

207. Monto AS, Malosh RE, Petrie JG, Thompson MG, Ohmit SE. Frequency of acute respiratory illnesses and circulation of respiratory viruses in households with children over 3 surveillance seasons. *J Infect Dis* 2014; **210**(11): 1792–9.

208. Morton JI and Siegel BV. Letter: Early autoantibody formation in lethally irradiated or drug-treated H-2-compatible recipients of pre-autoimmune NZB bone marrow or fetal liver cells. *Transplantation* 1974 Jun; **17**(6): 624-6.

209. Moskowitz DM, Zhang DW, Hu B, Le Saux S, Yanes RE, Ye Z, Buenrostro JD, Weyand CM, Greenleaf WJ, Goronzy JJ. Epigenomics of human CD8 T cell differentiation and aging. *Sci Immunol* 2017 Feb; **2**(8). pii: eaag0192.

210. Mullen AL, Benoit K, Keyes O, Selivanov D, Arnold J. Fast, Consistent Tokenization of Natural Language Text. *J Open Source Softw* 2018; **3**(23): 65.

211. Muls N, Dang HA, Sindic CJ, van Pesch V. Fingolimod increases CD39-expressing regulatory T cells in multiple sclerosis patients. *PLoS One* 2014 Nov 20; **9**(11): e113025.

212. Mundy CL, Patenge N, Matthews AGW, Oettinger MA. Assembly of the RAG1/RAG2 synaptic complex. *Mol Cell Biol* 2002; **22**: 69–77.

213. Muraro PA, Douek DC, Packer A, Chung K, Guenaga FJ, Cassiani-Ingoni R, Campbell C, Memon S, Nagle JW, Hakim FT, Gress RE, McFarland HF, Burt RK, Martin R. Thymic output generates a new and diverse TCR repertoire after autologous stem cell transplantation in multiple sclerosis patients. *J Exp Med* 2005 Mar 7; **201**(5): 805-16.

214. Muraro PA, Pasquini M, Atkins HL, Bowen JD, Farge D, Fassas A, Freedman MS, Georges GE, Gualandi F, Hamerschlak N, Havrdova E, Kimiskidis VK, Kozak T, Mancardi GL, Massacesi L, Moraes DA, Nash RA, Pavletic S, Ouyang J, Rovira M,

Saiz A, Simoes B, Trnený M, Zhu L, Badoglio M, Zhong X, Sormani MP, Saccardi R; Multiple Sclerosis–Autologous Hematopoietic Stem Cell Transplantation (MS-AHSCT) Long-term Outcomes Study Group. Long-term Outcomes After Autologous Hematopoietic Stem Cell Transplantation for Multiple Sclerosis. *JAMA Neurol* 2017 Apr 1; **74**(4): 459-469.

215. Muraro PA, Robins H, Malhotra S, Howell M, Phippard D, Desmarais C, de Paula Alves Sousa A, Griffith LM, Lim N, Nash RA, Turka LA. T cell repertoire following autologous stem cell transplantation for multiple sclerosis. *J Clin Invest*. 2014 Mar;**124**(3):1168-72.

216. Murray JM, Kaufmann GR, Hodgkin PD, Lewin SR, Kelleher AD, Davenport MP, Zaunders JJ. Naive T cells are maintained by thymic output in early ages but by proliferation without phenotypic change after age twenty. *Immunol Cell Biol* 2003 Dec; **81**(6): 487-95.

217. Myhr KM and Mellgren SI. Corticosteroids in the treatment of multiple sclerosis. *Acta Neurol Scand Suppl* 2009; **(189)**: 73-80.

218. Naismith RT, Piccio L, Lyons JA, Lauber J, Tutlam NT, Parks BJ, Trinkaus K, Song SK, Cross AH. Rituximab add-on therapy for breakthrough relapsing multiple sclerosis: a 52-week phase II trial. *Neurology* 2010 Jun 8; **74**(23): 1860-7.

219. Naito S, Namerow N, Mickey MR, Terasaki PI. Multiple sclerosis: association with HL-A3. *Tissue Antigens* 1972; **2**: 1–4.

220. Nakamura Y, Matsushita T, Sato S, Niino M, Fukazawa T, Yoshimura S, Hisahara S, Isobe N, Shimohama S, Watanabe M, Yoshida K, Houzen H, Miyazaki Y, Yamasaki R, Kikuchi S, Kira J; Japan Multiple Sclerosis Genetics Consortium. Latitude and HLA-DRB1*04:05 independently influence disease severity in Japanese multiple sclerosis: a cross-sectional study. Latitude and HLA-DRB1*04:05 independently influence disease severity in Japanese multiple sclerosis: a cross-sectional study. *J Neuroinflammation* 2016; **13**(1): 239.

221. Nash RA, Hutton GJ, Racke MK, Popat U, Devine SM, Griffith LM, Muraro PA, Openshaw H, Sayre PH, Stüve O, Arnold DL, Spychala ME, McConville KC, Harris KM, Phippard D, Georges GE, Wundes A, Kraft GH, Bowen JD. High-dose immunosuppressive therapy and autologous hematopoietic cell transplantation for relapsing-remitting multiple sclerosis (HALT-MS): a 3-year interim report. *JAMA Neurol* 2015 Feb; **72**(2): 159-69.

222. Neefjes J, Jongsma ML, Paul P, Bakke O. Towards a systems understanding of MHC class I and MHC class II antigen presentation. *Nat Rev Immunol* 2011 Nov 11; **11**(12): 823-36.
223. Nikolich-Zugich J, Slifka MK, Messaoudi I. The many important facets of T-cell repertoire diversity. *Nat Rev Immunol* 2004 Feb; **4**(2): 123-32.

224. Nielsen BR, Ratzer R, Börnsen L, von Essen MR, Christensen JR, Sellebjerg F. Characterization of naïve, memory and effector T cells in progressive multiple sclerosis. *J Neuroimmunol* 2017 Sep 15; **310**: 17-25.

225. Obermeier B, Lovato L, Mentele R, Brück W, Forne I, Imhof A, Lottspeich F, Turk KW, Willis SN, Wekerle H, Hohlfeld R, Hafler DA, O'Connor KC, Dornmair K. Related B cell clones that populate the CSF and CNS of patients with multiple sclerosis produce CSF immunoglobulin. *J Neuroimmunol* 2011; **233**: 245–248.

226. O'Connor PW, Goodman A, Kappos L, Lublin FD, Miller DH, Polman C, Rudick RA, Aschenbach W, Lucas N. Disease activity return during natalizumab treatment interruption in patients with multiple sclerosis. *Neurology* 2011 May 31; **76**(22): 1858-65.

227. O'Connor RA, Prendergast CT, Sabatos CA, Lau CW, Leech MD, Wraith DC, Anderton SM. Cutting edge: Th1 cells facilitate the entry of Th17 cells to the central nervous system during experimental autoimmune encephalomyelitis. *J Immunol* 2008 Sep 15; **181**(6): 3750-4.

228. Oksenberg JR, Baranzini SE, Sawcer S, Hauser SL. The genetics of multiple sclerosis: SNPs to pathways to pathogenesis. *Nat Rev Genet* 2008 Jul; **9**(7): 516-26.

229. Olerup O, Hillert J. HLA class II-associated genetic susceptibility in multiple sclerosis: a critical evaluation. *Tissue Antigens* 1991 Jul; **38**(1):1-15.

230. Orrell RW. Multiple Sclerosis: The history of a disease [Book Review]. *J R Soc Med* 2005; **98**:289.

231. Osgood EE, Riddle MC, Mathews TJ. Aplastic anemia treated with daily transfusions and intravenous marrow; case report. *Ann Intern Med* 1939; **13**: 357–67.

232. Owens GP, Ritchie AM, Burgoon MP, Williamson RA, Corboy JR, Gilden DH. Single-cell repertoire analysis demonstrates that clonal expansion is a prominent feature of the B cell response in multiple sclerosis cerebrospinal fluid. *J Immunol* 2003; **171**: 2725–2733.

233. Palanichamy A, Jahn S, Nickles D, Derstine M, Abounasr A, Hauser SL, Baranzini SE, Leppert D, von Büdingen HC. Rituximab efficiently depletes increased CD20-expressing T cells in multiple sclerosis patients. *J Immunol* 2014 **193**: 580-586.

234. Pannetier C, Cochet M, Darche S, Casrouge A, Zöller M, Kourilsky P. The sizes of the CDR3 hypervariable regions of the murine T-cell receptor beta chains vary as a function of the recombined germ-line segments. *Proc Natl Acad Sci USA* 1993 May 1; **90**(9): 4319-23.

235. Pardo G and Jones DE. The sequence of disease-modifying therapies in relapsing multiple sclerosis: safety and immunologic considerations. *J Neurol* 2017 Dec; **264**(12): 2351-2374.

236. Pearce JM. Historical descriptions of multiple sclerosis. *Eur Neuro*l 2005; **54**(1): 49-53.

237. Peeters LM, Vanheusden M, Somers V, Van Wijmeersch B, Stinissen P, Broux B, Hellings N. Cytotoxic CD4+ T Cells Drive Multiple Sclerosis Progression. *Front Immunol* 2017 Sep 20; **8**: 1160.

238. Peterson JW, Bo L, Mork S, Chang A, Trapp BD. Transected neurites, apoptotic neurons, and reduced inflammation in cortical multiple sclerosis lesions. *Ann Neurol* 2001; **50**(3): 389–400.

239. Phillips JT, O'Connor PW, Havrdova E, Hutchinson M, Kappos L, Miller DH, Polman CH, Lublin FD, Giovannoni G, Wajgt A, Lynn F, Panzara MA, Sandrock AW; AFFIRM Investigators. Infusion-related hypersensitivity reactions during natalizumab treatment. *Neurology* 2006 Nov 14; **67**(9): 1717-8.

240. Planas R, Metz I, Martin R, Sospedra M. Detailed Characterization of T Cell Receptor Repertoires in Multiple Sclerosis Brain Lesions. *Front Immunol* 2018 Mar 19; **9**: 509.

241. Polman CH, O'Connor PW, Havrdova E, Hutchinson M, Kappos L, Miller DH, Phillips JT, Lublin FD, Giovannoni G, Wajgt A, Toal M, Lynn F, Panzara MA, Sandrock AW; AFFIRM Investigators. A randomized, placebo-controlled trial of natalizumab for relapsing multiple sclerosis. *N Engl J Med* 2006 Mar 2; **354**(9): 899-910.

242. Polman CH, Reingold SC, Edan G, Filippi M, Hartung HP, Kappos L, Lublin FD, Metz LM, McFarland HF, O'Connor PW, Sandberg-Wollheim M, Thompson AJ, Weinshenker BG, Wolinsky JS. Diagnostic criteria for multiple sclerosis: 2005 revisions to the "McDonald Criteria". *Ann Neurol* 2005 Dec; **58**(6): 840-6.

243. Polman CH, Reingold SC, Banwell B, Clanet M, Cohen JA, Filippi M, Fujihara K, Havrdova E, Hutchinson M, Kappos L, Lublin FD, Montalban X, O'Connor P, Sandberg-Wollheim M, Thompson AJ, Waubant E, Weinshenker B, Wolinsky JS.

Diagnostic criteria for multiple sclerosis: 2010 revisions to the McDonald criteria. Ann Neurol 2011 Feb; 69(2): 292–302.

244. Praksova P, Stourac P, Bednarik J, Vlckova E, Mikulkova Z, Michalek J. Immunoregulatory T cells in multiple sclerosis and the effect of interferon beta and glatiramer acetate treatment on T cell subpopulations. *J Neurol Sci* 2012 Aug 15; **319**(1-2): 18-23.

245. R Core Team. R: A language and environment for statistical computing. R Foundation for Statistical Computing, Vienna, Austria. https://www.r-project.org/.

246. Radue EW, Stuart WH, Calabresi PA, Confavreux C, Galetta SL, Rudick RA, Lublin FD, Weinstock-Guttman B, Wynn DR, Fisher E, Papadopoulou A, Lynn F, Panzara MA, Sandrock AW; SENTINEL Investigators. Natalizumab plus interferon beta-1a reduces lesion formation in relapsing multiple sclerosis. *J Neurol Sci* 2010 May 15; **292**(1-2): 28-35.

247. Ramagopalan SV, Maugeri NJ, Handunnetthi L, Lincoln MR, Orton SM, Dyment DA, Deluca GC, Herrera BM, Chao MJ, Sadovnick AD, Ebers GC, Knight JC. Expression of the multiple sclerosis-associated MHC class II Allele HLA-DRB1*1501 is regulated by vitamin D. *PLoS Genet* 2009 Feb; **5**(2): e1000369.

248. Ransohoff R. Natalizumab for multiple sclerosis. *NEJM* 2007; **356**: 2622-2629.

249. Raj T, Rothamel K, Mostafavi S, Ye C, Lee MN, Replogle JM, Feng T, Lee M, Asinovski N, Frohlich I, Imboywa S, Von Korff A, Okada Y, Patsopoulos NA, Davis S, McCabe C, Paik HI, Srivastava GP, Raychaudhuri S, Hafler DA, Koller D, Regev A, Hacohen N, Mathis D, Benoist C, Stranger BE, De Jager PL. Polarization of the effects of autoimmune and neurodegenerative risk alleles in leukocytes. *Science* 2014 May 2; **344**(6183): 519-23.

250. Rasouli J, Ciric B, Imitola J, Gonnella P, Hwang D, Mahajan K, Mari ER, Safavi F, Leist TP, Zhang GX, Rostami A. Expression of GM-CSF in T Cells Is Increased in Multiple Sclerosis and Suppressed by IFN-β Therapy. *J Immunol* 2015 Jun 1; **194**(11): 5085-93.

251. Reboldi A, Coisne C, Baumjohann D, Benvenuto F, Bottinelli D, Lira S, Uccelli A, Lanzavecchia A, Engelhardt B, Sallusto F. C-C chemokine receptor 6-regulated entry of TH-17 cells into the CNS through the choroid plexus is required for the initiation of EAE. *Nat Immunol* 2009 May; **10**(5): 514-23.

252. Rezvany MR, Tehrani MJ, Karlsson C, Lundin J, Rabbani H, Osterborg A, Mellstedt H. Reconstitution of the T-cell repertoire following treatment with alemtuzumab (anti-CD52 monoclonal antibody) in patients with B-cell chronic lymphocytic leukaemia. *Br J Haematol* 2006 Nov; **135**(4): 475-85.

253. Richert N, Bloomgren G, Cadavid D. Imaging findings for PML in natalizumab-treated MS patients. *MS Journal* 2012; **18**(Suppl. 4): 27-28.

254. Rigby WF, Waugh M, Graziano RF. Regulation of human monocyte HLA-DR and CD4 antigen expression, and antigen presentation by 1,25-dihydroxyvitamin D3. *Blood* 1990; **76**: 189–197.

255. Rooney S, Sekiguchi J, Zhu C, Cheng HL, Manis J, Whitlow S, DeVido J, Foy D, Chaudhuri J, Lombard D, Alt FW. Leaky Scid phenotype associated with defective V(D)J coding end processing in Artemis-deficient mice. *Mol Cell* 2002 Dec; **10**(6): 1379-90.

256. Rosati G. The prevalence of multiple sclerosis in the world: an update. *Neurol Sci* 2001 Apr; **22**(2): 117-39.

257. Rudick RA, Sandrock A. Natalizumab: alpha 4-integrin antagonist selective adhesion molecule inhibitors for MS. *Expert Rev Neurother* 2004 Jul; **4**(4): 571-80.

258. Ruck T, Pfeuffer S, Schulte-Mecklenbeck A, Gross CC, Lindner M, Metze D, Ehrchen J, Sondermann W, Pul R, Kleinschnitz C, Wiendl H, Meuth SG, Klotz L. Vitiligo after alemtuzumab treatment: Secondary autoimmunity is not all about B cells. *Neurology* 2018 Dec 11; **91**(24): e2233-e2237.

259. Saccardi R and Gualandi F. Hematopoietic stem cell transplantation procedures. *Autoimmunity* 2008 Dec; **41**(8): 570-6.

260. Saccardi R, Kozak T, Bocelli-Tyndall C, Fassas A, Kazis A, Havrdova E, Carreras E, Saiz A, Löwenberg B, te Boekhorst PA, Gualandio F, Openshaw H, Longo G, Pagliai F, Massacesi L, Deconink E, Ouyang J, Nagore FJ, Besalduch J, Lisukov IA, Bonini A, Merelli E, Slavino S, Gratwohl A, Passweg J, Tyndall A, Steck AJ, Andolina M, Capobianco M, Martin JL, Lugaresi A, Meucci G, Sáez RA, Clark RE, Fernandez MN, Fouillard L, Herstenstein B, Koza V, Cocco E, Baurmann H, Mancardi GL; Autoimmune Diseases Working Party of EBMT. Autologous stem cell transplantation for progressive multiple sclerosis: update of the European Group for Blood and Marrow Transplantation autoimmune diseases working party database. *Mult Scler* 2006; **12**: 814–823

261. Saccardi R, Mancardi GL, Solari A, Bosi A, Bruzzi P, Di Bartolomeo P, Donelli A, Filippi M, Guerrasio A, Gualandi F, La Nasa G, Murialdo A, Pagliai F, Papineschi F, Scappini B, Marmont AM. Autologous HSCT for severe progressive multiple sclerosis in a multicenter trial: impact on disease activity and quality of life. *Blood* 2005 Mar 15; **105**(6): 2601-7.

262. Sallusto F, Geginat J, Lanzavecchia A. Central memory and effector memory T cell subsets: function, generation, and maintenance. *Ann Rev Immunol* 2004; **22**: 745-63.

263. Salou M, Garcia A, Michel L, Gainche-Salmon A, Loussouarn D, Nicol B, Guillot F, Hulin P, Nedellec S, Baron D, Ramstein G, Soulillou JP, Brouard S, Nicot AB, Degauque N, Laplaud DA. Expanded CD8 T-cell sharing between periphery and CNS in multiple sclerosis. *Ann Clin Transl Neurol* 2015 Jun; **2**(6): 609-22.

264. Sati P, Oh J, Constable RT, Evangelou N, Guttmann CR, Henry RG, Klawiter EC, Mainero C, Massacesi L, McFarland H, Nelson F, Ontaneda D, Rauscher A, Rooney WD, Samaraweera AP, Shinohara RT, Sobel RA, Solomon AJ, Treaba CA, Wuerfel J, Zivadinov R, Sicotte NL, Pelletier D, Reich D, NAIMS Cooperative. The central vein sign and its clinical evaluation for the diagnosis of multiple sclerosis: a consensus statement from the North American Imaging in Multiple Sclerosis Cooperative. *Nat Rev Neurol* 2016 Dec; **12**(12): 714-722.

265. Sawada M, Nagamine J, Takeda K, Utsumi K, Kosugi A, Tatsumi Y, Hamaoka T, Miyake K, Nakajima K, Watanabe T. Expression of VLA-4 on thymocytes. Maturation stage-associated transition and its correlation with their capacity to adhere to thymic stromal cells. *J Immunol* 1992 Dec 1; **149**(11): 3517-24.

266. Schneider-Hohendorf T, Mohan H, Bien CG, Breuer J, Becker A, Görlich D, Kuhlmann T, Widman G, Herich S, Elpers C, Melzer N, Dornmair K, Kurlemann G, Wiendl H, Schwab N. CD8(+) T-cell pathogenicity in Rasmussen encephalitis elucidated by large-scale T-cell receptor sequencing. *Nat Commun* 2016 Apr 4; **7**: 11153.

267. Schatz DG and Ji Y. Recombination centres and the orchestration of V(D)J recombination. *Nat Rev Immunol* 2011 Apr; **11**(4): 251-63.

268. Scheinberg P, Melenhorst JJ, Brenchley JM, Hill BJ, Hensel NF, Chattopadhyay PK, Roederer M, Picker LJ, Price DA, Barrett AJ, Douek DC. The transfer of adaptive immunity to CMV during hematopoietic stem cell transplantation is dependent on the specificity and phenotype of CMV-specific T cells in the donor. *Blood* 2009; **114**(24): 5071.

269. Schwarz BA and Bhandoola A. Trafficking from the bone marrow to the thymus: a prerequisite for thymopoiesis. *Immunol Rev* 2006 Feb; **209**: 47-57.

270. Serafini B, Rosicarelli B, Franciotta D, Magliozzi R, Reynolds R, Cinque P, Andreoni L, Trivedi P, Salvetti M, Faggioni A, Aloisi F. Dysregulated Epstein-Barr virus infection in the multiple sclerosis brain. *J Exp Med* 2007 Nov 26; **204**(12): 2899-912.

271. Serafini B, Rosicarelli B, Magliozzi R, Stigliano E, Aloisi F. Detection of ectopic B-cell follicles with germinal centers in the meninges of patients with secondary progressive multiple sclerosis. *Brain Pathol* 2004; **14**: 164–74.

272. Shannon P, Markiel A, Ozier O, Baliga NS, Wang JT, Ramage D, Amin N, Schwikowski B, Ideker T. Cytoscape: A Software Environment for Integrated

Models of Biomolecular Interaction Networks. *Genome Res* 2003; **13**(11): 2498–2504.

273. Shogren-Knaak M, Ishii H, Sun JM, Pazin MJ, Davie JR, Peterson CL. Histone H4‐K16 acetylation controls chromatin structure and protein interactions. *Science* 2006; **311**: 844–847.

274. Shugay M, Bagaev DV, Zvyagin IV, Vroomans RM, Crawford JC, Dolton G, Komech EA, Sycheva AL, Koneva AE, Egorov ES, Eliseev AV, Van Dyk E, Dash P, Attaf M, Rius C, Ladell K, McLaren JE, Matthews KK, Clemens EB, Douek DC, Luciani F, van Baarle D, Kedzierska K, Kesmir C, Thomas PG, Price DA, Sewell AK, Chudakov DM. VDJdb: a curated database of T-cell receptor sequences with known antigen specificity. *Nucleic Acids Res* 2018; **46**: D419–D427.

275. Sibley WA and Foley JM. Infection and immunization in multiple sclerosis. *Ann N Y Acad Sci* 1965 Mar 31; **122**: 457-66.

276. Simnica D, Akyüz N, Schliffke S, Mohme M, v.Wenserski L, Mährle T, Fanchi LF, Lamszus K, Binder M. T cell receptor next-generation sequencing reveals cancer-associated repertoire metrics and reconstitution after chemotherapy in patients with hematological and solid tumors. *Oncoimmunology* 2019; **8**:11.

277. Simpson BS and Coles AJ. Rationale for cytotoxic monoclonal antibodies in MS. *Int MS J* 2007; **14**: 48–56.

278. Sinnecker T, Dörr J, Pfueller CF, Harms L, Ruprecht K, Jarius S, Brück W, Niendorf T, Wuerfel J, Paul F. Distinct lesion morphology at 7-T MRI differentiates neuromyelitis optica from multiple sclerosis. *Neurology* 2012 Aug 14; **79**(7): 708-14.

279. Skon CN, Lee J, Anderson KG, Masopust D, Hogquist KA, Jameson SC. Transcriptional downregulation of S1pr1 is required for the establishment of resident memory CD8+ T cells. *Nat Immunol* 2013; **14**: 1285–1293.

280. Skulina C, Schmidt S, Dornmair K, Babbe H, Roers A, Rajewsky K, Wekerle H, Hohlfeld R, Goebels N. Multiple sclerosis: brain-infiltrating CD8+ T cells persist as clonal expansions in the cerebrospinal fluid and blood. *Proc Natl Acad Sci U S A* 2004 Feb 24; **101**(8): 2428-33.

281. Sobottka B, Harrer MD, Ziegler U, Fisher K, Wiendl H, Hünig T, Becher B, Goebels N. Collateral bystander damage by myelin-directed CD8+ T cells causes axonal loss. *Am J Pathol* 2009; **175**: 1160–6.

282. Soldan SS, Berti R, Salem N, Secchiero P, Flamand L, Calabresi PA, Brennan MB, Maloni HW, McFarland HF, Lin HC, Patnaik M, Jacobson S. Association of human herpes virus 6 (HHV-6) with multiple sclerosis: increased IgM response to HHV-6

early antigen and detection of serum HHV-6 DNA. *Nat Med* 1997 Dec; **3**(12): 1394-7.

283. Solomon AJ, Schindler MK, Howard DB, Watts R, Sati P, Nickerson JP, Reich DS. "Central vessel sign" on 3T FLAIR* MRI for the differentiation of multiple sclerosis from migraine. *Ann Clin Transl Neurol* 2015 Dec 16; **3**(2): 82-7.

284. Son NH, Murray S, Yanovski J, Hodes RJ, Weng N. Lineage-specific telomere shortening and unaltered capacity for telomerase expression in human T and B lymphocytes with age. *J Immunol* 2000; **165**: 1191–96.

285. Sorensen PS, Koch-Henriksen N, Petersen T, Ravnborg M, Oturai A, Sellebjerg F. Recurrence or rebound of clinical relapses after discontinuation of natalizumab therapy in highly active MS patients. *J Neurol* 2014; **261**: 1170–1177.

286. Sormani MP, Muraro PA, Schiavetti I, Signori A, Laroni A, Saccardi R, Mancardi GL. Autologous hematopoietic stem cell transplantation in multiple sclerosis. A meta-analysis. *Neurology* 2017; **88**: 2115–2122

287. Spelman T, Gray O, Trojano M, Petersen T, Izquierdo G, Lugaresi A, Hupperts R, Bergamaschi R, Duquette P, Grammond P, Giuliani G, Boz C, Verheul F, Oreja-Guevara C, Barnett M, Grand'Maison F, Edite Rio M, Lechner-Scott J, Van Pesch V, Fernandez Bolanos R, Flechter S, Den Braber-Moerland L, Iuliano G, Amato MP, Slee M, Cristiano E, Saladino ML, Paine M, Vella N, Kasa K, Deri N, Herbert J, Moore F, Petkovska-Boskova T, Alroughani R, Savino A, Shaw C, Vucic S, Santiago V, Bacile EA, Skromne E, Poehlau D, Cabrera-Gomez JA, Lucas R, Butzkueven H. Seasonal variation of relapse rate in multiple sclerosis is latitude dependent. *Ann Neurol* 2014; **76**(6): 880–90.

288. Steelman AJ. Infection as an environmental trigger of multiple sclerosis disease exacerbation. *Front Immunol* 2015; **6**: 520.

289. Steiner D. Natalizumab versus placebo in patients with secondary progressive multiple sclerosis (SPMS): results from ASCEND, a multicenter, double-blind, placebo-controlled, randomized phase 3 clinical trial. Paper presented at: American Academy of Neurology 2016 Annual Meeting; 2016; Vancouver, BC, Canada.

290. Steinman, L. A brief history of TH17, the first major revision in the TH1/TH2 hypothesis of T cell-mediated tissue damage. *Nat Med* 2007; **13**: 139–145.

291. Steinman L. No quiet surrender: molecular guardians in multiple sclerosis brain. *J Clin Invest* 2015 Apr; **125**(4): 1371-8.

292. Sui W, Hou X, Zou G, Che W, Yang M, Zheng C, Liu F, Chen P, Wei X, Lai L, Dai Y. Composition and variation analysis of the TCR β-chain CDR3 repertoire in

systemic lupus erythematosus using high-throughput sequencing. *Mol Immunol* 2015; **67**(2 Pt B): 455-64.

293. Swanson PC. The bounty of RAGs: recombination signal complexes and reaction outcomes. *Immunol Rev* 2004; **200:** 90–114.

294. Takada K and Jameson SC. Naive T cell homeostasis: from awareness of space to a sense of place. *Nat Rev Immuno* 2009; **9**: 823–832.

295. Takada K and Takahama Y. Positive-selection-inducing self-peptides displayed by cortical thymic epithelial cells. *Adv Immunol* 2015; **125**: 87–110.

296. Takaba H and Takayanagi H. The Mechanisms of T Cell Selection in the Thymus. *Trends Immunol* 2017 Nov; **38**(11): 805-816.

297. Tan I, McArthur J, Clifford DB, Major EO, Nath A. Immune reconstitution inflammation syndrome in natalizumab-associated PML. *Neurology* 2011; **77:** 1061-1067.

298. Tarlinton RE, Khaibullin T, Granatov E, Martynova E, Rizvanov A, Khaiboullina S. The Interaction between Viral and Environmental Risk Factors in the Pathogenesis of Multiple Sclerosis. *Int J Mol Sci* 2019 Jan 14; **20**(2). pii: E303.

299. Tejada-Simon MV, Zang YC, Hong J, Rivera VM, Zhang JZ. Cross-reactivity with myelin basic protein and human herpesvirus-6 in multiple sclerosis. *Ann Neurol* 2003; **53**: 189–197.

300. Teniente-Serra A, Hervás JV, Quirant-Sánchez B, Mansilla MJ, Grau-López L, Ramo-Tello C, Martínez-Cáceres EM. Baseline Differences in Minor Lymphocyte Subpopulations may Predict Response to Fingolimod in Relapsing-Remitting Multiple Sclerosis Patients. *CNS Neurosci Ther* 2016 Jul; **22**(7): 584-92.

301. Thapa DR, Tonikian R, Sun C, Liu M, Dearth A, Petri M, Pepin F, Emerson RO, Ranger A. Longitudinal analysis of peripheral blood T cell receptor diversity in patients with systemic lupus erythematosus by next-generation sequencing. *Arthritis Res Ther* 2015; **1**7: 132.

302. Thome JJ, Bickham KL, Ohmura Y, Kubota M, Matsuoka N, Gordon C, Granot T, Griesemer A, Lerner H, Kato T, Farber DL. Early-life compartmentalization of human T cell differentiation and regulatory function in mucosal and lymphoid tissues. *Nat Med* 2016 Jan; **22**(1): 72–77.

303. Thompson AJ, Banwell BL, Barkhof F, Carroll WM4, Coetzee T5, Comi G6, Correale J7, Fazekas F, Filippi M, Freedman MS, Fujihara K, Galetta SL, Hartung HP, Kappos L, Lublin FD, Marrie RA, Miller AE, Miller DH, Montalban X, Mowry EM, Sorensen PS, Tintoré M, Traboulsee AL, Trojano M, Uitdehaag BMJ, Vukusic S, Waubant E, Weinshenker BG, Reingold SC, Cohen JA. Diagnosis of multiple

sclerosis: 2017 revisions of the McDonald criteria. *Lancet Neurol* 2018 Feb; **17**(2): 162-173.

304. Tickotsky N., Sagiv T, Prilusky J, Shifrut E, Friedman N. McPAS-TCR: a manually curated catalogue of pathology-associated T cell receptor sequences. *Bioinformatics* 2017; **33**: 2924–2929.

305. Tony HP, Burmester G, Schulze-Koops H, Grunke M, Henes J, Kötter I, Haas J, Unger L, Lovric S, Haubitz M, Fischer-Betz R, Chehab G, Rubbert-Roth A, Specker C, Weinerth J, Holle J, Müller-Ladner U, König R, Fiehn C, Burgwinkel P, Budde K, Sörensen H, Meurer M, Aringer M, Kieseier B, Erfurt-Berge C, Sticherling M, Veelken R, Ziemann U, Strutz F, von Wussow P, Meier FM, Hunzelmann N, Schmidt E, Bergner R, Schwarting A, Eming R, Hertl M, Stadler R, Schwarz-Eywill M, Wassenberg S, Fleck M, Metzler C, Zettl U, Westphal J, Heitmann S, Herzog AL, Wiendl H, Jakob W, Schmidt E, Freivogel K, Dörner T. GRAID investigators. Safety and clinical outcomes of rituximab therapy in patients with different autoimmune diseases: experience from a national registry (GRAID). *Arthritis Res Ther* 2011 May 13; **13**(3): R75.

306. Traboulsee AL, Li DK. The role of MRI in the diagnosis of multiple sclerosis. *Adv Neurol* 2006; **98**: 125-46.

307. Trowbridge IS and Thomas ML. CD45: an emerging role as a protein tyrosine phosphatase required for lymphocyte activation and development. *Annu Rev Immunol* 1994; **12**: 85–116.

308. Tubridy N, Behan PO, Capildeo R, Chaudhuri A, Forbes R, Hawkins CP, Hughes RA, Palace J, Sharrack B, Swingler R, Young C, Moseley IF, MacManus DG, Donoghue S, Miller DH. The effect of anti-alpha4 integrin antibody on brain lesion activity in MS. The UK Antegren Study Group. *Neurology* 1999 Aug 11; **53**(3): 466-72.

309. Tzartos JS, Friese MA, Craner MJ, Palace J, Newcombe J, Esiri MM, Fugger L. Interleukin-17 production in central nervous system infiltrating T cells and glial cells is associated with active disease in multiple sclerosis. *Am J Pathol* 2008; **172**: 146–55.

310. Vanden Eijnden S, Goriely S, De Wit D, Willems F, Goldman M. IL-23 up-regulates IL-10 and induces IL-17 synthesis by polyclonally activated naive T cells in human. *Eur J Immunol* 2005; **35**: 469–75.

311. van der Geest KS, Abdulahad WH, Horst G, Lorencetti PG, Bijzet J, Arends S, van der Heiden M, Buisman AM, Kroesen BJ, Brouwer E, Boots AM. Quantifying Distribution of Flow Cytometric TCR-Vβ Usage with Economic Statistics. *PLoS One* 2015 Apr 29; **10**(4): e0125373.

312. van Gent DC, Ramsden DA, Gellert M. The RAG1 and RAG2 proteins establish the 12/23 rule in V(D)J recombination. *Cell* 1996 Apr 5; **85**(1): 107-13.

313. van Nierop GP, van Luijn MM, Michels SS, Melief MJ, Janssen M, Langerak AW, Ouwendijk WJD, Hintzen RQ, Verjans GMGM. Phenotypic and functional characterization of T cells in white matter lesions of multiple sclerosis patients. *Acta Neuropathol* 2017 Sep; **134**(3): 383-401.

314. Varadkar S, Bien CG, Kruse CA, Jensen FE, Bauer J, Pardo CA, Vincent A, Mathern GW, Cross JH. Rasmussen's encephalitis: clinical features, pathobiology, and treatment advances. *Lancet Neurol* 2014 Feb; **13**(2): 195-205.

315. Verma K, Ogonek J, Varanasi PR, Luther S, Bünting I, Thomay K, Behrens YL, Mischak-Weissinger E, Hambach L. Human CD8+ CD57- TEMRA cells: Too young to be called "old". *PLoS One* 2017 May 8; **12**(5): e0177405.

316. Virtanen JO and Jacobson S. Viruses and multiple sclerosis. *CNS Neurol Disord Drug Targets* 2012 Aug; **11**(5): 528-44.

317. Voelkerding KV; Dames SA, Durtschi JD. Next-Generation Sequencing: From Basic Research to Diagnostics. *Clinical Chemistry* 2009; **55**(4): 641–658.

318. Vrenken H, Pouwels PJ, Geurts JJ, Knol DL, Polman CH, Barkhof F, Castelijns JA. Altered diffusion tensor in multiple sclerosis normal-appearing brain tissue: cortical diffusion changes seem related to clinical deterioration. *J Magn Reson Imaging* 2006 May; **23**(5): 628-36.

319. Walsh P, Kane N, Butler S. The clinical role of evoked potentials. *J Neurol Neurosurg Psychiatry* 2005 Jun; **76**(Suppl 2): ii16–ii22.

320. Wandinger K, Jabs W, Siekhaus A, Bubel S, Trillenberg P, Wagner H, Wessel K, Kirchner H, Hennig H. Association between clinical disease activity and Epstein-Barr virus reactivation in MS. *Neurology* 2000 Jul 25; **55**(2): 178-84.

321. Wang HH, Dai YQ, Qiu W, Lu ZQ, Peng FH, Wang YG, Bao J, Li Y, Hu WQ. Interleukin-17- secreting T cells in neuromyelitis optica and multiple sclerosis during relapse. *J Clin Neurosci* 2011 Oct; **18**: 1313–7.

322. Wang W, Wang EQ, Balthasar JP. Monoclonal antibody pharmacokinetics and pharmacodynamics. *Clin Pharmacol Ther* 2008; **84**(5): 548–558.

323. Warnke C, Menge T, Hartung HP, Racke MK, Cravens PD, Bennett JL, Frohman EM, Greenberg BM, Zamvil SS, Gold R, Hemmer B, Kieseier BC, Stüve O. Natalizumab and progressive multifocal leukoencephalopathy: what are the causal factors and can it be avoided? *Arch Neurol* 2010 Aug; **67**(8): 923-30.

324. Waubant E. Spotlight on anti-CD20. *Int MS J* 2008; **15**: 19–25.

325. Weber MS, Hemmer B, Cepok S. The role of antibodies in multiple sclerosis. *Biochim Biophys Acta* 2011 Feb; **1812**(2): 239-45.

326. Wee Yong V, Chabot S, Stuve O, Williams G. Interferon beta in the treatment of multiple sclerosis: mechanisms of action. *Neurology* 1998 Sep; **51**(3): 682-9

327. Wessig C, Bendszus M, Stoll G. *In vivo* visualization of focal demyelination in peripheral nerves by gadofluorine M-enhanced magnetic resonance imaging. *Exp Neurol* 2007 Mar; **204**(1): 14-9.

328. Willinger T, Freeman T, Hasegawa H, McMichael AJ, Callan MF. Molecular signatures distinguish human central memory from effector memory CD8 T cell subsets. *J Immunol* 2005 Nov 1; **175**(9): 5895-903.

329. Winger RC and Zamvil SS. Antibodies in multiple sclerosis oligoclonal bands target debris. *Proc Natl Acad Sci U S A* 2016 Jul 12; **113**(28): 7696–7698.

330. World Health Organization. 64th Consultation on International Nonproprietary Names for Pharmaceutical Substances. Geneva, 4-7 April 2017. Executive Summary (PDF). 2017-07-31. Retrieved 2017-08-22.

331. Wucherpfennig KW and Strominger JL. Molecular mimicry in T cell-mediated autoimmunity: viral peptides activate human T cell clones specific for myelin basic protein. *Cell* 1995 Mar 10; **80**(5): 695-705.

332. Wuerfel E, Infante-Duarte C, Glumm R, Wuerfel JT. Gadofluorine M-enhanced MRI shows involvement of circumventricular organs in neuroinflammation. *J Neuroinflammation* 2010; **7**: 70.

333. Ye L, Li L, Wan B, Yang M, Hong J, Gu W, Wang W, Ning G. Immune response after autologous hematopoietic stem cell transplantation in type 1 diabetes mellitus. *Stem Cell Res Ther* 2017 Apr 18; **8**(1): 90.

334. Yednock TA, Cannon C, Fritz LC, Sanchez-Madrid F, Steinman L, Karin N. Prevention of experimental autoimmune encephalomyelitis by antibodies against alpha 4 beta 1 integrin. *Nature* 1992 Mar 5; **356**(6364): 63-6.

335. Yousry TA, Major EO, Ryschkewitsch C, Fahle G, Fischer S, Hou J, Curfman B, Miszkiel K, Mueller-Lenke N, Sanchez E, Barkhof F, Radue EW, Jäger HR, Clifford DB. Evaluation of patients treated with natalizumab for progressive multifocal leukoencephalopathy. *N Engl J Med* 2006 Mar 2; **354**(9): 924-33.

336. Yu J, Shi B, Ma L, Liu C, Sun S, Ma R, Qiu Y, Yao X. Case report for recurrent and new-onset SLE patients treated by high-dose glucocorticoid therapy: Characteristics of peripheral TCR beta chain CDR3 repertoires. *Medicine (Baltimore)* 2017; **96**(49): e9022.

337. Zhang Y, Smith CL, Saha A, Grill SW, Mihardja S, Smith SB, Cairns BR, Peterson CL, Bustamante C. DNA translocation and loop formation mechanism of chromatin remodeling by SWI/SNF and RSC. *Mol Cell* 2006 Nov 17; **24**(4): 559-68.

338. Zozulya AL and Wiendl H. The role of regulatory T cells in multiple sclerosis. *Nat Clin Pract Neurol* 2008 Jul; **4**(7): 384-98.

Ringraziamenti / Acknowledgements

Al termine del mio percorso di dottorato, ringrazio innanzitutto la mia tutor, **Clara Ballerini**, per la serietà e la cura con cui mi ha seguita in questi tre anni; fra gli ex-colleghi, ringrazio **Alessandra** per avermi dato un supporto scientifico e morale all'inizio del mio percorso di dottorato che non dimenticherò; **Elena** per la disponibilità e la pazienza non solo in laboratorio; **Antonio**, per i tanti momenti di condivisione di vita da dottorandi. Ringrazio il mio collega attuale, **Alberto**, con cui condividere esperimenti e vicissitudini da dottorandi mi ha un po' ricordato il piacere nostalgico di avere un compagno di scuola.
Ringrazio **i miei genitori e mio fratello** per essere supportivi in tutto ciò faccio e sempre incoraggianti. Ringrazio **Saul** per esserci sempre in qualsiasi circostanza. Infine, ma non per importanza, ringrazio il team di lavoro dell'Università di Oslo: grazie a **Victor Greiff** per avermi fatto da mentore nel periodo di sei mesi che ho trascorso nel suo team; grazie ai suoi colleghi **Igor**, **Mat** e **Milena** per avermi accolta e fatta sentire a casa da subito. *Tusen takk!*

At the end of my PhD journey, firstly I would like to thank my tutor, **Clara Ballerini**, who professionally and carefully guided me over the past three years; among my former colleagues, I would like to thank **Alessandra** who supported me in a scientific and moral way that I won't forget; **Elena** for her willingness and patience not only in the laboratory; **Antonio**, for sharing with me many PhD-students life moments. I would like to thank my current colleague, **Alberto**, with whom sharing experiments and PhD-students adventures reminded me the nostalgic pleasure to have a classmate.
I would like to thank **my parents and my brother** for being supportive in everything I do and always encouraging. I am grateful to **Saul** for being with me in every circumstance.
Last, but not least, I would like to thank the work team from University of Oslo: thanks to **Victor Greiff** for mentoring me during the period of six months that I spent in his team; thanks to his colleagues **Igor**, **Mat** and **Milena** for welcoming me and made feel home from the start. *Tusen takk!*